Exploring the role of cell-wall pectin cross-linking in freezing tolerance and guard cell dynamics in Arabidopsis thaliana

PANTER, PAIGE,ELIZABETH

Exploring the role of cell-wall pectin cross-linking in freezing tolerance and guard cell dynamics in *Arabidopsis thaliana*

Paige Elizabeth Panter

Submitted for the Degree of Doctor of Philosophy by Research

Department of Biosciences

September 2018

ABSTRACT

Freezing stress is detrimental to plants, resulting in major crop losses in temperate regions. The plant cell wall is a dynamic network of proteins and polysaccharides including cellulose, hemicellulose and pectins. It is essential for plant survival, providing structural integrity, strength and protection against pathogens. As the cell wall is the site of ice formation, it has also been suggested that the wall could contribute towards protection of the plant against freezing damage. The cell wall undergoes remodelling during cold acclimation, but it is unclear what specific role this restructuring may play in freezing tolerance.

The *sensitive to freezing8* (*sfr8*) mutant contains less cell wall fucose due do a mutation in the fucose biosynthetic gene *MUR1*. This was shown to result in a decrease in dimerisation of the cell wall pectic domain rhamnogalacturonan-II (RG-II), which in wild type plants is predominantly dimerised via a borate-ester cross-link. This decrease in dimerisation likely results in the observed freezing sensitivity of *mur1* mutants, as supplementation of plants with boric acid was shown to restore freezing tolerance. Guard cell dynamics were also compromised in the *sfr8* mutant, as stomata were found to be more restricted in their movements than wild type in response to ABA, CO_2 and changes in humidity.

The freezing and guard cell phenotypes of *sfr8* may be attributed to a decrease in the tensile modulus of the cell wall with reduced RG-II dimerisation. This makes the wall more vulnerable to deformation during freezing and prevents the guard cells from stiffening to allow an increase in stomatal aperture. RG-II dimerisation also mediates certain structural aspects of the cell wall that may facilitate supercooling by excluding ice nucleation and preventing ice growth. This research reveals the importance of RG-II dimerisation in cell wall dynamics and the impact cell-wall composition has on freezing and desiccation tolerance. These findings could lead to the identification of new targets for crop breeding.

TABLE OF CONTENTS

LIST OF FIGURES

LIST OF ABBREVIATIONS

The standard scientific conventions for protein and gene naming have been followed: wild type genes and proteins are in capitals and mutants are denoted by lower case, gene names are italicised whereas protein names are not.

Standard scientific abbreviations have been used for units of weight, length, amount, molarity, temperature and time.

Standard chemical element symbols, nucleic acid, amino acid and sugar codes are used.

ABA	Abscisic acid
AFP	Anti-freeze protein
AIR	Alcohol insoluble residue
BA	Boric acid
BOR	Boron transporter
CAS	Cold-acclimation specific
CBF	C-repeat/DRE binding factor
CESA	Cellulose synthase A
COR	Cold on regulated
CRT	C-repeat
CSL	Cellulose synthase-like
DRE	Drought responsive element
DREB	Drought responsive element binding
EIL	Expansion-induced lysis
EL	Electrolyte leakage
EPG	Endo-polygalacturonase
ESK1	Eskimo1
FUT	Fucosyltransferase
GalAT	Galactosyltransferase
GIPC	Glycosyl inositol phosphor ceramides
HG	Homogalacturonan
HOS1	High expression of osmotically responsive gene1
HOS9	High expression of osmotically responsive gene9
HPLC	High performance lipid chromatography
HSP	Heat shock protein
IAA	Indole acetic acid
IBP	Ice-binding protein
ICE1/2	Inducer of CBF expression1/2
IIF	Intracellular ice formation
LD	Light:dark
ML	Middle lamella

MS	Murashige and Skoog
MUR	Murus
PAE	Pectin acetyl-esterase
PAGE	Polyacrylamide gel electrophoresis
PAT	Pectin acetyl-transferase
PCR	Polymerase chain reaction
PCW	Primary cell wall
PG	Polygalacturonase
PM	Plasma membrane
PME	Pectin methyl-esterase
PMEI	Pectin methyl-esterase inhibitor
PMT	Pectin methyl-transferase
RG-I	Rhamnogalacturonan-I
RG-II	Rhamnogalacturonan-II
ROS	Reactive oxygen species
ROS	Reactive oxygen species
SCW	Secondary cell wall
SFR	Sensitive to freezing
SIZ1	siz/map1
SUMO	Small ubiquitin-related modifier
TCF1	Tolerant to chilling and freezing1
T-DNA	Transfer DNA
UV	Ultra violet
WT	Wild type
XT	Xylosyltransferase
XTH	Xyloglucan endotransglycosylase
XyG	Xyloglucan

STATEMENT OF AUTHORSHIP

I certify that all of the work described in this thesis is my own research unless otherwise acknowledged in the text or by references and has not been previously submitted for a degree in this or any other university.

STATEMENT OF COPYRIGHT

ACKNOWLEDGEMENTS

First and foremost, I would like to thank my supervisor, Dr Heather Knight, for her constant encouragement, support and advice throughout my PhD. Your supervision and your friendship have made these four years a pleasure.

I would like to thank all the collaborators and researchers I have worked with throughout the project. Most notably Ian Cummins for all his help with the sugar analysis and as a constant source of knowledge and patience in all the other measurements he attempted to do when I asked.

Thank you to Steve Fry and Dayan Sanhueza for hosting me several times at Edinburgh University. To Steve for all the effort he put into the chromatography as well as general cell wall chat, and to Dayan for all her help with PAGE analysis.

Thanks go also to Anne Borland for assistance with stomatal conductance measurements, Ankush Prashar for the use and advice of his thermal imaging camera, Tom Whale and Martin Daily for their help with the freezing experiments, Pablo Cubillas for his help in attempting AFM, to Mark Skipsey and Sarah Smith for their technical advice when I was starting out and of course to the BBSRC for the funding of the project.

I would like to thank everyone who has ever had the pleasure of gracing lab 19 for all the good times we have had. To Alice and Steph for keeping me sane, to Fieka, May and Kasia for all our hugs, to Tracey and Bryony for our constant chats and of course to Marc, mainly for his humour, but also for his advice.

Many thanks go to my family and friends for their encouragement. To my mum for always believing in me, to Molly for telling me to get on with it, and to everyone for putting up with my complaining even though no-one really knew why I was freezing plants all the time. Also, to Kylo for his company and cuddles.

Finally, my biggest thanks go to my amazing husband Jack. I could not have got through the past four years without you by my side. You have consoled me when things have gone wrong, encouraged me when I didn't know what to do next, and been immensely proud of me when things have actually come together. I cannot thank you enough for all the drafts you have read, for all our scientific conversations and for all the coffee you made in the morning. I can't wait for our next adventure together!

DEDICATION

This thesis is dedicated to my dad, David Martin Sleight, who I'm sure would have found it a thrilling read.

CHAPTER 1

INTRODUCTION

Environmental stress can have a major impact on plant survival and crop productivity. Plants growing in temperate to high latitudes, and at high altitudes, may experience low temperatures on a regular basis throughout their developmental lifespan, and due to their sessile nature, plants are unable to move to avoid these adverse conditions. Particularly damaging are the low temperatures plants may experience before cold hardening has taken place, and after tissues have de-hardened i.e. during early autumn and late spring frosts. With the threat of climate change, there is predicted to be an increase in the occurrence of these temperature fluctuations.

There is already evidence that these events can be devastating to agriculture, such as the 2007 eastern US spring freeze which caused severe and widespread damage to crops, resulting in agricultural losses of $111.7 million in one state alone (Gu *et al.* 2008). It is therefore an important endeavour to understand how plants withstand freezing, and how they can be made more tolerant in order to survive such future events and maintain crop yield for the increasing population.

This study aims to investigate the role of the plant cell wall as a mechanism for surviving freezing events. This chapter reviews our current knowledge of freezing injury and freezing tolerance in plants and looks at this in relation to the structure and dynamics of the plant cell wall.

1.1 Freezing Tolerance and Injury

1.1.1 Ice growth and propagation

In order to understand how a plant survives freezing events, it is necessary to know what processes occur within the plant during these events to cause damage. Different plants respond to freezing differently. Tropical plants which rarely, if ever, experience temperatures below 0°C often display chilling injury. These plants will experience damage such as chlorosis of leaves and loss of turgor and undergo physiological dysfunction at temperatures below 10-12°C (Lyons 1973). Temperate plants are generally chilling-resistant but can vary in their freezing tolerance. Most temperate plants increase their freezing tolerance through a process known as cold acclimation (Thomashow 1999), which will be discussed in section 1.2. This study will focus on temperate plants, and this section will summarise how they experience freezing and how they prevent or survive freezing injury.

For more information on the first 100 years of research into freezing injury and tolerance, the reader is referred to the extensive review by Levitt (1980) which covers many topics. This review will be used to reference early work and generalisations that have been established from many years of that work, and the reader is referred to references therein for further detail and progressions of ideas and discovery.

1.1.1.1 Ice nucleation

Freezing stress and cellular damage generally occur following the growth of ice crystals within the plant. In a bulk volume of water, ice crystals only form spontaneously in highly supercooled water, at temperatures below -40°C (Bigg 1953). Under such conditions, this homogeneous nucleation is effectively achieved once the forming crystal nucleus surpasses the critical radius of 1.13 nm (Sakai & Larcher 1987). However, in nature ice will readily form at much higher temperatures via heterogeneous ice nucleation, catalysed by ice-nucleating particles such as organic and inorganic molecules or ice-nucleating bacteria (Lindow, Arny & Upper 1982; Hirano & Upper 2000). There is evidence to suggest that in plants, ice nucleates first in the vessels (Asahina 1956), the large diameter and dilute solute of which facilitate freezing at higher temperatures than in epidermal cells, which have higher solute concentrations. Nucleation within the cells has been suggested to occur via nucleation sites associated with the cell wall (Salt & Kaku 1967). However, ice may also enter the plant from external sources: via growth of

ice nucleated on the outer surface through stomata, hydathodes or cracks in the cuticle surface (Wisniewski & Fuller 1999).

Plants that are able to survive freezing temperatures typically do so by tolerating ice formation in their tissues (Burke *et al.* 1976). There are two main compartments in plants in which water resides; the symplast and the apoplast. The symplast encompasses intracellular water of the cytoplasm and vacuole, and the apoplast encompasses water in the xylem-lumen space, the cell wall and other extracellular areas such as intercellular spaces (Canny 1995). Due to this separation, ice can form either intracellularly, in the symplast, or extracellularly, in the apoplast. Intracellular and extracellular ice occur under different conditions and have different damaging effects on plants.

1.1.1.2 Intracellular ice

Intracellular ice formation (IIF) has been observed in plants both *in vitro* and *in vivo* for example in non-hardy plants, in subepidermal and perivascular tissue (Pearce & Ashworth 1992) or in 'deep supercooled' (see section 1.5.3) tissues of freezing-tolerant plants at very low temperature (George & Burke 1976). IIF has also been observed using high-speed microscopy (Ninagawa *et al.* 2016), in which the formation pattern of ice inside the cell was influenced by the rate of cooling. It has been suggested that if cooling is rapid enough, ice crystals would form at very low temperatures that are small enough to penetrate the plasma membrane and induce intracellular freezing (Mazur 1963; Levitt 1980). Larger ice crystals may also damage membranes directly through shearing or laceration, disturbing their semi-permeability and resulting in the leaking of cell contents (Levitt 1980).

It has been suggested that intracellular freezing ultimately always results in cell death, likely due to the detrimental effects of the freezing of the cytoplasm, as well as subsequent dehydration stress and mechanical pressure due to ice formation (Asahina 1956). However, there is some evidence that this is not always the case, as IIF in seeds of *Acer saccharinum* was found to be non-lethal (Wesley-Smith *et al.* 2014), although this system is not necessarily typical of a hydrated plant cell. Nevertheless, IIF is believed to be a rare occurrence in nature, since it is usually observed during very rapid cooling that plants are unlikely to experience (Weiser 1970; Levitt 1980).

1.1.1.3 Extracellular ice

Most of the damage that occurs to plants in nature during freezing is due to extracellular ice formation. Ice will spread throughout the plant from nucleation points, forming mainly between cells where there is space for ice to grow (Levitt 1980). The hydrophobic lipid plasma membrane prevents the growth of ice into the cell at low rates of cooling (contrary to intracellular ice formation during fast cooling) (Chambers & Hale 1932). Effective structural ice barriers can also prevent the spread of ice through the plant, which may be related to the cell wall (Kuprian *et al.* 2014). This is particularly observed in plant organs such as flower buds, where ice is prevented from growing due to the presence of ice barriers in order to prevent damage to susceptible tissue (Wisniewski, Gusta & Neuner 2014). Ice crystals have frequently been observed to form on the surface of the cell wall facing the intercellular space, from water vapour and the surface film of water present on cell walls (Asahina 1956; Levitt 1980). Under natural freezing conditions, freezing may be gradual enough to prevent ice from spreading throughout the entirety of the plant. Ice crystals may be confined to specific regions, particularly if the membrane and cell wall structure prevent further ice growth (Ashworth & Abeles 1984). Ice must then grow at the expense of water diffusing to it from relatively distant unfrozen regions (Levitt 1980).

Extracellular freezing is believed to occur in two stages, a phenomenon that has been observed via infrared thermography (Pearce & Fuller 2001). An initial, rapid spread of extracellular ice is indicated by a low-intensity thermal signal (exotherm), due to the exothermic nature of ice nucleation. A small quantity of water moving from the cytoplasm to the apoplast down the water potential gradient created is enough to thaw the ice, after which a more intense freezing event occurs where water is drawn from cells and freezes extracellularly indicated by a second exotherm (Figure 1.1). The initial growth of ice can occur at a rate of between 4 to 40 mm per second (Hudson & Idle 1962; Pearce & Fuller 2001). Interestingly, a double freezing point of a different nature has also been observed in woody plants, where the first exotherm occurs at the beginning of extracellular freezing, and the second occurs at very low temperatures due to intracellular freezing of parenchyma cells (Burke *et al.* 1976).

It is important to note that the formation of ice within the plant relies on several factors including the rate of temperature decrease, the degree of supercooling, the water content of the cell and surrounding tissues and the hardiness of the plant (see section 1.2). All of these factors play a part in the incidence of ice nucleation, whether intra- or extracellular, and ultimately the damage that the plant sustains (Asahina 1956). As previously mentioned, most of

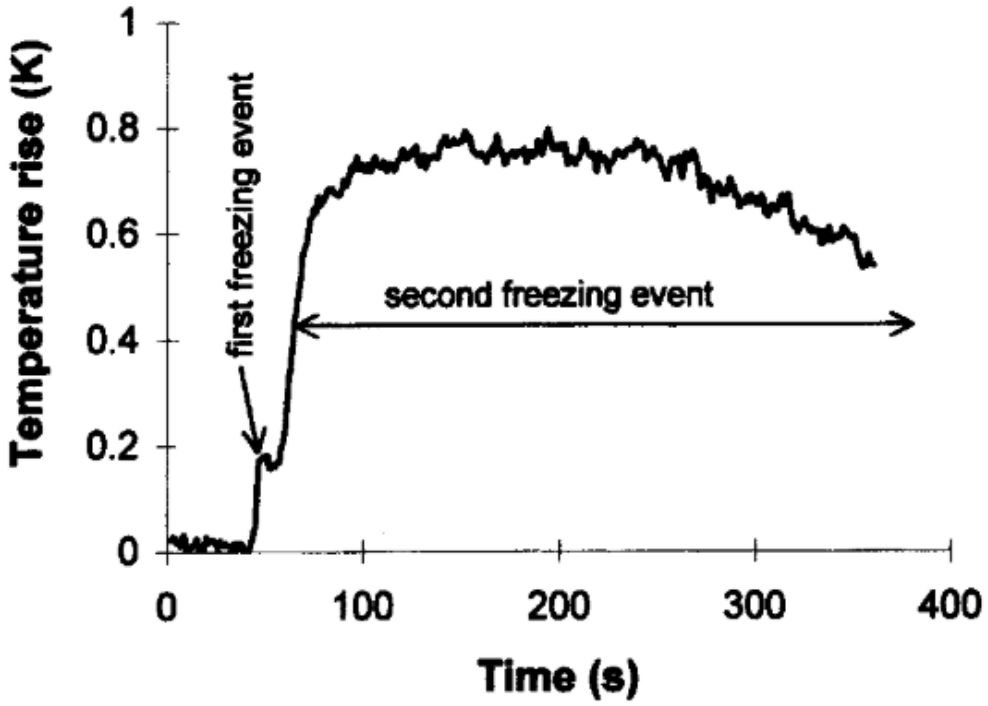

Figure 1.1: The double freezing point. Observation of two freezing points in leaf blades of barley during a typical freezing event, highlighted by the increase in temperature. From Pearce and Fuller (2001).

the damage sustained from freezing is due to the formation of extracellular ice, the various consequences of which will be discussed.

1.1.2 Mechanisms of freezing damage

1.1.2.1 Damage due to freeze-induced dehydration

The formation of extracellular ice within the plant results in a secondary dehydration stress that is believed to be the main cause of injury by extracellular ice (Levitt 1956, 1980; Pearce 2001). The formation of ice in intercellular spaces lowers the water potential of the apoplast. Consequently, cellular water at a higher potential diffuses through the plasma membrane to the intercellular ice, resulting in ice crystal growth (Gusta, Burke & Kapoor 1975). This results in the contraction or collapse of the cell, also known as cytorrhysis, as it experiences dehydration (Pearce 1988; Pearce & Ashworth 1992). If the temperature continues to decrease, water will continue to diffuse to points of extracellular ice, as the water potential of ice increases as temperature decreases, thus increasing dehydration (Gusta *et al.* 1975). The solute concentration within the cell thus increases, decreasing the freezing point further (Levitt 1941). Eventually temperature equilibrium and consequent water potential equilibrium may be

reached, and the plant can remain frozen indefinitely at constant temperature without the formation of ice occurring within the cell (Levitt 1980).

The rate of diffusion of water from the protoplasm to the apoplast is dependent upon the permeability of the plasma membrane. If the membrane is not permeable enough such that water movement is slowed, and the temperature decrease is rapid enough, diffusion cannot occur rapidly enough to increase the concentration of the cellular solute. The cell may therefore reach a temperature sufficiently lower than its freezing point to induce intracellular freezing (Levitt 1980). Studies have shown that the permeability of the cell membrane increases during cold acclimation (Yoshida & Uemura 1990; Uemura *et al.* 2006) which may account for the observance of intracellular freezing in non-hardy plants (Asahina 1956).

There is evidence to suggest that damage sustained during freezing events is mostly as a result of freeze-dehydration induced by extracellular ice nucleation and growth. Such dehydration results in constriction or even collapse of both the plasma membrane and the cell wall (Molisch 1897). This causes contraction of the tissues due to cell-cell adhesion, and ice has even been observed to split the cell walls of mosses, which typically have no intercellular spaces (Modlibowska & Rogers 1955). A particular site of injury is the plasma membrane, the structure of which is damaged when dehydration exceeds the tolerance of the cell (Steponkus 1984). This dehydration stress leads to a phase separation of the membrane from a bilayer to a non-bilayer structure, thus disrupting compartmentalisation and normal cellular function (Stout, Majak & Reaney 1980; Pearce & Willison 1985). Other membranes such as the thylakoid membrane (Steponkus *et al.* 1977) and the tonoplast (Murai & Yoshida 1998a) have been shown to incur damage, thus affecting photosynthetic and cellular processes. The increase in solute concentration has also been shown to damage membranes during freeze-induced dehydration due to so called “solution effects” (Levitt 1980; Steponkus 1984). This could occur through the direct interaction of solutes with the membrane resulting in the dissociation of proteins, or by the dissociation of the bilayer due to interaction of polar membrane components with aqueous solutions (Heber *et al.* 1981).

1.1.2.2 The effect of freeze-thaw cycles

Another form of damage due to dehydration presents itself upon thawing of plant tissues. During the cell collapse of freeze-induce dehydration, the cell membrane shrinks, and excess lipids are removed into endocytotic vesicles in order to maintain tension. The formation of these

vesicles is not believed to be a cause of membrane damage (Dowgert & Steponkus 1984). However, upon thawing, osmotic expansion causes membrane rupture as the vesicles are not able to be incorporated into the membrane quickly enough to reverse the large decrease in area (Wiest & Steponkus 1978), a form of injury termed 'expansion-induce lysis' (EIL).

A loss of osmotic responsiveness is another consequence of freeze-induced dehydration, where the membrane becomes flaccid and isotropic tension is lost (Yamazaki, Kawamura & Uemura 2009). This alteration to osmotic responsiveness effects the permeability of the membrane, and could occur for several reasons including the effect of toxic solutes, liquid crystal-to-gel phase transitions or the effects of dehydration (Steponkus 1984). The dehydration-induced lamellar-to-hexagonal-II phase transition has been observed in freeze-induced dehydrated protoplasts and occurs when the plasma membrane is brought into close contact with other endomembranes in the cell such as the chloroplast as it collapses (Gordon-Kamm & Steponkus 1984a; Nagao *et al.* 2008). Generally, the osmotic responsiveness of the protoplast is diminished during thawing, such that no lysis is observed but the protoplast is unable to return to its original size (Uemura *et al.* 2006). These events are likely the cause of the observation of "frost plasmolysis" in freeze killed cells, where the cell wall expands back to its nearly original shape during the influx of water after thawing, whilst the dead protoplast remains contracted (Levitt 1980).

1.1.2.3 Resistance to collapse and influence of cell tensions

As described previously, during the formation of extracellular ice, water moves down the potential gradient from inside the cell to outside, resulting in freeze-dehydration, which causes the membrane and cell wall to collapse. The movement of water allows the cell to reach freezing equilibrium where the water potential of the cells is identical to that of the ice (Levitt 1980). However, there is also evidence of non-equilibrium freezing resulting in the development of negative pressures within the cell. Negative pressures have been measured in an artificial cell during freezing (Zhu, Steudle & Beck 1989), and have been proposed in several plant species such as *Pachysandra terminalis* (Zhu & Beck 1991) and *Hordeum vulgare* (Hansen & Beck 1988). Negative pressures are formed due to the resistance of the cell wall to collapse during freeze-dehydration and can limit the extent of dehydration the cell experiences. The ability of the cell wall to resist collapse is believed to be associated with cell-wall strength (Rajashekar & Burke 1982), which has been shown to increase during cold acclimation (Rajashekar & Lafta 1996). Although resistance to collapse may lessen cellular dehydration during freezing events, the

formation of negative pressures can lead to cavitation i.e. the formation of vapour cavities in a liquid filled space (Tyree & Dixon 1986). Cavitation is mostly observed in xylem vessels during water stress, where negative pressures increase, and can lead to embolism where the xylem conduits fill with gases that come out of solution in the surrounding tissue to fill the space left by the cavitation event (Tyree & Sperry 1989).

1.1.2.4 Other effects of low temperature

Although membranes are believed to be the main site of injury during freezing, low temperatures and ice can have other detrimental effects on the cell. Such low temperatures have been shown to result in the denaturation of proteins due to a decrease in their conformational stability, impacting upon normal cellular processes (Guy, Haskell & Li 1998). The production of oxygen radicals (ROS) increases during freezing resulting in damage to membranes and other cell contents (Kendall & McKersie 1989). The formation of ice in intercellular spaces can also form adhesions to cell-wall polysaccharides and the plasma membrane often resulting in cell rupture (Olien & Smith 1977). It is clear that there are many aspects of freezing that are detrimental to plants, thus it is necessary for plants to have mechanisms in place in order to prevent damage from those events.

1.2 Cold Acclimation

Many temperate plants have the ability to undergo a process known as cold acclimation, through the exposure to low non-freezing temperatures between 0 and 5°C. This process allows the plant to gain a higher level of freezing tolerance, permitting it to survive at lower temperatures and often preventing injury from some of the events previously described. (Thomashow 1999). As early as the late 1800s plants were shown to increase in their freezing tolerance after exposure to low temperatures (Levitt 1980). These changes were hypothesised to result from metabolic and physiological modifications as a result of gene expression (Weiser 1970), and eventually it was established that cold exposure induced changes in gene expression (Guy, Niemi & Brambl 1985). The focus of this section will be on the regulation of cold acclimation, and what processes take place to allow the plant to become more freezing tolerant.

1.2.1 Cold sensing

The mechanism via which plants sense cold, and the events following this that occur upstream of cold-induced alterations in order for cold acclimation to occur are still uncertain. There is

evidence to suggest that the primary event in cold sensing is a change in membrane fluidity, as the fluidity of lipid membranes is known to decrease with decreasing temperature (Cossins 1994). Genetic and chemical alterations to membrane fluidity in cyanobacteria and plants respectively resulted in defects in cold-induced gene expression, suggesting fluidity plays an essential role in cold signalling (Orvar *et al.* 2000; Inaba *et al.* 2003). It has been hypothesised that a physical phase transition of the membrane from a liquid-crystal to a gel in response to a decrease in temperature may induce a conformational change in a hypothetical temperature sensor within the membrane (Murata & Los 1997). In animals, it has been shown that potassium channels are necessary for sensing temperature (Peier *et al.* 2002), although no conserved relatives of these proteins have been found in plants. It has been suggested that Ca^{2+} channels may play a role in temperature sensing, although no such channel has yet been identified (Knight & Knight 2012). However, there is ample evidence for this in that exposure of plants to low temperatures has been shown to result in an increase in cytosolic free Ca^{2+} concentration (Knight *et al.* 1991; Knight, Trewavas & Knighta 1996; Monroy & Dhindsa 1995), which is blocked by the addition of Ca^{2+} chelators or channel blockers (Monroy & Dhindsa 1995). This Ca^{2+} influx has been suggested to lead to depolarisation of the membrane (Lewis & Spalding 1998), and the degree of Ca^{2+} influx and depolarisation is dependent on the degree and rate of cooling (Plieth 1999). Research has shown that the cytoskeleton may also be involved downstream of perception but upstream of cytosolic Ca^{2+} influx, as the destabilisation of actin filaments resulted in cold-induced gene expression without the need for exposure to cold (Orvar *et al.* 2000). More evidence is required to ascertain the precise mechanism via which plants perceive cold, but this research suggests that membrane fluidity and Ca^{2+} signalling are likely early signalling events leading to downstream alterations to gene expression.

1.2.2 The CBF pathway

The most well studied pathway initialised during cold acclimation is that of the CBF (C-repeat/DRE Binding Factor) transcription factors (see Figure 1.2). These factors activate the expression of *COR* (Cold on Regulated) genes, which have roles in cold acclimation. These *COR* genes contain a specific DNA motif in their promotor region designated the CRT/DRE (C-Repeat/Drought Responsive Element) (Yamaguchi-Shinozaki & Shinozaki 1994), that was found to activate genes associated with cold acclimation (Jaglo-Ottosen *et al.* 1998; Liu *et al.* 1998). The first transcription factor found to bind this motif was CBF1 (Stockinger, Gilmour & Thomashow 1997),

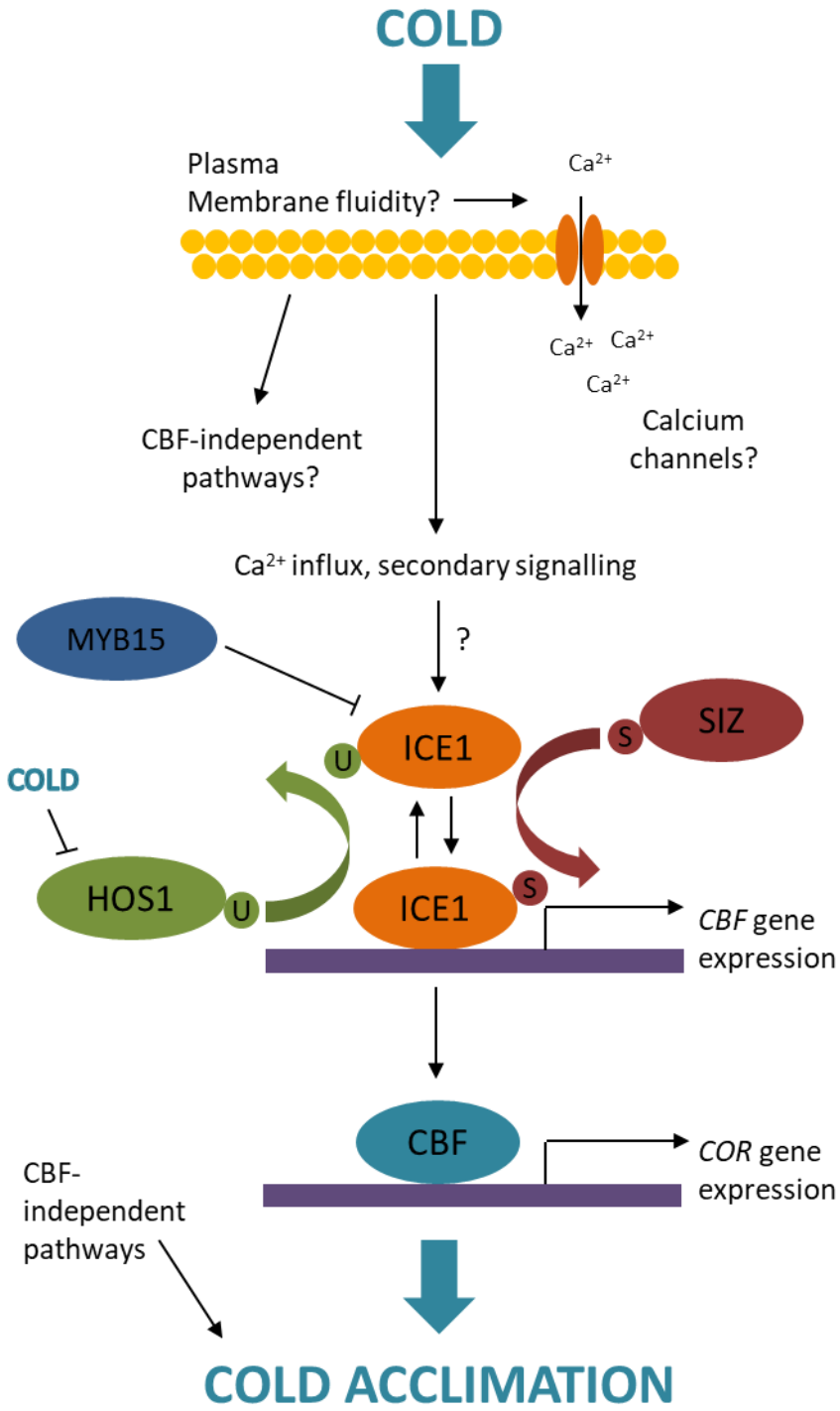

Figure 1.2: The CBF signalling pathway. Diagrammatic representation of the pathway leading to cold acclimation. CBF is used to denote CBFs 1, 2 and 3, SIZ is used to denote SIZ1 and 2. U stands for ubiquitin, S stands for SUMO.

which when overexpressed in *Arabidopsis* was found to confer freezing tolerance in non-acclimated plants (Jaglo-Ottosen *et al.* 1998).

It was later discovered that *CBF1* was only one of a small gene family of closely related transcription factors involved in freezing tolerance. These genes are denoted *CBF1, 2* and *3* or *DREB1B, 1C* and *1A* respectively and are physically linked on chromosome 4 of *Arabidopsis* (Gilmour *et al.* 1998; Liu *et al.* 1998; Shinwari *et al.* 1998). Evidence gathered from studying the overexpression of the three genes suggested that *CBF1, 2* and *3* play functionally redundant roles during cold acclimation (Gilmour, Fowler & Thomashow 2004). More recently it was shown that *CBF2* in particular may have a slightly different role than *CBF1* and *3* (Novillo, Medina & Salinas 2007). This is highlighted by the finding that CBF2 has been shown to regulate *CBF1* and *3* (Novillo *et al.* 2004), as well as the fact that analysis of single, double and triple *cbf* mutants suggest that CBF2 is the more important of the three (Zhao *et al.* 2016). Nevertheless, *CBF* expression is essential for full *COR* gene expression, as shown by the loss of *COR* gene expression despite exposure to cold in a mutant that had decreased activation of CBF proteins, possibly due to the loss of post-transcriptional regulation of CBFs (Knight *et al.* 1999, 2009).

Expression of the *CBF* genes themselves is positively regulated by the transcription factors ICE1 and ICE2 (inducer of CBF expression) (Zarka *et al.* 2003), which are also regulated by post translational modification. ICE1 is ubiquitinated by the E3 ligase HOS1 (high expression of osmotically responsive gene) resulting in the degradation of ICE1 under ambient conditions (Dong *et al.* 2006). ICE1 is also sumoylated by the SUMO (small ubiquitin-related modifier) E3 ligase SIZ1 (sap/miz) which confers stabilization of ICE1 (Miura *et al.* 2007), allowing binding to *CBF* promotors and consequent transcription leading to cold acclimation. Negative regulation of CBFs is achieved through the transcription factor MYB15, which binds to MYB-recognition sites in the promotors of *CBF* genes, as well as interacting with ICE1, possibly as a further control for the regulation of *CBF* expression (Agarwal *et al.* 2006). The CBF proteins themselves accumulate at low temperatures, but are very unstable at ambient temperatures suggesting aberrant expression of *COR* genes cannot take place above a certain temperature (Zarka *et al.* 2003).

Calcium has also been shown to be essential for *COR* gene expression, as described in section 1.2.1. Treatment of plants with Ca^{2+}-chelators was found to inhibit the expression of *COR* genes in *Arabidopsis* (Knight *et al.* 1996; Tahtiharju *et al.* 1997) and *CAS* (cold-acclimation specific) genes in Alfalfa (Monroy & Dhindsa 1995). It is unclear from this at what point Ca^{2+} is involved in the cold-acclimation pathway, although more recent research has suggested that Ca^{2+} is also

important downstream of cold-perception, with evidence suggesting that Ca^{2+} regulates *COR* gene expression via the CRT/DRE promotor motif (Whalley *et al.* 2011). The induction of *CBF* genes is also gated by the circadian clock; the extent to which *CBF* genes are expressed during cold exposure was found to be dependent upon the time of day (Fowler, Cook & Thomashow 2005), and in mutants deficient in two core clock genes, cold-induction of *CBF* genes was greatly diminished (Dong, Farré & Thomashow 2011). This suggests that there are various levels of regulation of the *CBF* pathway. This tight regulation of the pathway is necessary for growth, as overexpression of *CBF* genes in *Arabidopsis* was shown to result in a severe dwarf phenotype (Liu *et al.* 1998; Oakenfull, Baxter & Knight 2013). This is due to the fact that CBF1 reduces the amount of the plant hormone gibberellin, thus enhancing the accumulation of DELLA proteins which repress growth (Achard *et al.* 2008). Cold acclimation has also been shown to lead to the down-regulation of many growth- and hormone-related genes such as auxin-, gibberellin- and brassinosteroid-induced or responsive genes, which is likely related to the decrease in growth observed in plants exposed to low temperatures (Hannah, Heyer & Hincha 2005). The plant hormone ABA (abscisic acid) also plays a role in the perception and responses to abiotic stress (Gusta, Trischuk & Weiser 2005; Penfield 2008) and has been shown to induce an increase in the expression of *CBF1* (Knight *et al.* 2004).

1.2.3 CBF-independent pathways

Recent research into the targets of *CBF* genes has shown that approximately 414 genes are up-regulated and 68 down-regulated by the CBF transcription factors (Zhao *et al.* 2016). This number is much lower than the total number of genes differentially expressed by cold exposure, which is likely to be in excess of 10,000 (Hannah *et al.* 2005). This comparison highlights the fact that the CBF-regulon is not the sole pathway induced during cold acclimation for the acquisition of freezing tolerance. Some examples include the plant transcription factor ESK1 (eskimo1). Mutants of *esk1* are constitutively freezing tolerant (Xin & Browse 1998), and display altered expression of genes involved in abiotic stress responses that have little overlap with genes induced by CBFs. These results suggest that ESK1 is a negative regulator of cold acclimation (Xin *et al.* 2007). Another gene, *HOS9* (*high expression of osmotically responsive genes9*), a constitutively expressed homeodomain transcription factor, was shown to regulate genes that were not induced by CBFs (Zhu *et al.* 2004). These examples highlight the fact that there are several pathways that regulate the response to cold and thus freezing tolerance.

1.2.4 Cellular targets of cold acclimation

1.2.4.1 Lipid Membranes

As described in section 1.1.2, one of the most frequent sites of injury during freezing is the plasma membrane, brought about by freeze-induced dehydration. Thus, a key step during cold acclimation is to stabilise membranes to prevent damage from dehydration (Thomashow 1999). A process via which this is achieved is through alterations to the lipid composition of the membrane, observed in several different species including *Arabidopsis* (Lynch & Steponkus 1987; Yoshida & Uemura 1990; Uemura, Joseph & Steponkus 1995; Uemura *et al.* 2006). Cold acclimation induces an increase in the proportion of phospholipids within the membrane, a decrease in the proportion of free sterols and an increase in the proportion of di-unsaturated species (Uemura *et al.* 1995). It was observed that the formation of endocytotic vesicles did not occur during freeze-induced dehydration of acclimated cells, and instead the membrane formed exocytotic extrusions, meaning that the surface area of the membrane was conserved, and expansion-induce lysis did not occur in acclimated plants. This is believed to be associated with a higher proportion of phosphatidylcholine within the membrane (Gordon-Kamm & Steponkus 1984b). The formation of lamellar-to-hexagonal-II phases transitions was also not observed in acclimated protoplasts (Gordon-Kamm & Steponkus 1984a), possibly as a result of an increase in the proportion of highly hydrated lipid classes to increase bilayer hydration and maintain bilayer separation (Uemura *et al.* 1995). Injury to membranes can still occur in acclimated cells and is believed to be associated with 'fracture-jump-lesions' which is as a result of the formation of interlamellar attachments or the fusion of the plasma membrane with other endomembranes (Uemura *et al.* 1995).

Changes in lipid composition are key to preventing membrane damage during freeze-induced dehydration, but other mechanisms are also used to protect the membrane during freezing. The accumulation of sucrose and other simple sugars occurs during cold acclimation of *Arabidopsis* plants (Wanner & Junttila 1999). Sucrose has been shown to protect membranes during freeze-thawing, possibly by binding to the membrane or affecting adjacent water structure, and ultimately preventing membrane fusion and subsequent injury (Strauss & Hauser 1986). Other solutes such as proline and trehalose have also been shown to play a role in the maintenance of membrane integrity after freezing (Rudolph & Crowe 1985).

Many cold-induced *COR* genes encode hydrophilic polypeptides that play a role in mitigating injury due to freeze-induced dehydration (Thomashow 1998). An example of one of these genes

that has been found to contribute directly to membrane stabilisation during freezing is *COR15a*, a chloroplast stroma-localised protein which when constitutively expressed results in increased freezing tolerance of non-acclimated chloroplasts and protoplasts (Artus *et al.* 1996). This is believed to occur through the decrease in the incidence of lamellar-to-hexagonal-II phase transitions by the alteration of the intrinsic curvature of the chloroplast inner membrane by COR15am (Steponkus *et al.* 1998). Other proteins induced during cold acclimation also function to protect thylakoid membranes during freeze-thaw cycles by reducing membrane permeability during freezing and increasing membrane expandability during thawing (Hincha, Heber & Schmitt 1990). For example, SFR2 is a galactolipid remodelling enzyme of the outer chloroplast membrane that stabilises membranes during freezing events (Moellering, Muthan & Benning 2010). This gene was discovered after a screen of EMS-mutagenized plants was carried out to find mutants that were *sensitive to freezing* (see section 3.1) (Warren *et al.* 1996a).

1.2.4.2 Other cellular components

Other injury-reducing mechanisms are induced during cold acclimation besides those that prevent membrane damage. Analysis has shown that a multigene family of *HSP70* (heat shock protein 70) genes is induced during cold acclimation (Guy & Li 1998). These function as molecular chaperones and have been shown to interact with proteins in order to prevent denaturation (Guy *et al.* 1998). The damaging effects of reactive oxygen species are also reduced after cold acclimation by the expression of enzymatic scavengers such as superoxide dismutase (Mckersie *et al.* 1993) and ascorbate peroxidase (Tao, Oquist & Wingsle 1998).

An increased level of sugars such as sucrose, fructose and glucose observed within the apoplast after cold acclimation (Livingston III & Henson 1998) may function to protect membranes against ice adhesions. Anti-freeze proteins (AFPs), also known as ice-binding proteins (IBPs) (Thomashow 1998; Bredow & Walker 2017) have also been shown to accumulate within the apoplast during cold acclimation (Griffith *et al.* 1992; Zhang 2009). IPBs have a high structural and functional diversity (Bar Dolev, Braslavsky & Davies 2016) and evidence suggests that they reduce the temperature at which ice forms by adsorbing to the surface of ice nuclei and inhibiting growth, possibly by preventing the aggregation of water molecules (Griffith *et al.* 2005). It has only very recently been confirmed that AFPs are important for plant freezing tolerance through the observation that knockdown of AFPs results in an increase of freezing damage (Bredow, Vanderbeld & Walker 2016), and the expression of more than one isoform of

AFP expressed in *Arabidopsis* was found to increase freezing tolerance (Bredow, Vanderbeld & Walker 2017).

1.3 The Plant Cell Wall

It was not until many years after Robert Hooke's first observations of living plant cells (Hooke 1665) that the cell wall was considered a dynamic mosaic of diverse form and function rather than a simple static structure. Since then, major discoveries in the components and growth of the cell wall have led to models considering the wall to be a three-dimensional continuous matrix surrounding plant protoplasts (McNeil *et al.* 1984; Carpita & Gibeaut 1993; Cosgrove 1993; Höfte & Voxeur 2017). The plant cell wall plays key roles in structural integrity, strength, cell growth, cell differentiation, intercellular communication, water movement and pathogen defence (Cosgrove 2005), as well as more recently discovered roles in abiotic stress tolerance (Houston *et al.* 2016). It is essential for plant life, and the ability to carry out these roles is through its complex polysaccharide structure.

1.3.1 Structure of the plant cell wall

There are generally considered to be two types of cell wall in flowering plants; the type I cell wall of dicots and some monocot families, and type II cell walls present in Poaceae and other monocot families, which differ slightly in polysaccharide composition and structure (Carpita & Gibeaut 1993). This study will focus mainly on the structure of type I cell walls as this is more relevant to the dicots studied and researched here, although the stress responses of monocot cell walls will also be discussed.

In growing cells, the wall is a thin flexible layer between 0.1 and 1 µm thick comprising of a mixture of fibrous polysaccharides and structural proteins (Cosgrove 2005). The wall is typically made of three distinct sections identified via their polysaccharide composition; the primary cell wall (PCW), the secondary cell wall (SCW) and the middle lamella (ML). The PCW and the ML are secreted from the cell first, with the SCW normally being secreted after growth ceases and is usually only present in cells that require structural reinforcement such as xylem (Clarke 1938). The PCW is made up of a fibrous network of cellulose microfibrils embedded in a matrix of pectin and hemicellulosic polysaccharides as well as some protein. The ML is a shared layer of wall rich in pectins that connects two cells together (Brett & Waldron 1996). See figure 1.3 for a simplified model of the primary plant cell wall.

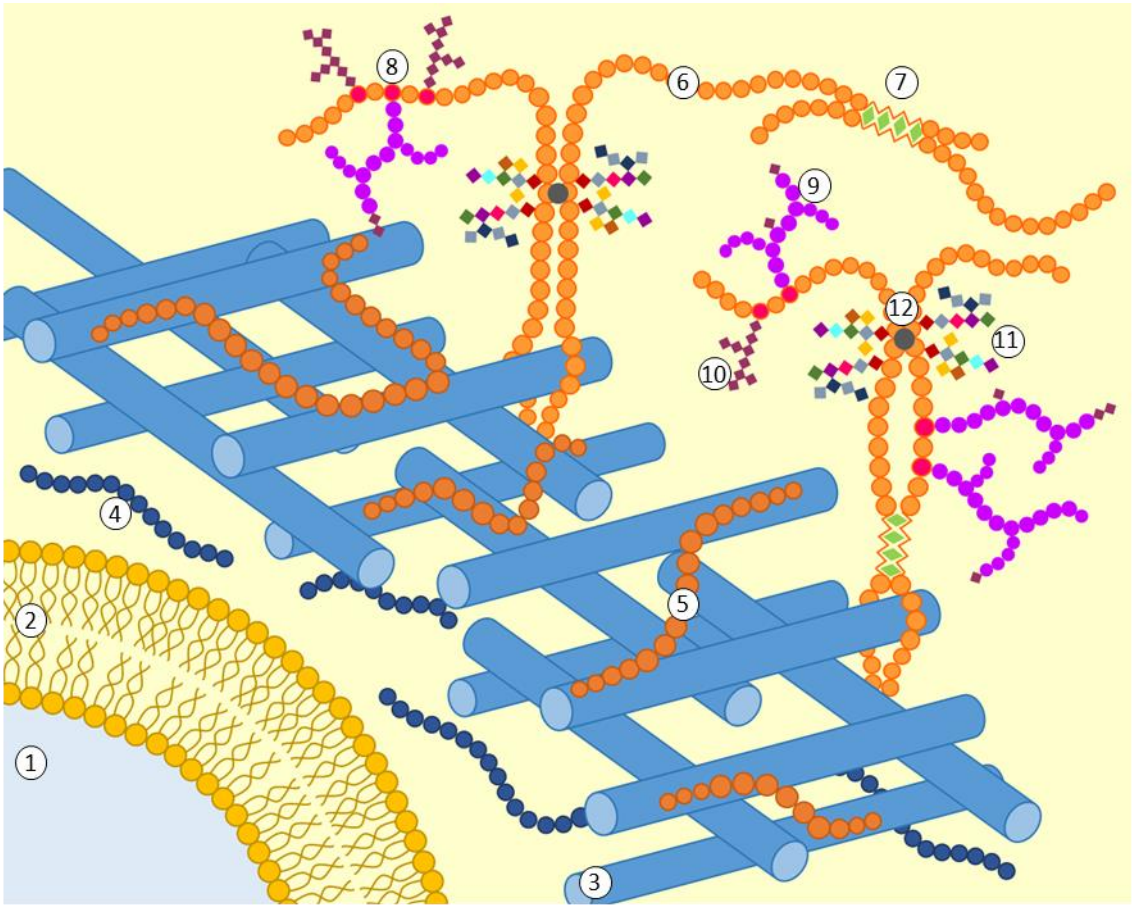

Figure 1.3: Polysaccharide composition of the primary plant cell wall. Diagrammatic representation of the primary plant cell wall. Components are labelled as follows; 1, cytosol; 2, lipid membrane; 3, cellulose microfibrils; 4, ;5, hemicellulose e.g. xyloglucan; 6, homogalacturonan; 7, calcium 'egg-box' cross-links; 8, rhamnogalacturonan-I; 9, galactan; 10, arabinan; 11, rhamnogalacturonan-II; 12, borate-ester cross-link. Adapted from Frankova and Fry (2013).

1.3.2 Growth of the cell wall

The ability for plant cell walls to expand is driven by wall stress relaxation, which relies on wall loosening (Ray, Green & Cleland 1972; Cosgrove 1993; Ortega 2017). This process allows the irreversible extension of the cell wall, often referred to as 'creep' (Cosgrove 2016a). It also relies on cell turgor pressure; during cell growth, cell volume increases as a result of water uptake resulting in an increase in wall surface area by the separation of cell wall components (Ray *et al.* 1972; Cosgrove 2016b). Cell growth is possible through the action of wall loosening enzymes such as expansins, endoglucanases, endotransglucosylases and pectin methyl-esterases (see section 1.3.4.1) (Cosgrove 2016a). Extension is also mediated by changes in cell wall pH, which is known to modulate the action of expansins (Cosgrove 2015); cell walls extend under acidic conditions, a process that supports the acid-growth hypothesis of auxin-induced elongation (Rayle & Cleland 1992). Cell growth can only occur under conditions of wall-loosening coupled with the action of wall deposition, otherwise the cell wall becomes thin, thus polysaccharide synthesis mechanisms are closely correlated to wall loosening (Refregier *et al.* 2004). It is believed that the cytoskeleton also plays a role in guiding wall machinery to supply cell-wall components at relevant locations in the cell (Szymanski & Cosgrove 2009).

1.3.3 The cellulose-hemicellulosic framework

1.3.3.1 Structure

Cellulose is common to most cell walls and makes up approximately 20-30% of the dry mass of PCWs (McNeil *et al.* 1984). Cellulose is an unbranched chain of β1,4-D-glucan sugars (Gardner & Blackwell 1974), with a degree of polymerisation as high as 15,000 subunits in SCW (Marx-Figini 1966), although PCWs have a slightly lower degree of polymerisation (Spencer & Maclachlan 1972). Between 30 and 100 cellulose chains come together to form a microfibril which can wind around the circumference of the cell many times in a perpendicular orientation to the axis of growth of the cell. This led to the view that cellulose could actually determine the axis of growth (McNeil *et al.* 1984). However, it has been shown in onion epidermal cells that the cell wall consists of layers of lamellae, in which microfibril organisation shifts by 30° to 90° between lamella, suggesting there are microfibrils with different organisations within the cell wall (Zhang, Zheng & Cosgrove 2016b). Recent work using atomic force microscopy (AFM) has visualised an alteration of microfibrillar connectivity during wall loosening suggesting dynamic movements of microfibrils are required for wall extension (Zhang *et al.* 2017). Microfibrils also form cellulose-

cellulose associations that may be mediated by hydrophilic or hydrophobic faces. These two faces may also facilitate interaction with other cell-wall polysaccharides (Cosgrove 2018).

The cellulose chains form a crystalline structure that contributes considerably to cell wall strength (Cosgrove 2005). This network is strengthened further via the cross-linking of microfibrils by polysaccharides known as hemicelluloses (see Figure 1.3). Hemicelluloses vary greatly in structure between species and even cell types, and the hemicellulosic fraction can consist of xyloglucans, xylans, mannans, mixed-link glucans and arabinogalactan-II among others (Brett & Waldron 1996). Xylan and arabinoxylan are the major hemicelluloses present in monocot cell walls (Burke *et al.* 1974), whereas xyloglucan is the main hemicellulosic constituent of dicots, comprising approximately 20-25% of the primary walls of sycamore cell cultures (McNeil *et al.* 1984), and approximately 20% in *Arabidopsis* (Zablackis *et al.* 1995). Xyloglucan consists of a backbone of β-1,4-linked glucose residues, to which various amounts of D-xylose, D-galactose and L-fucose are attached (Hayashi 1989). Xyloglucan chains have been shown to form hydrogen bonds with cellulose fibres, and can bridge cellulose microfibrils to form a strongly tethered network (Mccann, Wells & Roberts 1990). The substitution of different sugar side chains on the backbone of xyloglucan is believed to affect conformation and hence the ability to cross-link to cellulose (Levy, Maclachlan & Staehelin 1997).

1.3.3.2 Synthesis

Cellulose forms the main structural component of the cell wall and is synthesised at the plasma membrane by large cellulose synthase complexes (Arioli *et al.* 1998; Kimura *et al.* 1999). These complexes are formed into hexameric rosettes of different combinations of CESA subunits, each containing six CESA proteins (Doblin *et al.* 2002). There are currently ten known *CESA* genes in *Arabidopsis*, although there is evidence that there may be more, and that other proteins may also form part of the cellulose synthase complex (Richmond & Somerville 2000). Different combinations of CESA subunits are required for synthesis of the primary and secondary cell walls, for example it has been shown that CES4, 7 and 8 are required for the formation of secondary walls in developing xylem tissue (Gardiner, Taylor & Turner 2003). Each CESA protein synthesises one β-1,4-glucan chain which through bundling and crystallisation form into a cellulose microfibril of many chains (Doblin *et al.* 2002; Li *et al.* 2016a).

CESA genes belong to a larger superfamily of genes known as *cellulose synthase-like* (*CSL*), which is made up of eight other families of structurally related genes believed to be localised to the

Golgi (Richmond & Somerville 2000). Some of these proteins have been shown to be involved in the synthesis of the β-D-glycan backbone of hemicelluloses (Pauly *et al.* 2013). Xyloglucan synthesis, like many other non-cellulosic polysaccharides, has been localised to the Golgi (Moore & Staehelin 1988), where it is synthesised by proteins encoded by one or more members of the *CSLC* family of genes (Cocuron *et al.* 2007; Pauly *et al.* 2013). Activated nucleotide sugars are transferred to the backbone via the activity of enzymes such as xylosyltransferases (XT) (Pauly & Keegstra 2016) and fucosyltransferases (FUT) (Perrin 2003) which may form complexes with CSL proteins (Chou, Pogorelko & Zabotina 2012). Once deposited into the cell wall via vesicle transport, xyloglucan can associate with cellulose microfibrils (Hayashi, Marsden & Delmer 1987).

1.3.4 The pectin matrix

1.3.4.1 Structure

Pectic polysaccharides are rich in galacturonic acid (GalA), rhamnose (Rha), arabinose (Ara) and galactose (Gal), and along with hemicellulose they form the matrix component of the cell wall. They are found in the PCW of dicots and to a lesser extent in monocots and make up a large proportion of the ML in dicots. This group of polysaccharides is structurally diverse and is composed of homogalacturonan (HG), rhamnogalacturonan-I (RG-I) and rhamnogalacturonan-II (RG-II) as well as arabinans, galactans and arabinogalactans. Pectins are generally considered to form covalent links with each other, resulting in the formation of the complex structure of the cell wall (Jarvis 1984; Brett & Waldron 1996; Mohnen 2008; Caffall & Mohnen 2009) (see Figure 1.3). Pectins may also form non-covalent interactions with cellulose, although the evidence for this is still debated and may depend on growth status (Phyo *et al.* 2017).

HG linear polymers of α-1,4-linked-D-GalA residues make up approximately 65% of cell wall pectin (Caffall & Mohnen 2009), and approximately 23% of the *Arabidopsis* PCW (Zablackis *et al.* 1995). HG chains of up to 100 GalA residues have been found to form (Yapo *et al.* 2007), and these chains can be modified by the addition or removal of *O*-methyl and *O*-acetyl esters via the activity of pectin methyl-esterase (PME) (Pelloux, Rustérucci & Mellerowicz 2007) and pectin acetyl-esterase (PAE) (Philippe, Pelloux & Rayon 2017) enzymes respectively. The de-methyl-esterification of HG chains is generally believed to be associated with a cessation in growth (Goldberg & Prat 1982; Goldberg, Morvan & Roland 1986), as these regions form associations with other HG chains via Ca^{2+} ions to form so called 'egg-box' structures (Jarvis 1984). The use

of antibodies targeted towards areas of different levels of HG esterification have shown that HG in the ML is relatively un-esterified and could play a role in cell-cell adhesion (Willats *et al.* 2001).

RG-I is made up of a backbone of the disaccharide repeat [-α-D-GalA-1,2-α-L-Rha-1,4-] (Lau *et al.* 1985) with side chains of linear or branched α-L-arabinofuranosyl (Ara*f*) or β-D-galactopyranosyl (Gal*p*) residues, as well as other glycosyl residues, on 20-80% of the rhamnosyl residues dependent on species and cell type (Ridley, O'Neill & Mohnen 2001). RG-I represents approximately 20-35% of the pectin cell wall content, and makes up 11% of *Arabidopsis* PCW (Zablackis *et al.* 1995). RG-II, although similarly named, is structurally very different from RG-I. It represents approximately 10% of cell-wall pectin (O'Neill *et al.* 2004) and makes up 8% of the *Arabidopsis* primary cell wall (Zablackis *et al.* 1995). RG-II has a backbone of α-1,4-linked-D-GalA residues and is composed of many different sugars that make it the most structurally complex of the pectic polysaccharides (Darvill, McNeil & Albersheim 1978a). The structure of RG-II is shown in Figure 1.4 and will be discussed further in section 1.4.2.

It is generally believed that HG, RG-I and RG-II are all covalently cross-linked within the cell wall, since enzyme digestion is required to separate out the distinct domains (Ishii & Matsunaga 2001; Akamura *et al.* 2002). The model of current consensus suggests that the backbones of HG, RG-I and RG-II are continuous, thus pectin can be visualised as a tethered network with domains of HG, RG-I and RG-II (Caffall & Mohnen 2009; Franková & Fry 2013). There is also evidence that the pectic polysaccharides are covalently linked to or certainly associated with, other cell wall polysaccharides such as xyloglucans and xylans (Popper & Fry 2008). Figure 1.3 demonstrates the possible linkages formed between cell wall polysaccharides and highlights a model for the dynamic network formed.

1.3.4.2 Synthesis

Like hemicelluloses, pectins are synthesised in the Golgi, packed into vesicles and deposited in the apoplastic space (Zhang & Staehelin 1992). Many glycosyltransferases are required for pectin synthesis, which rely on the activity of nucleotide sugar interconverting enzymes which provide activated sugars (see Caffall & Mohnen (2009) for a list of glycosyltransferases and sugar synthesis enzymes). One example of an α-1,4-galactosyltransferase (GalAT) involved in the synthesis of HG chains is GAUT1 (Sterling *et al.* 2006) which transfers GalA from UDP-GalA onto endogenous acceptors in the Golgi (Sterling *et al.* 2018). *GAUT1* was found to form part of a bigger family of *GalAT* genes named *GalAT-like* (*GATL*), with mutants of these genes having a

significant reduction of GalA in cell walls (Sterling *et al.* 2006). RG-II synthesis is known to be much more complex, and only a handful of genes involved in RG-II-specific synthesis have currently been identified, namely genes *RGXT1-4,* which encode Golgi localised xylosyltransferases (Egelund *et al.* 2006, 2008; Petersen *et al.* 2009). Interestingly, it has been shown that polysaccharides can move a reasonable distance into the cell wall, a process driven by turgor pressure (Proseus & Boyer 2005)

1.3.5 Cell wall proteins

1.3.5.1 Extensins

Many of the proteins present in the cell wall are glycoproteins (Showalter 1993). One of the most well studied families of these glycoproteins are the hydroxy-proline rich extensins which are the major structural protein found in the cell wall (Carpita & Gibeaut 1993). An increased content of extensin within the wall is generally correlated with the cessation of growth (Sadava, Walker & Chrispeels 1973), and it is thought that binding of extensin to cellulose facilitates the 'locking' of microfibrils (Carpita & Gibeaut 1993).

1.3.5.2 Cell-wall modifying enzymes

As stated in section 1.3.2, cell walls can only grow after stress relaxation which requires the activity of wall loosening enzymes. The most common enzymes for wall loosening are the expansins (Cosgrove 2015). Plants contain two classes of expansins, α-expansin (EXPA) and β-expansin (EXPB), and their expression is closely correlated with wall expansion (Cosgrove 2000). Expansins have been shown to loosen the cell wall to allow growth, without impacting on wall strength, suggesting that they do not cut linkages (Yuan 2001). Expansins are also found in bacteria, and much that is known about the activity of expansins comes from the study of these proteins (Georgelis, Nikolaidis & Cosgrove 2015). The ability of expansins to facilitate wall loosening in believed to rely on interactions with cellulose microfibrils (Cosgrove 2015).

Xyloglucan endotransglycosylase (XTH) enzymes were also originally believed to be important for wall loosening (Fry *et al.* 1992). XTH enzymes cut xyloglucan chains and join the end onto that of another xyloglucan, or to water in a hydrolase activity (Cosgrove 2016a). *Arabidopsis* mutants of *xth* knock-outs eliminated hydrolase activity, but did not result in any discernible phenotype, suggesting that XTH enzymes are not imperative for growth (Kaewthai *et al.* 2013).

1.3.5.3 Pectin-modifying enzymes

Pectins are excreted into the apoplast in a highly methyl-esterified form (Lennon & Lord 2000) due to the action of pectin methyltransferases (PMTs) in the Golgi which are necessary for pectin biosynthesis (Caffall & Mohnen 2009). Pectin acetyltransferases transfer acetyl groups onto the backbone of HG and RG-I and on side chains of RG-II (Whitcombe *et al.* 1995; Ishii 1997). Once inside the cell wall, pectins are subject to modification by PMEs which remove methyl esters and affect the patterning of pectin methyl-esterification within the wall (Willats *et al.* 2001). *PME*s and *PME inhibitors* (*PMEI*s) belong to large multigene families which is likely to reflect the diversity of their role in cell-wall modification suggesting pectin de-methylation is a tightly controlled process (Pelloux *et al.* 2007). The activity of polygalacturonase (PG) enzymes is also believed to regulate plant development, and are particularly expressed during fruit ripening and at abscission zones highlighting their role of pectin disassembly (Hadfield & Bennett 1998).

1.3.6 The secondary cell wall

The SCW is not synthesised in all cells but is restricted to those that are no longer expanding and require supplementary strength such as sclerenchyma, tracheids and xylem vessels (Meents, Watanabe & Samuels 2018). Cellulose makes up approximately 60% of the SCW, and is structurally different from PCW cellulose due to a higher degree of crystallinity and polymerisation, resulting in microfibrils that are stronger and more rigid (McNeil *et al.* 1984). Hemicelluloses make up from 10 to 40% of the SCW dependent on species and cell type but are typically found to be xylan and mannans (Scheller & Ulvskov 2010). The final major component of SCWs is lignin comprising approximately 30% of woody cell wall biomass (Campbell & Sederoff 1996). Lignin is a heteropolymer of 4-hydroxyphenylpropanoids, which forms when three monolignols are oxidised to monolignol radicals and undergo coupling within the SCW. Monolignols are synthesised in the cytosol and excreted into the cell wall, where oxidative enzymes such as laccases and peroxidases carry out the lignification process (Meents *et al.* 2018). The shift from primary to secondary wall biosynthesis requires a remodelling of biosynthetic machinery, which switch to polysaccharide synthesis for the secondary wall, followed by lignification and often programmed cell death (Taylor-Teeples *et al.* 2015).

1.4 The use of mutants to elucidate cell wall polysaccharide function

1.4.1 The mur1 *mutant*

An EMS screen was carried out to find mutants in order to elucidate individual roles of cell wall polysaccharides. As elimination of particular cell wall polysaccharides would likely result in unviability of plants, alterations to the composition of the polysaccharides via changes to monosaccharides was a viable method in order to study this (Reiter, Chapple & Somerville 1997). From this screen, a mutation at one locus in particular resulted in plants with a marked reduction in cell-wall fucose levels down to 2% in shoot extracts and 60% in root extracts compared to wild type (Reiter, Chapple & Somerville 1993). These mutants, designated *mur1*, displayed some interesting visible phenotypes such as dwarfism, a reduction in petiole and internode length and reduced apical dominance, traits that could be reversed when grown in the presence of L-fucose. Another interesting trait displayed by *mur1* mutants was the decrease in force necessary to break inflorescence stems, highlighting an impact upon the mechanical properties of the cell walls (Reiter *et al.* 1993). This trait was also shown by Ryden *et al*. (2003), a study in which the tensile modulus and tensile strength of *mur1* hypocotyls were shown to be reduced suggesting a decreased stiffness and strength of cell walls.

The *mur1* mutation was eventually mapped to a gene that encodes a GDP-D-mannose-4,6-dehydratase, *GMD2*, an enzyme involved in the first step of the *de novo* synthesis of GDP-L-fucose (Bonin *et al.* 1997). Interestingly, two genes in *Arabidopsis* with high sequence similarity were identified in this research, designated *GMD1* and *GMD2* which were found to be differentially expressed. *GMD1* expression was confined to certain areas of the root, as well as stipules and pollen grains, whereas *GMD2* (*MUR1*) was expressed in all other parts of the plant (Bonin *et al.* 2003). The genetic redundancy of these two genes would account for the higher level of fucose observed in the roots of *mur1* plants (Reiter *et al.* 1993).

Fucose is a constituent of several cell-wall components but is predominantly found in xyloglucans, rhamnogalacturonans-I and II (RG-I and RG-II) as well as some glycoproteins. Investigations into whether alterations to any specific polysaccharide resulted in the observed phenotypes were therefore carried out. A mutant that lacked fucose in glycoproteins displayed no physiological differences to wild type plants, suggesting glycoproteins were not the culprit (Reiter *et al.* 1993; von Schaewen *et al.* 1993). Similarly, a mutant of a xyloglucan-specific fucosyltransferase gene *mur2*, displayed none of the morphological phenotypes of *mur1* mutants, despite the fact that 75-80% of fucose residues are found in xyloglucans (Zablackis *et*

al. 1995; Reiter *et al.* 1997; Vanzin *et al.* 2002). In *mur1* mutants, it was found that the lost L-fucose residues were replaced by L-galactose (Zablackis *et al.* 1996), a substitution that was also made in RG-II domains (O'Neill *et al.* 2001; Reuhs *et al.* 2004).

1.4.2 The pectic polysaccharide rhamnogalacturonan-II (RG-II)

The pectic polysaccharide RG-II is the most complex glycan known and unlike any other cell wall components (Figure 1.4A) (Darvill, McNeil & Albersheim 1978b). The latest research suggests it is formed of six side chains (A-F) that branch from a homogalacturonan chain that acts as the backbone (Ndeh *et al.* 2017). These side chains are made up of 13 different monosaccharides and 21 different glycosidic bonds that link them together to form the side chains (Stevenson, Darvill & Albersheim 1988; Pellerin *et al.* 1996; Ndeh *et al.* 2017). These sugars comprise mainly rhamnose, arabinose and galactose, but also comprise some rarer sugars such as apiose, aceric acid and 3-deoxy-manno-octulosonic acid (KDO), as well as methylated sugars (Darvill *et al.* 1978a). The backbone can comprise between 7 and 11 1,4-linked-α-D-galactosyluronic acid residues of the HG chains, dependent upon species (Whitcombe *et al.* 1995). The overall structure of RG-II is generally conserved throughout several plant kingdoms including dicots, monocots, gymnosperms, pteridophytes, bryophytes and lycophytes (Stevenson *et al.* 1988; Thomas, Darvill & Albersheim 1989; Kaneko, Ishii & Matsunaga 1997; Matsunaga *et al.* 2004), although there are slight variations in monosaccharides and methylation between species (Pabst *et al.* 2013). This conservation suggests a fundamental role within the cell wall.

An interesting structural aspect of RG-II is that 95% of RG-II in plant cell walls exists as a dimer covalently cross-linked by a borate-ester (Kobayashi, Matoh & Azuma 1996; O'Neill *et al.* 1996, 2001). The occurrence of this cross-link, like the structure of RG-II, is conserved across the plant kingdom (Matoh, Kawaguchi & Kobayashi 1996; Kaneko *et al.* 1997). The borate ester forms between two carbon atoms in D-apiose residues of side chain A of two RG-II domains (O'Neill *et al.* 1996; Pellerin *et al.* 1996; Ishii *et al.* 1999). The borate ester forms only on the more stable side chain A, not on the other apiosyl residue present on side chain B, which could contribute to the stability of the dimer and influence mechanics of the cell wall (Figure 1.4B) (Mazeau & Perez 1998; Ishii *et al.* 1999). Formation of the dimer is highly influenced by pH, as is the structure of the cell wall in general, with formation occurring far more quickly around pH 3.5 and the dimer being more stable at around pH 4. The amount of dimer formed *in vitro* was also shown to increase in the presence of large cations, such as strontium, lead and barium under cell wall pH conditions (pH 4.8-5.5), or with very high Ca^{2+} concentrations (O'Neill *et al.* 1996; Chormova &

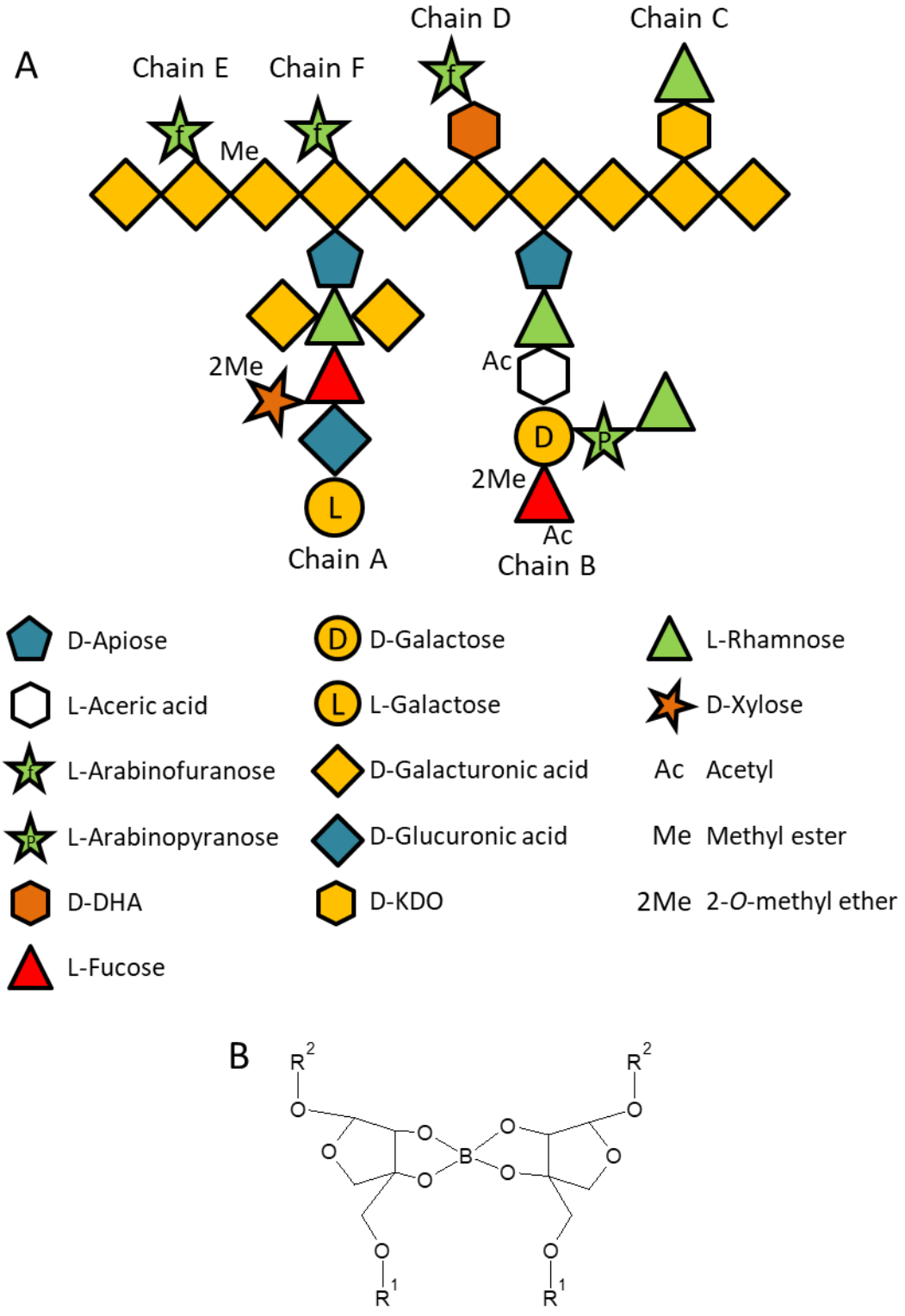

Figure 1.4: Structure of *Arabidopsis* rhamnogalacturonan-II. A) Structural representation of *Arabidopsis thaliana* rhamnogalacturonan-II (RG-II) showing sugar residue composition. Adapted from Sachet *et al*. (2018). **B**) Representation of the borate ester cross-link that forms between the D-apiose residue of side chain A between two RG-II domains. Orientation of RG-II is shown parallel, but chains may run anti-parallel.

Fry 2016). These ions were also found to bind and form complexes with dimeric RG-II, but not monomeric RG-II (O'Neill *et al.* 1996).

There is also evidence that *in vivo* formation of the dimer requires an enzymatic catalyst, as *in vitro* studies suggest formation in the absence of a catalyst is too slow to account for rapid wall expansion (O'Neill *et al.* 1996). Biological agents such as polyhistidine and wall glycoproteins have the ability to promote RG-II dimerisation. These agents could act catalytically to manoeuvre RG-II molecules into a position such that boron cross-linking is favourable (Chormova & Fry 2016). Although the exact mechanism for how this is achieved is not yet known, research suggests that membrane bound lipids such as GIPCs may be involved (Voxeur & Fry 2014). It is also believed that the process of RG-II dimerisation may occur through the formation of intermediates (O'Neill *et al.* 1996; Chormova & Fry 2016). Recent evidence suggests that dimerisation occurs specifically during synthesis of the molecule before secretion into the apoplast, possibly in the Golgi or at the plasma membrane. RG-II monomers are not thought to be able to dimerise once secreted to the apoplast (Chormova, Messenger & Fry 2014a; b).

1.4.3 RG-II domains in mur1 *mutants*

Further investigation found that although wild type and *mur1-1* plants contained the same amount of RG-II in their cell walls, dimerisation was reduced from 95% to approximately 50% in *mur1-1* and *mur1-2* mutants (O'Neill *et al.* 2001). This suggested that a loss of fucose in the side chains of RG-II affected the ability to dimerise, an effect that the replacement of fucose with galactose was unable to overcome (O'Neill *et al.* 2001). Supplementing *mur1* mutant plants with L-fucose had the ability to restore RG-II cross-linking, providing further evidence that fucose is essential for dimerisation. RG-II from *mur1* plants was found to dimerise less rapidly, irrespective of the presence of cations, and stability of the molecule was also reduced (O'Neill *et al.* 2001). The authors suggest that hydrophobic interactions may have a role in the formation of the dimer as the only difference between L-fucose and L-galactose is the presence of a methyl group rather than a hydroxymethyl group. More recent evidence however, suggests that side chain A may actually be truncated due to the loss of L-fucose (Pabst *et al.* 2013). Interestingly, exogenous application of excess boric acid (BA) to *mur1-1* and *mur1-2* plants was also able to restore cell-wall RG-II dimerisation, as well as the dwarfism and shortened petiole phenotypes observed in untreated mutant plants (O'Neill *et al.* 2001). This effect was also seen in measurements of cell-wall strength, in which hypocotyls of *mur1-1* and *mur1-2* supplemented with BA had restored tensile modulus and strength comparable to that of wild type (Ryden *et al.* 2003). These findings

provide evidence that the decrease in RG-II dimerisation following the loss of fucose residues is a possible candidate for the various phenotypes observed in *mur1-1* mutants, especially as the majority of boron within the cell wall is found to be associated with RG-II domains (Matoh *et al.* 1996).

1.4.4 The role of boron within the cell wall

1.4.4.1 Boron transport

Boron is an essential nutrient for plants and is necessary for normal growth in many species (Warington 1923; Arnon & Stout 1939). The control of boron transport is essential to ensure the availability under low boron conditions, but also to prevent the detrimental effects of toxicity under high boron conditions (Camacho-cristóbal, Rexach & González-Fontes 2008). Research has highlighted several mechanisms via which boron is transported throughout the plant. At physiological pH, boron exists in the undissociated form of boric acid ($B(OH)_3$) that is soluble and permeable through lipid membranes (Raven 1980; Dordas, Chrispeels & Brown 2000). The passive entry of boron through roots is generally the most accepted route of boron uptake in higher plants (Brown & Hu 1993; Hu & Brown 1997). As well as diffusion through lipid bilayers, BA can also cross membranes passively through channels such as aquaporins (Dordas & Brown 2001).

The other mechanism via which boron is transported throughout the plant is through active transporters most likely driven by the concomitant movement of H^+ ions across the membrane (Reid 2014). Many of these dedicated boron-transport channels have been identified; in *Arabidopsis*, BOR1 was the first boron efflux-transporter described and was shown to be important for xylem loading under low boron conditions, being expressed in mature endodermal cells and root tip cells (Takano *et al.* 2002). BOR2 is a paralog of BOR1 but is more strongly expressed in epidermal cells of the root, suggesting complementary activity to BOR1 (Miwa *et al.* 2013). Interestingly, both of these efflux transporters are degraded under high boron conditions (Takano *et al.* 2005; Miwa *et al.* 2013). Other efflux transporters have also been described including BOR4, which is important for the export of boron from the root to the soil under high boron conditions (Miwa *et al.* 2007), and several other BOR transporters whose precise functions are not yet fully understood (Reid 2014). The expression of genes encoding several channels are also up-regulated under boron deficiency; NIP5;1 is necessary for boron uptake in the roots under boron-deficient conditions (Takano *et al.* 2006) and NIP6;1 is

potentially required for the normal distribution of BA in developing shoot tissues (Tanaka *et al.* 2008). Through the use of boron transporter mutants, it has been shown that the regulation of boron levels throughout the plant is necessary to prevent the damaging effects of both boron deficiency and toxicity.

1.4.4.2 Boron deficiency and toxicity

Boron deficiency can be exacerbated under conditions of high rainfall where boron is leached from the soil and results in a wide range of symptoms affecting crop yield and quality (Shorrocks 1997). Boron deficiency has been shown to result in decreased root growth, reduced leaf expansion, male sterility and possible abnormal growth of vascular tissues (Dell & Huang 1997). Boron deficiency has also been shown to affect the physical properties of the cell wall; rinsing of squash and bean roots in boron-free medium resulted in a decrease of cell-wall elastic modulus (Findeklee & Goldbach 1996); hypocotyls of boron-deficient squash were shown to have decreased extensibility, with typically more brittle and rigid tissues (Hu & Brown 1994); boron-deficient pumpkin cells had thickened cell walls concomitant with a reduction in RG-II dimerisation (Ishii, Matsunaga & Hayashi 2001a) and growth of *Chenopodium album* cells in boron-deficient medium resulted in cell walls that had decreased RG-II dimerisation and an increase in cell-wall pore size (Fleischer, Titel & Ehwald 1998; Fleischer, O'Neill & Ehwald 1999). These findings are consistent with the role of boron in cross-linking two domains of the cell-wall pectin RG-II (Kobayashi *et al.* 1996; O'Neill *et al.* 1996; Ishii *et al.* 1999). More recent research has shown that boron deficiency resulted in a decrease of pectin covalently attached to the cell wall, and significantly increased the relative amounts of hemicellulose and cellulose in leaves of orange plants (Liu *et al.* 2014). This could hint at a role for boron other than the cross-linking of RG-II domains, or particular secondary effects of the loss of RG-II dimerisation due to boron deficiency.

Indeed there are several other effects that result from boron deficiency including a decrease in plasma membrane-bound calcium and subsequent increase in apoplastic calcium content in roots and leaves of bean (Muhlung, Wimmer & Goldbach 1998), a reduction in the translocation of indole-acetic acid (IAA), possibly linked to alterations of IAA transport genes (Li *et al.* 2016b), and an increase in the amount of actin and tubulin detected in the cytoskeleton (Goldbach *et al.* 2001). It is possible that the consequences of boron deficiency may occur as secondary effects due to alterations to cell-wall architecture. However, it cannot be ruled out that boron may play

a more complex role than just cross-linking of RG-II, and there are hypotheses that boric acid may act as a signalling molecule (Goldbach *et al.* 2001; Redondo-Nieto *et al.* 2012).

As well as being detrimental to plants when deficient, boron can also have significant adverse effects on plants when present at high concentrations, which occurs especially in semi-arid regions where boron can accumulate (Nable, Banuelos & Paull 1997). Boron toxicity results in chlorosis and necrosis of leaves and a reduction in shoot and root growth, particularly in the younger expanding tissues such as the root tip (Reid *et al.* 2004). These damaging effects may occur as a result of the inhibition of cellular process, as toxicity has been linked to the accumulation of intracellular boron (Hayes & Reid 2004), although the exact mechanism via which boron toxicity occurs is yet to be elucidated (Reid *et al.* 2004).

1.5 Freezing tolerance and the cell wall

There is contradictory evidence as to the role the cell wall plays in plant freezing tolerance, particularly in studies investigating the freezing of protoplasts. Several studies have reported no difference in freezing tolerance between intact tissues and isolated protoplasts (Siminovitch 1979; Singh 1979). Other studies have suggested that the cell wall is actually detrimental during freezing events as protoplasts were found to have a higher freezing tolerance than intact cells (Tao, Li & Carter 1983; Murai & Yoshida 1998b). Nevertheless, there is increasing evidence to suggest that the cell wall is a necessary component for the acquisition of freezing tolerance, and could act as a barrier to ice nucleation (Ashworth & Abeles 1984) and growth of ice (Yamada *et al.* 2002).

1.5.1 Cell wall modifications during cold acclimation

There are several studies that show modifications occur to the cell wall during cold acclimation in a variety of different species. Cell wall thickness was found to increase in cold-hardened cells of puma rye (Huner *et al.* 1981), as well as in oilseed rape (Stefanowska *et al.* 1999), and was hypothesised to be associated with an increase in cell wall pectin content. The limiting pore size of cell walls, i.e. the available space between the matrix of cell wall polysaccharides that determines the size of molecules that are able to move through the cell wall and interact with the cell (Carpita *et al.* 1979), decreases with cold acclimation. Pore size decreased from 3.5 to 2.2 nm in cultured cells of grape stems, and from 2.9 to 2.2 nm in cultured apple fruit cells after exposure to 4°C for 3 to 5 weeks (Rajashekar & Lafta 1996). This structural characteristic of cell walls has been linked to pectins. Treating cell walls of soybean roots with a pectinase resulted

in the increase in pore size without affecting cell viability, whereas treatment with protease or cellulysin had no effect (Baron-Epel, Gharyal & Schindler 1988). Cell-wall pore size has been correlated more specifically with the dimerisation of RG-II domains; cultured cells of *Chenopodium album* grown in a boron-deficient medium had larger pores than those supplemented with BA, as the mean size limit decreased from 5.62 to 3.41 nm in growing cells with 100 µM BA (Fleischer *et al.* 1998). Cells with smaller pore sizes were shown to contain only monomeric RG-II domains, whilst supplementing with BA resulted in an increase in the presence of dimerised RG-II associated with the decreased pore size (Fleischer *et al.* 1999).

The levels and modifications of specific cell-wall contents also exhibit alterations during cold acclimation. The pectin content of the cell wall of oil-seed rape was found to increase, along with a marked increase of cell wall content in general (Solecka, Zebrowski & Kacperska 2008). During cold acclimation in peas, cell-wall content of arabinosyl (a side chain of pectins) and hydroxyproline was found to increase, both of which are major components of the glycoprotein extensin, and extensin mRNA was found to increase by a factor of three after cold exposure (Weiser, Wallner & Waddell 1990). More recently, cold acclimation was shown to affect the levels of pectic polysaccharides in peas, with an increase in sugar residues indicative of homogalacturonan, xylogalacturonan and RG-I (Baldwin *et al.* 2014). Studies using antibodies against differential levels of pectin methyl-esterification have suggested that cold induces a decrease in esterification and thus a probable increase in pectin cross-linking in the pit membranes of xylem vessels of peach (Wisniewski & Davis 1995). Contrary to this, pectin methyl-esterification was found to increase in peas after cold acclimation, possibly correlated with a decrease in PME activity (Baldwin *et al.* 2014). In chicory roots, PME activity was found to be correlated with ambient temperature, with activity decreasing as temperature decreased (Thonar, Liners & Van Cutsem 2006). In oil-seed rape plants, PMEI activity was shown to increase with exposure to cold temperatures, and overexpression of a *PMEI* gene resulted in a decrease in freezing tolerance, possibly related to the enhanced degree of methylation of pectin chains (Chen *et al.* 2018). In oilseed rape plants, galactose, arabinose and glucose residues of pectic cell-wall fractions were found to increase with cold acclimation, along with galactose and arabinose in hemicellulosic fractions (Kubacka-Zebalska & Kacperska 1999).

Other cell-wall localised proteins are found to be regulated with cold exposure, such as XTH enzymes and members of the expansin family; the differences in expression of each of the members of the XTH and expansin gene families between shoot and root found in this study

highlight the differential transcriptional control required in different tissues (Tenhaken 2015). This could explain the differences observed in alterations to PME activity with cold exposure described above as *PME*s and *PMEI*s are also members of a large gene family (Pelloux *et al.* 2007). A similar pattern was observed in wheat crowns as many different cell-wall modifying enzymes responded differentially to cold exposure in the shoot apical meristem and the vascular transition zone, suggesting cell wall modifications in response to cold are specific to cell type (Willick *et al.* 2018). The authors also showed that these differences in expression of cell-wall modifying enzymes resulted in the enhanced methyl-esterification status of pectins in the vascular transition zone, but not the shoot apical meristem (Willick *et al.* 2018). Interestingly, recent research has shown that the CBF transcription factors regulate cell-wall modifying proteins such as PMEs (Zhao *et al.* 2016).

Analysis has also shown that genes associated with lignin biosynthesis in winter barley increase after cold acclimation (Janská *et al.* 2011). Lignin was found to increase in *Arabidopsis* plants overexpressing antioxidant enzymes that were also shown to have increased freezing tolerance (Shafi *et al.* 2014). Interestingly, analysis of a cold-induced nuclear protein TCF1 (Tolerant to Chilling and Freezing 1) led to the discovery of a role in regulating lignin biosynthesis in *Arabidopsis*. Loss of *TCF1* function resulted in a decrease in lignin content, but an increase in freezing tolerance. This was verified by the fact that a *pal1pal2 (phenylalanine ammonia lyase*) double mutant which acts downstream of TCF1 had a 30% decrease in lignin content and an increase in freezing tolerance (Ji *et al.* 2015b). In a similar vein, the *esk1* mutant described in section 1.2.3 which is constitutively freezing tolerant had altered secondary cell wall composition and subsequent xylem malformation (Lefebvre *et al.* 2011). These findings do not necessarily fit with the hypothesis described above that increased cell-wall stiffness automatically translates to increased freezing tolerance, as lignin is a major determinant of cell wall stiffness (Özparpucu *et al.* 2017).

1.5.2 Functional significance of cell wall modifications for freezing tolerance and the process of supercooling

One mechanism for limiting damage from freezing events is by freeze-avoidance, and one way this is carried out is by supercooling which is the "depression of the freezing temperature of a liquid below its equilibrium freezing point" (Pearce 2001). Some woody plants can 'deep supercool' to as low as -40°C in the winter allowing the avoidance of freezing in some tissues (Burke *et al.* 1976). Interestingly, research has suggested that the main freezing-resistance

mechanism for *Arabidopsis* is freezing avoidance by the process of supercooling (Reyes-Diaz *et al.* 2006). Supercooling is facilitated by anything that depresses the freezing point of water in the plant. For example, the production of AFPs may decrease nucleation temperature in the apoplast (Bar Dolev *et al.* 2016), and the production of compatible solutes may reduce freezing temperature in the apoplast (Livingston III & Henson 1998). Supercooling is also associated with plant structure for example small cell size, and a lack of intercellular spaces which may partly be facilitated by the cell wall (Asahina 1956). Indeed, smaller xylem conduits have been shown to be less prone to cavitation and have also been associated with a decrease in ice nucleation temperature in the xylem (Lintunen, Holtta & Kulmala 2013).

There is ample evidence to suggest that cell wall modifications during cold acclimation may facilitate supercooling. The decrease in pore size could serve functionally in reducing the occurrence of ice nucleation in the cell wall; water in pores with a diameter less than 100 nm froze at a lower temperature than bulk water, with the additions of solutes reducing the freezing point even further (Ashworth & Abeles 1984). The freezing points measured in pores of different sizes were found to agree with the predicted values calculated from previously developed equations (Mazur 1965; Homshaw 1980). Using these equations, the authors predicted that in pores of diameter less than 4 nm, ice nucleation would occur between -15 and -25°C, thus smaller pores could facilitate supercooling (Ashworth & Abeles 1984). The proportion of cells that contained intracellular ice was measured to be approximately 4.3% in cells of grape cultures that had been cold acclimated, compared to ca. 37.6% in cells that had not. This was correlated with a decrease in pore size, supporting the idea of a reduction of ice nucleation events in cell walls with smaller pores (Rajashekar & Lafta 1996). The authors, among others, suggest that smaller pores may also restrict the growth of ice through the apoplast (Ashworth & Abeles 1984; Rajashekar & Lafta 1996). The structure and permeability of walls, particularly in pit membranes, have also been hypothesised to determine the rate of water movement and therefore the loss of water from cells to sites of extracellular ice during freezing events, which could limit damage from freeze-induced dehydration (Wisniewski, Ashworth & Schaffer 1987).

1.6 Summary

There is evidence to suggest that the plant cell wall plays a role in preventing damage from freezing events. This role is related to the structure of the cell wall, which is highly dynamic and regulated by abiotic stresses. Whilst studies have provided insight into the modifications that take place in the wall during cold acclimation, it is not clearly understood what precise details of

these alterations provide the mechanism for freezing tolerance. A greater understanding of this mechanism would be beneficial not only to increase our understanding of freezing tolerance mechanisms in plants, but also to highlight targets for the improvement of crops in the future.

1.7 Objectives and hypotheses

The objectives of this study are to increase our knowledge of what aspects of the plant cell wall can influence freezing tolerance by utilising a mutant of the model organism *Arabidopsis* which has altered cell-wall structure, and to attempt to understand how cell-wall structure may influence the tolerance to low temperature in plants. It is hypothesised that the alteration to the cell wall will have a negative impact upon the freezing tolerance of the plants, which will be investigated using a combination of electrolyte leakage and whole plant freezing assays. As previous studies have revealed that the phenotypic traits observed in the mutant in question are related to cell-wall pectin cross-linking (O'Neill *et al.* 2001), it is hypothesised that restoring cross-linking would restore freezing tolerance in these plants. It is possible that the influence that the loss of cross-linking has on cell-wall structure is the reason for an alteration in freezing tolerance. This hypothesis will be tested by exploring the different mechanisms via which the plant increases freezing tolerance, in particular in relation to the cell wall. Other potential dynamic impacts of the loss of cell-wall cross-linking and whether these are linked to freezing tolerance will also be explored.

CHAPTER 2

MATERIALS AND METHODS

2.1 Plant Materials and growth conditions

2.1.1 Seed material

Arabidopsis thaliana plants used were either of the Columbia (Col-0) or *Lansberg erecta* (Ler-0) background. Complemented lines were made by expressing the *MUR1* gene in the *sfr8* mutant background with a 35S promotor (Skipsey, Knight and Knight, unpublished). The *pme6* transposon insertion line (SGT6342) in a Landsberg background, the *pme6* T-DNA insertion line (GK278G11) in the Columbia background and the *bor1* T-DNA insertion line (SALK_149460C) in the Columbia background were obtained from the Nottingham *Arabidopsis* Stock Centre (NASC). Accession numbers are as follows: *MUR1* (At3g51160), *MUR2* (At2g03220), *BOR1* (At2g47160), *PME6* (At1g23200), *PEX4* (At5g25760).

2.1.2 Growth conditions

Arabidopsis seeds were surface sterilised by shaking with 70% ethanol in a 1.5 mL centrifuge tube for 5 min before being transferred to sterile filter paper and allowed to dry in a laminar flow hood. Seeds were then transferred to 9 cm diameter Petri dishes of ½ x Murashige and Skoog (MS) medium (Murashige & Skoog 1962) comprising of 0.8% plant tissue culture grade agar and ½ x MS with added vitamins (Duchefa Biochemie, Netherlands) with pH adjusted to 5.8 with 0.1 M KOH before sterilisation. All growth medium was sterilised by autoclaving at 121°C for 20 min. Seeds were then stratified at 4°C in the dark for a minimum of 48 h to ensure uniform germination and growth before being transferred to a Percival CU-36L5D growth chamber (CLF PlantClimatics, Wertingen, Germany) set to 16:8 Light:Dark (LD) cycles at 20°C with a light intensity of 150 µmol/m²/s.

For growth of mature plants, seedlings were transferred to 44 mm diameter Jiffy pellets (LBS Horticulture, UK) at 8-11 days old and covered with cling-film to allow acclimation to the change in humidity. Clingfilm was removed after 2 days and plants grown in short days, 12:12 LD cycles at 20°C, 70% humidity for a further 3 to 5 weeks as necessary. During growth on plugs, all plants were watered with deionised water.

2.1.2.1 Cold acclimation

Mature plants were transferred to acclimating conditions of 5°C, 10:14 LD cycles in a MLR-351 environmental test chamber (Sanyo) at 5 weeks old. Plants were acclimated for 14 days and used in experiments at 7 weeks old.

2.1.2.2 Boric acid supplementation

Seeds were grown on ½ x MS medium with the conditions as before. Once transferred to plugs, plants were watered with deionised water containing 10 mg/mL boric acid (BA) where applied throughout growth and cold acclimation. For the updated BA watering regime, seeds were grown on ½ x MS agar plates containing 1 mM BA for 8-11 days, then watered with deionised water containing 20 mg/mL BA where applied throughout growth and acclimation.

2.1.2.3 Fucose supplementation

Seeds were grown on ½ x MS medium with the conditions as before. Once transferred to plugs, plants were watered with deionised water and each tray of 22 plugs was sprayed with 60 mL of 10 mM fucose once a week where applied throughout growth and cold acclimation.

2.1.2.4 2F-fucose treatment

Peracetylated 2-fluoro 2-deoxy-L-fucose (2F-fucose, Merck Millipore) was dissolved in DMSO to 10 mM. For the electrolyte leakage assay with different concentrations, Col-0 wild type seeds were grown on ½ x MS medium containing 0.25% DMSO for the control and 2.5 µM, 10 µM and 25 µM of 2F-fucose for inhibitor treated seedlings. For the boric acid supplemented 2F-fucose treated assay, Col-0 seeds were grown on ½ MS medium supplemented with the following for the four different treatments; 0.1% DMSO; 0.1% DMSO and 0.75 mM boric acid; 10 µM 2F-fucose; 10µM 2F-fucose and 0.75mM boric acid. Seeds were grown in a Percival growth chamber as before for 14 days.

2.2 Molecular biology techniques

2.2.1 gDNA extraction

DNA extraction was carried out using a modification of the method described by Edward's (Edwards, Johnstone & Thompson 1991). Plant tissue was harvested into a 1.5 mL centrifuge tube and placed into liquid nitrogen. Samples were removed from the liquid nitrogen and

ground briefly using a micropestle before adding 400 µL of Edward's extraction buffer (200 mM Tris-HCl, pH 7.5/250 mM NaCl/25 mM EDTA, pH 8/0.5% SDS) and homogenising with an electric micropestle. Samples were then vortexed briefly and centrifuged for 1 min at 16000 *g*. 300 µL of supernatant was then transferred to a new 1.5 mL centrifuge tube and 300 µL of isopropanol added, mixed and incubated for 2 min. Samples were centrifuged for 5 min at 16000 *g* and the supernatant removed. Samples were centrifuged again for 1 min at the same speed and the remaining supernatant removed before samples were dried for 5 min in a vacuum desiccator. The pellet was re-suspended in 50 µL of TE buffer (10 mM Tris, pH 8, 1 mM EDTA) and incubated at 5°C overnight for the DNA to dissolve into solution. DNA was then stored at -20°C.

2.2.2 Polymerase chain reaction (PCR)

For amplification of DNA, PCR reactions were carried out using DreamTaq DNA polymerase (Thermo Scientific). A 50 µL reaction was made up in a 500 µL centrifuge tube as follows; 10 x DreamTaq green buffer, 5 µL; 10 mM dNTPs, 1 µL; forward primer, 0.25 µL; reverse primer, 0.25 µL; DreamTaq polymerase, 0.25 µL; DNA, 1 µL; nuclease-free H_2O, 42.25 µL. Reagents were vortexed and centrifuged briefly before being placed in a 96-well Px2 PCR thermocycler (Thermo Electron Corporation, Waltham, Massachusetts, USA) and run on the following programme; 95°C, 2 min x 1; (95°C, 30 s; Ta, 30 s; 72°C, 1 min) x 35; 72°C, 5 min x 1. The annealing temperature (Ta) for each primer pair was chosen to be 5°C lower than the melting temperature of the primer with the higher of the two. PCR products were analysed using gel electrophoresis.

2.2.2.1 Oligonucleotides

Primers were designed to be a minimum of 20 bp in length and to have a GC content of 40-60% for optimal annealing. The program Primer3Plus (https://primer3plus.com/) was used to assist with primer design. A full list of oligonucleotides used for PCR can be found in Appendix C.

2.2.3 Gel electrophoresis

DNA was separated by size using agarose gel electrophoresis. Gels were prepared by melting 0.8% molecular grade agarose (Bioline) in 0.5 x TBE buffer (1.1 M Tris, 900 mM borate, 25 mM EDTA, pH 8) with 2 µL of MIDORI^{Green} dye (Nippon Genetics, Europe) per 50 mL of agarose. The gel was poured into a gel tank with a comb to create wells and allowed to set. 0.5 x TBE buffer was using as running buffer with 10 µL of PCR product loaded into each well and 5 µL of 1 Kb Hyperladder 1 (Bioline) loaded into one well for size comparison. Gels were run at 35 mA for

approximately 1 h and imaged under UV light using an uvidoc trans-illuminator (Uvitec Limited, Cambridge, UK).

2.2.4 DNA clean-up

PCR products were cleaned for sequencing using MicroCLEAN (Microzone, UK). Briefly, an equal volume of MicroCLEAN and DNA were mixed by pipetting in a 1.5 mL centrifuge tube and left at room temperature for 5 min. Samples were then centrifuged at 16000 *g* for 7 min and the supernatant removed. Samples were centrifuged again for 1 min and all liquid removed. The pellet was re-suspended in 50 µL TE buffer and left for 5 min to rehydrate DNA.

2.2.5 Sequencing

Sequencing of PCR product was carried out after DNA clean-up by the DNA sequencing laboratory (Department of Biosciences, Durham University) using one of the primers used for amplification (Appendix C). Sequence alignment was carried out using Clustal alignment in Jalview (http://www.jalview.org/).

2.2.6 RNA extraction

For the assessment of gene expression, RNA extraction was carried out on two-week-old seedlings grown as previously described. Samples were placed immediately into liquid nitrogen and stored at -80°C until extraction of RNA was carried out according to the Promega ReliaPrep RNA Tissue Miniprep System (Promega, Wisconsin, US) protocol for non-fibrous tissue. Tissue was harvested into a 1.5 mL centrifuge tube and placed into liquid nitrogen. Samples were removed from liquid nitrogen and ground briefly with a micropestle before adding 500 µL of LBA with added thioglycerol and using the micropestle to homogenise the material. Samples were vortexed briefly and then centrifuged for 3 min at 14000 *g*, removing the supernatant to a new 1.5 mL centrifuge tube. 170 µL of isopropanol was then added and samples vortexed for 5 s. The lysate was then transferred to a Minicolumn placed into a Collection tube and centrifuged for 1 min at 14000 *g*. The flow-through was discarded and 500 µL of RNA wash solution added to the Minicolumn before centrifuging for 30 s at 14000 *g*. The liquid was again discarded, and DNase digestion carried out by pipetting 30 µL of DNase 1 incubation mix (24 µL Yellow Core Buffer, 3 µL 90 mM $MnCl_2$, 3 µL DNase 1) directly to the Minicolumn membrane and incubating at room temperature for 15 min. The column was then washed by adding 200 µL od Column Wash Solution with added ethanol and centrifuging for 30 s at 14000 *g*. The flow-through was

discarded and 500 µL of RNA Wash Solution with added ethanol added to the samples, which were then centrifuged for 30 s at 14000 *g*. The Minicolumn was placed into a new collection tube and the RNA wash step repeated, adding 300 µL of RNA Wash Solution and centrifuging for 2 min at 16000 *g*. The Minicolumn was then placed into a 1.5 mL centrifuge tube and 30 µL of nuclease-free water pipetted directly onto the membrane. Samples were then centrifuged for 1 min at 14000 *g* to elute the RNA into the centrifuge tube. RNA was stored at -80°C.

2.2.7 cDNA synthesis

cDNA was synthesised from RNA extracted as above using an Applied Biosystems High Capacity cDNA synthesis kit (Applied Biosystems, California, US). For each sample, solutions were made up on ice as follows in a 500 µL centrifuge tube; 2 µL 10x RT buffer; 0.8 µL 100 mM 25x dNTP mix; 2 µL 10x RT random primers; 1 µL Multiscribe™ reverse transcriptase; 4.2 µL nuclease-free H_2O; 2 µg RNA made up in 10 µL nuclease-free H_2O, making a total reaction volume of 20 µL. Two controls were also made up; a 'no reverse transcriptase control' (NRT) containing 1 µL of water in place of reverse transcriptase, and a 'no template control' (NTC) containing 10 µL H_2O in place of RNA. Samples were vortexed briefly and centrifuged to bring the contents to the bottom. Samples were then placed in a PCR machine and run on the following programme; 25°C, 10 min; 37°C, 120 min; 85°C, 5 s. The resulting cDNA was diluted 1:50 with nuclease free water before use in qPCR and stored at -20°C until required.

2.2.8 Gene expression measurements using qPCR

The relative transcript level of genes was determined by qPCR using an Applied Biosystems 7300 real time PCR machine and Go Taq qPCR master mix (Promega). All experiments used triplicate wells for each sample and included NTC and NRT controls as described in section 2.2.7. Samples were loaded into a 96 well plate (STARLAB UK, Milton Keynes, UK). Each well contained; 7.5 µL 2 x Go Taq qPCR mastermix; 0.9 µL 5 µM forward primer; 0.9 µL 5 µM reverse primer; 0.7 µL nuclease free water; and 5 µL of the appropriate 1:50 dilution of cDNA synthesis from RNA extractions. The Go Taq qPCR master mix contains ROX reference dye to account for optical differences between the wells. *PEX4* was used as an endogenous control (Moffat *et al.* 2012). Primers were designed with an amplicon size of 80-120 bp. Gene expression levels were analysed using the ΔΔCt method (Applied Biosystems). The algorithm described in the Applied Biosystems user bulletin in 2007 entitled 'Relative Quantitation (RG) algorithms, Applied Biosystems Real-Time PCR Systems Software' was used for the statistical analysis of the qPCR

data (Moffat *et al.* 2012). Error bars represent RQ_{MIN} and RQ_{MAX} and constitute the acceptable error level for a 95% confidence level according to the student's t-test.

2.3 Assessment of freezing and freezing damage

2.3.1 Electrolyte leakage

2.3.1.1 Electrolyte leakage of mature plants

Quantitative assessment of freezing damage to plants was carried out using a modification of the method described by Helmsley *et al.* (2014). Leaf discs were excised from three leaves of comparable size from each plant with six replicate test tubes, each with three leaf discs, prepared for each measurement. Test tubes were held on ice until all samples had been prepared and were then washed in deionised water. The water was removed and leaf discs blotted gently on tissue paper to remove excess water. Test tubes were then transferred in a randomised order to a freezing bath set at -2°C where they were allowed to equilibrate for 1 h. An ice chip made using deionised water was then added to each test tube to initiate freezing, and samples incubated at -2°C for a further 2 h. The temperature was then turned down to the first temperature and after 30 min at this temperature one set of tubes (six tubes for each plant type) were removed and placed on ice before decreasing the bath to the next temperature. After 30 min at this temperature the next set of tubes were removed and placed on ice before decreasing to the lowest temperature. After 30 min at this temperature the final set of tubes was removed and placed on ice and all samples were allowed to thaw overnight in a cold chamber at 5°C. Temperatures used were -3°C, -5.5°C and -8°C for non-acclimated plants and -7°C, -9.5°C and -12°C for acclimated plants.

The following day 5 mL of deionised water was added to each tube and tubes shaken gently for 3 h at room temperature. The liquid from each tube was decanted into a respective tube and the conductivity (µS/cm) of each sample measured using a hand-held conductivity meter (Mettler Toledo). The tubes containing leaf discs were transferred to a -80°C freezer for 1 h to allow complete release of ions from the plant tissue. The liquid was then decanted back into each respective tube and the tubes shaken again for 3 h at room temperature before the leaf discs were removed and the conductivity was measured again. Percentage electrolyte leakage could then be calculated by expressing the first reading as a percentage of the second.

2.3.1.2 Electrolyte leakage of 2F-fucose treated seedlings

Seedlings treated with 2F-fucose were used in the electrolyte leakage experiment at 14 days old. For seedlings treated with different concentrations of 2F-fucose, seedling size varied so numbers were increased so that all samples contained approximately the same mass of tissue. This equated to using 3 seedlings in each tube for the DMSO control, 5 seedlings for the 2.5 µM, 10 seedlings for the 10 µM and 15 seedlings for the 25 µM 2F-fucose treated plants. The experiment was carried out as before, but the temperatures used were -3, -5 and -7°C as the seedlings were more fragile and had not undergone cold acclimation. For the seedlings supplemented with boric acid, seedling size also varied so different numbers of seedlings were used from each treatment to obtain a similar mass. This equated to 3 seedlings in each tube for the DMSO and DMSO + BA controls, 5 seedlings for the 2F-fucose + BA treated plants and 15 seedlings for the 2F-fucose treated plants. The temperatures used were -2, -4 and -6°C.

2.3.2 Visual freezing assays

Plants were grown as before and at 5 weeks old were transferred to cold acclimating conditions for 14 days, being used in the experiment at 7 weeks old. Plants were then placed randomly on to a large tray to deter positional effects and placed into a freezing chamber at -8.5°C in the dark for 24 h. After freezing, plants were transferred to an MLR-351 environmental test chamber (Sanyo) at 5°C for 24 h to allow defrosting and prevent heat shock. Plants were then moved to a growth room at 20°C and watered as necessary with recovery assessed after 7 days.

2.3.3 Droplet freezing assays

A droplet freezing assay was carried out as described by Whale *et al.* (2015) modified for use with ground plant samples. Plants were grown as before and used in the experiment at approximately 7 weeks old or 5 weeks with 2 weeks of cold acclimation. 0.5 g of leaf material was harvested from five plants of each genotype and washed in deionised water, then blotted dry. Samples were ground in a pestle and mortar with 10 mL of deionised water added in 2.5 mL increments to make sure the samples were as homogenous as possible. Samples were transferred to a 50 mL centrifuge tube and stored at 4°C until required. Samples were vortexed briefly before use in the assay to make sure plant material was present in the fractions to be frozen. For the assay, a 22 mm glass slide was washed with deionised water, followed by isopropanol and finally deionised water again and then dried with N_2. The slide was placed onto an aluminium square attached to the cryo-plate of a VIA Freeze Duo controlled rate freezer

(Asymptote). Up to 40 1 µL droplets were pipetted onto the glass slide and the atmosphere maintained by enclosing the slide with a plastic chamber via which a camera was attached (Figure 2.1A). The cryo-plate was then cooled to 4°C at a rate of 2°C per min, after which nitrogen was pumped through the chamber at 0.3 L per min to maintain a dry atmosphere. The plate was maintained at 4°C for 2 min before cooling at a rate of 1°C per min. Below 0°C, images were taken every second and cooling continued until all the droplets were frozen. For the freezing of droplets containing RG-II standards, the procedure was carried out in the same way using 0.1 and 1 µg/mL solutions of RG-II monomer and dimer from sugar beet provided by the Edinburgh Cell Wall Group. Droplets of 1 µL were pipetted onto a slide and frozen as before on a Grant EF600 controlled rate freezer.

For the preliminary droplet freezing assays, plants were approximately 4-5 weeks old and only 0.3 g of leaf tissue was ground into 10 mL of deionised water using a homogeniser. Droplets were frozen on a Grant EF600 controlled rate freezer (Asymptote), but all other technicalities of the procedure were the same. For freezing of supernatant, 1 mL of ground leaf sample was transferred to a 1.5 mL centrifuge tube and centrifuged at 10000 *g* for 1 min to collect large material in the pellet. Microlitre droplets of supernatant were pipetted onto a glass slide and frozen as before on a VIA Freeze DUO controlled rate freezer (Asymptote) as before. The images obtained from freezing experiments were used to deduce the temperature at which each droplet froze, and these results used to calculate the fraction of droplets frozen with temperature (Figure 2.1B).

2.3.4 Ice nucleation in epidermal peels

Plants were grown as before and used in the experiment at 4 weeks old with 2 weeks of cold acclimation where stated. Epidermal peels were obtained as described in section 2.5.2. Peels were placed on a 1 cm diameter glass coverslip, a rubber 'O' ring placed on top sealed with high vacuum grease and another glass coverslip placed on top of this, also sealed with high vacuum grease (Figure 2.2A). Samples were placed onto an Olympus Bx53 microscope stage modified to be used as a cold stage (Figure 2.2B), with a seal made between the coverslip and the cold stage using high vacuum grease. A plastic chamber was placed between the stage and the microscope lens to maintain the atmosphere. Samples were cooled from 20°C to 2°C at 10°C per min, followed by cooling to -25°C at 2°C per min, during which stage nitrogen was pumped through the chamber to maintain a dry atmosphere and prevent the production of condensation on the slide. Ice nucleation occurred during the cooling step and was imaged using a MIRO M310 high

A

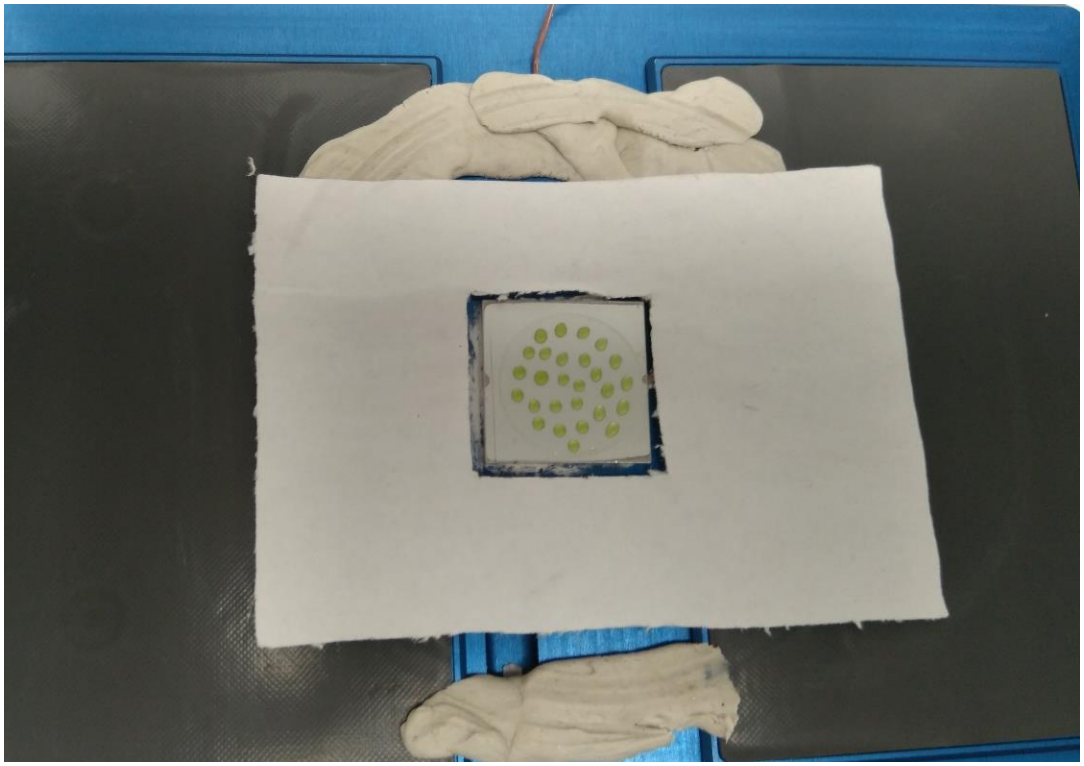

B

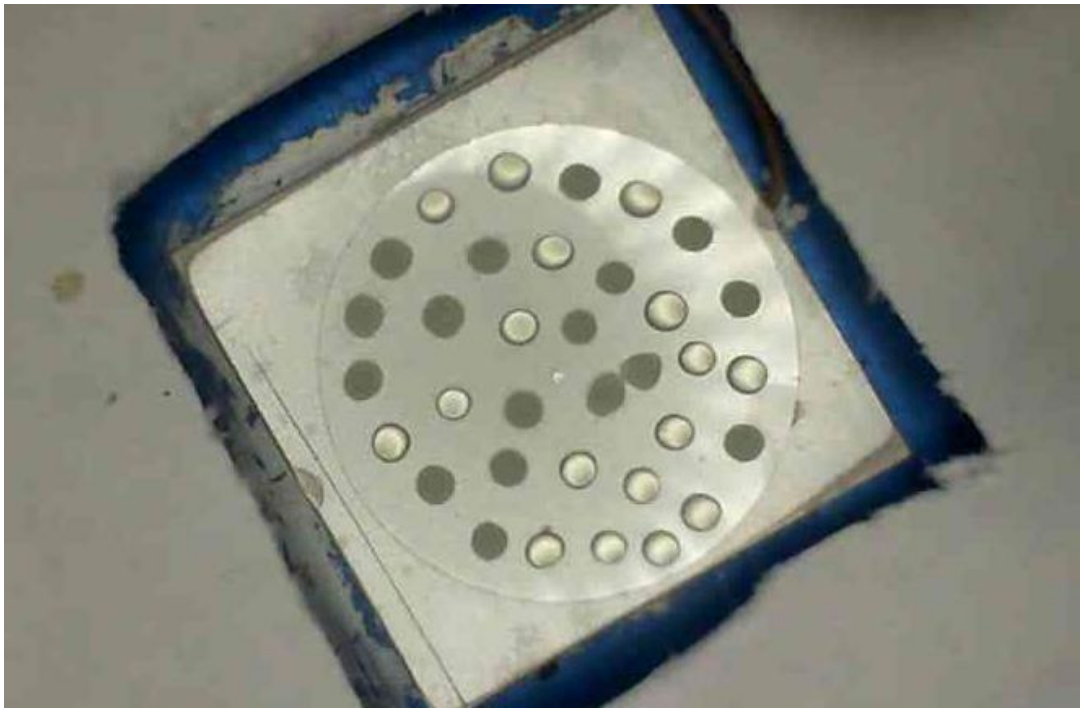

Figure 2.1: Experimental set-up of the droplet freezing assay. A) Set-up of the droplet freezing assay on the cryocooler. **B**) Droplets of supernatant from whole plant extracts on glass slides used in the droplet freezing assays. Darker droplets indicate frozen status, lighter droplets are unfrozen.

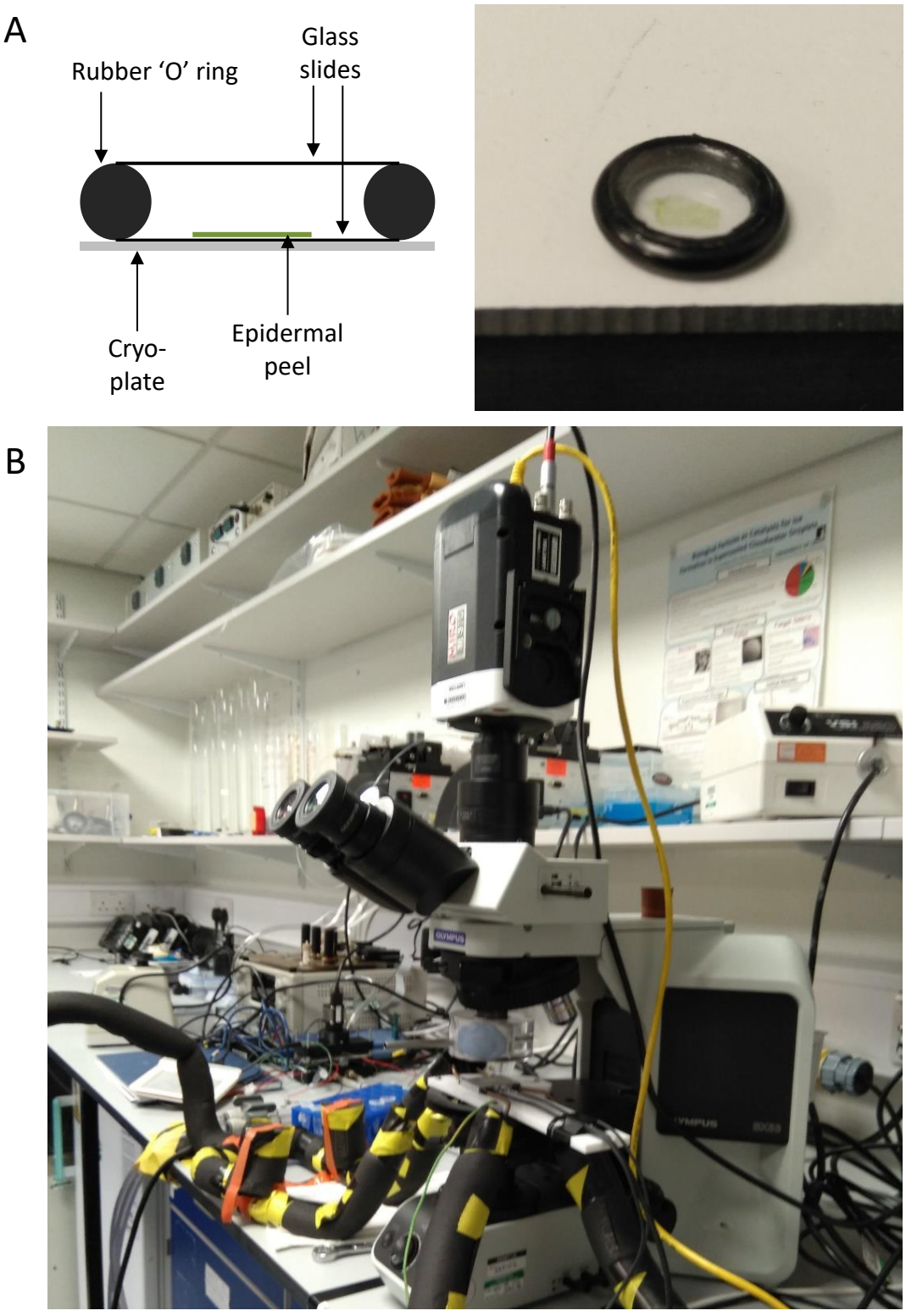

Figure 2.2: Experimental set-up for the freezing of epidermal peels. Microscope set-up used for the freezing of epidermal peels. **A**) Microscope fitted with high-speed camera cryoplate cooled with liquid nitrogen. **B**) Diagram and real-life set up of the epidermal peel in a contained environment for freezing.

speed camera (AMETEK) attached to the microscope. The temperature at which nucleation occurred was recorded. Videos were edited using Phantom Camera Control (PCC) 2.7 video software (AMETEK).

2.4 Cell wall analysis

2.4.1 Analysis of cell wall sugars using GC-MS

Plants were grown on ½ MS medium as before for 14 days. At 14 days old, approximately 100 mg of tissue was harvested into a 1.5 mL centrifuge tube and placed into liquid nitrogen. Samples were removed from liquid nitrogen and ground using a micro-pestle, after which 1 mL of 70% ethanol was added, tubes vortexed briefly and the samples incubated at 70°C for 15 min. Samples were centrifuged for 5 min at 16000 *g* and the supernatant discarded. The tissue was then washed twice in hot 70% ethanol, homogenising tissue again with a micro-pestle during the first wash, centrifuged as before and the supernatant discarded. Two to three holes were made in the lid of the centrifuge tube and the samples frozen and dried overnight in a vacuum bell. The next day, 500 µL of water was added to each sample and tubes placed into a sonicating water bath for 30 min to rehydrate the material. The lids were then replaced and 500 µL of 4 M trifluoroacetic acid (TFA) added to the tubes for a final concentration of 2 M. A 100 µg inositol internal standard was also added. Tubes were vortexed to break down the material and the samples incubated at 110°C for 2 h in a fume hood with heavy blocks on top of the tubes to prevent explosions. After incubation, tubes were vortexed briefly and then centrifuged for 15 min at 14000 *g*, with 800 µL of the brownish supernatant transferred to a glass sample tube. The liquid was then evaporated under N_2 at 40°C, after which 400 µL of 1 M MeOH-HCl was added and samples incubated at 80°C overnight. The next day, samples were allowed to cool and then dried under N_2 at 40°C until completely dry, after which 400 µL of TMSI-pyridine was added and samples incubated at 80°C for 30 min. After incubation, samples were dried under N_2 at 40°C and the brownish oil left re-suspended in 1 mL of hexane and vortexed vigorously. Samples were then centrifuged for 5 min at 500 *g* to remove the remaining brown salt formed and the supernatant transferred to clean glass sample tubes using a glass pipette. The samples were partitioned with an equal volume of water to hexane. Upon addition a white salt is formed, and samples were vortexed vigorously to dissolve this and the samples separate into an upper phase and a lower phase. The upper hexane phase was then transferred to a GC-MS vial using a glass pipette. Samples were run on the GC-MS machine.

2.4.2 Analysis of cell wall rhamnogalacturonan II (RG-II) content

2.4.2.1 Measurement of cell-wall RG-II content

2.4.2.1.1 Preparation of alcohol insoluble residue (AIR) and digestion with endo-polygalacturonase (EPG)

Plants were grown as before, and leaf tissue was harvested from plants at 5 weeks for non-acclimated plants and 7 weeks for cold acclimated plants (5 weeks growth and 2 weeks of cold acclimation) and placed into liquid nitrogen. To prepare the AIR, tissue was ground in liquid nitrogen with a pestle and mortar to a fine powder. From this, 50 mg (+/- 1) of powder was placed into a 1.5 mL centrifuge tube with 1 mL of 100% EtOH and samples incubated shaking at 250 rpm, room temperature for 4 h. Samples were then centrifuged for 3 min at 16000 *g* and the supernatant aspirated off, after which 1 mL of fresh 100% EtOH was added and samples incubated shaking as before at 37°C overnight (16 h). Samples were centrifuged as before and the supernatant removed, followed by incubation in 350 µL of Na_2CO_3 shaking at 4°C for 16 h. Samples were again centrifuged as before, and the supernatant removed. Tissue was then neutralised with an excess of acetic acid and washed in 500 µL of EtOH, before drying with 20 µL of acetone and incubating at 40°C to dry the tissue completely. Once dry, 1 mg of material was placed into a new 1.5 mL centrifuge tube and centrifuged to bring the powder to the bottom. Then 100 µL of 10 U/mL endo-polygalacturonase (EPG - Merck) in pyridine/acetic acid/0.5% chlorobutanol (1:1:98, pH 4.7) was added to each tube and samples incubated at 37°C shaking for 16 h.

2.4.2.1.2 Gel electrophoresis and silver staining

Samples were centrifuged for 3 min at 16000 *g* and 8 µL of the supernatant added to 2 µL of loading buffer (0.63 M Tris HCl/0.25% w/v bromophenol blue/50% glycerol, pH 8.8). Samples were then loaded into the wells of a 26.4% polyacrylamide gel run at 200 V, room temperature for 75 min in electrode buffer (50mM Tris/38 mM glycine). A 5 mL gel was made from the following; 834 µL 1.5 M Tris, pH 8.8; 3.33 mL 40% acrylamide/bis acrylamide (29:1); 46.7 µL 10% APS; 3.9 µL TEMED; 834 µL H_20. All reagents were added to a 50 mL centrifuge tube and mixed by pipetting up and down before being pipetted into the gel apparatus and allowed to dry. Once finished, the gel was removed from the glass slides and placed into a tray. The gel was fixed in ethanol/acetic acid/water (4:1:5) shaking gently for 30 min and then washed with H_2O for 1 min, three times. The gel was then treated with 400 µM sodium thiosulphate for 1 min then washed with H_2O for 1 min, three times. Staining was achieved by adding 6 mM $AgNO_3$/10 mM

formaldehyde solution and shaking gently for 20 min, after which the gel was washed with H_2O for 20 s, two times. For colour development, 0.28 M Na_2CO_3/8 µM sodium thiosulphate/64 mM formaldehyde solution was added, and the gel shaken gently until the desired colour strength was reached. Colour development was stopped by adding 0.33M Tris/2% acetic acid and the gels scanned.

2.4.2.2 Measurement of cell-wall RG-II content during cold acclimation

2.4.2.2.1 Preparation of AIR and EPG digestion

Plants were grown as before and at 5 weeks were transferred to cold acclimating temperatures of 5°C. Tissue was harvested from wild type plants after 3, 12 and 48 h, and 7 and 14 days of cold acclimation, frozen in liquid nitrogen and stored at -80°C until required. Sample preparation was carried out as described in section 2.4.2.1.1 with a few minor changes. After grinding in a pestle and mortar, 500 mg (+/- 5) of leaf tissue was added to a 50 mL centrifuge tube with 10 mL of 100% EtOH and incubated for 6 h shaking at room temperature. After incubation, tubes were centrifuged at 4500 rpm for 3 min and the supernatant removed. 10 mL of fresh 100% EtOH was added and the tubes incubated at 37°C shaking for 22 h. Samples were then centrifuged at 4500 rpm for 3 min and the supernatant removed, after which 7 mL of Na_2CO_3 was added and samples incubated at 4°C shaking for 16 h. After incubation, samples were centrifuged as before, and the supernatant removed. Tissue was then neutralised with an excess of acetic acid, washed with 5 mL of EtOH, before drying with 1 mL of acetone and incubating at 40°C to dry the tissue completely. Once dry, 10 mg of material was placed in a 1.5 mL centrifuge tube and centrifuged to bring the powder to the bottom. 1 mL of 10 U/mL EPG in pyridine/acetic acid/0.5% chlorobutanol (1:1:98, pH 4.7) was added to each tube and samples incubated at ambient temperature shaking for 16 h. Gel electrophoresis was then carried out as described before.

2.4.2.2.2 Separation of RG-II monomer and dimer

AIR was prepared as before and digested in EPG. Approximately 500 µL of EPG digested cell wall material was freeze dried and resuspended in 100 µL of 50 mM ammonium formate pH 5. An aliquot of 50 µL was injected into a gel filtration column (Superdex peptide, 10 mm x 300 mm and Superdex G75, 10 mm x 300 mm) and eluted at 800 µL/min in ammonium formate as above using an AKTA Purifier system. 800 µL fractions were collected and freeze dried. 50 µL of sample was also run on a Superdex S200, 5 mm x 150 mm with 200 µL fractions eluted at 200 µL/min

which were freeze dried as before. Samples were re-suspended in 40 µL of deionised water and used in PAGE analysis as described in section 2.4.2.1.2. Briefly, 8 µL of sample was added to 2 µL of loading buffer and loaded onto a 26.4% polyacrylamide gel. The gel was run for 4 h before fixing in ethanol:acetic acid:water as before and treating with silver nitrate/formaldehyde solution to stain RG-II monomer and dimer bands.

2.4.2.2.3 Quantitative analysis of RG-II

Quantification of RG-II was performed using a high-performance anion-exchange chromatography with a Dionex HPLC system. The system comprised an AS50 autosampler and GP50 pump and equipped with an ED50A electrochemical detector fitted with a gold electrode and a pH reference cell. The column used was a Dionex PA100 (4.5 mm x 250 mm). The amount of sample injected was 25 µL and flow rate was 1 mL/min. Elutents were prepared from 50% sodium hydroxide stock solution and from electrochemical-grade sodium acetate (Fisher) using degassed HPLC-grade water. Gradients from 100 mM NaOH to 800 mM NaOH, or from 100 mM NaOH to 100 mM NaOH + 500 mM sodium acetate were used to try to obtain peaks corresponding to RG-II.

For measurement of RG-II from digested cell wall samples prepared as described in 2.4.2.1.1; 950 µL of EPG-digested material was transferred to a clean 1.5 mL centrifuge tube and freeze dried completely. Samples were re-suspended in 25 µL sodium acetate as above and injected into the column to detect carbohydrate peaks as described. For qualitative analysis of samples, PAGE analysis of the EPG digested product was carried out as described in 2.4.2.1.2. Briefly, 8 µL of sample was added to 2 µL of loading buffer and loaded onto a 26.4% polyacrylamide gel. The gel was run for 4 h before fixing in EtOH:acetic acid:water as before and treating with silver nitrate/formaldehyde solution to stain RG-II monomer and dimer bands.

2.4.2.3 Measurement of RG-II synthesis using radiolabelling

2.4.2.3.1 Radiolabelling

Plants were grown as previously described and treatments were as follows: 5-week-old plants kept at ambient temperature (A); 7-week-old plants kept at ambient temperature (B); 5-week-old plants placed in the cold (C); 5-week-old plants plus 2 weeks of cold acclimation kept in the cold (D). Leaves were excised from plants with as much petiole as possible and placed into 5 µL of [^{14}C]-fructose in 200 µL centrifuge tubes which were put into a glass beaker. The beaker containing leaves to be kept cold was placed into a beaker with ice. Samples to be kept at

ambient temperature were placed in an identical beaker without ice and both beakers covered with Clingfilm and placed in fume hood for 16 h. Leaves were observed during incubation and once all the [^{14}C]-fructose had been taken up, 50 µL of water was added to each tube on an individual basis. After incubation, leaves were removed from tubes, washed with deionised water and placed into 15 mL centrifuge tubes containing 14 mL of 1 M NaOH in 75% EtOH and shaken gently at ambient temperature for 16 h to remove methyl ester groups. Samples were washed in 12 mL 75% EtOH for 30 min, then 12 mL 100% EtOH for 30 min and finally 12 mL 100% EtOH/0.5% acetic acid for 30 min to neutralise alkaline NaOH.

2.4.2.3.2 Preparation of AIR and EPG digestion

Leaves (L) and petioles (P) were transferred to separate 1.5 mL centrifuge tubes. Tissue was frozen in liquid nitrogen, ground using a micropestle and incubated in 500 µL 100% EtOH for 30 min shaking at room temperature. Tubes were centrifuged as before, and the supernatant removed before washing in 75% EtOH/0.5% acetic acid, followed by drying in 20 µL acetone and drying completely at 40°C. Once dry, 100 µL of 10 U/mL EPG in pyridine/acetic acid/0.5% chlorobutanol (1:1:98, pH 4.7) was added to each tube and incubated at ambient temperature shaking for 16 h.

2.4.2.3.3 Chromatography

To each EPG digested sample, 10 µL of 1% EPG digested homogalacturonan was added as an internal marker-mixture containing GalA, $GalA_2$ and $GalA_3$, and 60 µL spot loaded onto Whatman No. 20 chromatography paper as 4 x 15 µL spots with a 3 cm centre-to-centre spacing between samples. Chromatography papers were run in EAW (ethyl acetate/acetic acid/water) (10:5:6) for 50 h. GalA, $GalA_2$ and $GalA_3$, the expected products of homogalacturonan digestion migrated along the chromatography paper, whereas undigested RG-I and RG-II remained at the origin. Autoradiograms were made of the origin spots by exposing the paper chromatograms to film which were then developed and imaged.

The origin zones of these paper chromatograms were cut out, with pieces averaging approximately 40 mg. Each piece was placed into a 15 mL centrifuge tube with 500 µL 2 M TFA + 50 µg each of internal sugar markers comprising GalA, Gal, Glc, Man, Ara, Xyl, Fuc, Rib, Rha and Api. Samples were heated at 115°C for 1.33 h. The supernatant was removed and placed into a 1.5 mL centrifuge tube. A further 1 mL of ethanol was added to the paper samples, shaken and then removed and pooled with the first supernatant. This sample was now expected to

contain the monosaccharides released by acid hydrolysis of the rhamnogalacturonans. The samples were vacuumed dry overnight and the residue re-suspended in 30 µL of 0.5% aqueous chlorobutanol. Samples were then spot-loaded onto Whatman No. 20 chromatography paper with a 2.75 cm centre-to-centre spacing between each sample plus external markers of the ten sugars previously stated and run in EPW (ethyl acetate:pyridine:water) (8:2:1) for 31 h. Autoradiograms were made by exposing the paper chromatograms to film for 2-3 months which were then developed and imaged.

The mobile regions from the chromatograms run in EAW displayed a large number of mobile spots. Two representative tracks (P1C1 and P3A1) were therefore taken in the form of the 24 zones highlighted from the run. Each of the 24 zones was cut out and placed into a 15 mL centrifuge tube with 1.5 mL 2 M TFA for 2-3 days. The papers were removed, and the remaining solution heated at 120°C for 1 h so that the oligosaccharides would be converted to monosaccharides and then vacuum dried. The residue was re-suspended in 50 µL 0.5% chlorobutanol and spot-loaded onto Whatman No. 20 chromatography paper along with external sugar markers (excluding fucose), which was then run in EPW (8:2:1) for 33 h. The radioactivity of the paper chromatograms was measured in counts per 10 min per 0.576 cm using a LabLogic AR2000 radioactivity scanner.

2.5 Stomatal analysis

2.5.1 Measurement of water loss from leaves

Plants were grown as before and used in the experiment at 5 weeks old. The day before the experiment was carried out, plants were covered with a plastic bag to provide an approximate 100% humidity environment. One leaf was harvested from each of seven plants, blotted dry, weighed immediately and then placed in a weighing boat with the abaxial side facing upwards. Leaves were kept at an ambient temperature of approximately 22°C and 50% humidity and weighed every hour for eight hours to gain a measurement of percentage mass. Leaves were then weighed at 24 h and finally at 7 days. Each measurement was expressed as a percentage of the original mass.

2.5.2 Stomatal aperture measurements using epidermal peels

Plants were grown as before and used in the experiment at 4 weeks old as younger leaves were easier to obtain epidermal peels from. One leaf was excised from each plant and placed adaxial

side down on a microscope slide with a few drops of water to hold the leaf in place and assist peeling of the epidermis. The top and one edge of the leaf were removed with a scalpel and an incision made near the bottom of the leaf from the cut edge to the vein. Tweezers were used to grip the top of the cut section and pull the leaf down parallel to the slide to peel the epidermis away from the rest of the tissue. The peel was then placed into 10 mM MES/50 mM KCl_2 solution, pH 6.15 with the outside face of the peel facing upwards and incubated at 20°C for 2 h (Gonzalez-Guzman *et al.* 2012). After incubation, peels were carefully transferred to a microscope slide with a little MES solution and a coverslip placed on top. Samples were imaged using a light microscope with attached camera at 20x magnification, with 15 stomata imaged on each peel using a scanning method across the sample. Images were analysed using ImageJ to measure the aperture of each stoma imaged. Each experiment was repeated three times.

2.5.2.1 Treatment with Abscisic acid

The experiment was carried out as before but after the first incubation step in MES/KCl_2, abscisic acid (ABA) was added to a final concentration of 5 µM, the solution mixed gently, and samples incubated for a further 2 h before transferring the peels to microscope slides and imaging stomata.

2.5.3 Stomatal density/index

Epidermal peels were obtained as described in section 2.5.2 from 4-week-old plants grown as before. Images of leaf epidermis were taken on a light microscope with attached camera at 10x magnification. Stomatal density was measured as the number of stomata per unit area of leaf. Stomatal index was measured using the following equation where I = stomatal index, S = stomata per unit area of leaf and E = epidermal cells per unit area of leaf;

$$I = \frac{S}{S + E}\ x\ 100$$

Density and index were measured from 15 images obtained from 3 different leaves, and each experiment was repeated twice.

2.5.4 Stomatal conductance measurements

Plants were grown as before and used in the experiment at 6 weeks old. Stomatal conductance was measured using a LICOR-6400 photosynthetic system with attached leaf chamber. One leaf was placed into the chamber and allowed to acclimate at 400 ppm for 30 min, after which the

reference CO_2 value was decreased to 50 ppm for 1 h, and then increased to 1000 ppm for 1 h. The machine was matched between every reference CO_2 change and a measurement taken every 60 s (calculated as 15 s averages). Flow rate was maintained at 300 µmol/s; leaf temperature at 20°C and humidity at 45-50%. Six repeats were carried out for each genotype and the experiment was carried out twice.

2.5.5 Thermal Imaging

2.5.5.1 Excised rosette imaging

Plants were grown as before and used in the experiment at 5 weeks old. Rosettes were excised from the root at the base of the rosette and placed on a matte white surface and allowed to desiccate. Thermal images were obtained using a FLIR T1030sc infrared camera (FLIR systems, USA) that operates in the spectral range of 7.5–13 µm and has a focal plane array (FPA) uncooled microbolometer detector with a spatial resolution of 1024 x 768 pixels (Figure 2.3). Images were taken from a distance of 1 m from rosettes, with images taken every 1 min. Emissivity was set at 0.95, ambient temperature at 23°C and humidity at 50%.

2.5.5.2 Whole plant imaging

2.5.5.2.1 Whole plants in plugs

Plants were grown as before and used in the experiment at 5 weeks old. Plants were watered and placed in a clear bag to create a high humidity environment the evening before the experiment. Plants were removed from the bag, set up randomly in small petri dishes on a matte white surface and allowed to acclimate to the change in humidity for 40 min (see Figure 2.3 for set-up). A thermal imaging camera was set up to image plants at a distance of 1 m every 30 min for 4 days in constant light. Emissivity was set at 0.95, ambient temperature at 23°C and humidity at 50%. Four plants of each genotype were imaged, with two of each watered morning and evening and the other two given no further water.

2.5.5.2.2 Whole plants in pots

Plants were grown as before and used in the experiment at 5 weeks old. Netting was removed from plugs and plugs placed into small pots to protect the roots from droughting. Plants were watered well the evening before the experiment and then removed from water and weighed. At the start of the experiment, plants to be watered were given water, whilst plants to be

Figure 2.3: Experimental set-up for the thermal imaging of droughted plants in plugs. Plants were imaged under constant light, with or without water, with images taken every 30 minutes.

droughted were not. Pots were set up randomly on a metal bench in a greenhouse of approximately 16:8 LD cycles with temperatures ranging from 21°C during the day to 13°C during the night. A thermal camera was set up to image plants at a distance of 1 m every 30 min for 4 days. Emissivity was set at 0.95, ambient temperature at 21°C and humidity at 50%. Plants were subsequently weighed every morning and evening, and watered plants given water morning and evening. Eight Col-0 plants were used in the experiment; 4 droughted, 4 watered, and 4 *sfr8* mutant plants; 2 droughted, 2 watered.

2.6 Statistical analyses

All statistically significant results are shown using asterices, where * indicates $P \leq 0.05$, ** indicates $P \leq 0.01$ and *** indicates $P \leq 0.001$.

2.6.1 Electrolyte leakage assays

All statistical analysis was carried out using R software (R-Core-Team 2016). For electrolyte leakage experiments, percentage electrolyte leakage values from three biological replicate experiments were arcsine-transformed so they followed a normal distribution. A linear mixed effects model (Kuznetsova, Brockhoff & Christensen 2016) with genotype and any treatment (i.e. BA or fucose supplementation) specified as fixed terms, and experiment specified as a random effect. For the fucose and BA supplemented experiments, results were analysed by a two-way ANOVA at each temperature point with an interaction term specified between genotype and fucose/BA. For other electrolyte leakage experiments, a one-way ANOVA was carried out to determine the effect of genotype on the level of electrolyte leakage. Significant differences in leakage between genotypes and/or treatments was assessed using a least-squares means comparison (Lenth 2016) at each temperature point.

2.6.2 Stomatal aperture measurements

Statistical differences between stomatal aperture measurements were ascertained by carrying out a one-way ANOVA followed by a post-hoc Tukey test for pairwise comparisons.

2.6.3 Stomatal conductance measurement

Slopes of lines were compared using an analysis of covariance (ANCOVA).

2.6.4 Root growth assays

Differences in root growth were assessed by carrying out a two-sample student's t-test.

CHAPTER 3

THE *SENSITIVE TO FREEZING8* MUTANT IS DEFICIENT IN RHAMNOGALACTURONAN-II DIMERISATION

3.1 Introduction

In earlier studies, a population of EMS-mutagenized plants was screened to assess sensitivity to freezing temperatures after a period of cold acclimation. This screen highlighted a number of mutants that were designated *sensitive-to-freezing* (*sfr*) that were affected in the development of freezing tolerance (Warren *et al.* 1996b). Mapping of the mutations to the chromosome in several of these mutants (Thorlby *et al.* 1999) led to the discovery of specific roles for *SFR* genes in freezing tolerance. For example, SFR2 is involved in the protection of the chloroplast membrane during freezing (Fourrier *et al.* 2008; Moellering *et al.* 2010), whilst SFR6 is a subunit of the plant mediator complex which plays a role in the control of gene expression during cold acclimation as well as other abiotic stresses (Hemsley *et al.* 2014).

The *Arabidopsis sfr8* mutation was mapped to the *MUR1* gene (Skipsey, Knight and Knight, unpublished) which encodes a GDP-D-mannose-4,6-dehydratase enzyme involved in the production of GDP-L-fucose; the activated form of L-fucose. Specifically, MUR1 converts GDP-deoxy-D-mannose to GDP-deoxy-L-galactose within the fucose biosynthetic pathway (Bonin *et al.* 1997). GDP-L-fucose is incorporated into several cell wall polysaccharides such as hemi-cellulosic xyloglucan (XyG), and pectic rhamnogalacturonans-I and -II (RG-I and RG-II) (Bauer *et al.* 1973; Darvill *et al.* 1978a; Lau *et al.* 1985), as well as arabinogalactan proteins (AGPs) (van Hengel & Roberts 2002) and *N*-linked glycans (Rayon *et al.* 1999). Previous studies have shown that *mur1* mutants are thus deficient in cell-wall fucose (Reiter *et al.* 1993). This deficiency has been shown to result in several morphological phenotypes such as dwarfism, shortened petioles and early flowering time that can be reversed with exogenous application of L-fucose (Reiter *et al.* 1993). The leading hypothesis for these phenotypic traits is thus the impact that the loss of fucose residues has on cell-wall polysaccharides.

Xyloglucan makes up approximately 20% of *Arabidopsis* primary plant cell walls, whilst RG-I constitutes 11% and RG-II makes up approximately 8% (Zablackis *et al.* 1995). Despite constituting a relatively small part of the wall, RG-II is perhaps the most structurally complex

polysaccharide known with its structural attributes being regularly revised (Ndeh *et al.* 2017). Unlike XyG and RG-I, whose fucose residues typically occur at the end of branched chains, RG-II domains contain intrinsic fucose residues that have been shown to be necessary for their structure. As described in Chapter 1, the loss of fucose in *mur1* mutants has an impact on the dimerisation status of RG-II domains within cell walls (O'Neill *et al.* 2001). Either by replacement of the lost L-fucose residue with L-galactose (Reuhs *et al.* 2004) or the complete truncation of side chain A due to L-fucose deficiency (Pabst *et al.* 2013), the *mur1* mutation results in the inability of RG-II monomers to cross-link via a borate-ester linkage between apiose residues of that side chain (O'Neill *et al.* 1996, 2001). Evidence for the decrease in RG-II dimerisation resulting in the phenotypes observed in *mur1* mutants comes from the fact that supplementing plants with boric acid (BA) has the ability to reinstate the majority of dimerisation of RG-II in the cell walls of mutants, as well as restoring wild-type traits such as petiole length and plant size (O'Neill *et al.* 2001). This suggests that RG-II dimerisation controls several phenotypic traits, including some aspects of plant growth. This phenomenon has also been observed in L-galactose deficient tomato plants (Voxeur *et al.* 2011), and L-galactose deficient *Arabidopsis* (Sechet *et al.* 2018), both of which display a decrease in RG-II dimerisation that is restored with BA application. RG-II dimerisation has also been shown to control other structural aspects of the plant cell wall such as pore size (Fleischer *et al.* 1999) and cell wall strength (Ryden *et al.* 2003). In this chapter, the hypothesis that RG-II dimerisation is required for freezing tolerance is addressed experimentally, and the damage that results from the loss of that dimerisation explored.

3.2 Results

3.2.1 Phenotypic assessment of mur *mutants*

The visible appearance of mutants was examined and compared to Col-0 wild type plants under non-stress conditions. The *mur1-1* mutant displayed clear differences to wild type plants in the form of dwarfism and shortened petioles (Figure 3.1A). Plants exhibited an early flowering phenotype (data not shown), with dwarfed inflorescence stems, as has been previously described (Reiter *et al.* 1993). *mur1-1* plants displayed an obvious difference in leaf shape which although observed is rarely alluded to in previous literature; leaves were squat, rounded and crumpled, a trait possibly exaggerated by the shortening of the petioles. Interestingly, *sfr8* plants exhibited similar visible differences to wild type as *mur1-1*, but not to the same extent. Petioles were shortened but not to the extent of *mur1-1* plants, and leaves were rounder but not as short and did not crumple (Figure 3.1A). This could suggest that the amino acid change caused by the

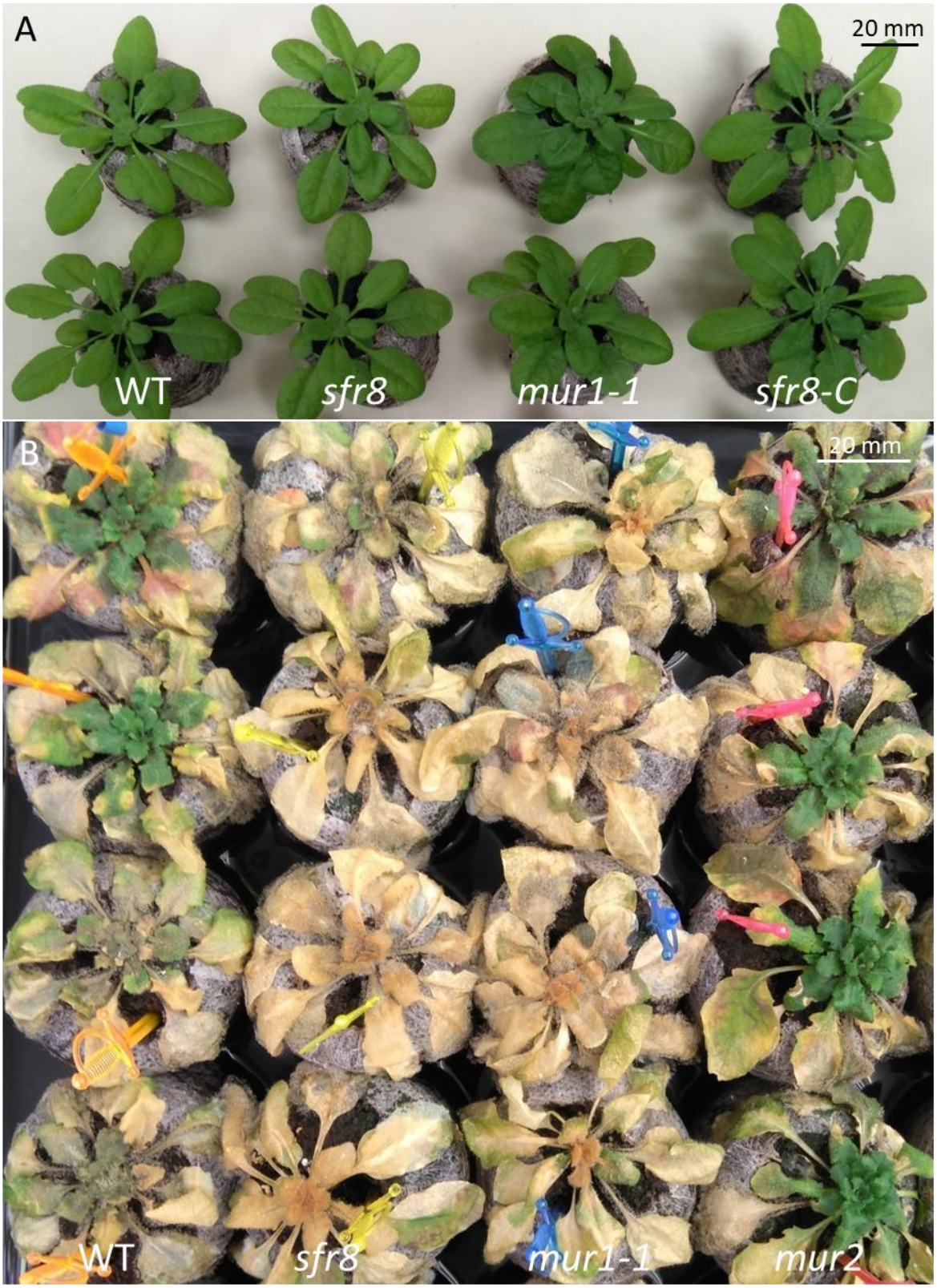

Figure 3.1: Assessment of growth and freezing tolerance in mature wild type and *sfr8, mur1-1, sfr8-C* and *mur2* mutant plants. A) Visual assessment of mature 6-week-old Col-0 wild-type (WT), *sfr8*, *mur1-1* and *sfr8-C* (*sfr8* plants complemented with the *MUR1* gene) plants. **B**) Assessment of Col-0 wild-type (WT), *sfr8*, *mur1-1* and *mur2* plants after exposure to freezing temperatures. 6-week-old plants were exposed to -8.5°C for 24 h, before returning to ambient growth conditions. Recovery was assessed after 7 days.

base substitution in the *MUR1* gene of *sfr8* mutants was less detrimental than that in *mur1-1* (see Appendix A).

In plants of a *sfr8* mutant background complemented with the *MUR1* gene (*sfr8-C*), the appearance of mature plants was similar to wild type, although leaves displayed a slightly more toothed edge, a contrasting appearance to the rounder leaves of *sfr8* and *mur1-1* (Figure 3.1A). A mutant of the xyloglucan specific fucosyl-transferase gene *MUR2* (Vanzin *et al.* 2002) was also assessed as this mutation also resulted in a decrease in cell-wall fucose due to a lack of fucose residues of xyloglucan (Reiter *et al.* 1997). These plants were very similar in appearance to wild type, showing none of the visual phenotypes observed in *sfr8* and *mur1-1* (data not shown), suggesting that xyloglucan fucosylation was not the cause of the visual appearance of *sfr8* and *mur1-1* plants.

3.2.2 Assessment of freezing tolerance

3.2.2.1 Visual assessment of freezing damage

Freezing damage was visually assessed by subjecting mature plants that had been cold acclimated at 5°C to temperatures of -8.5°C for 24 h, with recovery assessed after 7 days. Both the *sfr8* and *mur1-1* mutants showed decreased survival after exposure to freezing, whilst Col-0 wild type and *mur2* plants still showed signs of growth (Figure 3.1B). Assessment of the complemented line of *sfr8*, *sfr8-C*, showed similar freezing tolerance to wild type, as *sfr8-C* plants also maintained signs of growth after freezing (Figure 3.2A). These results suggested that a mutation in the *MUR1* gene was detrimental to freezing tolerance. Thus, a more quantitative assessment was carried out to assess the extent of freezing damage via an electrolyte leakage assay.

3.2.2.2 Electrolyte leakage

Electrolyte leakage (EL) assays were carried out on mature plants to quantitatively assess the damage incurred from exposure to freezing temperatures. Leaf discs were excised from plants and frozen at three different temperatures, and the percentage of electrolytes that leaked from cells taken as a measure of damage. A one-way ANOVA followed by a least-squares means (LSM) comparison was used to assess the significance in differences of EL and thus freezing sensitivity. Results showed that the *sfr8* mutant had a significantly increased leakage of electrolytes than wild type plants at all three temperatures This sensitivity was reversed in the complemented

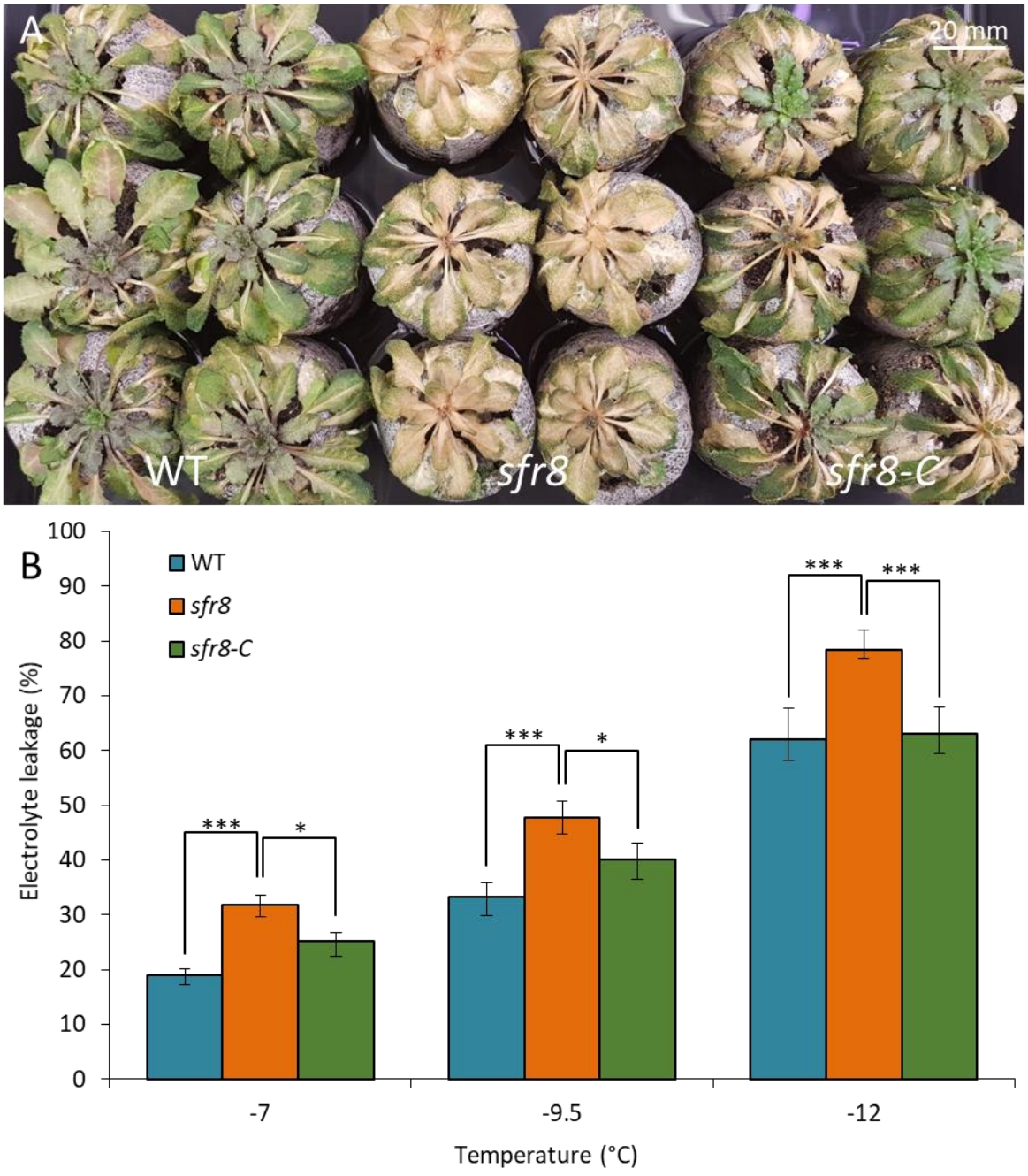

Figure 3.2: Visual freezing damage and electrolyte leakage from leaf discs of wild type, *sfr8* and *sfr8-C* plants. A) Assessment of Col-0 wild-type (WT), *sfr8*, and *sfr8-C* plants after exposure to freezing temperatures. 6-week-old plants were exposed to -8.5°C for 24 h, before returning to ambient growth conditions. Recovery was assessed after 7 days. **B)** Electrolyte leakage in Col-0 wild type (WT), *sfr8* and *sfr8-C* (complemented line) *Arabidopsis thaliana*. Plants were grown for five weeks before acclimating at 5°C for two weeks. Values represent percentage loss of electrolytes from leaf discs when exposed to temperatures of -7, -9.5 and -12°C. Each data point represents the average of three separate biological replicate experiments. Each experiment used six replicate tubes per genotype per temperature, with three leaf discs per tube. Arcsine transformed percentage leakage data were analysed by a least-squares means comparison at each temperature point (*, $P \leq 0.05$, ***, $P \leq 0.001$). Error bars represent +/- 1 SE calculated from arcsine transformed data and then converted back to percentage data.

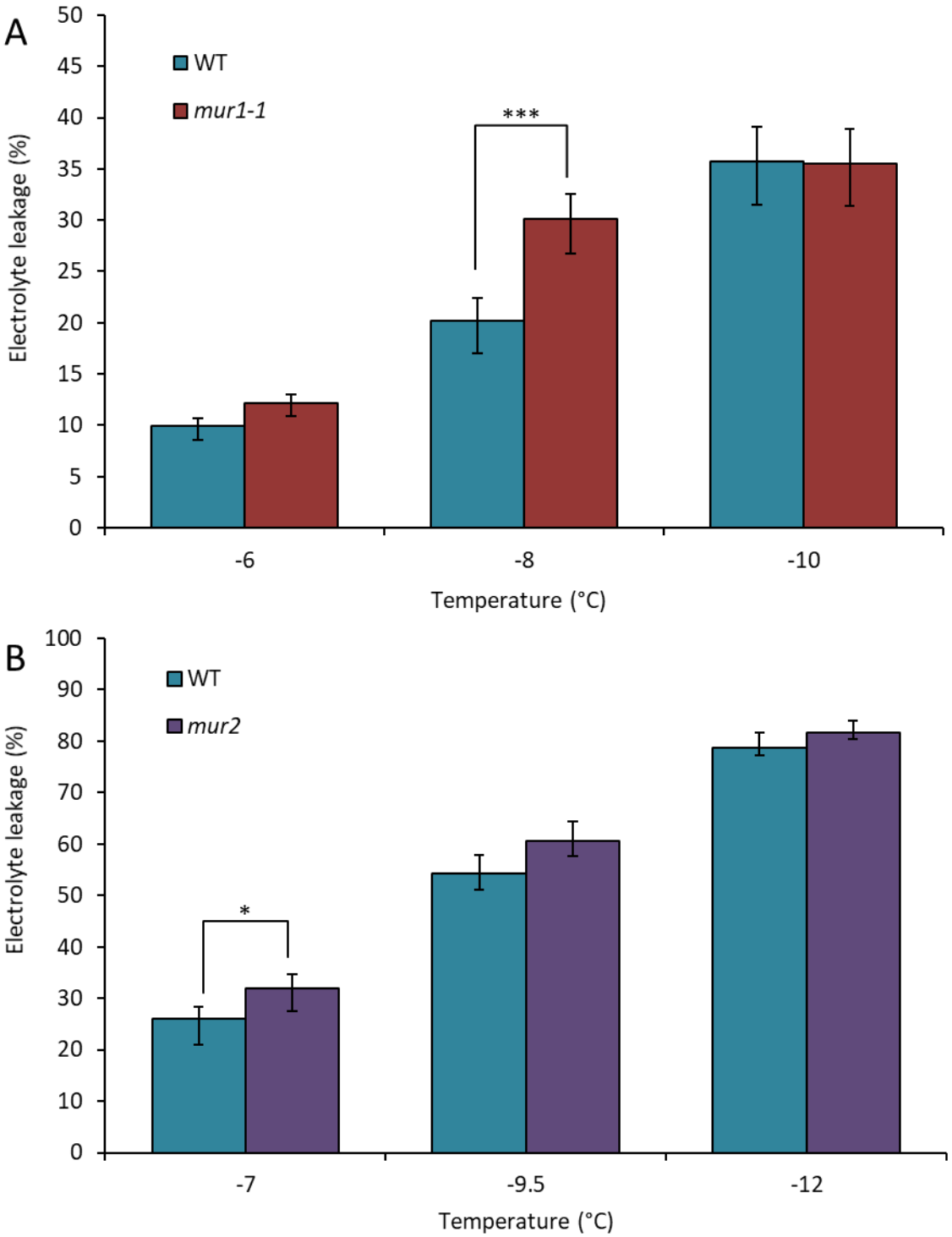

Figure 3.3: Electrolyte leakage from leaf discs of wild-type, *mur1-1* and *mur2* mutant plants. Electrolyte leakage in Col-0 wild type (WT) and *mur1-1* **(A)** or *mur2* **(B)** mutant *Arabidopsis thaliana.* Plants were grown for five weeks before acclimating at 5°C for two weeks. Values represent percentage loss of electrolytes from leaf discs when exposed to temperatures of -6, -8 and -10°C **(A)** or -7, -9.5 and -12°C **(B)**. Each data point represents the average of three separate biological replicate experiments. Each experiment used six replicate tubes per genotype per temperature, with three leaf discs per tube. Arcsine transformed percentage leakage data were analysed by a least-squares means comparison at each temperature point (*, $P \leq 0.05$, *** $P \leq 0.001$). Error bars represent +/- 1 SE calculated from arcsine transformed data and then converted back to percentage data.

line, *sfr8-C*, which had leakage levels significantly lower than *sfr8* and much closer to that of wild-type values (Figure 3.2B; one-way ANOVA/LSM, ***, $P \leq 0.001$, *, $P \leq 0.05$).

An increase in EL and thus freezing sensitivity was also observed in *mur1-1* plants, which showed significantly higher EL levels than wild type at exposure to -8°C (Figure 3.3A; one-way ANOVA/LSM, ***, $P \leq 0.001$). An EL assay carried out on *mur2* plants showed no increase in leakage compared to wild-type plants at two of the three temperature measured, and only a slight increase in leakage at -7°C (Figure 3.3B, one-way ANOVA/LSM, $P = 0.047$). This significance was much lower than that observed in *sfr8* and *mur1-1* mutant plants, suggesting that the *mur2* mutation did not impact on freezing tolerance to the same extent that the *mur1* mutation did. Following this finding that plants with a mutation in the *MUR1* gene displayed a freezing-sensitive phenotype, experiments were carried out to assess what attributes of *sfr8* and *mur1-1* were the cause of this.

3.2.3 Cell-wall fucose

3.2.3.1 Measurement of cell-wall fucose in mur *mutants*

Previous analysis of *mur1* and *mur2* mutants highlighted a decrease in cell-wall fucose content (Reiter *et al.* 1997). Thus, the cell-wall fucose levels of *sfr8* mutant plants were assessed in comparison to wild type, *mur1-1*, *mur2* and the complemented line to highlight any possible links with freezing sensitivity. A plant cell-wall extract was obtained from two-week-old seedlings and hydrolysed to monosaccharides with trifluoracetic acid. The concentration of fucose was measured using GC-MS and values expressed as percentages of wild-type cell-wall fucose. Results showed that both *sfr8* and *mur1-1* had decreased cell-wall fucose levels in comparison to wild type, with a decrease to approximately 27% for *sfr8* and 20% for *mur1-1*. A decrease is also seen in the *mur2* mutant, although not to the same extent as the *mur1* mutants, with approximately 40% of wild-type fucose levels (Figure 3.4A). Cell-wall fucose levels were much closer to wild-type levels in the complemented line, containing approximately 80% fucose of wild-type levels (Figure 3.4B).

3.2.3.2 Fucose supplementation of sfr8

In order to assess if the decrease in fucose observed in *sfr8* plants affected the increase in freezing sensitivity, an EL leakage assay was carried out on plants that had been supplemented with fucose during growth. Wild type and *sfr8* plants were sprayed with 10 mM fucose

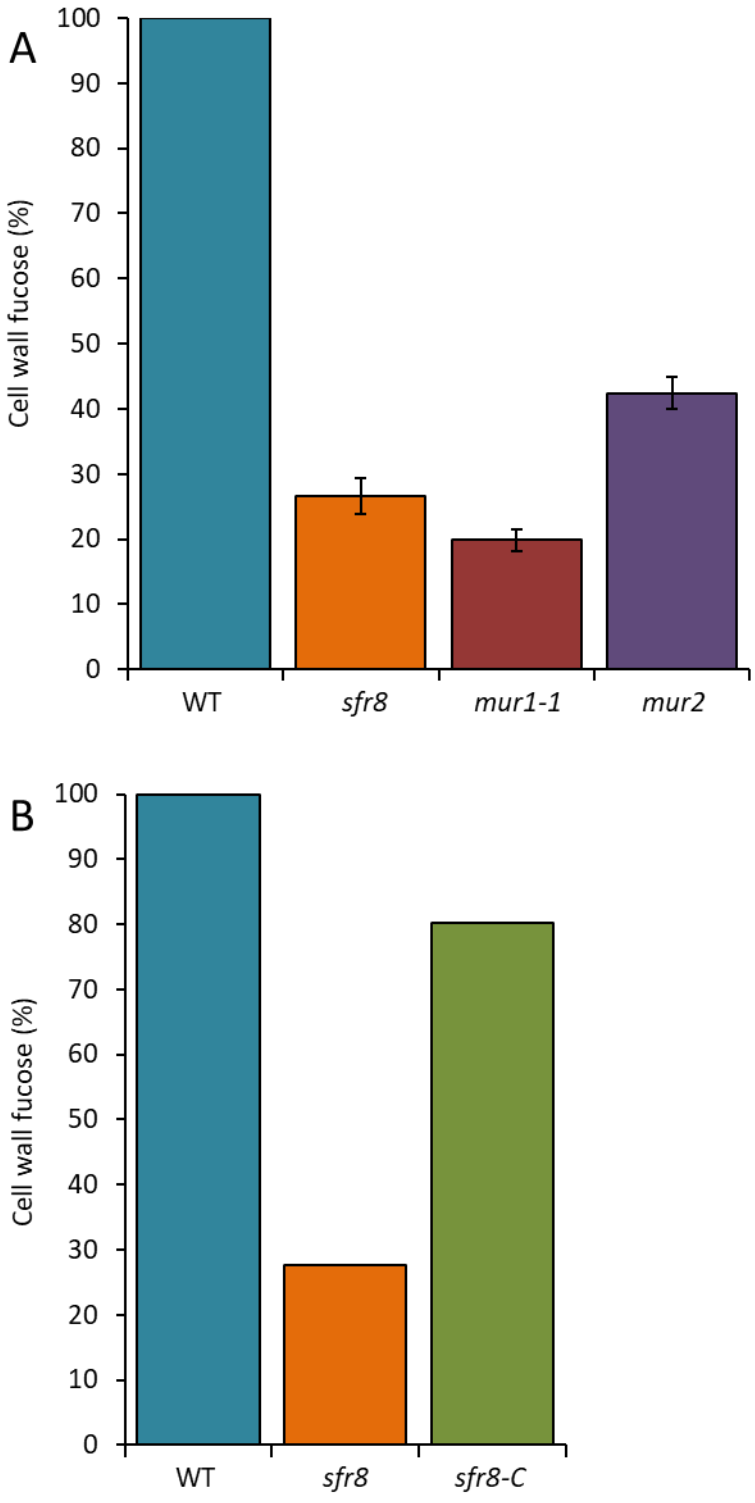

Figure 3.4: Cell-wall fucose content in *mur1-1, sfr8, mur2* and *sfr8-C* plants in comparison to wild type. Measurement of cell-wall fucose levels by GC-MS analysis of plant cell wall extract from Cold-0 wild-type (WT), *sfr8, mur1-1, mur2* and *sfr8-C Arabidopsis thaliana*. Seedlings were harvested after 2 weeks growth on ½ MS. Results are an average of three separate experiments with three repeats for each genotype **(A)** or one experiment with three repeats for each genotype **(B)**. Values are expressed as a percentage of WT cell wall fucose levels. Error bars represent +/- 1 S.E.

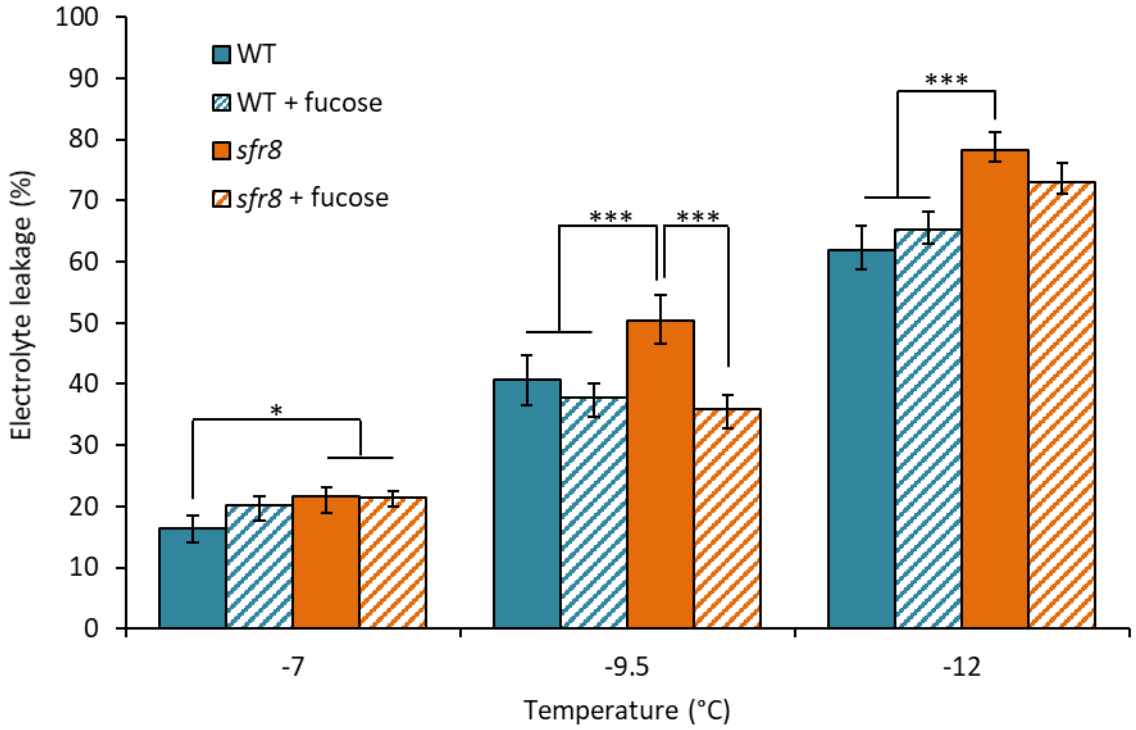

Figure 3.5: Electrolyte leakage from leaf discs of wild and *sfr8* supplemented with fucose. Electrolyte leakage in Col-0 wild type (WT) and *sfr8 Arabidopsis thaliana* with and without L-fucose supplementation. Plants were grown for five weeks before acclimating at 5°C for two weeks. Values represent percentage loss of electrolytes from leaf discs when exposed to temperatures of -7, -9.5 and -12°C. Each data point represents the average of three separate biological replicate experiments. Each experiment used six replicate tubes per genotype/treatment per temperature, with three leaf discs per tube. Arcsine transformed percentage leakage data were analysed by a least-squares means comparison at each temperature point (*, $P \leq 0.05$, ***, $P \leq 0.001$). Error bars represent +/- 1 SE calculate from arcsine transformed data and then converted bac to percentage data.

throughout five weeks of growth and two weeks of cold acclimation to replace that lost as a result of the mutation. This supplementation had the ability to reverse the increased EL of *sfr8* at -9.5°C, as supplemented plants had significantly lower leakage levels than non-supplemented *sfr8* plants. No significant effect on EL was seen in wild type plants supplemented with fucose. A two-way ANOVA was used to test significance in order to account for the interacting effects of genotype and fucose treatment on EL (Figure 3.5; two-way ANOVA/LSM, *, $P \leq 0.05$, ***, $P \leq 0.001$). These results suggest fucose levels are in some way linked to freezing tolerance, as a decrease in fucose is correlated with an increase in freezing sensitivity.

3.2.3.3 2F-fucose treatment of wild type seedlings

A chemical approach to decrease cell-wall fucose content was undertaken through the use of an inhibitor of fucosylation to support the initial genetics-based approach used. The small molecule 2-fluoro-L-fucose (2F-fucose) competitively inhibits the fucosylation of polysaccharides resulting in a reduced cell-wall fucose content (Villalobos, Yi & Wallace 2015). This inhibitor was used on wild type seedlings to simulate the decreased cell wall fucose content observed in *sfr8* plants. Wild type seedlings were grown on MS agar plates supplemented with DMSO as a control (the inhibitor was dissolved in DMSO) and varying concentrations of 2F-fucose for two weeks. EL assays showed a dose-dependent increase in EL with treatment of the inhibitor at all three temperatures (Figure 3.6A). A significant increase in EL was seen at -3°C for the two higher concentrations of 2F-fucose (one-way ANOVA/LSM, $P \leq 0.001$), and for all three concentrations at the two lower temperatures (one-way ANOVA/LSM $P \leq 0.001$ or 0.01) (Figure 3.6A). This provided further evidence that fucose is essential for normal plant freezing tolerance.

3.2.3.4 Assessment of root growth

Previous studies have shown that plants treated with the 2F-fucose inhibitor of fucosylation display a decrease in root growth and root morphology (Dumont *et al.* 2015; Villalobos *et al.* 2015). This phenotype was also observed in this study, with a concentration-dependent decrease in root growth (data not shown). Since chemically decreasing cell-wall fucose content resulted in a decrease in root growth, the growth of *sfr8* roots was measured to see if the decrease in fucose had the same effect. Seven-day-old seedlings of wild type and *sfr8* were transferred to 1.2% agar and grown vertically for 5 days. Results showed a significant decrease in root growth in *sfr8* seedlings compared to wild type (Figure 3.6B, two-way t-test, $P \leq 0.001$), suggesting a decrease in cell-wall fucose does affect root growth.

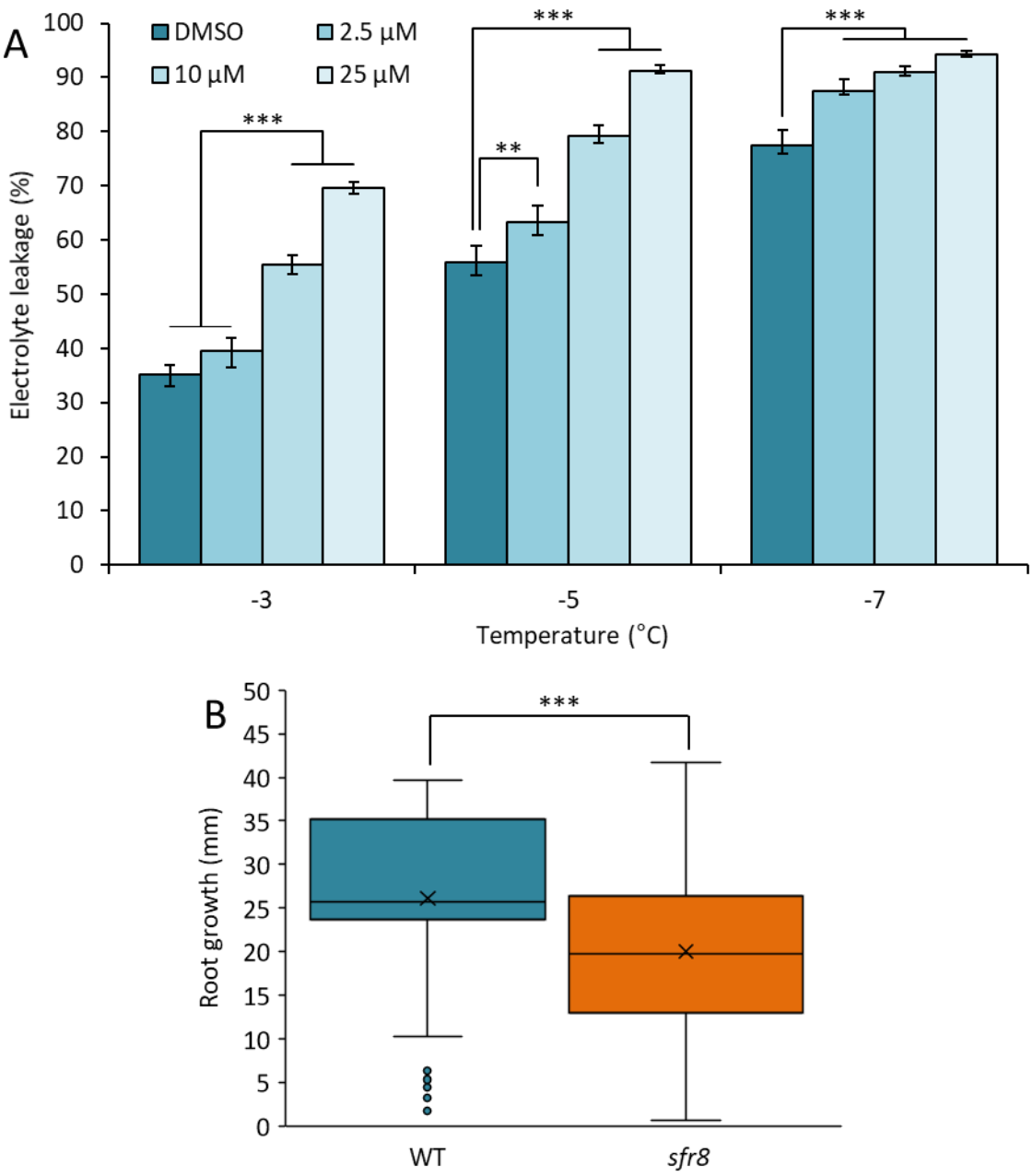

Figure 3.6: Electrolyte leakage from wild type seedlings treated with 2F-fucose, and analysis of root growth of wild type and *sfr8*. A) Electrolyte leakage in Col-0 wild type (WT) *Arabidopsis thaliana.* Seedlings were grown for two weeks on ½ MS agar plates supplemented with DMSO, 2.5, 10 or 25 µM fucosyl inhibitor. Values represent percentage loss of electrolytes from seedlings when exposed to temperatures of -3, -5 and -7°C. Each data point represents the average of three separate biological replicate experiments. Each experiment used six replicate tubes per treatment per temperature. Arcsine transformed percentage leakage data were analysed by a least-squares means comparison at each temperature point (**, $P \leq 0.01$, ***, $P \leq 0.001$). Error bars represent +/- 1 SE calculated from arcsine transformed data and then converted back to percentage data. **B)** Root growth of Col-0 wild type (WT) and *sfr8* seedlings. Seedlings were grown on ½ MS medium with 0.8% agar for 7 days, before being transferred to 1.2% agar and grown vertically. Roots were measured 5 days after transfer. For boxplots, coloured box represents inter-quartile range with centre line representing median, and 'x' representing mean. Bars represent maximum and minimum values, separate data points represent outliers. Data were analysed using a two-sample t-test (***, $P \leq 0.001$).

3.2.4 Cell-wall rhamnogalacturonan-II dimerisation

Assessment of *mur1* mutants in earlier studies highlighted a significant impact of the decrease in fucose for the pectic polysaccharide rhamnogalacturonan-II. As described in section 3.1, RG-II contains a fucose residue that is essential for dimerisation of RG-II domains within the cell wall, as *mur1-1* mutants display a decrease in RG-II cross-linking that can be reversed by supplementing plants with L-fucose during growth (O'Neill *et al.* 2001). The dimerisation status of plant cell-wall RG-II was therefore assessed in *sfr8* plants via the method of polyacrylamide gel electrophoresis (PAGE) previously described (Chormova *et al.* 2014a). A cell-wall extract was obtained from leaves of 5-week-old wild type, *sfr8* and *mur1-1* plants. The extract was digested with endo-polygalacturonase (EPG) and the RG-II monomer and dimer separated via PAGE analysis and visualised by silver staining. RG-II monomer and dimer standards purified from sugar beet were used for comparisons. The results showed that the majority of RG-II in the cell walls of wild type plants was dimerised. The *sfr8* lane showed an increase in the presence of RG-II monomer, and a slight decrease in the size of the RG-II dimer band, suggesting that the loss of cell-wall fucose resulted in a decrease of RG-II dimerisation within the cell wall (Figure 3.7). Analysis of the *mur1-1* mutant also showed a decrease in the size of the dimer band, consistent with previous observations (O'Neill *et al.* 2001). There was also a monomer band present but interestingly not at the intensity of that seen for *sfr8* (Figure 3.7A).

As described in section 3.1, the observed decrease in RG-II dimerisation in *mur1* mutants was shown to be reversible by supplementing plants with boric acid (BA) (O'Neill *et al.* 2001). To see if this was possible in *sfr8* plants, PAGE analysis of digested cell-wall extracts was carried out on wild type, *sfr8* and *mur1-1* plants that had been supplemented with BA during growth. The results showed that BA was able to restore the presence of primarily dimerised RG-II in the *sfr8* mutant, as the monomer band had almost disappeared (Figure 3.7A). This did not appear to be the case for the *mur1-1* plants supplemented with BA, as the size and intensity of the RG-II monomer and dimer bands did not differ from those of the non-BA-supplemented plants (Figure 3.7A). This could suggest that RG-II from the *sfr8* and *mur1-1* mutants differed in their ability to dimerise with BA supplementation.

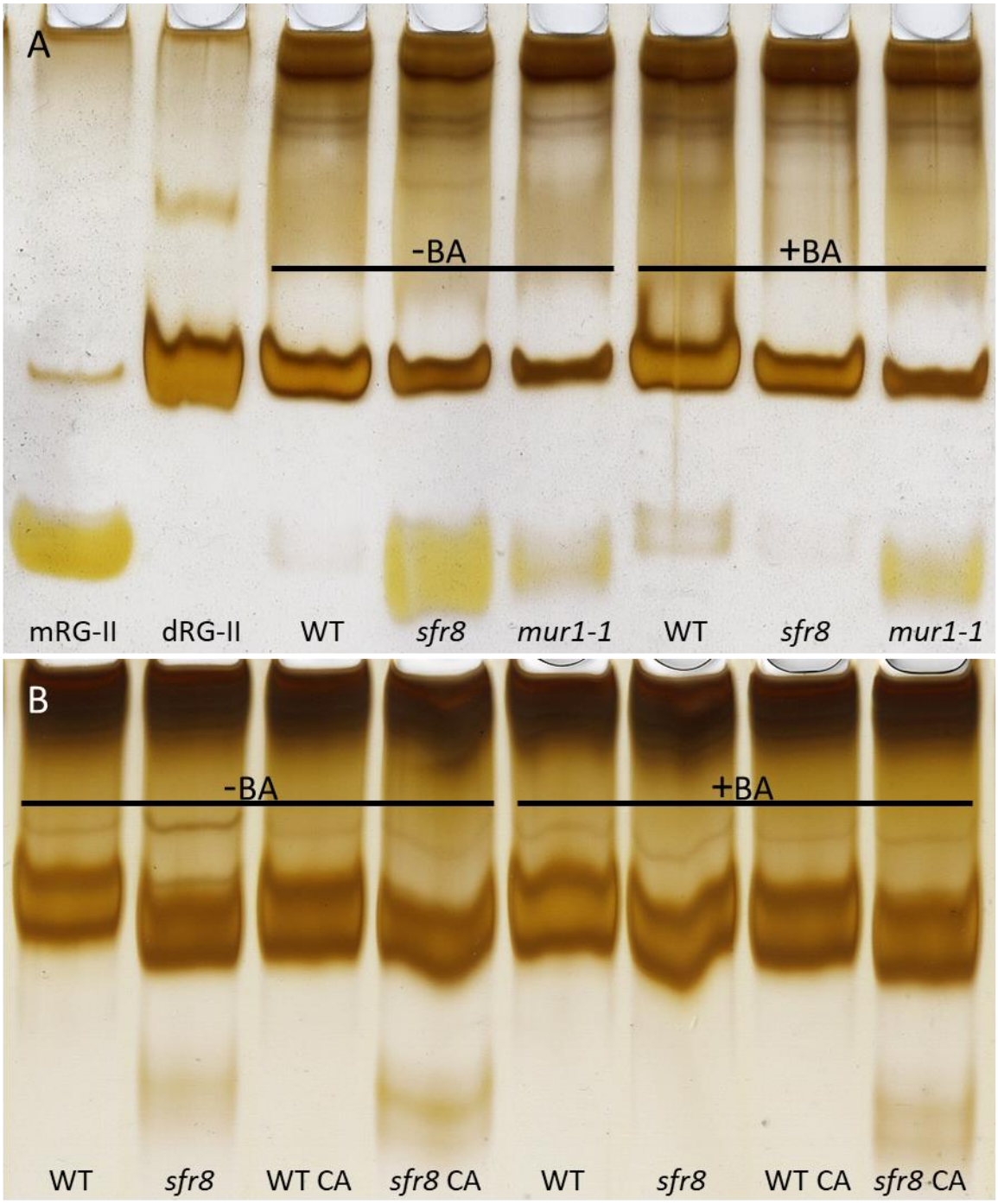

Figure 3.7: PAGE analysis of cell-wall extracts from wild type, *sfr8* and *mur1-1* plants. Polyacrylamide gel electrophoresis of endo-polygalacturonase digested cell wall extracts from 5-week-old *Arabidopsis thaliana.* Gels were stained with silver nitrate and purified RG-II standards show where monomer (mRG-II) and dimer (dRG-II) bands of rhamnogalacturonan-II should appear. **A)** Col-0 wild type (WT), *sfr8* and *mur1-1* plants with an without boric acid (BA) supplementation. **B)** Col-0 wild type and *sfr8* with and without BA supplementation, before and after 2 weeks of cold acclimation (CA) at 5°C.

3.2.5 Assessment of freezing damage with boric acid supplementation

3.2.5.1 BA supplementation of sfr8 *plants*

With the finding that BA supplementation could restore RG-II dimerisation in the *sfr8* mutant, EL assays were carried out on plants that had been supplemented with BA during growth to assess the necessity of dimerised RG-II for freezing tolerance. Assays carried out on non-acclimated plants showed no significant difference between *sfr8* and *sfr8* supplemented with BA, although a significant difference between WT and *sfr8* was still observed (Figure 3.8A; two-way ANOVA/LSM, ***, $P \leq 0.001$). Assays were then carried out on wild type and *sfr8* plants with and without BA supplementation that had also been cold acclimated for two weeks at 5°C. Interestingly, these experiments did show a difference in EL, with leakage of BA supplemented *sfr8* plants significantly lower than those that were not treated with BA at all three temperatures (Figure 3.8B; two-way ANOVA/LSM, **, $P \leq 0.01$, ***, $P \leq 0.001$). This showed that BA supplementation was able to reverse the freezing-sensitive phenotype in *sfr8* plants, but only after a period of cold acclimation. Interestingly, analysis of the dimerisation status of RG-II in wild type and *sfr8* plants after cold acclimation, with and without BA supplementation suggested that RG-II monomer accumulated during cold acclimation, as a monomer band was present in the *sfr8* sample even when plants were supplemented with BA (Figure 3.7B). This may hint that RG-II monomer is important for freezing tolerance, perhaps as a borate-ester cross-link between the cell wall and plasma membrane, which has been shown to occur (Voxeur & Fry 2014). It may be that up-regulation of the monomer during cold acclimation is required for freezing tolerance.

3.2.5.2 BA supplementation of 2F-fucose treated seedlings

In *sfr8* mutant plants, BA was able to restore RG-II dimerisation and freezing tolerance. Previous research into fucosylation inhibitors showed that treatment with BA was able to restore the root growth phenotype of 2F-fucose treated plants, suggesting that the phenotypic defects observed are as a result of a loss of RG-II dimerisation, similar to the *sfr8* mutant (Dumont *et al.* 2015; Villalobos *et al.* 2015). Thus, it was tested whether BA could reverse the freezing sensitivity observed in 2F-fucose treated seedlings. The concentration of 10 µM 2F-fucose was chosen as this was the lowest inhibitor concentration that showed a significant increase in electrolyte leakage at all three temperatures (Figure 3.6A). Treatments were as follows; 0.1% DMSO, 0.1% DMSO + 0.75 mM BA, 10 µM 2F-fucose and 10 µM 2F-fucose + 0.75 mM BA. DMSO-treated wild-type seedlings were used as the control as DMSO was the solvent for the fucosylation inhibitor

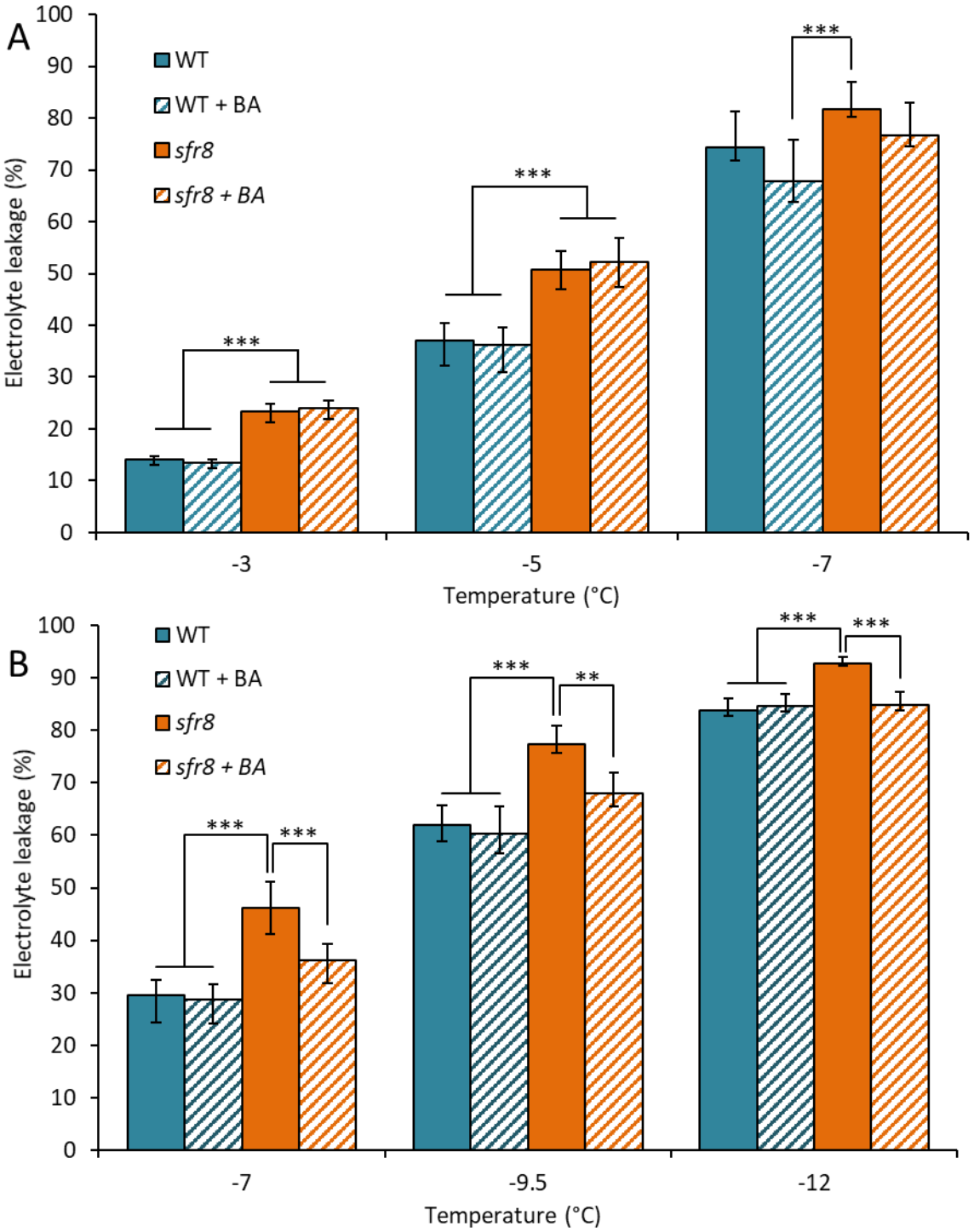

Figure 3.8: Electrolyte leakage from leaf discs of wild type and *sfr8* supplemented with BA. Electrolyte leakage in Col-0 wild type (WT) and *sfr8 Arabidopsis thaliana* with and without boric acid (BA) supplementation. Plants were used in the experiment at 5-weeks-old **(A)** or were grown for five weeks before acclimating at 5°C for two weeks **(B)**. Values represent percentage loss of electrolytes from leaf discs when exposed to temperatures of -3, -5 or -7°C **(A)** or -7, -9.5 and -12°C **(B)**. Each data point represents the average of three separate biological replicate experiments. Each experiment used six replicate tubes per genotype/treatment per temperature, with three leaf discs per tube. Arcsine transformed percentage leakage data were analysed by a least-squares means comparison at each temperature point (**, $P \leq 0.01$, ***, $P \leq 0.001$). Error bars represent +/- 1 SE calculated from arcsine transformed data and then converted back to percentage data

and thus the concentration of DMSO also present in the 2F-fucose treated seedlings. Analysis of root growth showed that BA supplementation was able to partially reverse the decrease in root length resulting from 2F-fucose treatment (Figure 3.9E), as previously described (Dumont *et al.* 2015; Villalobos *et al.* 2015). Following this pattern, an initial EL experiment carried out showed that the increase in EL observed in 2F-fucose treated plants was reversible with BA treatment, as EL was reduced to wild-type levels in 2F-fucose and BA treated seedlings (Figure 3.9A). However, the assay was repeated a further three times, and although EL of 2F-fucose + BA treated seedlings was shown to be less than that of 2F-fucose treated seedlings in all experiments, an increase in EL of the DMSO treated seedlings as well as the 2F-fucose treated ones was also observed, even though seedlings treated with DMSO and BA did not show an increased EL (Figure 3.9B-D).

The increase in EL observed in seedlings treated with DMSO could be a result of the increased membrane permeability effect of DMSO (Notman *et al.* 2006). To see if DMSO's suggested effects on membrane permeability resulted in an increased EL after freezing, an EL assay was carried out on seedlings with and without DMSO treatment. A third treatment of autoclaved DMSO was also used to see if this process affected DMSO stability or mode of action. However, no differences in EL were observed between the three treatments, suggesting that DMSO treatment did not impact upon EL from seedlings after freezing (Figure 3.10A).

3.2.5.3 RG-II dimerisation status in 2F-fucose treated plants

To see whether freezing sensitivity was correlated with a decrease in the dimerisation of RG-II in fucosylation inhibitor-treated plants, RG-II gel analysis was carried out on WT seedlings with the four different treatments described in section 3.2.5.2. A cell-wall extract was obtained from the same batch of two-week-old seedlings as those used in the EL for Figure 3.9D, digested with EPG and run on a polyacrylamide gel. The bands present after silver staining show that all samples contained RG-II dimer, although perhaps slightly less dimer was present in the two treatments with 2F-fucose (Figure 3.10B). The only sample to show clear presence of the RG-II monomer was that derived from 2F-fucose plus BA treated seedlings. This is contrary to findings by Dumont *et al.* (2015) who showed that treatment with 2F-fucose resulted in a loss of dimerised RG-II and an increase in the RG-II monomer. These discrepancies may have arisen due to differences in the experimental protocol – further analysis is required to verify if RG-II dimerisation is disrupted in 2F-fucose-treated plants, and if this is reversible with BA supplementation.

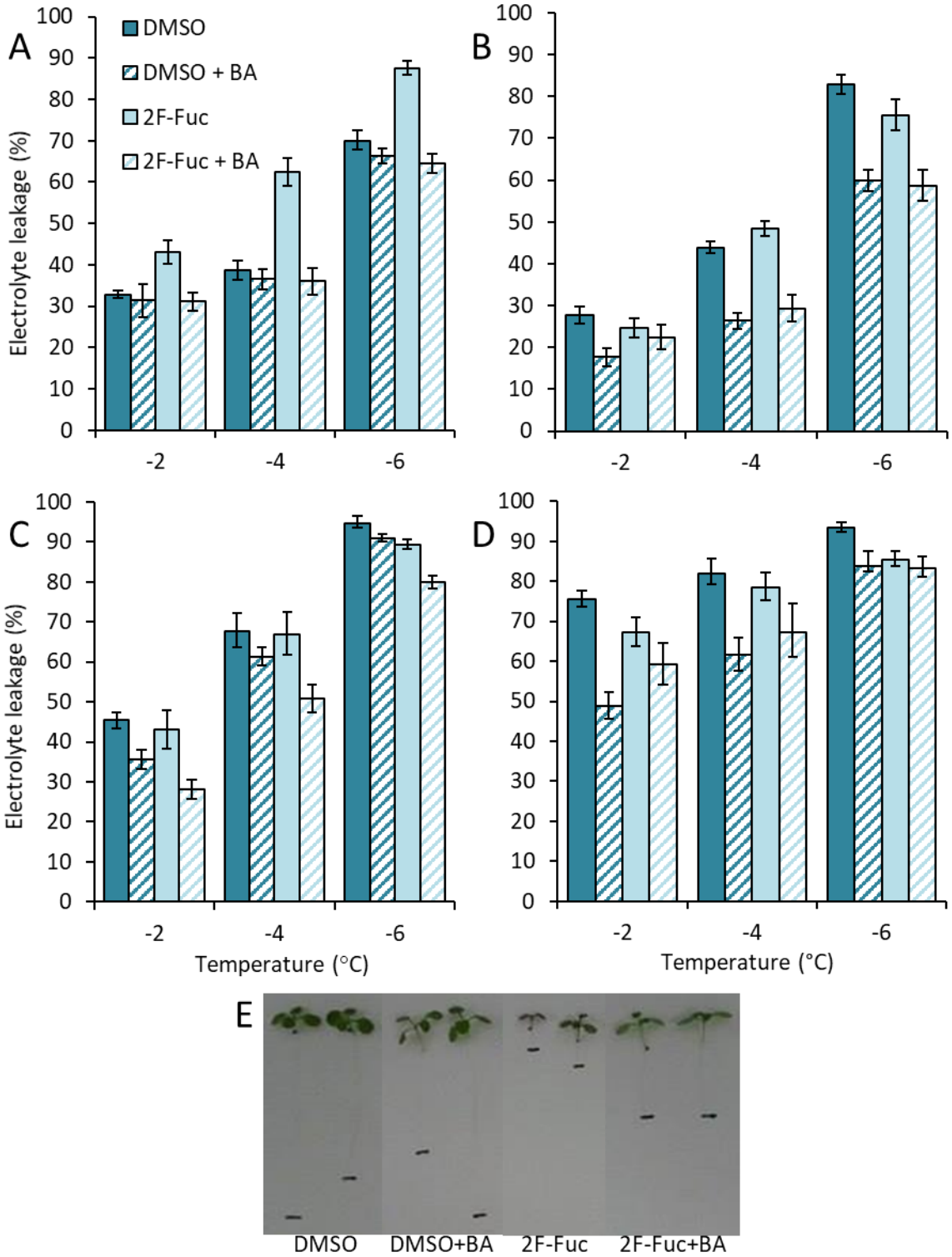

Figure 3.9: Electrolyte leakage from wild type seedlings treated with 2F-fucose and BA. A-D) Repeat electrolyte leakage assays of Col-0 wild type (WT) *Arabidopsis thaliana.* Seedlings were grown for two weeks on ½ MS agar plates supplemented with 0.1% DMSO, 0.1% DMSO and 7.5 µM boric acid (BA), 10 µM fucosylation inhibitor (2F-Fuc) or 10 µM 2F-Fuc and 7.5 µM BA. Values represent percentage loss of electrolytes from seedlings when exposed to temperatures of -2, -4 and -6°C. Each experiment used six replicate tubes per treatment per temperature. Error bars represent +/- 1 SE calculated from arcsine transformed data and then converted back to percentage data. **E)** Differences in root length of DMSO, DMSO + BA, 2F-Fuc and 2F-Fuc + BA treated seedlings. Black line indicates root tip.

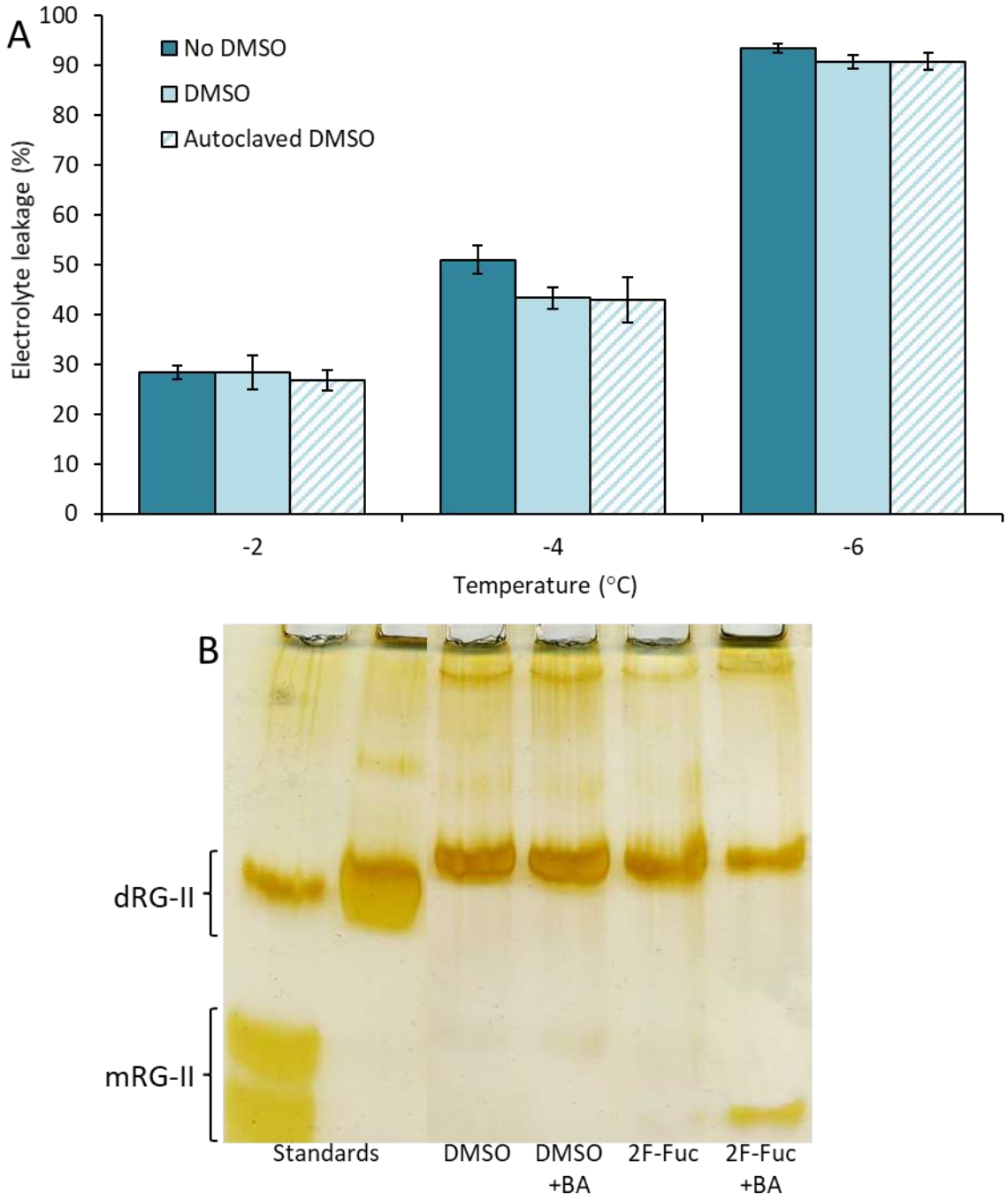

Figure 3.10: Electrolyte leakage from DMSO treated seedlings, and assessment of RG-II dimerisation in 2F-fucose and BA treated seedlings. A) Electrolyte leakage assay of Col-0 wild type (WT) *Arabidopsis thaliana.* Seedlings were grown for two weeks on ½ MS agar plates supplemented with DMSO, autoclaved DMSO or no DMSO. Values represent percentage loss of electrolytes from seedlings when exposed to temperatures of -2, -4 and -6°C. The experiment used six replicate tubes per treatment per temperature. Error bars represent +/- 1 SE calculated from arcsine transformed data and then converted back to percentage data. **B)** Polyacrylamide gel electrophoresis of endo-polygalacturonase digested cell wall extracts. Two-week-old *Arabidopsis thaliana* Col-0 wild type (WT) seedlings were grown on ½ MS agar supplemented with 0.1% DMSO, 0.1% DMSO and 7.5 µM boric acid (BA), 10 µM fucosylation inhibitor (2F-Fuc) or 10 µM 2F-Fuc and 7.5 µM BA. Gels were stained with silver nitrate and purified RG-II standards show where monomer (mRG-II) and dimer (dRG-II) bands of rhamnogalacturonan-II should appear.

3.2.6 Assessment of a bor1 *mutant*

3.2.6.1 Electrolyte leakage

The necessity of boric acid for freezing tolerance was assessed by carrying out an electrolyte leakage assay on plants with a mutation in *BOR1,* a gene encoding a boron efflux transporter involved in loading boron ions into the xylem under boron-limiting conditions. As boron is essential for RG-II dimerisation, a mutation that reduces the amount of boron available to the plant should also reduce RG-II dimerisation, as has been previously observed in the *bor1-1* mutant (Noguchi *et al.* 2003). However, an electrolyte leakage assay showed no significant differences between wild type and *bor1-1* mutant plants at any of the three temperatures tested (Figure 3.11A). To ensure that the mutation had the hypothesised effect on RG-II i.e. a decrease in cross-linking due to the absence of boron, PAGE analysis was carried out on wild type and *bor1-1* plant cell walls.

3.2.6.2 RG-II dimerisation status

The RG-II dimerisation status of the *bor1-1* mutant was assessed via PAGE analysis. A cell wall extract was obtained from wild type and *bor1-1* plants, digested with EPG and run on a polyacrylamide gel. The RG-II dimer band was present in both samples, as was a small RG-II monomer band. The size and intensity of the bands for both samples was very similar, suggesting that there was no decrease in RG-II dimerisation in the *bor1-1* mutant (Figure 3.11B). This suggests that the plants did not experience a great enough boron deficiency, as under non-limiting boron conditions, *bor1-1* mutants had near wild type levels of dimerised RG-II (Noguchi *et al.* 2003), similar to that shown here. If RG-II dimerisation and freezing tolerance are correlated, this could explain why no increase in freezing sensitivity was observed.

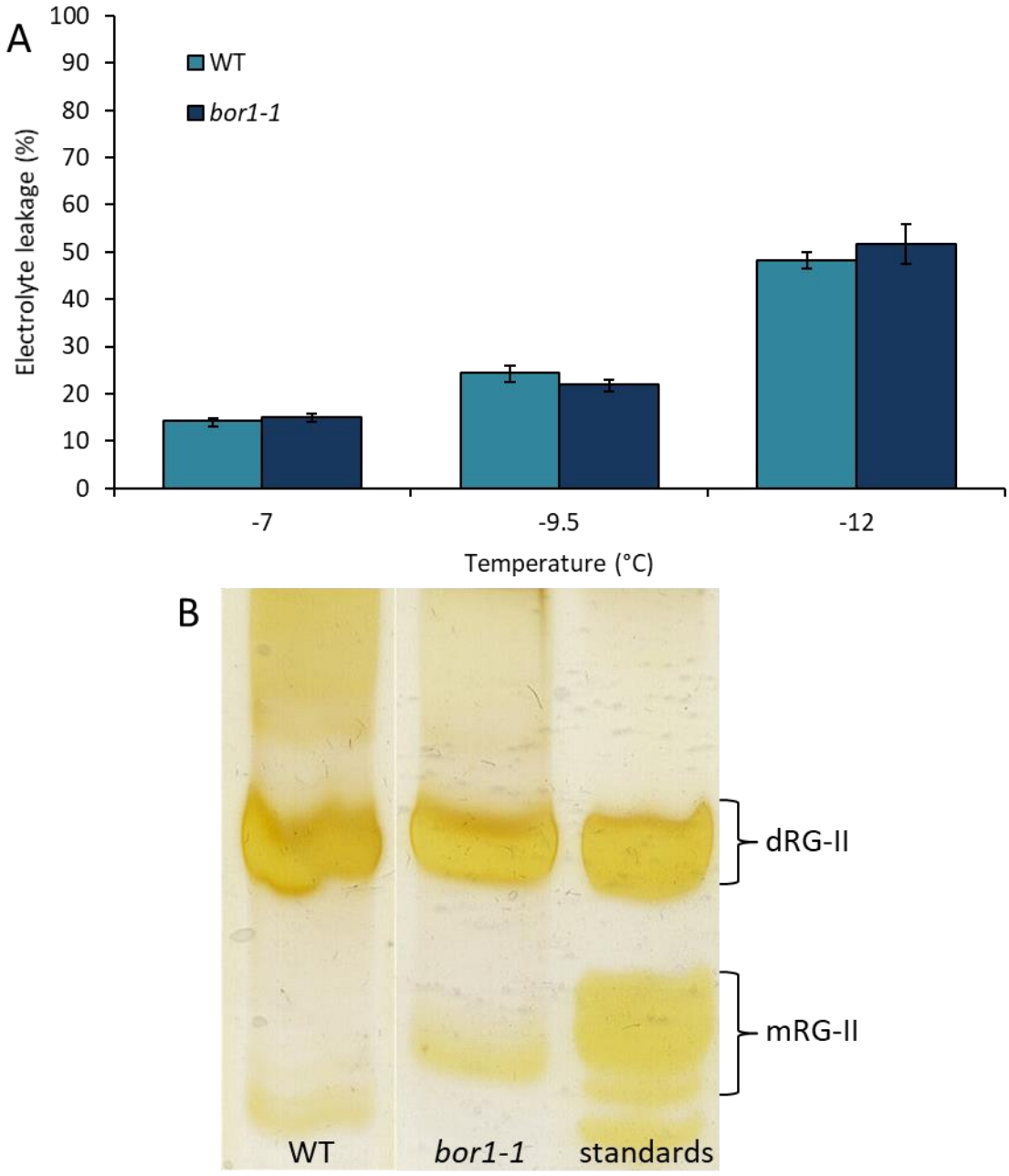

Figure 3.11: Electrolyte leakage and RG-II dimerisation from wild type and *bor1-1* mutant plants. A) Electrolyte leakage in Col-0 wild type (WT) and *bor1* mutant *Arabidopsis thaliana.* Plants were grown for five weeks before acclimating at 5°C for two weeks. Values represent percentage loss of electrolytes from leaf discs when exposed to temperatures of -7, -9.5 and -12°C. Each data point represents the average of three separate biological replicate experiments. Each experiment used six replicate tubes per genotype per temperature, with three leaf discs per tube. A least-squares means comparison of arcsine transformed data at each temperature point showed no significant difference in electrolyte leakage. Error bars represent +/- 1 SE calculated from arcsine transformed data and then converted back to percentage data. **B)** Polyacrylamide gel electrophoresis of endo-polygalacturonase digested cell wall extracts from 5-week-old *Arabidopsis thaliana* Col-0 wild type (WT) and *bor1-1* plants. Gels were stained with silver nitrate and purified RG-II standards show where monomer (mRG-II) and dimer (dRG-II) bands of rhamnogalacturonan-II should appear.

3.2.7 Genotyping the sfr8 *mutant*

An observation that some of the *sfr8* plants did not display the phenotypic traits associated with a mutation in the *mur1* gene led to an investigation into the *sfr8* seed stock. As shown in Figure 3.12A, some plants (1 to 3) did not display the distinctive leaf shape and shortened petiole length normally observed (e.g. plants 4 to 7). It was possible that there was some phenotypic variation between the mutants, as plants 4 to 7 did display differences in the intensity of the leaf shape phenotype. To see if this was the case, the seven plants chosen along with a wild type plant were genotyped by sequencing part of the *MUR1* gene. The *sfr8* mutation is identified as a base change from G to A at nucleotide 629 of the gene (Bonin *et al.* 1997) (Appendix A). This base change was observed in the four plants exhibiting a typical *sfr8* appearance, but not in the three plants that were within the *sfr8* stock but did not resemble *sfr8* plants (Figure 3.12B). This highlighted a possible contamination within the *sfr8* seed stock.

To measure the extent of this contamination, bulk sequencing was carried out using 50 seedlings from the *sfr8* stock used for most of the experiments in this study (A), and a previous stock that was used in earlier experiments (such as the non-acclimated BA supplementation EL assay) and for bulking (i.e. it is the parent of A) (B). Sequencing of Col-0 wild type plants shows that base 629 is a G, whilst sequencing of *sfr8* stock B shows that the nucleotide present at base 629 is an A (Figure 3.13A and B). However, sequencing of *sfr8* stock A shows a mixture of bases A and G at position 629, suggesting either that a mixture of wild type and *sfr8* plants were present in the 50 seedlings used for analysis, or that they are all heterozygous (this is unlikely due to sequencing of individual plants displaying no heterozygosity) (Figure 3.13C). This suggests that experiments carried out using stock A of *sfr8* seeds would have wild type plants present at around 50%. Experiments comparing wild type and *sfr8* plants are unlikely to have been significantly affected by this contamination, as plants carrying the mutation were identifiable due to the morphological traits of *sfr8.* Even if wild type plants were chosen for EL assays, results still show significant differences between wild type and *sfr8*, so it may even be the case that these significances are underestimated. In experiments where reversal of the phenotype was possible, e.g. in fucose and BA supplemented experiments, it is difficult to say whether those plants appearing to show a reversed phenotype were actually wild type plants.

To verify if this was the case, RG-II analysis was carried out on known *sfr8* plants from stock B supplemented with BA using the same watering regime as that used for the previous BA treated experiments i.e. Figure 3.7 and 3.8. The analysis showed that in fact, the BA watering regime

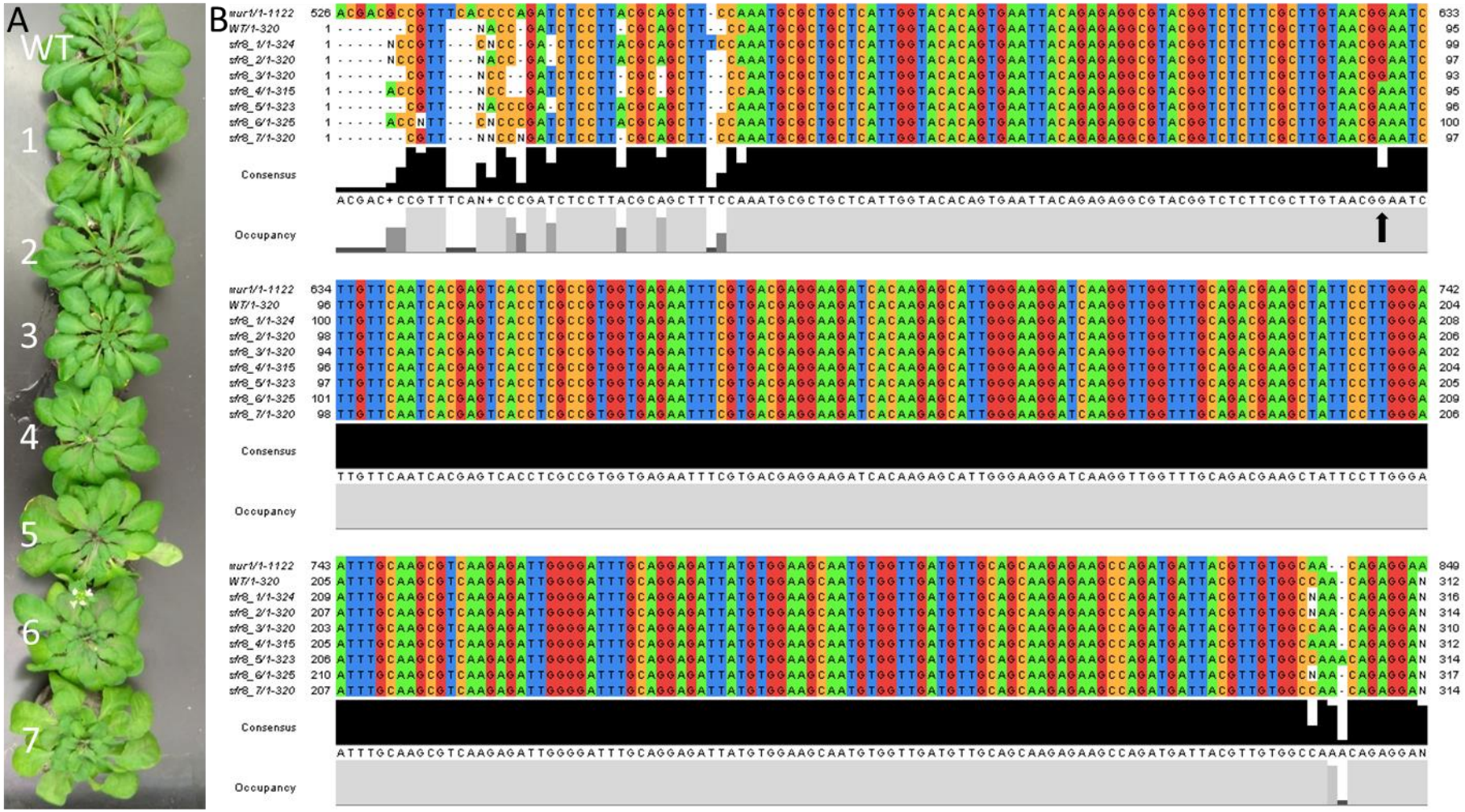

Figure 3.12: Sequencing of putative *sfr8* plants. A) Col-0 wild type (WT) *Arabidopsis thaliana* compared to *sfr8* plants that do not display described phenotypic traits (1-3) and those that do (4-7). **B)** Sequence of *MUR1* gene from WT and the seven *sfr8* plants in **A** compared to known gene sequence from TAIR (top sequence - 'mur1'). Site of base change in *sfr8* is indicated by the black arrow.

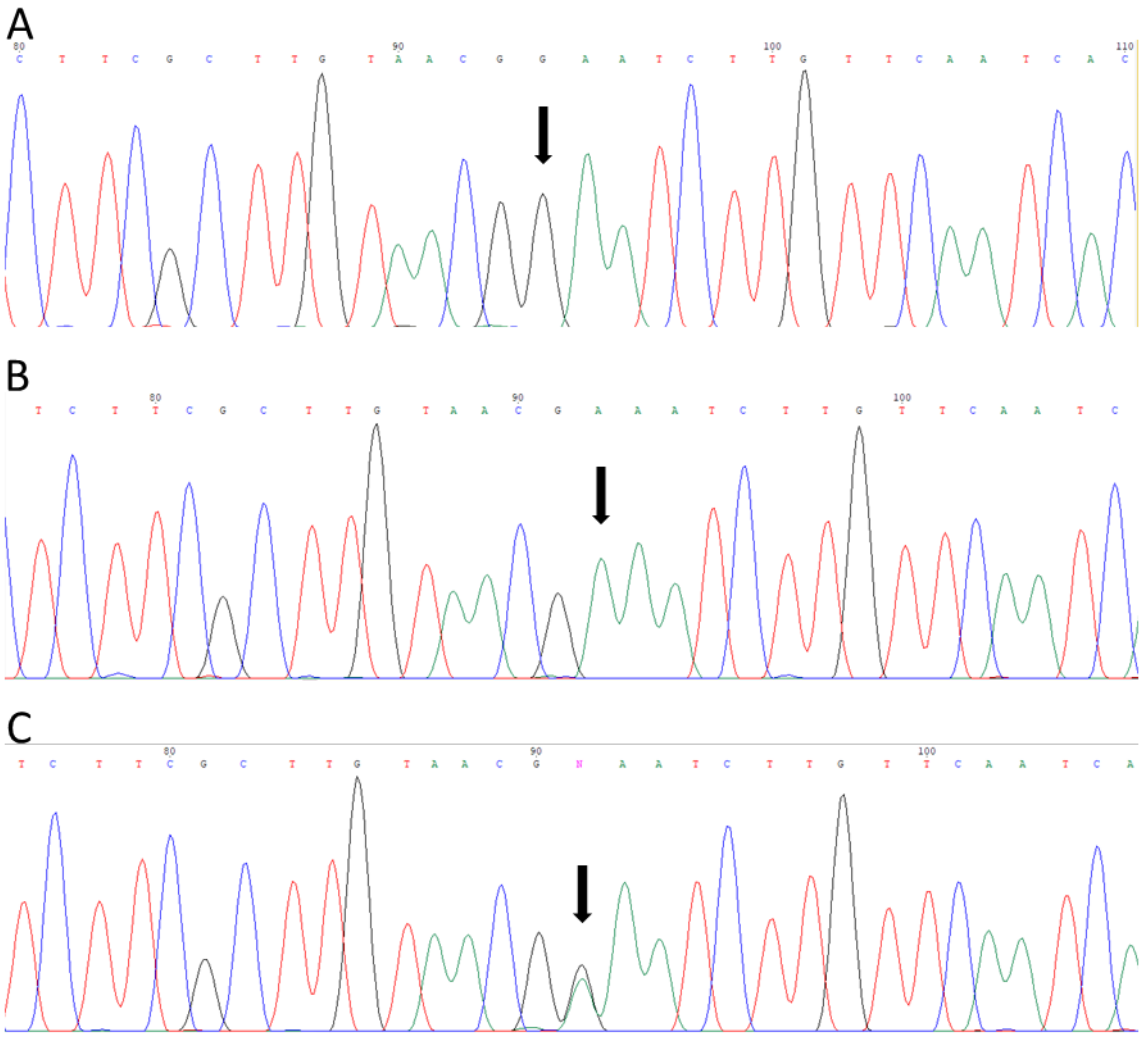

Figure 3.13: Sequencing of wild type and two separate *sfr8* seed stocks. Sequencing of the *MUR1* DNA sequence of Col-0 wild type **(A)**, *sfr8* seed stock B **(B)** and *sfr8* seed stock A **(C)**. Sequencing was carried out on 50 two-week-old seedlings of each genotype. Black arrows indicate site of base change in *sfr8*.

was unable to reverse the presence of monomer in *sfr8* plant cell walls (Figure 3.14A). Wild type and *sfr8-C* plants had mainly dimerised RG-II in their cell walls both with and without BA supplementation. These results show that it is likely that the "sfr8" plants used in BA supplementation electrolyte leakage measurements were contaminated with wild type plants and could explain the difference observed between cold acclimated and non-acclimated plants. It is likely that the non-acclimated EL (Figure 3.8A) used seed stock B which was not contaminated, and that the cold-acclimated EL (Figure 3.8B) used seed stock A which was contaminated with wild type seeds. Thus, the decrease in EL observed in '*sfr8* + BA' in Figure 3.8B was as a result of the presence of wild type plants, since BA was not able to reinstate a majority of dimerised RG-II in *sfr8* cell walls (Figure 3.14A). It is also possible that the fucose-supplemented EL used the contaminated seed stock and did not show a true reversal of leakage in *sfr8* mutants (Figure 3.5). This finding could also explain why RG-II dimerisation status was not changed in *mur1-1* plants supplemented with BA (Figure 3.7A).

3.2.8 Reassessing RG-II dimerisation and freezing damage of BA supplemented plants

It was possible that the BA watering regime used was unable to re-instate RG-II dimerisation because there was not enough boron present to overcome the effect of the loss of fucose, since BA supplementation has been shown to reinstate RG-II dimerisation in previous studies (O'Neill *et al.* 2001). In previous studies that found a reversal of *mur1-1* phenotypes with BA treatment, seeds were germinated on plates containing BA as well being provided with supplementation throughout growth (Reiter *et al.* 1993), which was not initially done in this study. Thus, the BA watering regime was modified, and seeds grown on 1 mM BA-supplemented agar and watered with 20 mg/L of BA once transferred to soil pellets. RG-II dimerisation was assessed as before by carrying out PAGE analysis of EPG digested cell wall extracts. Interestingly, this watering regime also did not appear to be able to alter the dimerisation status of RG-II in five-week-old plants as no difference was seen in the RG-II bands of *sfr8* and *mur1-1* plants with and without BA supplementation (Figure 3.14B). However, the visual phenotypes observed in *mur1-1* were less apparent in plants treated with BA as petioles appeared to be longer and leaves less rounded (Figure 3.15A). Thus, an electrolyte leakage assay was carried out to assess freezing sensitivity.

An EL assay carried out on the same set of *mur1-1* plants as those used in the RG-II analysis again highlighted the increase in leakage of *mur1-1* plants compared to wild type as was observed in Figure 3.3A. The experiment also showed that BA was able to reverse the leakage of *mur1-1* plants closer to levels of wild type at all three temperatures (Figure 3.15B). There was no

consistent decrease in leakage of wild type plants supplemented with BA compared to those that were not, and leakage was even higher in wild type plus BA plants compared to wild type at the lowest temperature. This may have been a result of the BA toxicity observed in the wild type plants after 7 weeks of BA supplementation of yellowing and chlorosis of the leaves (not shown) (Nable *et al.* 1997). This effect was also seen in BA supplemented *mur1-1* plants, however, the rescuing effects of BA supplementation appear to have outweighed any detrimental effects that BA toxicity may have had on freezing tolerance.

Taking into consideration the results from the RG-II analysis and the assessment of freezing damage, it may be that it is not RG-II dimerisation that is correlated with freezing tolerance, but some other trait that BA influences within the plant. It may also be the case that gel analysis of RG-II dimerisation is not a robust enough way to observe if RG-II dimerisation is restored in *sfr8* and *mur1-1* plants. It would also be necessary to analyse RG-II dimerisation after cold acclimation, as it may be that the two weeks of acclimation altered the RG-II dimerisation status and may hint at an association after all.

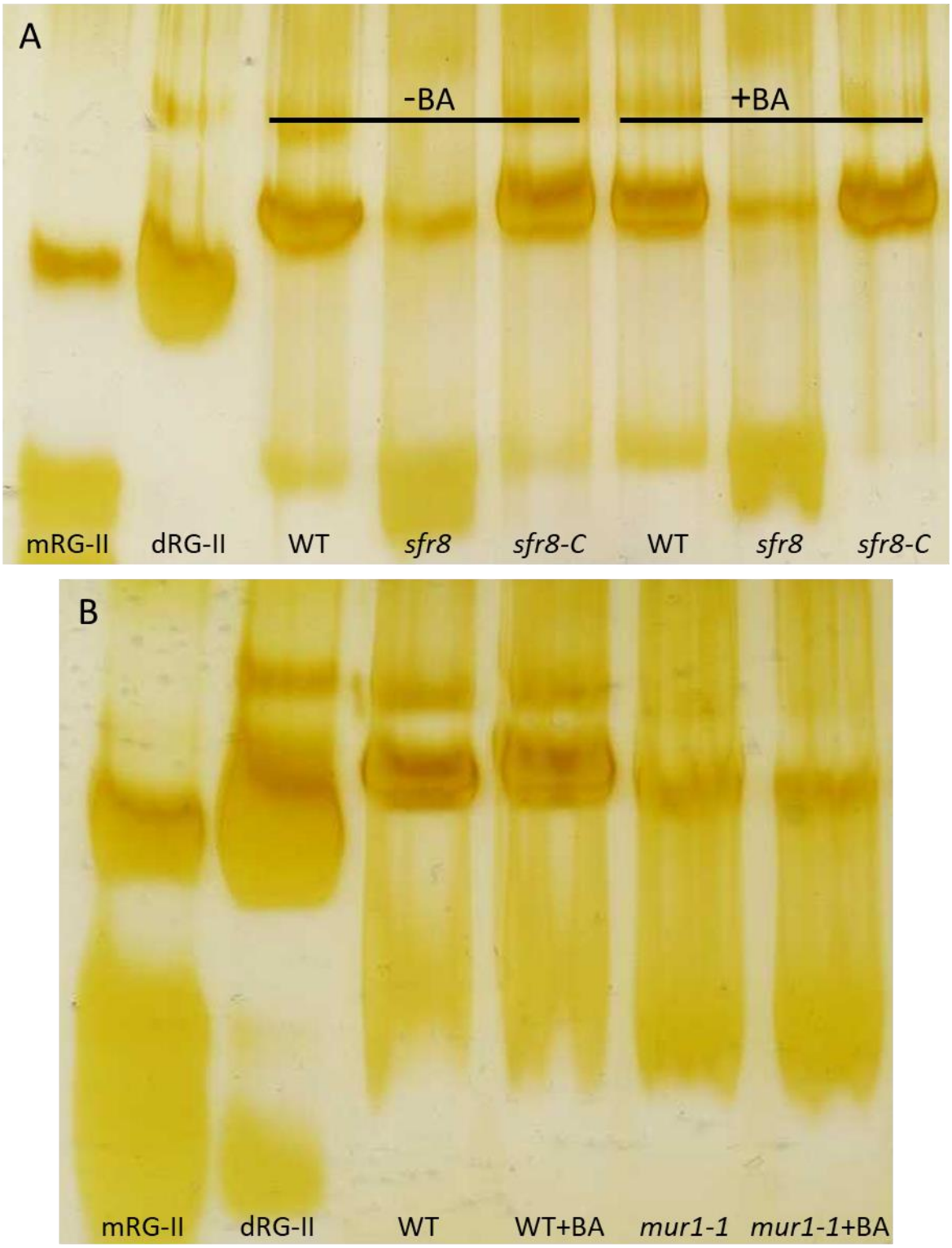

Figure 3.14: RG-II dimerisation status in wild type, *sfr8* and *mur1-1* mutants supplemented with BA. A) Polyacrylamide gel electrophoresis of endo-polygalacturonase digested cell wall extracts from five-week-old *Arabidopsis thaliana* Col-0 wild type (WT), *sfr8* and *sfr8-C* **(A)** and WT and *mur1-1* **(B)** plants with and without boric acid (BA) supplementation. Gels were stained with silver nitrate and purified RG-II standards show where monomer (mRG-II) and dimer (dRG-II) bands of rhamnogalacturonan-II should appear.

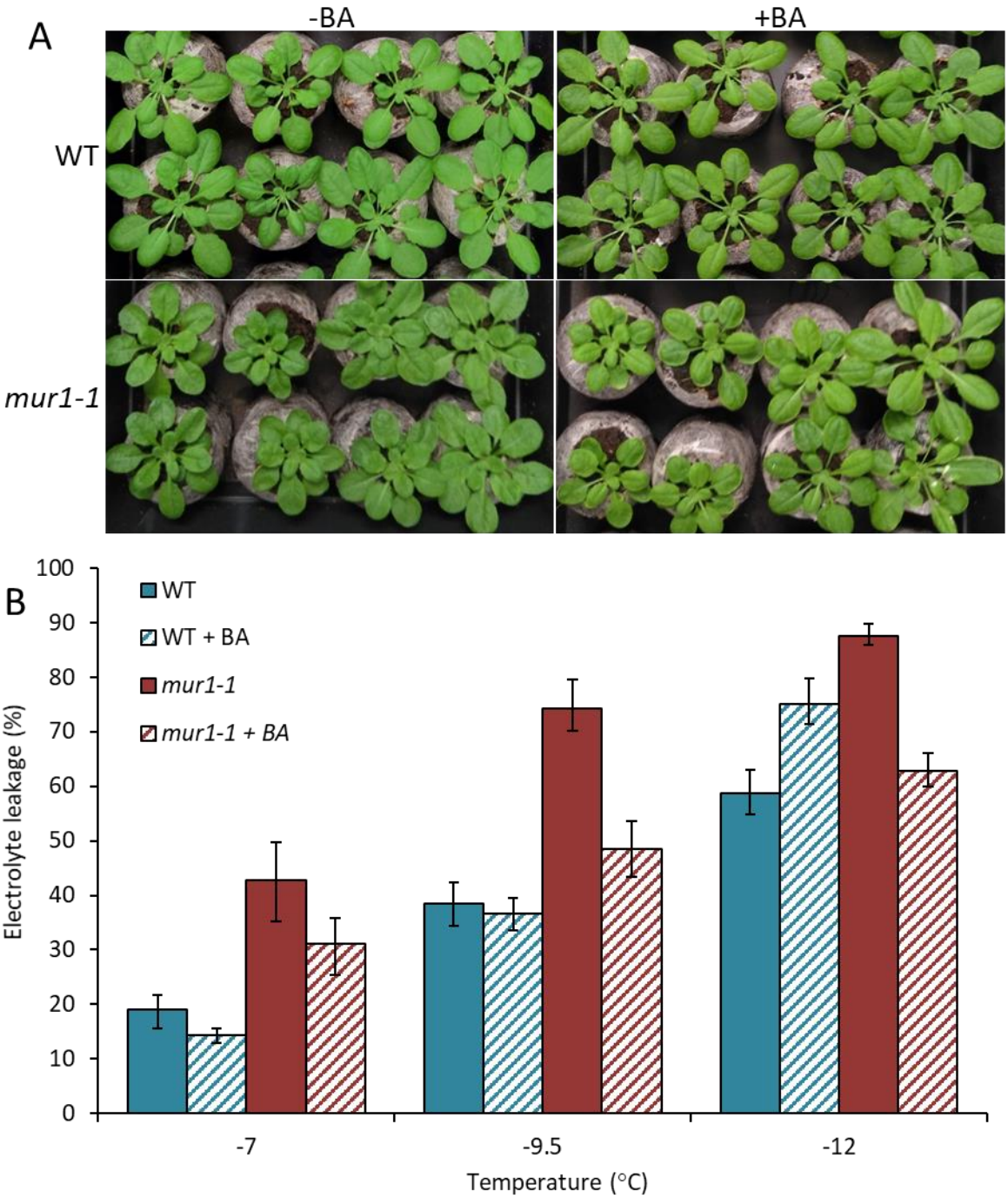

Figure 3.15: Visual assessment and electrolyte leakage from leaf discs of wild type and *mur1-1* mutant plants supplemented with BA. A) Visual assessment of five-week-old Col-0 wild type (WT) and *mur1-1* plants with and without boric acid (BA) supplementation during growth. **B)** Electrolyte leakage in Col-0 wild type (WT) and *mur1-1* mutant *Arabidopsis thaliana* with and without boric acid supplementation throughout growth. Plants were grown for five weeks before acclimating at 5°C for two weeks. Values represent percentage loss of electrolytes from leaf discs when exposed to temperatures of -7, -9.5 and -12°C. Each data point represents the average of six replicate tubes per genotype per temperature, with three leaf discs per tube. Error bars represent +/- 1 SE calculated from arcsine transformed data and then converted back to percentage data.

3.3 Discussion

3.3.1 Discovery of contamination of sfr8 seed stock

As described in section 3.2.1, *mur1-1* and *sfr8* plants display a clear visible phenotype of shortened petioles and rounded leaves compared to wild type plants. After the somewhat confusing results from the acclimated and non-acclimated EL assays of *sfr8* with and without BA supplementation and concomitant RG-II analysis (Figures 3.7 and 3.8), a critical analysis of the plants highlighted the fact that some plants that were supposedly *sfr8* looked more like wild type plants in their leaf shape and petiole length. Thus, a selection of these plants were individually genotyped; three plants that resembled wild type, and four that resembled *sfr8* and compared to known wild type plants (Figure 3.12A). Sequencing of the *MUR1* gene showed that plants that resembled wild type were in fact wild type plants, suggesting a contamination of the *sfr8* seed stock used to carry out experiments in this study (Figure 3.12B). Indeed, further analysis of this seed stock compared to an earlier one along with wild type showed that the stock likely consisted of up to 50% wild type seeds (Figure 3.13). It is likely then that the experiments carried out using the contaminated *sfr8* stock display false results. As previously stated, this is likely to have impacted more on the plants that had undergone fucose or BA supplementation such as the fucose and BA supplemented electrolyte leakage assays, and the assessment of RG-II dimerisation with BA supplementation (Figures 3.5, 3.7 and 3.8), where it would have been difficult to assess whether plants that displayed wild type characteristics were *sfr8* that had successfully been rescued, or were simply wild type. The fact that a decrease in leakage was only seen after a period of cold acclimation could highlight where the new (contaminated) stock began to be used (Figure 3.8). Although it is possible that the other experiments contained wild type plants, particularly those using seedlings where it would have been more difficult to identify wild type plants, the differences observed between *sfr8* and wild type were still found to be significant (Figures 3.2, 3.4 and 3.7). It may even have been the case that the increase in EL was underestimated (Figure 3.2), and the decrease in fucose was overestimated, and fucose levels may even be decreased to the extent of *mur1-1* plants (Figure 3.4). In order to verify if the decrease in RG-II dimerisation observed in *sfr8* plants could indeed be reversed with BA, PAGE analysis of digested cell-wall extracts (Chormova *et al.* 2014a) was carried out on plants from the known *sfr8* stock. Interestingly, the results were the same for the *sfr8* plants with and without BA supplementation, suggesting that BA was not able to rescue the RG-II phenotype (Figure 3.14A).

3.3.2 Cell-wall fucose content is correlated with freezing tolerance

Despite the discovery of contamination, the results that display clear differences between wild-type and *sfr8* plants, and the results that do not use *sfr8* plants still stand true. The *mur1* mutation has previously been described to result in certain phenotypic traits such as shortened petioles, dwarfed stature and early flowering (Reiter *et al.* 1993). These traits were also observed in *sfr8* mutant plants (Figure 3.1A) and genetic analysis showed that the *sfr8* mutation is identical to that of *mur1-4* (Reiter *et al.* 1997, Skipsey, Knight and Knight unpublished, Appendix A). Interestingly, *mur1-1* mutants seem to display a stronger visible phenotype than *sfr8* in the shortening of petioles and rounding of leaves (Figure 3.1A), suggesting that the amino acid change in *mur1-1* is more detrimental than that of *sfr8*. However, there is little discussion in the literature of the different effects of each allelic mutation, and most research has centred around *mur1-1* or *mur1-2* mutants (Reiter *et al.* 1993, 1997).

Using two mutant alleles, *mur1-1* and *sfr8* (*mur1-4*), and a complemented line (*sfr8-C*) genetic linkage was shown between the *MUR1* gene and plant freezing tolerance. Electrolyte leakage assays and visual assessment of plants exposed to freezing temperatures highlighted a significant increase in electrolyte leakage and freezing damage in both *mur1-1* and *sfr8* plants (which may have been underestimated for *sfr8*) that was reversed in the complemented line (Figures 3.1B, 3.2 and 3.3A). The *MUR1* gene encodes an enzyme functional in the fucose biosynthetic pathway (Bonin *et al.* 1997) and analysis has shown that *mur1* mutant plants are deficient in cell-wall fucose content (Reiter *et al.* 1997). Fucose was decreased to 2% of wild-type levels in *mur1-1* leaf material, and 40% in the roots (Reiter *et al.* 1993, 1997). The cell-wall fucose content of *sfr8* and *mur1-1* plants was measured in this study and showed a decrease to 27% and 20% respectively of wild-type levels (Figure 3.4A). The slight discrepancy with respect to the literature is likely because whole seedlings i.e. both shoot and root material were used in this study. This decrease in fucose was reversed in *sfr8-C* plants which had cell-wall fucose levels much closer to wild type at 80% (Figure 3.4B). These results suggest that cell-wall fucose content is correlated to plant freezing tolerance, and that a decrease in cell-wall fucose is associated with an increase in freezing sensitivity. Due to the contamination, the fucose supplementation experiments would need to be repeated to explicitly verify that freezing sensitivity can be reversed with fucose application, but fucose has previously been showed to reverse the morphological phenotypes of *mur1-1* (Reiter *et al.* 1993).

This association between fucose and freezing sensitivity was further evidenced by treating plants with a fucosylation inhibitor 2-fluoro-L-fucose (2F-fucose). Treatment with 10 µM inhibitor was shown to reduce cell-wall fucose in seedlings to less than 50% of wild-type levels in the shoots and less than 10% in the roots (Dumont *et al.* 2015). Electrolyte leakage assays of seedlings treated with 2F-fucose showed a significant concentration-dependent increase in leakage and thus freezing damage (Figure 3.6A). Interestingly, 2F-fucose treatment also resulted in a decrease in root length of seedlings (Dumont *et al.* 2015; Villalobos *et al.* 2015). Assessment of wild type and *sfr8* seedling roots showed a decrease in root growth in *sfr8* seedlings, suggesting that cell-wall fucose is also correlated with root growth (Figure 3.6B). This decrease in root growth has been observed previously in *mur1-1* mutants, and has been suggested to be as a result of alterations to arabinogalactan proteins (AGPs) in the roots due to L-fucose deficiency (van Hengel & Roberts 2002). AGPs have previously been shown to play a role in root elongation (Willats & Knox 1996). However, there is also evidence that RG-II may play a role in this phenotype, as mutations in the *RGXT4* gene involved in RG-II synthesis led to lethal root growth defects (Liu *et al.* 2011). Root cell-wall integrity was also decreased in another mutant that had a decrease in RG-II dimerisation (Sechet *et al.* 2018). Indeed, the finding that the decrease in root growth of 2F-fucose treated plants could be partially reversed with BA supplementation lends further evidence to this (Figure 3.9E) (Dumont *et al.* 2015).

Recent research has shown that GDP-L-fucose also plays a specific role in leaf development (Gonçalves *et al.* 2017) which could account for the differences in leaf shape observed in *mur1-1* and *sfr8*. There are several hypotheses for how L-fucose influences leaf shape. One of these hypotheses is that *MUR1* acts in the same pathway as the transcription factor cup-shaped cotyledon 2 (CUC2), which controls plant boundary formation and is required for leaf serration (Hasson *et al.* 2011), and that post-translational fucosylation of proteins may affect the upstream regulation of *CUC2* expression (Gonçalves *et al.* 2017). Another hypothesis is that modifications of cell-wall polysaccharides as a result of L-fucose deficiency may indirectly impact *CUC2* expression, or that cell-wall properties may affect leaf growth independently or downstream of *CUC2* expression (Gonçalves *et al.* 2017). It is still unclear therefore, exactly why *mur1-1* and *sfr8* mutants display this leaf shape phenotype, but evidence suggests that fucose has an important role to play.

3.3.3 The sfr8 *mutant has decreased RG-II dimerisation*

As previously discussed in section 3.1, there are several components of the cell wall that contain L-fucose residues including XyG, RG-I, RG-II, AGPs and *N*-linked glycans. The loss of fucose in any of these polysaccharides or proteins could potentially be a major cause for the freezing-sensitive phenotype of *sfr8*. One of the most common fucosylated polysaccharides in the cell wall is the hemicellulose xyloglucan, which accounts for approximately 20% of *Arabidopsis* cell walls (Zablackis *et al.* 1995). The *Arabidopsis mur2* mutant contains less than 50% of wild-type cell-wall fucose levels (Reiter *et al.* 1997). This value agrees with measurements taken in this study where *mur2* mutant seedlings were found to have a reduced cell-wall fucose content of 42% that of wild type (Figure 3.4A). The *mur2* mutation was found to reside in the fucosyl-transferase gene *FUT1* (Vanzin *et al.* 2002), which encodes an enzyme that catalyses the addition of L-fucose onto XyG molecules (Perrin *et al.* 1999; Sarria *et al.* 2001). XyG is believed to function primarily in a structural capacity as part of the cellulose-xyloglucan framework of the cell wall (Hayashi 1989). EL assays carried out on *mur2* mutants showed that, although there was a small significant increase in leakage at one temperature, overall there was little effect on freezing tolerance (Figure 3.3B). This suggests that a loss of L-fucose residues on XyG molecules, which has been shown to be replaced with L-galactose in *mur2* mutants (Zablackis *et al.* 1996), did not affect XyG in a way that would result in increased freezing sensitivity, despite the fact that xyloglucan comprises more than 50% of the fucose content of the cell wall. The organisation of different sugar residues on the xyloglucan backbone is believed to affect the conformation of binding to cellulose (Levy *et al.* 1997); this study suggests that the loss of fucose side chains may not affect that link. However, recent analysis of a xyloglucan-deficient double mutant *xxt1/xxt2* that did not display detrimental cell-wall defects suggests xyloglucan may not be a main load-bearing wall component as previously thought (Cosgrove 2016b). Interestingly, it appears to take only a further 15% decrease in cell-wall fucose to result in the significant increase in freezing sensitivity observed in the *sfr8* mutant (Figure 3.2B, 3.4A). This would suggest that it is the loss of another fucose containing cell-wall component that is necessary for full freezing tolerance.

It is possible that loss of L-fucose residues on *N*-linked glycans could result in reduced freezing tolerance, although mutants that lack L-fucose on glycoproteins display none of the morphological characteristics of *mur1-1* mutants (von Schaewen *et al.* 1993). It is also possible that a loss of fucose in AGPs may be a contributing factor, as this has been shown to affect the root length of *mur1-1* plants (van Hengel & Roberts 2002), although mutants deficient in

arabinose that specifically alter AGP structure do not display a dwarf phenotype (Reiter *et al.* 1997). However, previous analysis of *mur1* mutants has shown that a major consequence of fucose deficiency is the decrease in dimerisation of the cell-wall pectin domain rhamnogalacturonan-II (O'Neill *et al.* 2001). The structure of RG-II described in section 1.4.2 and shown in Figure 1.4, is a complex branched network of many different sugar residues, with RG-II monomers being dimerised via a borate ester cross-link between the apiose residues of side chain A (Ishii & Matsunaga 1996; Matoh *et al.* 1996; O'Neill *et al.* 1996). Research has shown that a loss of the L-fucose residue in side chain A decreases the ability of RG-II monomers to cross-link, possibly due to structural and conformational changes that reduce the stability of the borate cross-link, resulting in a decrease in RG-II dimerisation in *mur1-1* and *mur1-2* mutants (O'Neill *et al.* 2001).

The RG-II dimerisation status was analysed in *sfr8* mutant cell walls by carrying out PAGE analysis of digested cell-wall extracts. The results showed that the cell wall of the *sfr8* mutant does contain more RG-II monomer than wild type plants, as well as appearing to contain less dimer (Figures 3.7A and 3.14A), a phenotype also observed in *mur1-1* plants (Figure 3.7A). This is comparable to previous analysis of *mur1-1* mutants which have been shown to contain approximately 56% dimerised RG-II compared to 95% in wild-type cell walls, a trait that can be reversed by supplementing plants with L-fucose (O'Neill *et al.* 2001). This phenotype can also be reversed by expressing the *MUR1* gene in the *sfr8* mutant background, as results for *sfr8-C* plants show that they contain primarily dimer, as is observed in wild type plants (Figure 3.14A).

3.3.4 BA can reverse the freezing sensitivity of mur1-1 *but cannot restore RG-II dimerisation*

Studies have shown that providing plants with excess BA has the ability to restore RG-II dimerisation; *mur1-1* plants treated with BA had near similar petiole length, plant size and leaf shape to wild type, and the amount of dimerised RG-II in the cell wall was increased to approximately 78% (O'Neill *et al.* 2001). These experiments provide evidence that it is the loss of RG-II dimerisation that results in the phenotypes observed. However, in this study, BA did not have the ability to reverse the RG-II phenotype observed in *sfr8* and *mur1-1* mutant plants (Figures 3.7A and 3.14A), even after the amount of BA provided during growth was increased (Figure 3.14B). Despite this, an EL assay showed that *mur1-1* plants supplemented with BA had leakage levels closer to that of wild type plants after freezing (Figure 3.15B), and morphological phenotypes of *mur1-1* were also partially reversed with BA supplementation (Figure 3.15A).

It was also tested whether BA had the ability to reverse the freezing-sensitive phenotype of plants treated with the fucosylation inhibitor 2F-fucose. BA was previously shown to rescue the decrease in root length observed with 2F-fucose treatment (Villalobos *et al.* 2015), and this result was also observed in this study as although roots of seedlings treated with 2F-fucose and BA were shorter than the control treated seedlings, they were consistently longer than seedlings treated with 2F-fucose alone (Figure 3.9E). These results could suggest that 2F-fucose has an effect on RG-II synthesis, leading to a decrease in dimerisation that can be overcome via treatment with BA (see discussion on roots in section 3.3.2). Indeed, it has been shown that treatment of 10 µM 2F-fucose is enough to decrease the occurrence of dimeric RG-II and increase monomeric RG-II within the cell wall, and treatment with 25 µM had an even greater impact on RG-II dimerisation (Dumont *et al.* 2015). However, analysis of RG-II dimerisation of 2F-fucose treated seedlings in this study did not show the same results. Although there appeared to be slightly less RG-II dimer in 2F-fucose treated seedlings, there was no evidence of RG-II monomer, which only appeared in 2F-fucose and BA treated seedlings (Figure 3.10A). Despite these results, an initial EL leakage experiment carried out on 2F-fucose treated seedlings supplemented with BA showed that leakage was much closer to wild type levels (Figure 3.9A), suggesting that BA was able to reverse the effects of the fucosylation inhibitor that resulted in freezing sensitivity (Figure 3.9A). However, three repeat experiments consistently showed that DMSO treated seedlings also had increased leakage of electrolytes (Figure 3.9B-D). It is known that DMSO can cause an increase in membrane permeability (Notman *et al.* 2006) so it was possible that DMSO treatment was having some adverse effects on the seedlings. However, analysis of the effects of DMSO on electrolyte leakage as a result of freezing damage showed no significant increases in leakage with DMSO treatment (Figure 3.10B). It is unknown, therefore, as to why an increase in leakage was so consistently seen in the DMSO treated seedlings and thus further experiments would be needed to be carried out to determine the cause of this.

Analysis of the freezing tolerance of a *bor1-1* mutant was not able to link BA and RG-II with freezing tolerance. BOR1 is a boron efflux transporter involved in xylem loading that is essential for the plant during boron deficiency (Takano *et al.* 2002). The *bor1-1* mutant was shown to contain lower levels of boron than wild type (Noguchi *et al.* 1997), and also had reduced dimerisation of RG-II to 40% under boron limiting conditions (Noguchi *et al.* 2003). However, an EL showed no significant difference between leakage of wild type and *bor1* plants (Figure 3.11A). Analysis of the RG-II dimerisation status suggested there was no decrease in RG-II dimerisation, as no significant increase in RG-II monomer was observed (Figure 3.11B). This is likely because

there was sufficient boron available to the plant, as under non boron-limiting conditions, it was shown that 85-90% of RG-II present in the cell wall of *bor1-1* plants was dimerised (Noguchi *et al.* 2003). Further analysis would need to be carried out on truly boron deficient plants that therefore have decreased RG-II dimerisation to assess if this does indeed result in increased freezing sensitivity.

The results described here could suggest one of two things; 1. that there is another role that BA is playing within the plant in relation to freezing tolerance or 2. that the method for visualising the presence of RG-II monomer and dimer in the cell wall via gel electrophoresis is not robust enough for analysis with *sfr8* and *mur1-1* mutants. RG-II domains from *mur1-1* mutant plants have been shown to be much less stable that RG-II from wild type plants (O'Neill *et al.* 2001). It is thus possible that the process of cell-wall extraction and EPG digestion is detrimental to any borate ester cross-links formed between RG-II domains of *mur1-1* and *sfr8* plants, and that the gel analysis carried out in this study is not truly representative of the RG-II levels in plant cell walls. No previous studies have attempted to measure dimerisation of RG-II in *mur1-1* plants via gel electrophoresis, and only a handful of studies directly show that RG-II can be forced to dimerise with excess BA application in mutants where RG-II structure effects dimerisation ability (O'Neill *et al.* 2001; Voxeur *et al.* 2011; Sechet *et al.* 2018). It is important to note that the RG-II analysis in Figure 3.14B was carried out on five-week-old non-acclimated plants, thus it would also be necessary to measure RG-II dimerisation in the same seven-week-old acclimated plants on which the EL leakage analysis was performed to ensure cold acclimation does not induce changes to RG-II structure, although cold acclimation was not required for the rescue of RG-II dimerisation in previous studies (O'Neill *et al.* 2001; Voxeur *et al.* 2011; Sechet *et al.* 2018). Thus, it would be necessary to carry out analysis of RG-II dimerisation using different techniques such as those used in the studies mentioned where analysis has been successful, or by *in vivo* techniques such as antibodies directed against monomeric RG-II (Matoh *et al.* 1998), in order to assess if RG-II dimerisation is indeed rescued and thus correlated with freezing tolerance.

3.3.5 What roles does boron play within the plant?

It is generally believed that the primary role of boron is as a structural component of the cell wall. This comes from the finding 90% of boron in the plant is localised to the cell wall (Loomis & Durst 1992). Indeed the first symptoms of boron deficiency include abnormalities in the cell wall (Hu & Brown 1994; Liu *et al.* 2014). It was later discovered that boron formed a complex with a pectic polysaccharide, to which up to 80% of cell-wall boron was localised (Matoh *et al.*

1993). This pectin was eventually shown to be RG-II, which was dimerised via a borate-ester cross-link (Ishii & Matsunaga 1996; Kobayashi *et al.* 1996; O'Neill *et al.* 1996), and it was suggested that RG-II was the sole boron-binding molecule within the plant cell wall (Matoh *et al.* 1996). However, it has been suggested that boron may bind to other biomolecules (Goldbach & Wimmer 2007), and that it may even bind to transcription factors and thus regulate plant transcription (González-Fontes *et al.* 2008). Evidence for this comes from the fact that boron seems to exert effects on a number of different plant processes including root and pollen tube growth, plasma membrane function (Blevins & Lukaszewski 1998), nitrogen fixation and carbohydrate metabolism (Camacho-Cristobal & Gonzalez-Fontes 1999), and even cytoskeletal processes (Bassil 2004).

Interestingly, boron has also been shown to form a complex with RG-II and the plasma membrane sphingolipid GIPC (Voxeur & Fry 2014). This interaction could influence membrane processes and even be part of a cell wall-plasma membrane-cytoskeletal continuum that could be important for signalling between extracellular and intracellular compartments (Goldbach & Wimmer 2007). This would still involve the binding of boron to RG-II, suggesting it may be cell wall-plasma membrane connections that are important for freezing tolerance (see Chapter 5). Indeed, many of the processes affected by boron deficiency have also been linked to RG-II dimerisation, including root and pollen tubes growth (Liu *et al.* 2011; Dumont *et al.* 2014). Many of the phenotypic traits of boron-deficient plants are also observed in mutants deficient in RG-II dimerisation. For example, boron deficiency in roots of squash and bean was shown to reduce the cell-wall tensile elastic modulus (Findeklee & Goldbach 1996; Findeklee, Wimmer & Goldbach 1997), and these findings are concurrent with the decrease of tensile modulus in *mur1-1* and *mur1-2* hypocotyls measured by Ryden *et al*. (2003). Boron-deficient plants have been shown to have brittle leaves (Loomis & Durst 1992; Hu & Brown 1994), a phenotype of *mur1-1* tissues initially reported by Reiter *et al*. (1993). RG-II existed principally in monomer form in boron-deficient *C. album* cells, which resulted in a decrease in the limiting cell-wall pore size. Supplementing cells with BA restored RG-II dimerisation and also cell-wall pore size (Fleischer *et al.* 1998, 1999). Boron-deficient cells were also mechanically unstable, as cells ruptured due to overexpansion (Fleischer *et al.* 1998).

Although it cannot be ruled out that boron may play a signalling role in plants, it is still the case that most of the boron within the plant is located in the cell wall as a cross-linking molecule. It is also the case that some of the cell wall structures that have been shown to be influenced by

boron cross-linking of RG-II molecules such as pore size and cell wall strength, are also correlated with freezing tolerance mechanisms (Ashworth & Abeles 1984; Rajashekar & Burke 1996; Rajashekar & Lafta 1996). How these mechanisms may be influenced in the *sfr8* mutant will be discussed further in Chapter 5.

3.4 Conclusions

The results of the experiments carried out here demonstrate a significant effect of cell-wall fucose deficiency on freezing tolerance. There are several cell-wall polysaccharides that contain fucose residues, alterations to which could result in the freezing-sensitive phenotypes of *sfr8* and *mur1-1* observed. The *mur2* mutant did not show a consistently significant increase in electrolyte leakage, suggesting it is not alterations to xyloglucan chains that result in freezing sensitivity. Although previous analysis has shown that *N*-linked glycans and AGPs do not display the same morphological phenotypes as *mur1-1*, it would be necessary to verify that alterations to these cell-wall components do not result in freezing sensitivity, as it may be possible that these traits are independent of each other. Little attention is given to RG-I in previous studies of *mur1* mutants, possibly because fucose residues tend to exist terminally and are unlikely to result in any severe structural changes. Also, there is compelling evidence that many of the morphological traits observed in *sfr8* and *mur1-1* mutants are linked to RG-II dimerisation, which is shown to be affected by fucose deficiency, both in this and previous studies. Although RG-II dimerisation was not restored with BA supplementation in this study, it has been observed in other studies, and the decrease in freezing sensitivity of BA-treated *mur1-1* plants suggests a correlation between RG-II dimerisation and freezing tolerance given the role of boron described in the literature. Taking these results into account, the initial hypothesis that the cell-wall influences freezing tolerance within the plant can be accepted. There is also strong evidence to suggest that the structure of the RG-II cross-linking influences this as reversing the loss of the cross-link with BA is able to reverse the increase in freezing sensitivity in mutant plants.

CHAPTER 4

SFR8 MUTANTS DISPLAY ALTERED GUARD CELL DYNAMICS

4.1 Introduction

4.1.1 Stomata and stomatal regulation

Stomata are small pores located mainly on the lower epidermis of leaves that allow gaseous exchange between the plant and the environment. They are essential for plant life, allowing the influx of CO_2 for photosynthesis, and the efflux of waste products such as O_2 and water vapour, as well as playing a major role in the transpiration stream that allows the movement of water and other molecules through the plant (Zeiger 1983). In monocots the guard cells are dumb bell-shaped and are surrounded by subsidiary cells (Franks & Farquhar 2007), whilst in dicots, the stomatal complex consists of two kidney-shaped guard cells which are surrounded by epidermal cells or sometimes subsidiary cells. The guard cells control the opening and closing of the stomatal pore to regulate gas exchange as well as plant-water relations. Several environmental signals induce changes to stomatal aperture i.e. the width of the stomatal pore, including light, CO_2 concentration, water content, humidity and temperature (Araújo, Fernie & Nunes-Nesi 2011).

Stomata open via the action of ion channels localised at the plasma membrane and the integration of many stomata-regulating signals (Schroeder *et al.* 2001a; Araújo *et al.* 2011; Kollist, Nuhkat & Roelfsema 2014). During opening of the stomata, H^+-ATPases pump H^+ ions out of the guard cells resulting in a hyperpolarisation of the membrane (Shimazaki & Kondo 1987), which provides a driving force for the passive uptake of K^+ and Cl^- ions and in some cases malate^{2-} into the guard cells (Gotow *et al.* 1985; Schroeder 1988). This results in a decrease in the osmotic potential of the guard cells leading to an influx of water and an increase of turgor and cell volume that contributes to the opening of the pore. Conversely, stomatal closure is driven by a decrease in guard cell turgor due to efflux of K^+ ions (Hosy *et al.* 2003). There is also evidence to suggest that sucrose plays a role in the regulation of stomatal opening and closing (Daloso & Fernie 2016). There are different guard cell signalling pathways that regulate stomata, for example, stomatal opening is initiated by the blue-light activation of H^+-ATPase pumps (Shimazaki *et al.*

2007). Abscisic acid (ABA) is also an important guard cell signalling component, and is induced in response to abiotic stresses such as drought, causing the stomata to close (Schroeder, Kwak & Allen 2001b). ABA activates a complex signalling network involving the influx of Ca^{2+} ions into the cytosol and a decrease in cytosolic pH that ultimately induce the efflux of K^+ through membrane channels, thus resulting in a decrease of guard cell turgor and stomatal closure (Li, Assmann & Albert 2006). As well as inducing stomatal closure, ABA also prevents opening by Ca^{2+}-regulated inhibition of H^+-ATPase channels (Kinoshita, Nishimura & Shimazaki 1995). The complex signalling network induced by ABA and the many other cellular components involved has been reviewed by various groups (Hetherington 2001; Li *et al.* 2006; Daszkowska-Golec & Szarejko 2013; Pantin *et al.* 2013). Ca^{2+} signalling plays a central role in the regulation of stomatal movement, with cytosolic Ca^{2+} increases being induced not only by ABA, but also other stimuli that induce stomatal closure such as CO_2 and pathogens (Webb *et al.* 1996; Klusener *et al.* 2002).

4.1.2 Guard cell walls

A distinctive feature of guard cells that is essential for stomatal-regulation is the guard cell wall. Early studies of stomata led to the observation that the inner radial walls of guard cells are thickened, leading to a stiffening of the wall that allows the cells to bend and successfully open the stomatal pore (Mohl 1856; Zeiger 1983). More recently, modelling of stomatal movements has taken into account cell wall mechanics in an effort to better understand the mechanism via which the cell wall influences stomata opening and closure (Rui *et al.* 2016). Immuno-histochemical studies and microscopy techniques have led to the observation that guard cell walls contain a specific polysaccharide make-up compared to other cells (Majewska-Sawka, Mu & Rodriguez-Garcia 2002; Verhertbruggen *et al.* 2009; Rui & Anderson 2016), that can also vary between species (Shtein *et al.* 2017). This led to the hypothesis that these components are important for guard cell function. Indeed, research has shown that altering guard cell-wall composition results in aberrant guard cell dynamics, and several pectin modification enzymes in particular have been implicated as necessary for proper stomatal function (Amsbury *et al.* 2016; Huang *et al.* 2017; Rui *et al.* 2017). In this chapter, it is hypothesised that the *sfr8* mutants display altered guard cell dynamics and that this may be related to the loss of RG-II cross-linking described in Chapter 3. Possible reasons for this guard-cell phenotype are discussed in relation to cell-wall structure and mechanics.

4.2 Results

4.2.1 Leaf water loss

A leaf drying assay was carried out where single leaves were excised from mature wild type, *sfr8*, *mur1-1, mur2* and *sfr8-C* plants and left to dry at ambient temperature and humidity with the abaxial side facing upwards. The mass of the leaves was measured every hour for eight hours then at 24 hours and 7 days and decrease in mass used as a measure of water loss. The results showed that both *sfr8* and *mur1-1* leaves lost a greater proportion of their original mass than wild type, *mur2* and *sfr8-C*, suggesting a greater water loss in plants with a mutation in the *mur1* gene (Figure 4.1). Upon initial excision, wild type, *sfr8-C* and *mur2* leaves lost mass at a comparable rate to *sfr8* and *mur1-1*. However, after this first measurement, the mass of wild type, *sfr8-C* and *mur2* leaves decreased at a much steadier rate and leaves even decreased in mass between 24 h and 7 days. Contrary to this, *sfr8* and *mur1-1* leaves decreased in mass at a continually high rate and reached almost complete dryness after only 6 h.

To assess if this was a result of a decrease in RG-II dimerisation, plants were supplemented with boric acid (BA) during growth and the experiments carried out as before. Interestingly, both wild type and *sfr8-C* plants show an increased water loss when grown with BA supplementation (Figure 4.2), whereas water loss appeared to be partially reversed in *mur1-1* and *sfr8* leaves (Figure 4.3). Although the differences seen for *sfr8* could be due to the contamination with wild type seeds described in Chapter 3, this would not be the case for the difference seen in *mur1-1* plants. It is possible that because the opposite difference is seen in wild type and *sfr8-C* plants, that it is simply within the margin of error of the experiment and BA does not affect water loss. However, as reported in Chapter 3, the BA watering regime used did not appear to be enough to reform RG-II borate-ester linkages. Further experiments utilising the new BA supplementation regime that was shown to alter freezing tolerance in *mur1-1* plants (Figure 3.14) are required to ascertain if the water loss phenotype is due to a loss of RG-II dimerisation (although further proof is also required that RG-II domains are dimerised in BA treated mutants – see Chapter 3).

As described in previous chapters, there are several effects of a loss of RG-II dimerisation in the cell wall that could result in this phenotype if it is indeed as a result of this. An increase in cell wall pore size concomitant with a loss of RG-II dimerisation (Fleischer *et al.* 1999) could mean that water is able to move through the apoplast quicker, or changes to water binding properties of RG-II could also result in an increased rate of water movement. However, the pattern of water loss described earlier, and the immense difference in water loss observed in *mur1-1* and *sfr8*

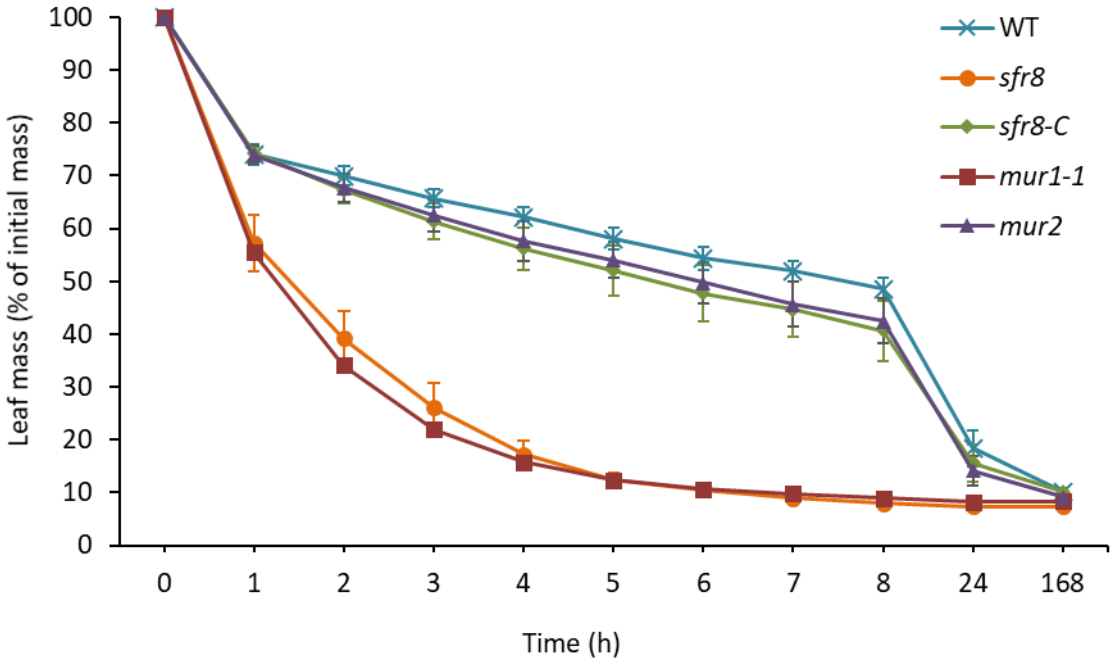

Figure 4.1: Water loss from excised leaves. Mass of leaves excised from mature plants and weighed every hour for 8 h then at 24 h and 7 days shows differences in water loss. Results are an average of three separate experiments each with seven repeats. Error bars show +/- 1 S.E. between averages of the three experiments.

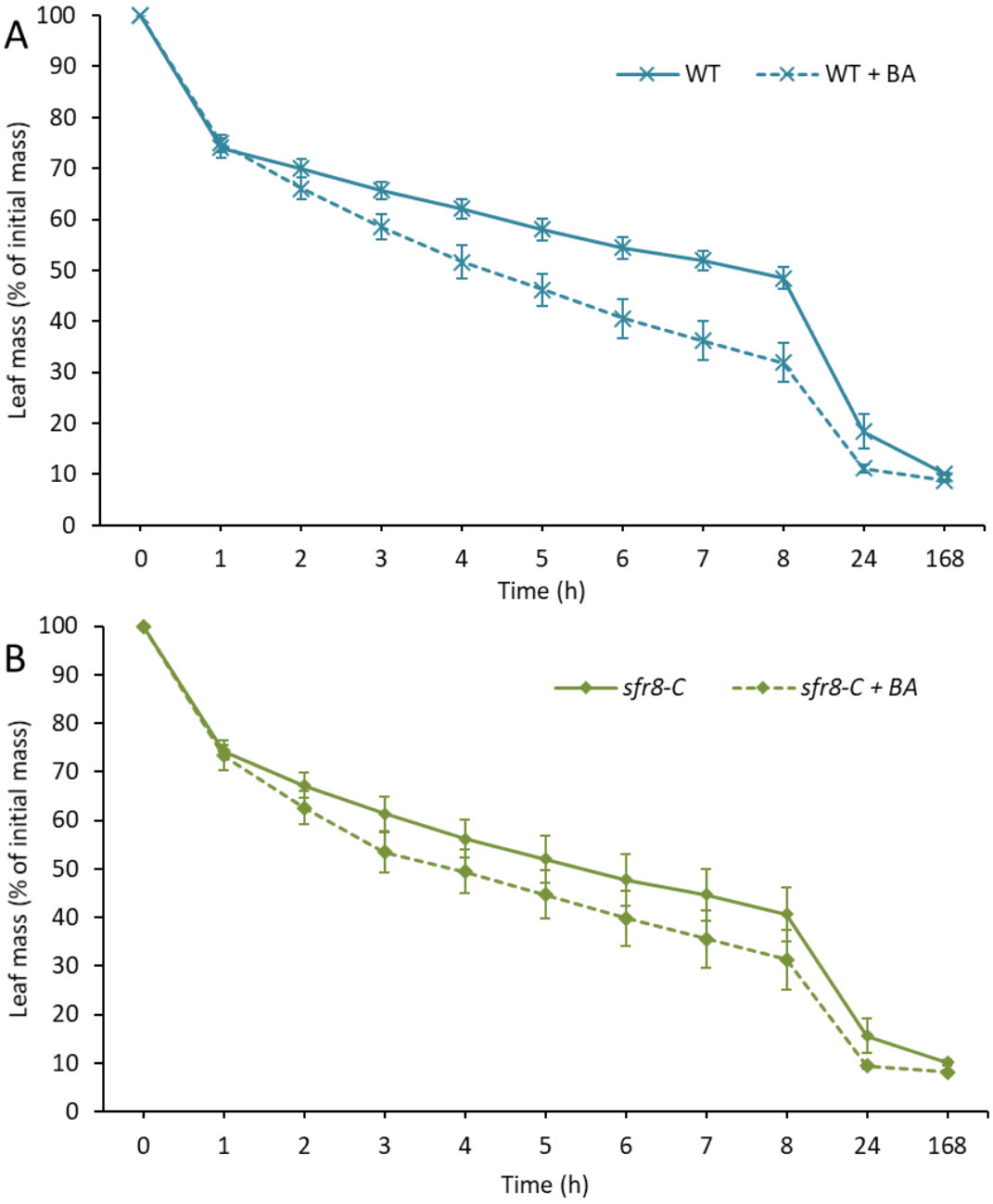

Figure 4.2: Water loss from excised leaves of wild type and *sfr8-C* supplemented with BA. Mass of leaves excised from mature plants of Col-0 wild type (WT) (**A**) and *sfr8-C* (**B**) with and without boric acid (BA) supplementation weighed every hour for 8 h then at 24 h and 7 days. Results are an average of three separate experiments each with seven repeats. Error bars show +/- 1 S.E. between averages of the three experiments.

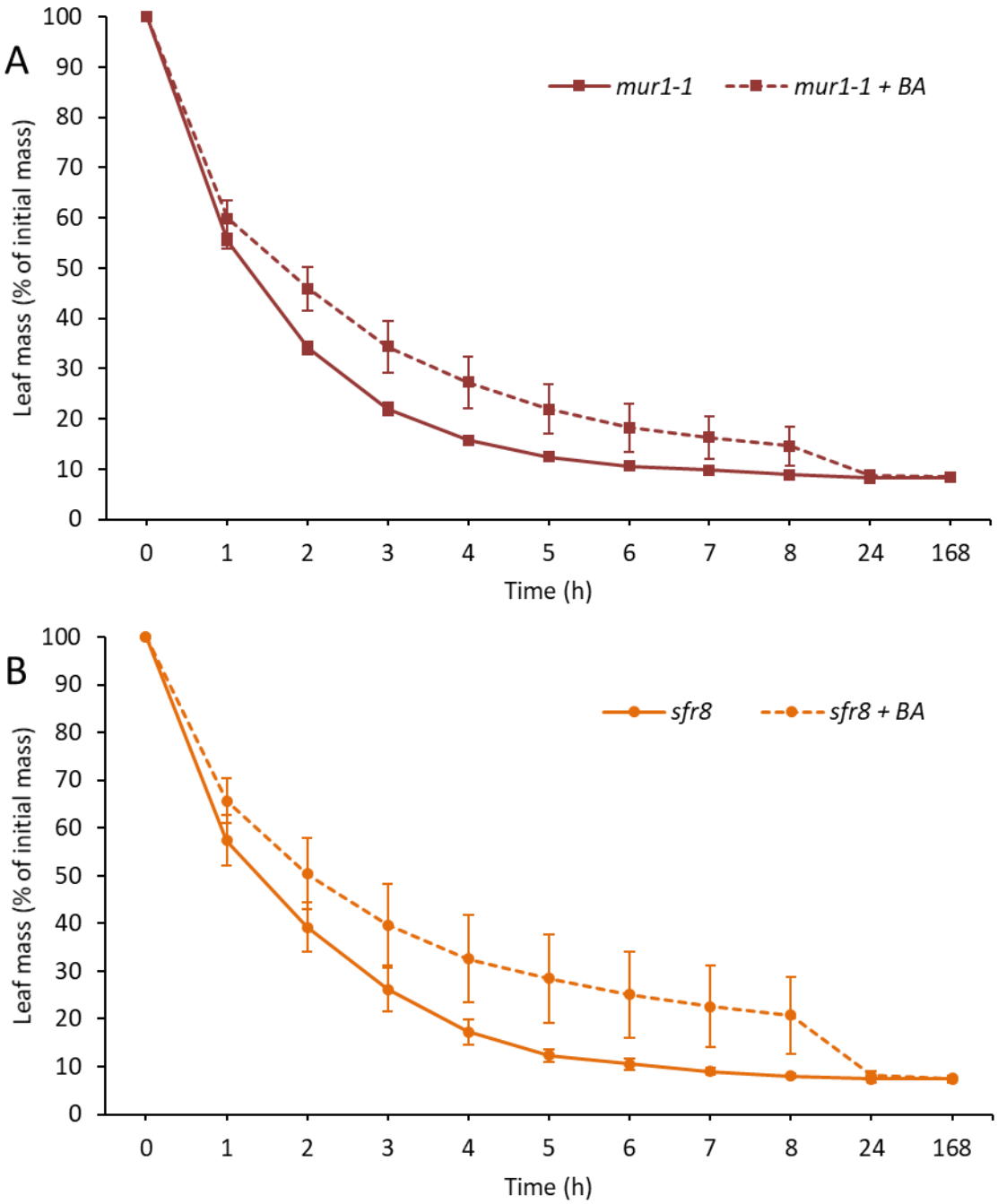

Figure 4.3: Water loss from excised leaves of *sfr8* and *mur1-1* supplemented with BA. Mass of leaves excised from mature plants of *mur1-1* (A) and *sfr8* (B) with and without boric acid (BA) supplementation weighed every hour for 8 h then at 24 h and 7 days. Results are an average of three separate experiments each with seven repeats. Error bars show +/- 1 S.E. between averages of the three experiments.

hinted at the involvement of stomata, as this is the easiest and quickest way that plants lose water. This hypothesis was investigated further using several different experimental methods.

4.2.2 Stomatal analysis

4.2.2.1 Stomatal density, index and size

To assess if stomata were involved in the increased water loss from *sfr8* plants, the first step was to measure stomatal density and index to assess if this was affected by the *mur1* mutation. Epidermal peels were taken from wild type and *sfr8* plants and measurements of stomatal density and stomatal index measured by counting the number of stomata, and the number of stomata in relation to the number of cells respectively for a given area. Results showed that there was no significant difference between wild type and *sfr8* for both stomatal density and index (two-sample T-test, Figure 4.4A and B). This suggested it could be the stomatal dynamics that are affected in *sfr8* and *mur1-1* mutants, which was assessed by measuring stomatal aperture.

4.2.2.2 Stomatal aperture after incubation in opening buffer

To assess if the *mur1* mutation affected stomatal dynamics, stomatal aperture was measured by taking epidermal peels from the abaxial side of mature leaves and imaging using a light microscope. Epidermal peels were incubated in a stomatal opening buffer (MES/KCl) for 2 h as previously described (Gonzalez-Guzman *et al.* 2012) to give a baseline of maximal stomatal aperture. The aperture of the stomatal pore was then measured in ImageJ. A one-way ANOVA and post-hoc Tukey test showed that there was no significant difference between wild type and *sfr8* stomatal aperture (Figure 4.5A). There was, however, significance observed between wild type and *sfr8-C* ($P \leq 0.05$), and *sfr8* and *sfr8-C* stomatal aperture ($P \leq 0.001$, Figure 4.5A). This could be a result of an observed difference in stomatal size in which *sfr8-C* stomata appeared much smaller than wild type, but further analysis would need to be carried out to verify this. There was also no significant difference found between wild type and *mur1-1* stomatal aperture, or wild type and *mur2* aperture (Figure 4.5B). These results suggest that *mur1-1, sfr8* and wild type plants are able to reach the same maximal aperture when incubated in opening buffer. It was possible that differences may only occur when stomata of *mur1* mutants were exposed to a closure signal, as was the case in the leaf drying experiment as with the excision of leaves and concurrent loss of the transpiration stream, stomata would receive a signal to close.

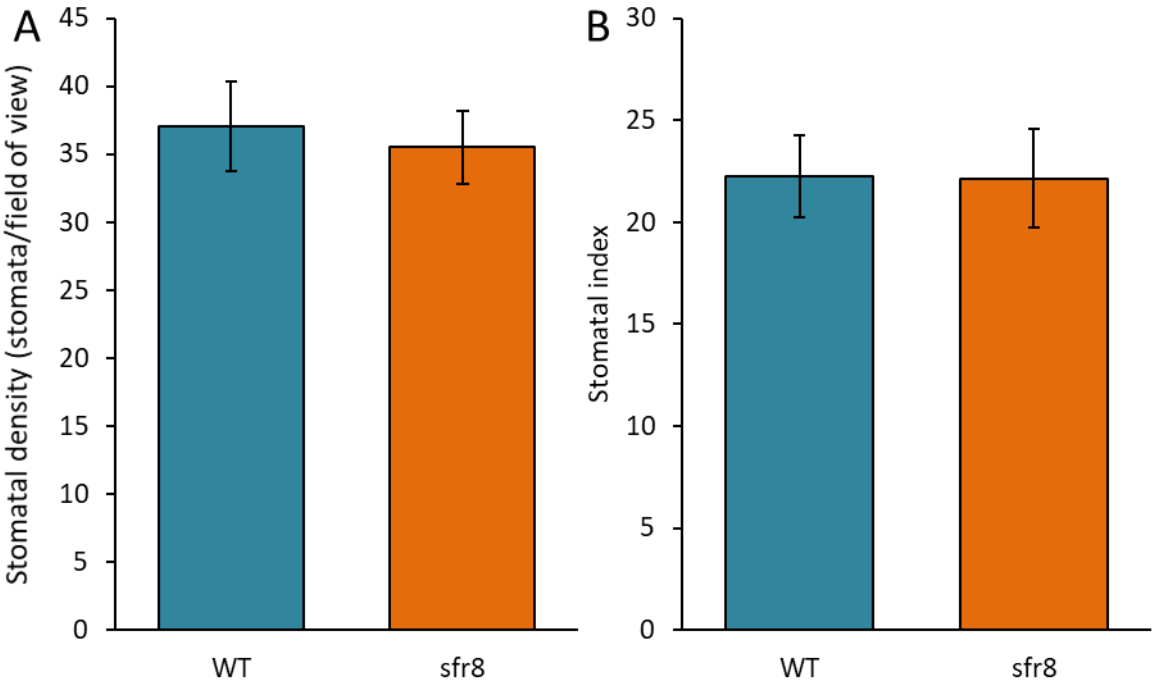

Figure 4.4: Stomatal density and index in wild type and *sfr8* plants. Stomatal density **(A)** and stomatal index **(B)** measurements of Col-0 wild type (WT) and *sfr8* plants. Each data point is an average from two experiments each with 15 repeats. Stomatal index is calculated as (S/(S+E))*100 where S is the number of stomata and E is the number of epidermal cells in the same given area. Error bars represent +/- 1 S.D. A two-way T-test carried out for each experiment showed no significant differences.

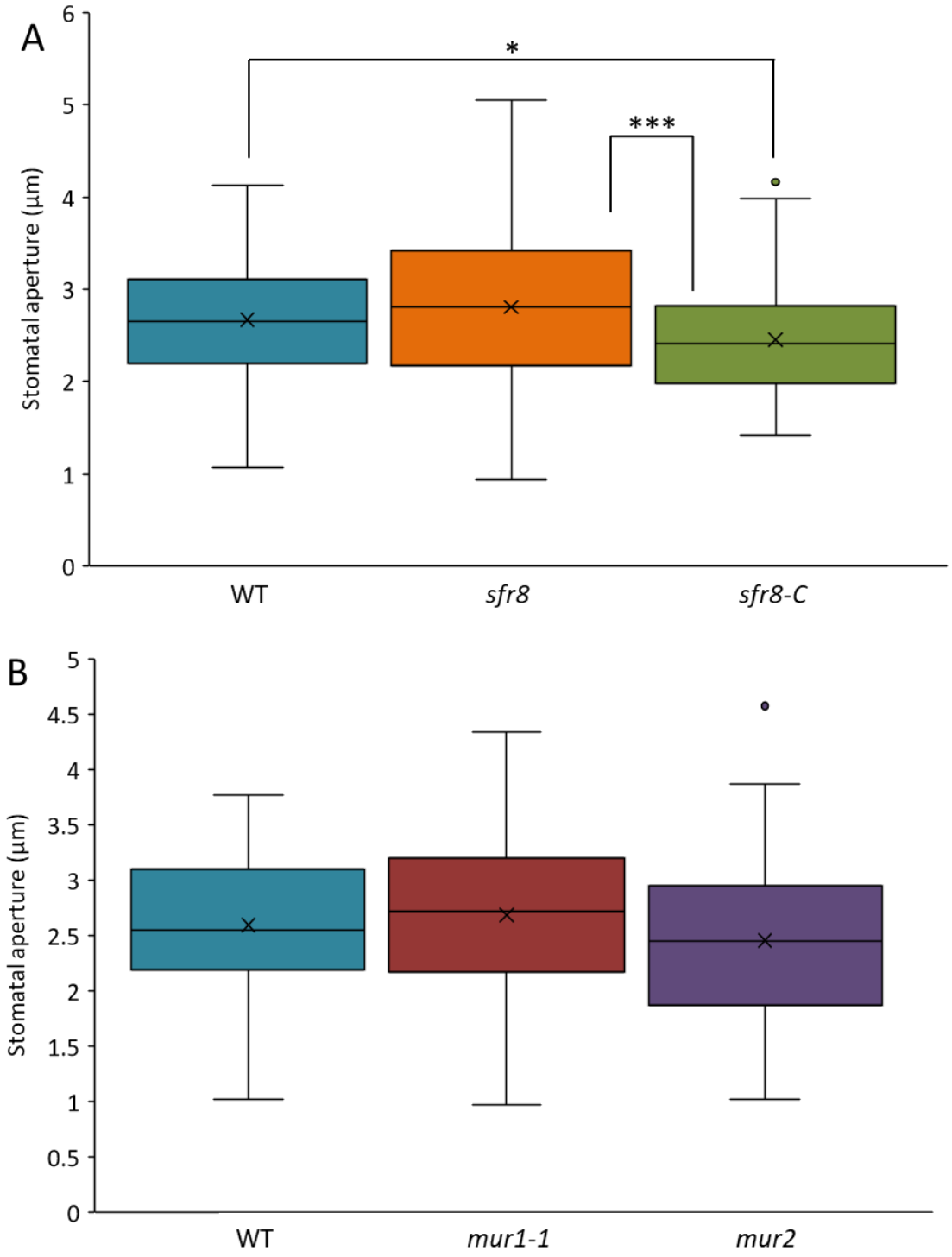

Figure 4.5: Stomatal aperture in epidermal peels treated with stomatal opening buffer. Stomatal aperture of Col-0 wild type (WT), *sfr8* and *sfr8-C* **(A)** and WT, *mur1-1* and *mur2* **(B)** measured after 2 h incubation in stomatal opening buffer. Apertures were measured by taking epidermal peels of leaves and imaging using a light microscope, using ImageJ to measure aperture. Boxplots show results from two **(B)** or three **(A)** separate experiments, each with 15 stomata measured from each of 3 separate leaf peels. For boxplots, coloured box represents inter-quartile range with centre line representing median, and 'x' representing mean. Bars represent maximum and minimum values, separate data points represent outliers. A one-way ANOVA followed by a post-hoc Tukey test was carried out on each experiment (*, $P \leq 0.05$, ***, $P \leq 0.001$).

4.2.2.3 Stomatal aperture after incubation with ABA

Although no differences were seen with incubation in opening buffer, it was possible that a difference could be observed after the stomata have been stimulated by a closure signal. Thus, abscisic acid (ABA), a well-known stomata closure signal (Walton 1980), was used as a chemical signal to induce stomatal closure. Epidermal peels were obtained as before and incubated in opening buffer for 2 h, followed by incubation in 5 µM ABA for 2 h. Images were taken as before on a light microscope and analysed in ImageJ. A one-way ANOVA followed by a post-hoc Tukey test showed a significant difference between wild type and *sfr8* stomatal aperture, as well as between *sfr8* and *sfr8-C* (Figure 4.6A, $P \leq 0.001$). Similarly, *mur1-1* stomatal aperture was found to be significantly greater than both wild type and *mur2* (Figure 4.6B, $P \leq 0.001$). No significant difference was found between wild type and *sfr8-C* and wild type and *mur2* aperture (Figure 4.6A and B). These results show that under conditions where stomata are required to decrease their stomatal aperture, such as in the presence of ABA, *sfr8* and *mur1-1* plants are not able to respond to the same extent as wild type plants, and this phenotype was reversable in the *sfr8* complemented line. The results also show that a loss of xyloglucan fucosylation did not appear to impact upon guard cell dynamics as *mur2* stomata responded in the same way as wild type, as was observed in the water loss assay. In order to assess if the phenotype observed in *sfr8* and *mur1-1* is as a result of a decrease in RG-II dimerisation, measurements would need to be carried out on plants supplemented with BA during growth.

4.2.3 Infrared thermography

4.2.3.1 Imaging of excised rosettes

Several studies have utilised infrared thermography for analysing differences in stomatal responses (Merlot *et al.* 2002; Wang *et al.* 2004; Amsbury *et al.* 2016). Infrared thermography was therefore used in this study to measure the temperature of plants as a way of observing differences in evaporative cooling and thus stomatal responses. In order to observe the effect of cutting leaves, as was done in the leaf drying assay, imaging was first carried out on cut rosettes. Mature wild type and *sfr8* plants were cut at the base of the plant just above the soil and placed on an even white surface. Images were taken every minute until plants showed clear signs of desiccation. In Figure 4.7A, both wild type and *sfr8* plants are reasonably cool compared to the ambient temperature, showing that the stomata were open, and the plants were carrying out evaporative cooling. A difference began to be observed approximately 25 minutes after the

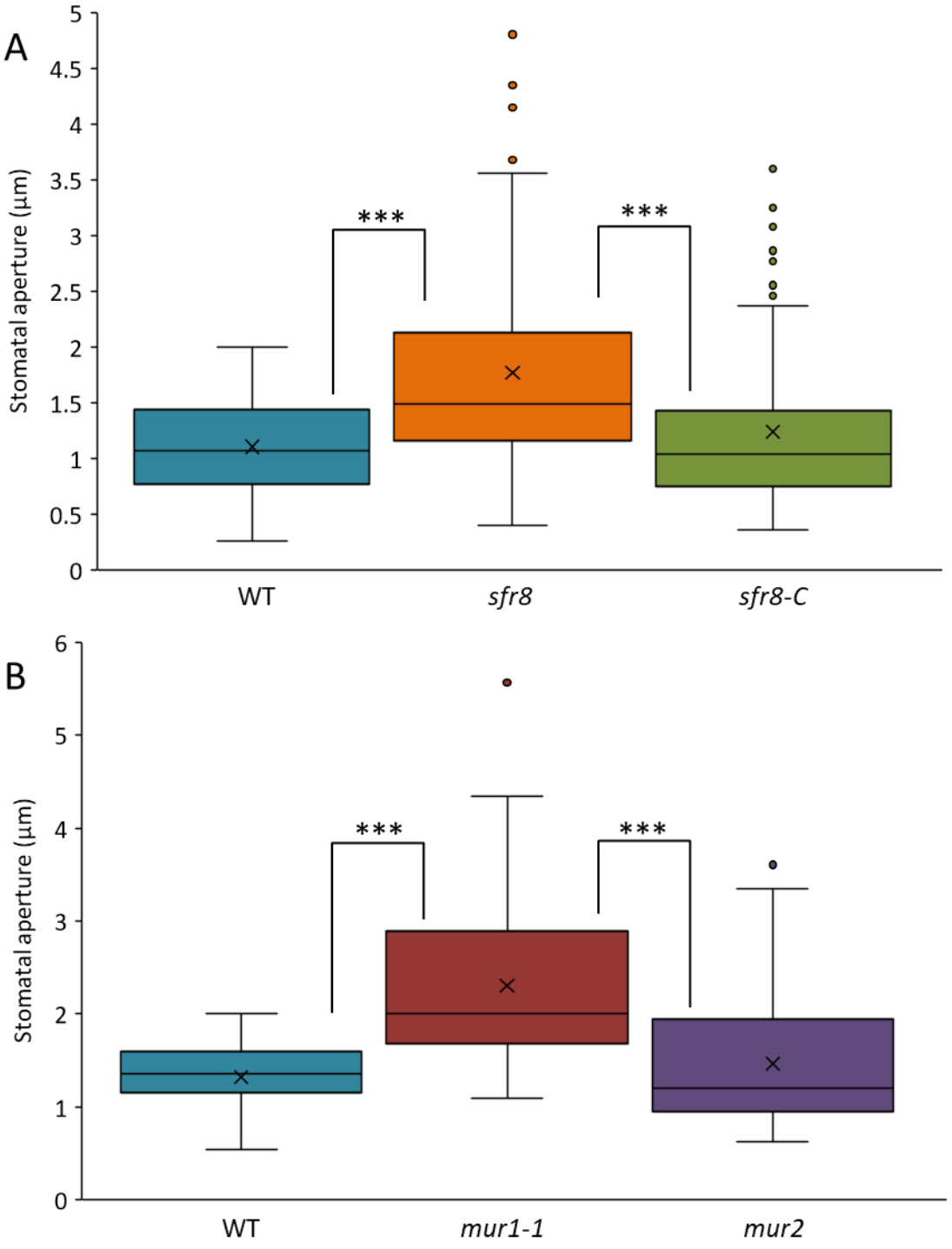

Figure 4.6: Stomatal aperture in epidermal peels treated with ABA. Stomatal aperture of Col-0 wild type (WT), *sfr8* and *sfr8-C* **(A)** and WT, *mur1-1* and *mur2* **(B)** measured after 2 h incubation in stomatal opening buffer, followed by 2 h incubation in ABA. Apertures were measured by taking epidermal peels of leaves and imaging using a light microscope, using ImageJ to measure aperture. Boxplots show results from two **(B)** or three **(A)** separate experiments, each with 15 stomata measured from each of 3 separate leaf peels. For boxplots, coloured box represents inter-quartile range with centre line representing median, and 'x' representing mean. Bars represent maximum and minimum values, separate data points represent outliers. A one-way ANOVA followed by a post-hoc Tukey test was carried out on each experiment (***, $P \leq 0.001$).

rosettes were cut as the wild type plants showed a higher temperature compared to *sfr8* (Figure 4.7B). This difference is even greater 40 minutes after cutting as wild type plants were clearly warmer than *sfr8* plants (Figure 4.7C), suggesting that in response to being cut and losing the transpiration stream, the stomata closed to conserve water and plants were no longer carrying out evaporative cooling. This was not the case in the *sfr8* plants, which although appeared warmer than the initial temperature measured after cutting as shown in Figure 4.7C, were not able to respond as quickly as wild type. These results concur with those seen in the leaf drying assay.

Eventually *sfr8* rosettes did increase in temperature as shown in Figure 4.7D, indicating that evaporative cooling was no longer taking place. However, it is likely that this was because of the rosettes drying out due to extensive water loss rather than a response of the stomata. These images support the results obtained from measuring water loss and stomatal aperture in suggesting that *sfr8* stomata are unable to respond in the same way as wild type when exposed to a closure signal. They also allow for observation of the whole plant response and infer consequences for plant-water relations in *sfr8* plants that are unable to properly regulate stomata. To gain more insight into these consequences however, it was necessary to see how drought affected intact wild type and *sfr8* plants under normal conditions of growth.

4.2.3.2 Imaging whole plants in plugs

A more authentic response of stomata and overall plant responses to drought was measured via thermal imaging using whole plants growing in soil pellets. To accelerate the stomatal response, a change in humidity was applied as has been previously used when measuring stomatal responses with infrared thermography (Wang *et al.* 2004). Plants were watered and placed at ca. 100% humidity for 16 h the night before imaging began. Approximately 40 minutes before the first image was taken, plants were transferred from ca. 100% to ca. 50% humidity and arranged as shown in Figure 4.8G (see also Figure 2.4), after which water was withheld from droughted plants, and watered plants were given water twice daily. Seventy minutes after transfer from high to low humidity, the leaf edges of *sfr8* plants showed a slight difference in temperature to wild type (Figure 4.8A). This was clearer after a further six hours, when wild type plants appeared significantly warmer than *sfr8* plants (Figure 4.8B), suggesting that wild type plants responded to the decrease in humidity by closing their stomata, whereas the *sfr8* plants were unable to respond as quickly and so were still carrying out evaporative cooling. *sfr8* plants did eventually respond; after 24 hours (Figure 4.8C) and more clearly after 72 hours (Figure

4.8D), the temperature of wild type and *sfr8* plants was more comparable. This was likely because *sfr8* plants *were* able to respond to signals, but at a slower rate. Therefore, under normal conditions when not exposed to a specific closure signal, *sfr8* stomata were able to open and close in a similar way to wild-type. However, a slight difference in temperature was always visible, suggesting that *sfr8* stomata were not able to reach the extent of closure that wild type stomata did (Figure 4.8D-F).

Another observation made during the imaging was that *sfr8* plants desiccated earlier than wild type plants (Figure 4.7E), with droughted *sfr8* plants beginning to wilt 20 hours before wild type plants showed signs of desiccation (Figure 4.7F). This suggests that the inability of *sfr8* plants to fully close their stomata has an impact on desiccation of plants under drought conditions. One observation that was not made, however, was any clear difference in leaf temperature between watered and droughted wild type plants. It was expected that droughted wild type plants would be warmer as the plants respond to a lack of water by closing their stomata. One hypothesis as to why this was not seen was because the soil plugs that the plants were grown in were open to the environment. Thus, although the watered plants appeared to be well watered, their roots may have experienced drought conditions through exposure to dry air. Other factors such as the transfer from high to low humidity and imaging in constant light may also have masked differences between watered and droughted wild type plants. For these reasons the experiment was repeated using conditions that represented a more realistic environmental setting.

4.2.3.3 Imaging of whole plants in pots

Whole plant imaging under drought conditions was repeated but without transferring plants from high to low humidity and observing light dark cycles of a normal British summer's day. Plants were grown in soil plugs as before, but the day preceding the start of imaging, the outer netting of the plugs was removed, and the pellet placed into a pot with extra soil where required. Plants to be watered were given water twice daily by standing in water and directly applying to the soil surface to assure saturation, whereas water was withheld from plants to be droughted after the last watering the evening before imaging began. Twice as many wild type plants were used to increase the probability of observing drought responses in wild type. After 19 hours with no additional water, there did not appear to be any differences between watered and droughted wild type plants (Figure 4.9A). Neither were differences observed between wild type and *sfr8* plants. Temperatures appear to differ between wild type and *sfr8* in Figure 4.9B which could be indicative of the transition between light and dark states where stomata were closing more

quickly in wild type plants than in *sfr8*. However, a simpler explanation could be that the leaves of the *sfr8* plants were much closer to the soil, and thus the temperature of the leaves appeared lower due to the cool temperature of the soil. Wild type leaves were held much higher above the soil, likely experiencing more turbulent air conditions, and no particular differences in temperature were observed in the morning in transition from dark to light (Figure 4.9C).

The first observable differences between watered and droughted wild type plants were seen approximately 138 hours after last watering of the droughted plants (Figure 4.9D). This difference can be seen more clearly in Figure 4.9E, 162 hours after the last watering. This image, taken in the morning, suggests that as the stomata of watered plants were opening, the stomata of the droughted wild type plants were not as they had reached a point where it was necessary to conserve water. None of the plants, including *sfr8*, reached a point where the leaves wilted or looked desiccated in any way during the course of the experiment. The most obvious conclusion from these results is that the experimental design when using infrared thermography is highly important, and perhaps further modification is necessary to observe the hypothesised results, i.e. differences between *sfr8* and wild type, and differences between droughted and non-droughted plants, within one experiment. Although the stomatal response to drought was observed in wild type plants, it was not clear in *sfr8* plants as no difference in temperature was seen between watered and droughted *sfr8* during the experiment. One factor that may have masked any differences was the closeness of the *sfr8* leaves to the soil, amplified by the transfer from plugs to pots. The shortened petiole length of *sfr8* plants may also have had an impact here (see Chapter 3), as wild type leaves had the ability to move upwards and be held further away from the soil, whilst *sfr8* leaves did not. The effect of this was two-fold – the soil temperature impacted upon the temperature measurements of *sfr8* leaves, but not wild type, and the wild type leaves were more exposed to turbulent airflow, which would result in an increase in evaporative cooling where water was plentiful (Costa, Grant & Chaves 2013). Alternatively, it could be that under normal conditions, where there are no changes in humidity, *sfr8* stomata are able to function at close to wild-type levels. Although thermal imaging provides insights into stomatal movements, the results obtained in this particular experiment were too variable to conclude that alterations to stomatal dynamics was detrimental to plant-water relations under drought conditions compared to wild type. In order to gain a more quantitative measure of stomatal aperture, it was necessary to employ a technique that would provide more detail of the dynamic process of the opening and closing of stomata.

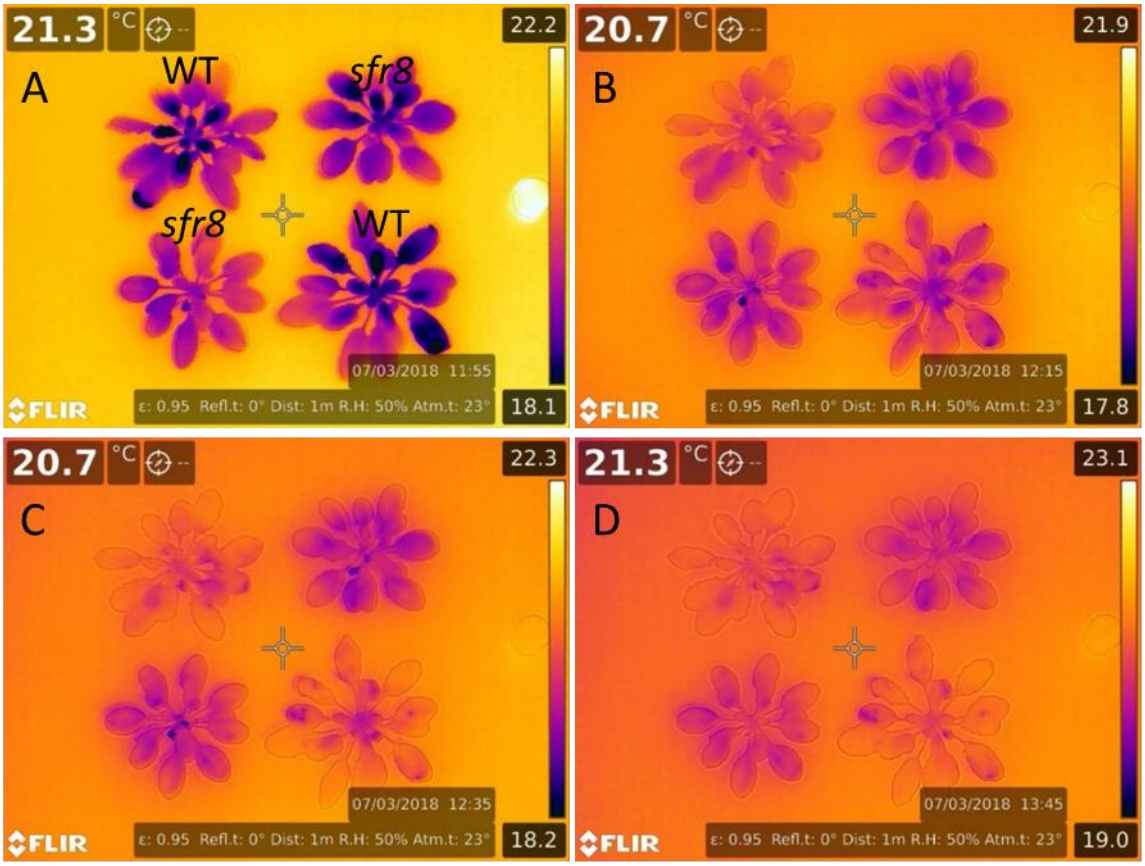

Figure 4.7: Thermal imaging of cut rosettes of wild type and *sfr8*. Infrared thermography of cut rosettes of mature Col-0 wild type (top left and bottom right) and *sfr8* plants (top right and bottom left). Genotypes are labelled in **(A)** and are the same in each image **A)** Rosettes 5 min after cutting, **B)** rosettes 25 min after cutting, **C)** rosettes 40 min after cutting, **D)** rosettes 110 min after cutting. All images show ambient temperature (top left) and colour temperature scale (right).

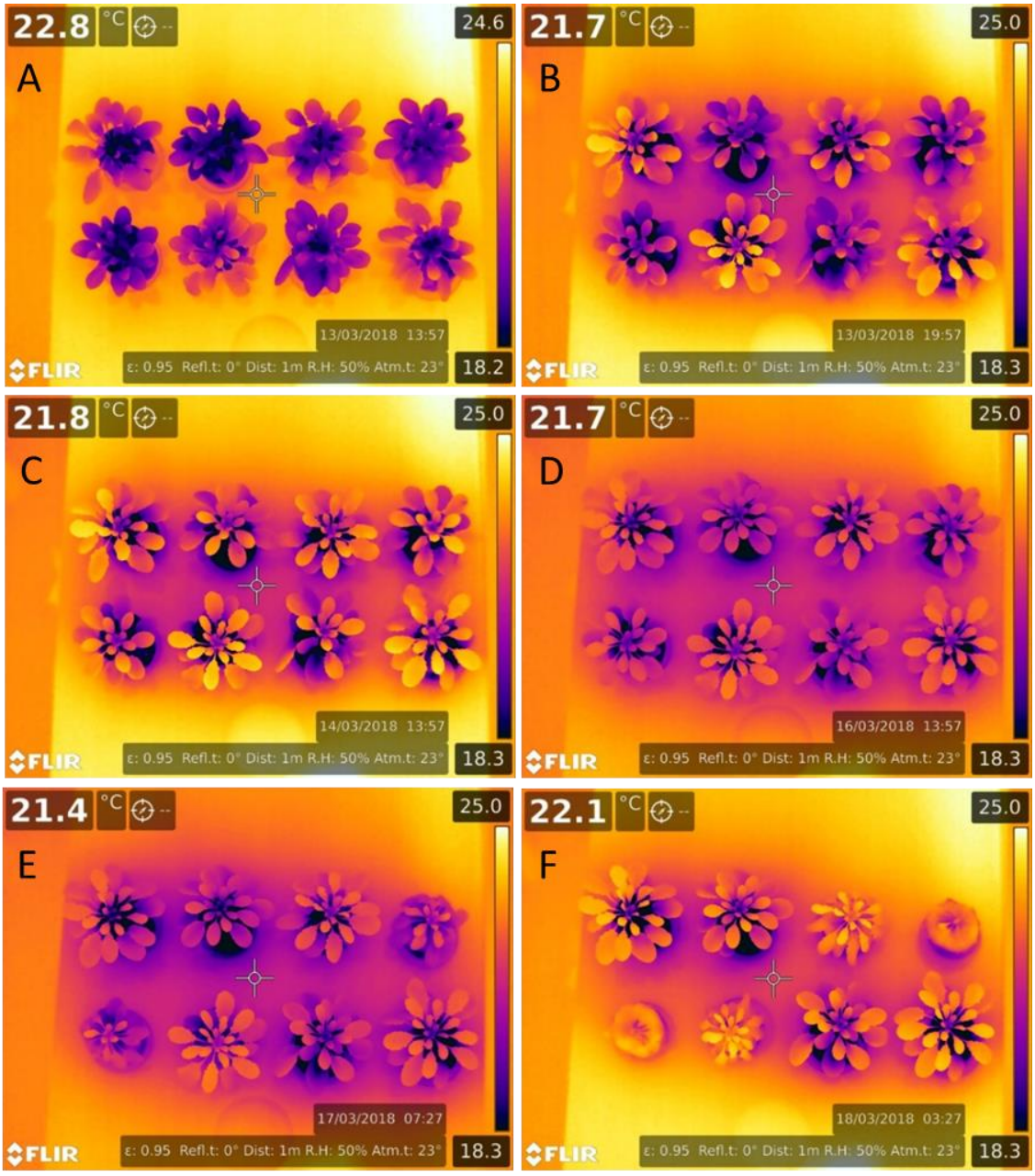

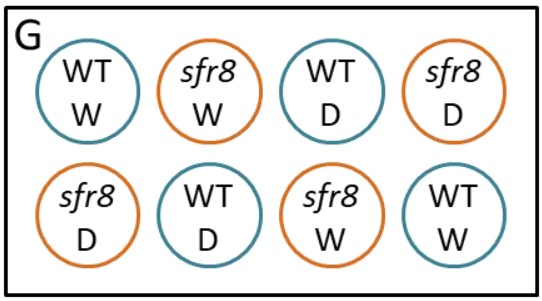

Figure 4.8: Thermal imaging of whole plants of wild type and *sfr8*. Infrared thermography of mature Col-0 wild type (WT) and *sfr8* plants under watered (W) and droughted (D) conditions as shown in **G**. Images show plants **A)** 70 min after transfer from 100% to 50% humidity; **B)** 6 h after A; **C)** 24 h after A; **D)** 72 h after A; **E)** upon clear desiccation of droughted *sfr8* plants and **F)** upon clear desiccation of droughted WT plants. All images show ambient temperature (top left) and colour temperature scale (right).

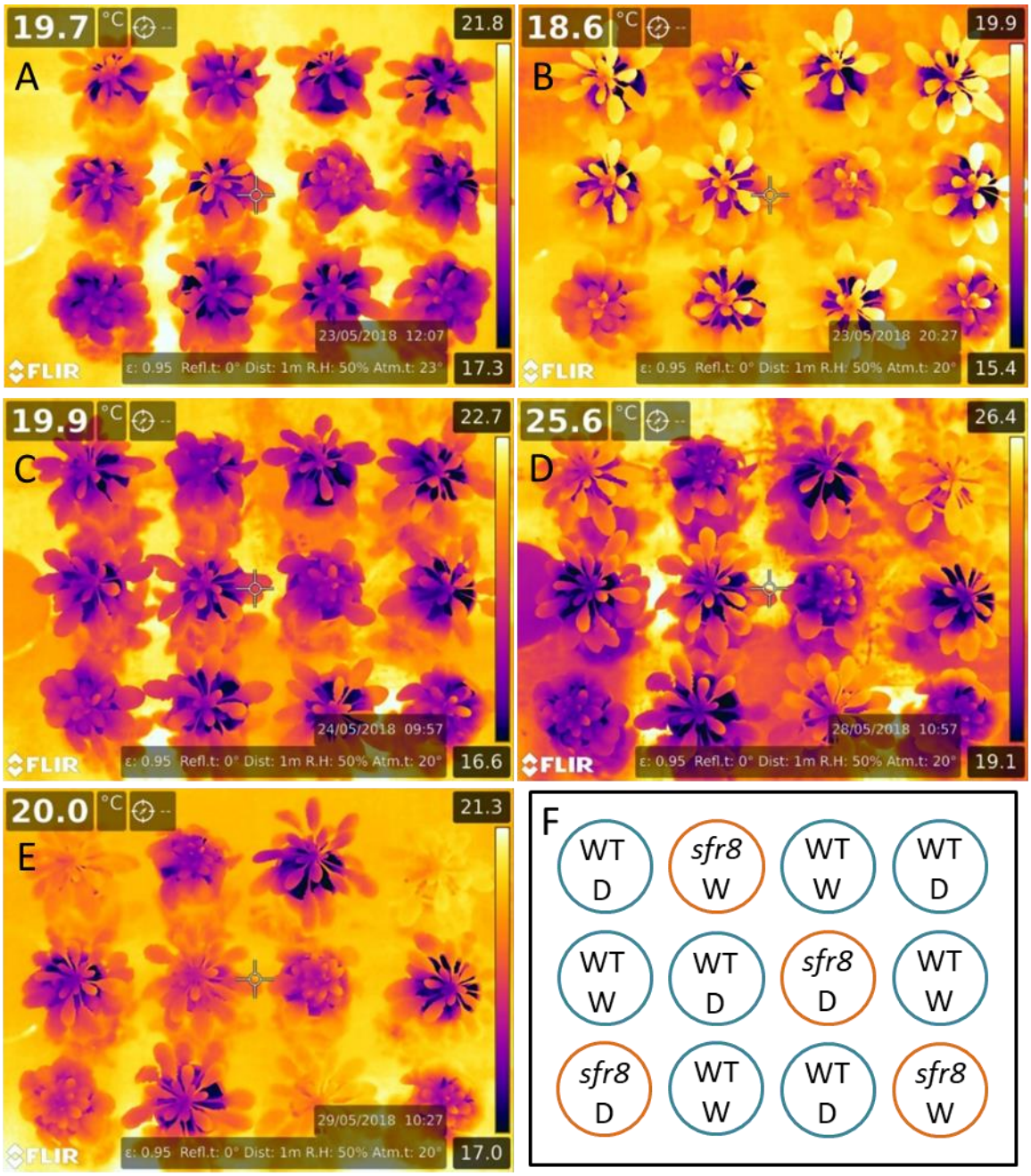

Figure 4.9: Thermal imaging of whole plants of wild type and *sfr8* in pots. Infrared thermography of mature Col-0 wild type (WT) and *sfr8* plants under watered (W) and droughted (D) conditions as shown in **F**. Images show plants **A)** 19 h after last watering of droughted plants; **B)** 27 h after watering; **C)** 41 h after watering; **D)** 138 h after watering and **E)** 162 h after watering. All images shown ambient temperature (top left) and colour temperature scale (right).

4.2.4 Stomatal conductance

To quantitatively assess stomatal responses in a more representative system than epidermal peels, and in a more robust experimental set-up than the thermal imaging, a LICOR portable photosynthesis system that could measure stomatal conductance in mature intact plants was used. Changes in CO_2 concentration were used as a stimulus; an increase in environmental CO_2 concentration is a signal for plants to close their stomata, whereas a decrease in CO_2 is a signal to open them (Heath 1948; Xu *et al.* 2016). One leaf still attached to a mature plant was placed into a leaf chamber attached to the LICOR photosynthesis system and allowed to acclimate at 400 ppm CO_2 (approximate to ambient concentrations) for ca. 25 mins. The CO_2 concentration was decreased to 50ppm for ca. 60 mins, then increased to 1000ppm for ca. 60 mins. Analysis of results showed that *sfr8* plants were able to respond to changing CO_2 concentrations by opening and closing their stomata, but not to the extent of wild type plants (Figure 4.10). Conductance measurements at the higher concentration of CO_2 were similar for wild type and *sfr8*, suggesting they were both able to close their stomata to the same extent. Results for *sfr8-C* show that conductance levels were higher than that for *sfr8* but did not reach values obtained by wild type plants. Interestingly, the conductance level started lower than wild type, and appeared to follow a similar pattern but at values that were shifted downwards by about 0.05 mol m^{-2} s^{-1}. The rates of opening and closing were analysed by measuring the slope of the first fifteen minutes of the increase and decrease in stomatal conductance after the decrease and increase in CO_2 concentration respectively and carrying out an ANCOVA (Figure 4.11A and B). This analysis showed that the rates of opening and closing for wild type and *sfr8-C* did not significantly differ, whereas *sfr8* had a slower rate in both instances, highlighted by the significant difference of the slope (Figure 5.11A and B, $P \leq 0.005$). These results show that *sfr8* stomata are able to open and close, but at a rate that is significantly slower than that of wild type stomata.

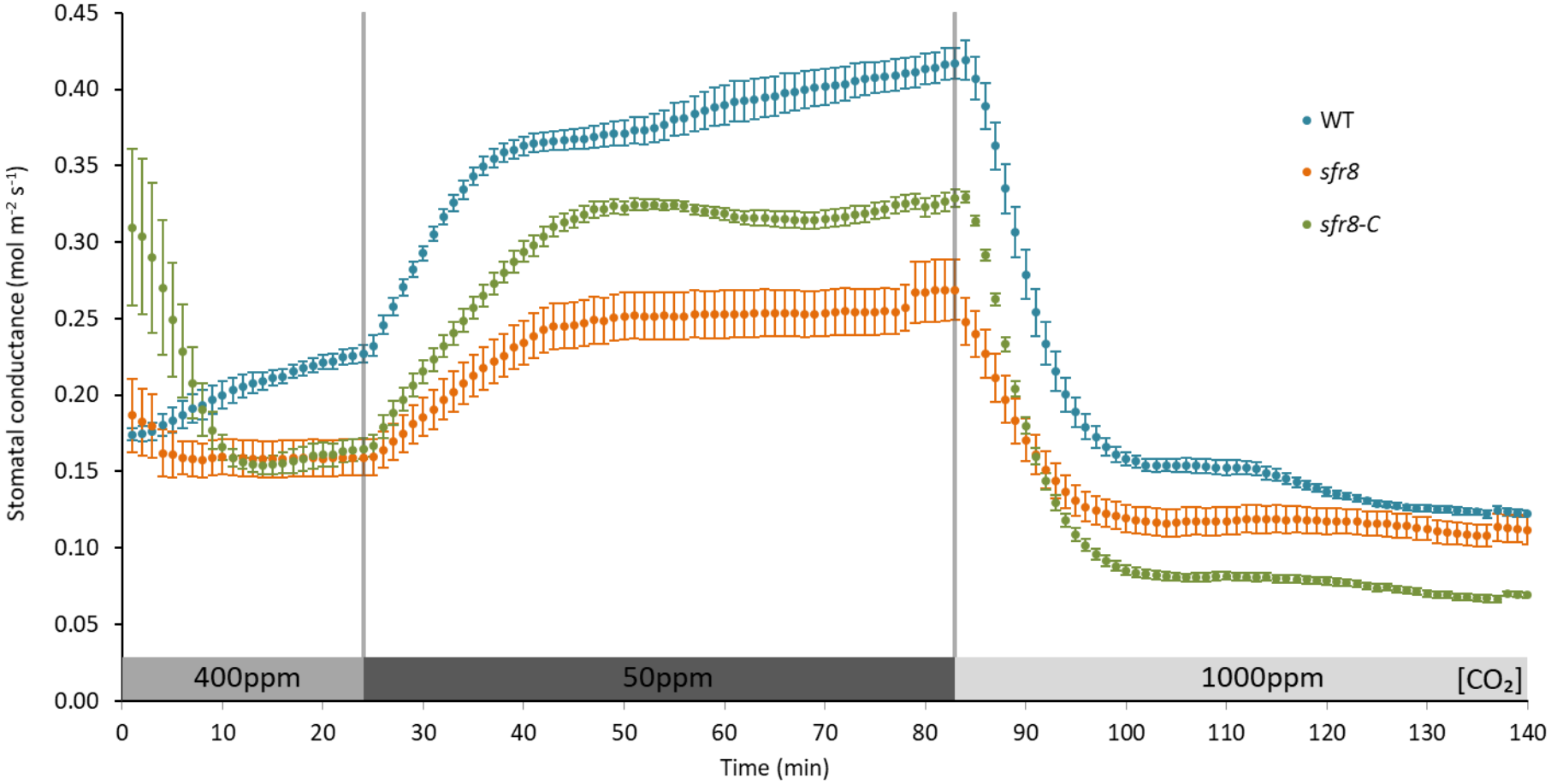

Figure 4.10: Stomatal conductance of wild type, *sfr8* and *sfr8-C* plants exposed to changing CO_2 conditions. Stomatal conductance of mature Col-0 wild type (WT), *sfr8* and *sfr8-C* plants measured using a LICOR plant photosynthesis system (LI-6400). Plants were acclimatised at 400ppm of CO_2 for 25 min before CO_2 concentration was decreased to 50ppm for approximately 60 min, then increased to 1000ppm for approximately 60 min. Results are an average of measurements from six individual plants of each genotype. Error bars are +/- 1 S.E.

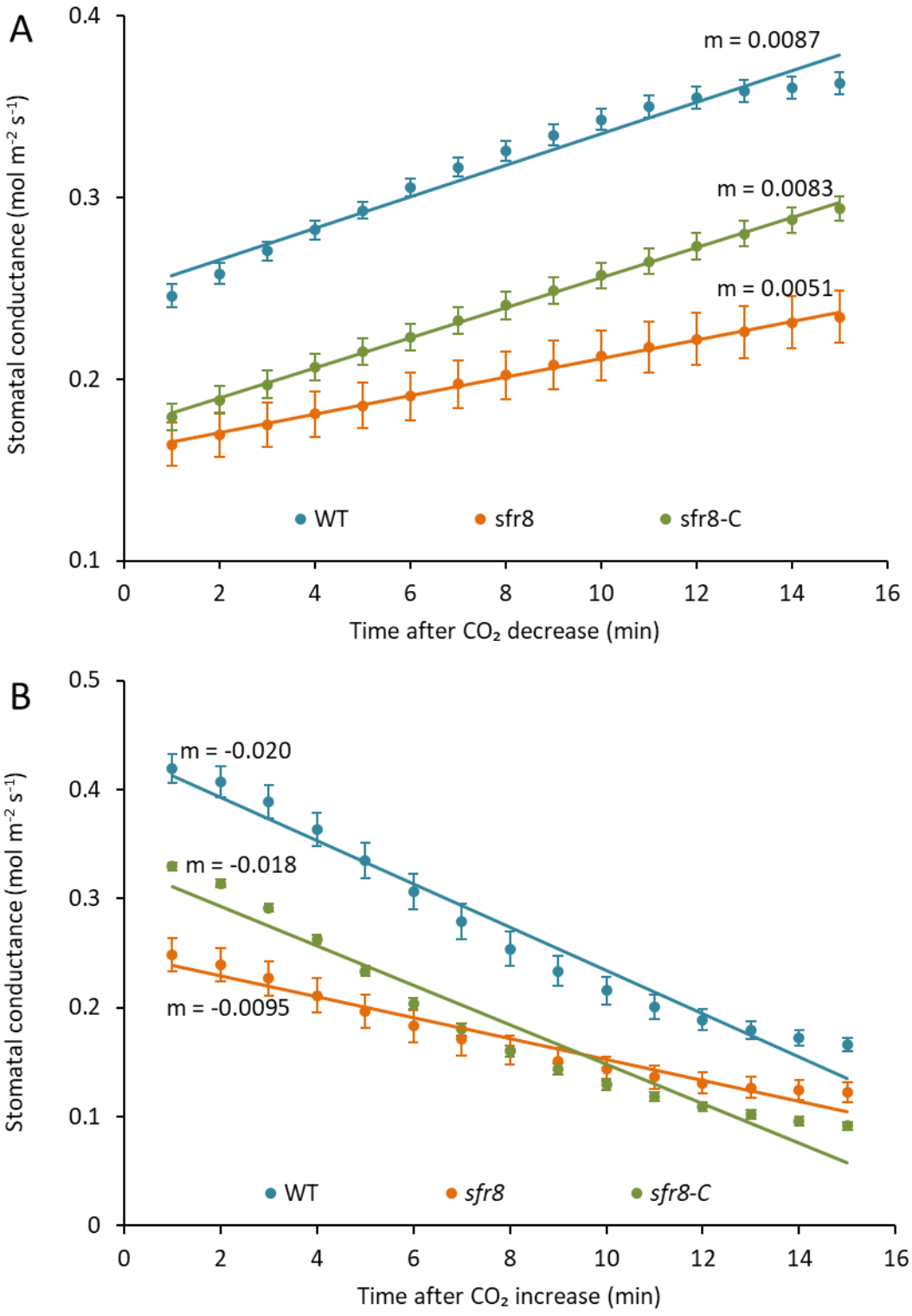

Figure 4.11: Analysis of the increase and decrease in stomatal conductance with changing CO_2 conditions. Comparison of the first 15 min of the increase **(A)** and decrease **(B)** in stomatal conductance of Col-0 wild type (WT), *sfr8* and *sfr8-C* plants following a decrease from 400 ppm to 50 ppm **(A)** or an increase from 50 ppm to 1000 ppm **(B)** CO_2 concentration. Slope values (m) are given for each line with units of mol m^{-2} s^{-1} min^{-1}. ANCOVA analysis showed that the slope of *sfr8* was statistically different to that of wild type and *sfr8-C* for both sets of data ($P \leq 0.005$).

4.3 Discussion

4.3.1 Guard cell dynamics are compromised in plants with a mutation in the MUR1 *gene*

A preliminary investigation into water loss from *sfr8* leaves suggested that the mutant may exhibit a desiccation phenotype. Further experiments in the form of a leaf drying assay confirmed that both *sfr8* and *mur1-1* leaves decreased in mass much more quickly than wild type, a complemented line, and the *mur2* mutant (Figure 4.1). This decrease in mass suggested that leaves of *mur1* mutants were experiencing an increased water loss. It is well-known that the main pathway of water loss in plants is via transpiration through stomata (Maercker 1965), but water can also be lost via evaporation from the cuticle (Lendzian & Kerstiens 1991). Alterations to these structures could result in increased water loss. It is also possible that alterations to how water moves through the plant could affect water loss. The main routes of water movement are apoplastic (extracellular) and symplastic (intracellular) routes (House 1974). Taking into consideration that a mutation in the *MUR1* gene was shown to result in a decrease in RG-II dimerisation (see Chapter 3), it could be that alterations to cell wall structure impact upon water movement via the apoplast. A decrease in RG-II dimerisation results in an increased cell wall pore size (Fleischer *et al.* 1999), which may allow water to move more rapidly through the cell wall and thus be lost from the plant more quickly. It is possible that RG-II monomer could bind water differentially to the dimer, again allowing more rapid movement of water through the cell wall, however there are no specific studies to support this hypothesis.

Considering stomata are the principal site of water loss from the plant, an investigation into whether stomata were modified in *sfr8* plants in any way was carried out. One way in which this could occur is as a result of an increase in stomatal density which has been shown to affect gas exchange (Yoo *et al.* 2010). However, analysis of this showed no difference in stomatal density (Figure 4.4A), or the number of stomata per cell i.e. stomatal index (Figure 4.4B) between wild type and *sfr8* plants. As no difference was seen in the number of stomata, it was then investigated as to whether the stomatal pore size was altered and thus the guard cell dynamics. Several different approaches were taken in order to measure this. Firstly, measurements of stomatal aperture were carried out on epidermal peels obtained from leaves of mature plants using a method previously described by Gonzalez-Guzman *et al.* (2012). Incubation in an opening buffer gave a measurement of the maximum stomatal aperture, as the stomata would have been open when the peels were taken, and the opening buffer would maintain them this way. These measurements would show if there were any intrinsic differences in stomatal aperture in

the absence of a closure stimulus. Results showed that there was no significant difference between wild type, *sfr8* and *mur1-1* mutants, suggesting the stomata were able to reach the same maximal opening (Figure 4.5A and B). There was, however, a significant difference in aperture found between *sfr8* and *sfr8-C,* and wild type and *sfr8-C* stomata. This could be a result of the decrease in size of the guard cell pair which was observed in *sfr8-C* plants, although further analysis would need to be carried out to verify this. Interestingly, research has shown that plants that have higher rates of response to stomatal stimuli often have smaller stomatal size (Drake, Froend & Franks 2013). Thus, it could be hypothesised that that stomata of *sfr8-C* respond faster because they are smaller. However, this was not observed in the conductance experiments, as *sfr8-C* stomata responded at the same rate as wild type to changing CO_2. Stomatal size has also been correlated with stomatal density (Drake *et al.* 2013), so it may be that stomatal density is increased in *sfr8-C* plants, possibly in relation to fucose content, but this would need to be measured.

Although no intrinsic increase in stomatal pore size was observed in the *sfr8* mutant, treatment with abscisic acid (ABA), a well-known stomatal closure stimulus (Trejo, Carlos, Davies & Ruiz 1993), resulted in a significant difference in aperture between *sfr8* and wild type, and *sfr8* and *sfr8-C* (Figure 4.3). This suggests that in the two-hour incubation period, wild type and *sfr8-C* stomata were able to respond to the closure signal elicited by ABA, whereas the *sfr8* stomata were not. This result was also observed between *mur1-1* and wild type stomata. Infrared thermography was also carried out as a less invasive method to imply stomatal aperture from temperature measurements of whole plants and allowed further insight into the desiccation phenotype observed from the leaf drying assay. Infrared thermography has previously been used to identify *Arabidopsis* mutants compromised in stomatal dynamics by observing changes in temperature as a measure of evaporative cooling (Merlot *et al.* 2002; Wang *et al.* 2004). Results showed a clear difference in temperature and therefore evaporative cooling between wild type and *sfr8* plants in response to excision of whole rosettes, providing evidence that the behaviour seen in the leaf drying assay was as a result of the inability of stomata to close in the *sfr8* mutant (Figure 4.6). Imaging plants after changes to humidity, a method used by Wang *et al.* (2004), provided further evidence of the reduced ability of *sfr8* plants to close their stomata, but showed that eventually, *sfr8* and wild type plants had very similar temperatures, suggesting that the stomata *are* able to close (Figure 4.7). Plants in this experiment were also subjected to drought and results highlighted that the inability of *sfr8* to control stomatal aperture resulted in earlier desiccation of *sfr8* plants.

Thermal imaging clearly showed differences between *sfr8* and wild type plants in terms of stomatal dynamics, and provided evidence that stomata were not 'stuck' open. Jones *et al* (1999) demonstrated that thermal imaging could even be used to estimate stomatal conductance, as leaf temperature varies with evaporation and is thus a function of stomatal conductance (Tanner 1963). However, It was clear especially from the final thermography experiment, that there are potential areas of error with the technique, and it has been suggested that estimations of conductance from thermal imaging are sensitive to errors in reference surface temperatures (Jones 1999). Thus, direct measurements of stomatal conductance using a LICOR photosynthesis system were also carried out to analyse in more detail the patterns of opening and closing in mutant and wild type plants.

The stimulus chosen was CO_2 as this was easy to modify and observe changes in conductance in response to this, as has been shown in previous studies (Farquhar, Dubbe & Raschke 1978; Engineer *et al.* 2017). The results showed a clear difference in the response of wild type, *sfr8* and *sfr8-C* stomata to increases and decreases in CO_2 concentration (Figure 4.9). Most importantly, it is clear that *sfr8* stomata are able to open and close their stomata and shows that they are not impeded from closing as the aperture measurements after incubation with ABA may have suggested. This also suggests that the mutants are not unresponsive to ABA like other mutants with altered stomatal dynamics have been shown to be (Merlot *et al.* 2002), as ABA stomatal signalling pathways have been shown to be required for CO_2 induced stomatal responses (Chater *et al.* 2015). Interestingly, wild type stomata appear to be able to reach a much higher conductance than *sfr8*, which plateaus at about 0.25 mol m^{-2} s^{-1} whilst both reached a similar *lower* level of conductance in response to increased CO_2, suggesting that the range of movement of *sfr8* stomata is more restricted. These differences in maximal aperture observed are contrary to those seen when measuring aperture in epidermal peels after incubation in opening buffer, as in these experiments, apertures were shown to be the same. This could be a consequence of obtaining the epidermal peel, as environmental factors such as the temperature and humidity the peel was taken in can affect results (Zeiger 1983). Further artefacts could occur with the removal of the mesophyll layer or rupture of epidermal cells, as guard cell dynamics are also influenced by neighbouring cells (Starlfelt 1966). Although taking conductance measurements can impact upon leaf behaviour as stated earlier, it is more likely that the conductance measurements are closer to the 'true' values of stomata openness, since they are taken from guard cells in an *in vivo* environment.

Another observation apparent from these results is that stomata from *sfr8-C* plants were not able to reach the same level of conductance as wild type but *were* more open than *sfr8* and showed a similar range of movement to wild type that appeared to be shifted down. This could be another consequence of the difference in stomatal size observed between wild type, *sfr8* and *sfr8-C* (data not shown), which could mean that the conductance levels of wild type are not achievable by *sfr8-C* because the pore simply cannot open wide enough (Drake *et al.* 2013). As well as demonstrating that *sfr8* stomata are not stuck open, the conductance results also indicate that there is a difference in the rates of opening and closing between wild type and *sfr8*. Analysis of the first fifteen minutes of conductance after changes in CO_2 showed a significant difference in the slope and therefore the rate of increase and decrease in stomatal conductance (Figure 4.10). This suggests that *sfr8* guard cells are much slower to adapt from turgid to flaccid and vice versa, a process that is reversed in the complemented line, which shows rates similar to that of wild type.

4.3.2 Why do sfr8 *stomata have a decreased rate of movement?*

There are several factors affecting the rapidity of guard cell movements that have previously been categorised into anatomical (e.g. size and density), biochemical (e.g. activity of ion channels) or structural (e.g. cell wall elasticity) (Lawson & Vialet-Chabrand 2018). In terms of anatomical, factors, as previously stated smaller stomata have been suggested to have increased rate of movement (Drake *et al.* 2013), which may be related to a more rapid change in solutes due to an increased surface area to volume ratio (Hetherington & Woodward 2003; Raven 2014). Although the observation was made that *sfr8-C* stomata were slightly smaller than wild type and *sfr8*, there were no obvious differences in size between wild type and *sfr8*, although this would of course need to be explicitly verified. Measurements of stomatal density and index also showed no significant difference between wild type and *sfr8*, suggesting anatomical factors were not influencing differences in stomatal conductance.

Stomatal opening relies on changes in guard cell turgor pressure stimulated by the movement of ions across the membrane to induce osmotic adjustments (Blatt 2000). Several studies have shown that the rapidity of stomatal movements is linked to the capacity for solute transport across the plasma membrane, and how quickly components such as ion channels are able to respond to environmental stimuli (Lawson & Blatt 2014). Indeed, in grass species, the rapid transport of ions between guard cells and subsidiary cells allows fast and efficient stomatal movements (Cai *et al.* 2017; Jezek & Blatt 2017). However, although sugars such as sucrose are

suggested to play a role in stomatal movements (Daloso & Fernie 2016), there is no evidence that fucose is involved, which if it were, could result in alterations to stomatal dynamics as seen in *sfr8* and *mur1-1* mutants. It is also generally accepted that most L-fucose in the plant is used up in fucosylation (see Chapter 3). It cannot be ruled out that fucosylation of proteins involved in ion transport or osmotic regulation of stomata may be affected in the *sfr8* mutant but again, there is little evidence to suggest fucosylation is important for stomatal movements. Considering the primary role of fucose within the plant as a component of cell wall polysaccharides (see Chapter 3), it is more likely that the alterations to stomatal dynamics observed in *sfr8* mutants is as a consequence of structural alterations to the cell wall. One way to verify that biochemical factors i.e. ion transport, are not altered in the mutant would be to observe volume changes in guard cell protoplasts that are unhindered by any influences of the cell wall (Zhu *et al.* 2015).

4.3.3 How does the cell wall influence guard cell dynamics?

Recently, more and more research is emerging that highlights the necessity of guard cell wall pectins for normal stomatal function. In work by Atkinson *et al.* (2002), overexpression of a fruit polygalacturonase enzyme (catalyses the breakdown of galacturonic acid chains) in leaves of apple trees resulted in aberrant stomatal responses to dark and ABA stimuli, although this also resulted in perturbations to cell adhesions around the guard cells which may have influenced the findings. In *Arabidopsis*, the loss of a polygalacturonase enzyme prevented normal stomatal closure, and conversely overexpression of that enzyme accelerated stomatal opening (Rui *et al.* 2017). Another study has shown that arabinan is essential for guard cell function as digesting cell walls with arabinase resulted in a reduced ability of *Commelina communis* stomata to open in response to fusicoccin treatment. Interestingly, treating cell walls with pectin methyl-esterase (PME) and endo-polygalacturonase (EPG) resulted in stomata that were more open than wild type (Jones *et al.* 2003). The same observations were made in stomata of other plant species, including *Zea mays,* a monocot which is known to have a cell wall that generally contains less pectin than dicots (Jones *et al.* 2005). In *Arabidopsis,* cellulose also appears to play a role in stomatal movements, as a mutant of the cellulose synthase locus *AtCesA7* had smaller stomatal apertures than wild type both with and without ABA induction (Liang *et al.* 2010). Work by Amsbury et al (2016) has shown that *Arabidopsis* plants with a mutation in a pectin methyl-esterase, *pme6*, which is highly expressed in the guard cells, have stomata with a smaller range of movement in response to changing CO_2 conditions, display a more restricted response to ABA treatment and an inability to prevent evaporative cooling by closing stomata under drought

conditions, as shown via thermal imaging. The authors show that a reduction in *PME6* expression results in guard cell walls with increased homogalacturonan (HG) methyl-esterification, whilst under normal conditions guard cell HG chains are relatively un-esterified (Amsbury *et al.* 2016). Methylation status is generally believed to influence HG cross-linking; with a decrease in methyl-esterification, HG chains are able to cross-link via Ca^{2+} cations, bringing the chains closer together (Jarvis 1984; Willats *et al.* 2001).

These findings could be summarised in a recent model developed by Woolfenden *et al* (2017) that attempts to elucidate the mechanism via which the guard cell wall influences turgor changes and thus stomatal opening and closing. The findings of the model suggest that guard cell dynamics rely on certain properties, namely anisotropy of the cell wall in the form of reinforced microfibril hoops, and strain-stiffening of the cell wall matrix. The model predicts that a stoma will be less open when the cell wall matrix is stiffer, and conversely will open more when the matrix is less stiff. This is because the cell-wall matrix must stiffen significantly as strain increases to limit the aperture of the pore with increasing pressure. Thus if the cell wall is less stiff, the size of the obtainable aperture will increase (Woolfenden *et al.* 2017). The authors go on to suggest that pectins that contribute to the stiffness of the matrix can be identified by degrading pectins and comparing the effects on stomatal dynamics. This was demonstrated by showing that stomatal apertures in two mutants that have an increased pectin content, namely arabinan, were larger than those of wild type stomata, suggesting that this is because the cell walls had reduced stiffness (Woolfenden *et al.* 2017). This hypothesis can be applied to research described earlier; for example, in Jones *et al.* (2003), a decrease in arabinan resulted in a smaller stomatal aperture, suggesting that the guard cells have become stiffer. The authors suggest that arabinan may maintain pectin fluidity by hindering the direct interaction of HG chains, whereas treatment with arabinase allows HG chains to come together and associate via Ca^{2+} cross-links, making cells stiffer. Conversely, treating cell walls with PME and EPG which results in the breakdown of pectins, causes the cell walls to become less stiff and the stomata to be more open.

This model does not seem to agree with work by Amsbury *et al.* (2016) in which a decrease in *pme6* expression results in an increase in HG methyl-esterification and a subsequent hypothesised decrease in Ca^{2+} cross-linking. This should technically result in less stiff cells, as it is the opposite to the observation of that in Jones *et al.* (2003). However, there are other consequences of a decrease in HG methylation, as de-methyl-esterification can also result in a

softening of the cell wall due to susceptibility to degradation by cell wall enzymes (Hocq, Pelloux & Lefebvre 2017), and de-methyl-esterification was also shown to result in an increase in elasticity during shoot meristem initiation (Peaucelle *et al.* 2011). Thus, it is unclear what the effects of the *pme6* mutation are without direct measurements of cell wall stiffness (Amsbury *et al.* 2016).

If the findings of Woolfenden *et al's.* (2017) model are applied to results observed in *sfr8,* an observation that stomatal pores are smaller than wild type when given an opening signal as seen in the conductance measurements, would suggest that guard cell walls are stiffer in the mutant. This is logical as the stomata have a smaller dynamic range, as well as a slower rate of movement. Although the model does not go into detail about how rate of movement may be affected by stiffness, it is reasonable to expect that an increased stiffness would result in slower movements (Lawson & Vialet-Chabrand 2018). This could result from a similar pattern seen in Jones *et al.* (2003) where, like with the removal of arabinans, which are hypothesised to keep HG chains apart, the eradication of the boric acid cross-link could allow HG chains to come together and associate via Ca^{2+} cross-links. However, there is no evidence to support this, and this hypothesis also does not fit with measurements of tensile properties made by Ryden *et al.* (2003). In this study, *mur1-1* mutants were shown to have a decreased tensile strength and decreased tensile modulus, suggesting that the cell walls were less stiff than wild type. This would perhaps agree with a scenario in which the loss of RG-II dimerisation resulted in the HG chains being held further apart from each other, which agrees with findings that a decrease in cell-wall RG-II dimerisation results in thickened cell walls (Ishii, Matsunaga & Hayashi 2001b).

Without understanding the structural consequence of the loss of RG-II dimerisation on HG chains, it is difficult to hypothesise what effect this has on the mechanics. It may be that a decrease in RG-II dimerisation *does* result in less stiff guard cell walls, and that stiffness is an important factor necessary for guard cell dynamics. This hypothesis is supported by the finding that pectin-regulated polar stiffening of guard cells is important for guard cell opening, as this helps to hold the stomatal poles in place and fix stomatal complex length during opening. Guard cell poles have also been shown to have specific pectin make-up suggesting they are important for stomatal dynamics (Carter *et al.* 2017; Woolfenden *et al.* 2018). In *sfr8* guard cells, a decreased stiffness may prevent the poles from being fixed, thus when turgor increases, the guard cells elongate without the concomitant opening of the stomata, exacerbated by a decreased stiffness in the surrounding cells. This would agree with the finding that *sfr8* stomata

do not reach the same level of openness as wild type in the conductance experiments (Figure 4.10). It is possible that both an increase and a decrease in guard cell wall stiffness may result in alterations to guard cell dynamics.

4.3.4 Consequences for plant growth

Although the reason for the alterations to stomatal dynamics in *sfr8* and *mur1-1* mutants require verification, there is evidence to suggest that cell wall alterations in the mutant result in aberrant stomatal movements. As discussed in section 4.1, stomata are essential for the life of the plant allowing for the movement of gases for photosynthesis and respiration and the evaporation of water to create the transpiration stream, essential for transporting sugars and metabolites, as well as water, throughout the plant (Zeiger 1983). Stomatal regulation is necessary to ensure metabolic processes can take place within the plant, whilst controlling overall plant water status. Indeed early work suggested a close relationship between photosynthesis and stomatal conductance (Wong, Cowan & Farquhar 1979). More recently, it has been shown that the speed of stomatal opening can result in nonsynchronous behaviour between photosynthesis and conductance, with knock-on effects for water-use-efficiency (Lawson & Blatt 2014; Vialet-Chabrand *et al.* 2017; Lawson & Vialet-Chabrand 2018). Research has shown that a slow increase in conductance can limit photosynthesis, whilst a slow decrease can result in unnecessary water loss for a limited carbon gain due to a lag between the drop in photosynthesis and the stomatal response to closure stimulus, thus reducing water-use-efficiency (Hetherington & Woodward 2003; Franks & Farquhar 2007; Mcausland *et al.* 2016; Lawson & Vialet-Chabrand 2018). This is observable in *sfr8* plants during droughting as plants were quicker to desiccate than wild type. It is also possible that growth and development are impacted by a decrease in stomatal responsiveness. Interestingly, growing *pme6* plants at high CO_2 was able to overcome the dwarf phenotype observed in these plants (Amsbury *et al.* 2016), suggesting slower stomatal movements limit carbon assimilation. It would be interesting to grow *sfr8* mutant plants under increased CO_2 conditions to see if this has an impact upon plant growth.

4.4 Conclusions

sfr8 and *mur1-1* mutants display a clear alteration to guard cell dynamics in response to several stimuli including ABA and CO_2 meaning that the hypothesis stated in section 4.1.2 can be accepted. Although verification is required that these changes are as a result of a decrease in RG-II dimerisation, there is evidence to suggest that cell-wall structure, particularly that of

pectins, is integral to guard cell mechanics. Additional analysis is required to assess if the decrease in stomatal responsiveness is due to an increase or a decrease in cell-wall stiffness, possible through the use of atomic force microscopy as has been previously employed (Carter *et al.* 2017). Still, it is likely that the decreased responsiveness observed has consequences for water use efficiency and growth of *sfr8* plants, highlighting further the importance of cell-wall structure.

CHAPTER 5

HOW DOES CELL-WALL CROSS-LINKING INFLUENCE PLANT FREEZING TOLERANCE?

5.1 Introduction

The results presented in Chapter 3 identified a freezing-sensitive phenotype in plants with a mutation in the *MUR1* gene (Reiter *et al.* 1993). These plants exhibited a decrease in cell-wall fucose, resulting in a decrease in the dimerisation of pectic polysaccharide rhamnogalacturonan-II (RG-II) domains within the cell wall (O'Neill *et al.* 2001). Freezing sensitivity was found to be reversable with the addition of boric acid (BA) in the *mur1-1* mutant, but PAGE analysis did not reveal a reversal in the RG-II dimerisation phenotype. It is known however that RG-II is the primary site of boron binding in the cell wall (Matoh *et al.* 1996), suggesting that PAGE analysis is not a reliable technique to measure RG-II dimerisation in these mutants. Therefore, it is investigated here whether RG-II dimerisation is important for freezing tolerance. As the most complex glycan present in the cell wall, RG-II has been shown to impact upon several different aspects of cell wall structure. However, it is not clear what the consequences of altering that structure may have for freezing tolerance, so much so that damage from freezing increases when RG-II dimerisation is lost.

5.1.1 Roles of rhamnogalacturonan-II in the cell wall

Although RG-II is only a relatively small component of the plant cell wall (Zablackis *et al.* 1995), it has been shown to have several possible roles. Several studies have researched into the impacts of the loss of RG-II dimerisation in order to study these roles. The cell wall was shown to be swollen in boron-deficient *Cucurbita pepo* plants, concomitant with a decrease in RG-II dimerisation in the wall. Supplementing plants with BA resulted in rapid formation of dimerised RG-II and a decrease in the thickness of the cell wall (Ishii *et al.* 2001a). The authors suggest that this swelling is thus due to a lack of RG-II borate ester cross-linking. RG-II dimerisation has been shown to regulate pore size, i.e. the mean size limit (Carpita *et al.* 1979), of the cell wall. *Chenopodium album* cells grown in boron-deficient medium had a pore size of 5.1-6.2 nm, whereas cells grown with boron had a pore size of 3.3-3.7 nm (Fleischer *et al.* 1998). This observation was correlated with the formation of dimerised RG-II, which accounted for 85% of

RG-II in boron grown cells but was absent in boron deficient cells. Other factors that influence the ratio of mRG-II to dRG-II such as pH and divalent cation activity also influenced cell wall pore size (Fleischer *et al.* 1999). There is evidence that RG-II may form borate-ester cross-links with plasma membrane localized proteins, thus facilitating cell wall-membrane adhesion (Voxeur & Fry 2014).

These structural aspects that relate to the dimerisation status of RG-II may influence the mechanical properties of the cell wall. Indeed, inflorescence stems of *mur1-1* plants require less force and energy input to break (Reiter *et al.* 1993), whilst hypocotyls of *mur1-1* have decreased tensile strength and tensile modulus, which is reversible with boric acid treatment (Ryden *et al.* 2003). There is evidence that these mechanical aspects are crucial for freezing tolerance in order for the plant to survive freezing events (Rajashekar & Burke 1996).

5.1.2 The cell wall is essential for mediating freezing tolerance

As discussed in Chapter 1, freezing is a multi-factorial stress which can cause damage via several different mechanisms including ice nucleation, ice growth and cellular dehydration (Levitt 1980). The plant thus utilises structural aspects to prevent damage from freezing events. Studies have shown that water in small pores freezes at a lower temperature than bulk water (Ashworth & Abeles 1984). The authors, among other researchers, also suggest that smaller pores may impede the spread of ice through the cell wall (Ashworth & Abeles 1984; Wisniewski & Davis 1995), which may limit the likelihood that ice will damage cell membranes as well as slowing the rate of cellular dehydration by water moving out of the cell. Interestingly, cold acclimation has been shown to induce a decrease in cell wall pore size in cells of *Vitis spp* and *Malus domestica*, resulting in a decrease in the presence of intracellular ice (Rajashekar & Lafta 1996). For ice to spread in the plant it must first nucleate. Studies have shown that plants can prevent ice nucleation through the expression of ice-binding proteins (Bredow & Walker 2017), and it has even been suggested that plant polysaccharides may influence ice nucleation and growth (Olien & Smith 1981).

Cell wall rigidity has also been shown to increase during cold acclimation (Rajashekar & Lafta 1996; Solecka *et al.* 2008; Scholz *et al.* 2012; Arias *et al.* 2015), and several studies have suggested that plants with more rigid cell walls are able to resist collapse during freezing events and thus withstand freezing to lower temperatures (Rajashekar & Burke 1996; Scholz *et al.* 2012; Zhang *et al.* 2016a). There is increasing evidence that the presence of pectins within the cell wall

has a major role in determining its stiffness (Jones *et al.* 2003; Amsbury *et al.* 2016) and the finding that modifications and increases in pectin in the cell wall occurs during cold acclimation (Weiser *et al.* 1990; Kubacka-Zebalska & Kacperska 1999; Solecka *et al.* 2008; Domon *et al.* 2013; Baldwin *et al.* 2014; Bilska-Kos *et al.* 2017; Chen *et al.* 2018) could provide further evidence that rigidity afforded by pectic polysaccharides is an important characteristic of the cell wall to provide tolerance to freezing.

This chapter begins the investigation into *why* RG-II dimerization-deficient mutants are freezing-sensitive. Considering the structural aspects of the cell wall such as pore size and rigidity that RG-II has been shown to mediate, and the correlation of these factors with freezing tolerance, there is evidence that RG-II is necessary for freezing tolerance and it is hypothesised that structural aspects imposed by RG-II cross-linking influence the ability for plants to withstand freezing temperatures. It is possible that a combination of particular phenotypes bought about by the loss of RG-II dimerisation may influence the sensitivity to freezing events observed. It is also possible that RG-II could be specifically targeted for modification or upregulation during cold acclimation in order to increase freezing tolerance. Although studies have shown that cell-wall pectins are modified during the cold e.g. (Baldwin *et al.* 2014), there is as yet no clear evidence that RG-II in particular is targeted as a way to increase freezing tolerance.

5.2 Results

5.2.1 Electrolyte leakage of pme6 *mutants*

5.2.1.1 Freezing sensitivity of pme6 *in the Ler-0 background*

As well as resulting in a freezing-sensitive phenotype, the *sfr8* mutation had an effect on desiccation tolerance due to the inability to control guard-cell dynamics under different conditions such as drought and ABA treatment (see Chapter 4). The consequence of this was the inability of stomata to close to the same degree as wild type plants when given a closure signal. It is possible that another consequence of this alteration to guard cell dynamics could be the increase in freezing sensitivity observed in *sfr8* and *mur1-1*. Stomata have been identified as a point of entry for ice to grow into the leaf and thus cause damage (Pearce & Ashworth 1992; Pearce & Fuller 2001). It would thus be favourable for the plants to be able to close their stomata quickly under these situations to prevent such events. However, in plants that are not able to regulate their stomata as quickly, an increase in the occurrence of ice growth through stomata could result in more damage within the leaf, rendering them freezing sensitive.

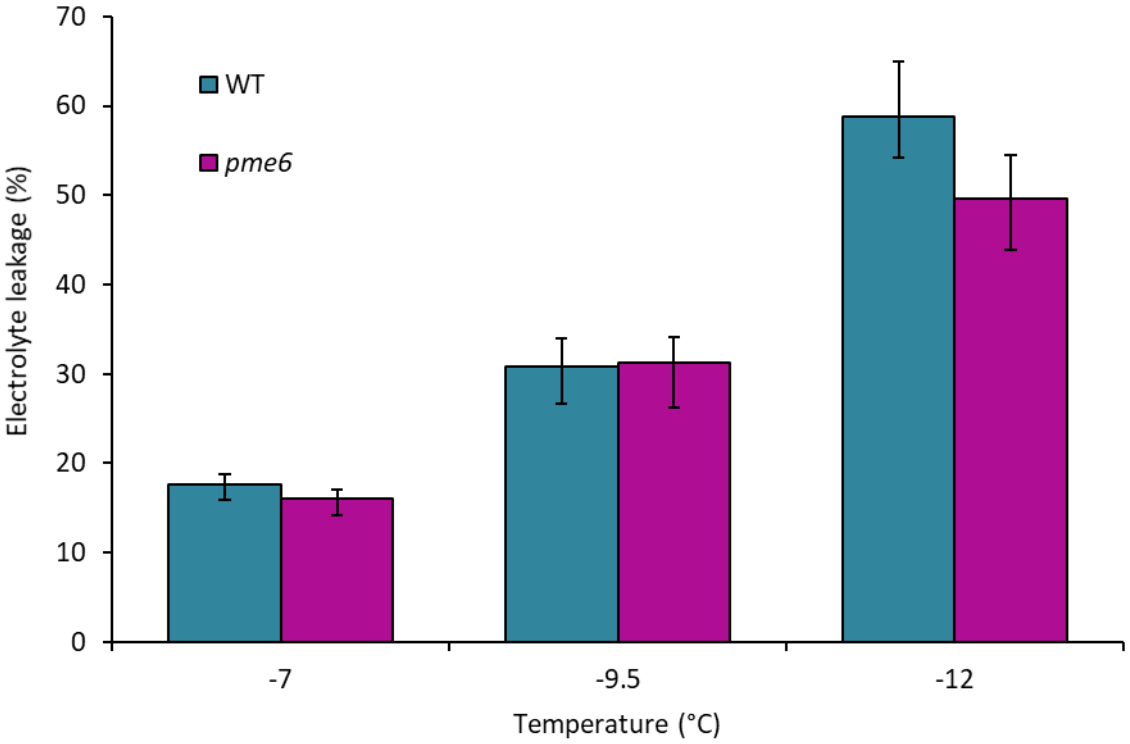

Figure 5.1: Electrolyte leakage of *pme6* mutants in the Landsberg background. Electrolyte leakage in Ler-0 wild type (WT) and *pme6* mutant *Arabidopsis thaliana*. Plants were grown for five weeks before acclimating at 5°C for two weeks. Values represent percentage loss of electrolytes from leaf discs when exposed to temperatures of -7, -9.5 and -12°C. Each data point represents the average of three separate biological replicate experiments. Each experiment used six replicate tubes per genotype per temperature, with three leaf discs per tube. Arcsine transformed percentage leakage data were analysed by a least-squares means comparison at each temperature point, but showed no significant differences in leakage. Error bars represent +/- 1 SE calculated from arcsine transformed data, then converted back to percentage data.

To test this hypothesis, the freezing sensitivity of a mutant that displayed a decreased response to closure signals similar to *sfr8* plants was tested via an electrolyte leakage assay. A mutation in the *PECTIN METHYLESTERASE6* (*PME6*) gene resulted in increased homogalacturonan methylation, which had knock-on effects for guard cell dynamics that the authors suggest was due to an increase in cell-wall stiffness (Amsbury *et al.* 2016). The results showed that electrolyte leakage did not differ significantly between wild type and *pme6* plants (Figure 5.1), which may suggest that alterations to guard cell dynamics in *pme6* did not increase freezing sensitivity. However, before drawing conclusions from this, a mutational analysis of the supposed *pme6* mutant was carried out.

5.2.1.2 Mutant analysis

Although the freezing tolerance of *pme6* was shown to be the same as wild type, there were some attributes that suggested the mutant was not compromised in guard cell dynamics as previously reported (Amsbury *et al.* 2016). Thermal imaging was carried out on rosettes that were cut at the base of the plant and left to dry. As described in Chapter 4, and shown in Figure 5.1A and B, wild type and *sfr8* plants had similar temperatures 5 min after excision. However, after 45 min, wild type plants were warmer than *sfr8* plants due to a decrease in evaporative cooling as the stomata closed to conserve water. This response was not seen in *sfr8* which remained cool, suggesting evaporative cooling was still taking place (see Chapter 4). As *pme6* was postulated to display a guard cell phenotype similar to that of *sfr8*, the same pattern should have been observed between wild type and *pme6* plants. However, although a small difference in temperature was observed between wild type and *pme6* rosettes in the thermal imaging analysis, the difference was incomparable to that seen between wild type and *sfr8* and was mainly concentrated around the apical meristem (Figure 5.2A and B). This is also inconsistent with thermal imaging carried out by Amsbury *et al.* (2016) which clearly showed differences between wild type and *pme6* plants.

To verify this finding, a leaf drying assay was carried out on wild type and *pme6* plants, with results demonstrating no visible difference in water loss between leaves of wild type and those of *pme6* (Figure 5.2C). Taking these results into account, it seemed plausible that these plants did not contain the insertion in the *PME6* gene that would result in a mutational response. To investigate this hypothesis, DNA analysis was carried out on wild type and mutant plants to assess the presence of the insertion, results from which suggested that it was indeed not present (see Appendix D). Expression levels of the *PME6* gene were also analysed in wild type and in

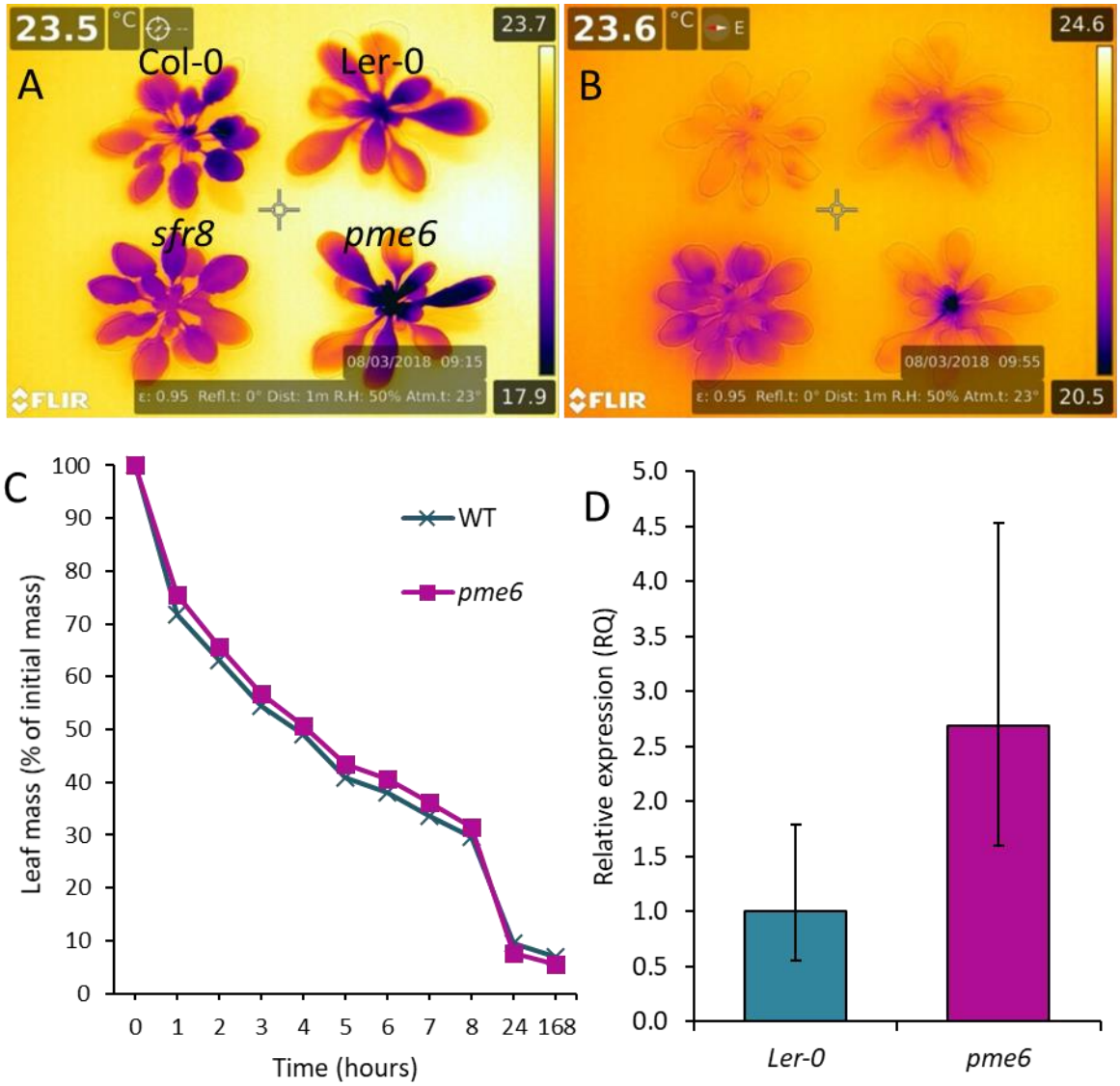

Figure 5.2: Mutational analysis of the *pme6* mutant in the Landsberg background. A, **B**) Infrared thermography of cut rosettes of mature Ler-0 wild-type (top right) and *pme6* (bottom right) plants in comparison to Col-0 wild type (top left) and *sfr8* (bottom left) as shown in **A**, 5 minutes after cutting (**A**) and 45 minutes after cutting (**B**). **C**) Percentage mass of leaves excised from mature Ler-0 wild type (WT) and *pme6* plants weighed every hours for 8 hours then at 24 hours and 7 days, relative to original mass. **D**) Relative expression of *PME6* in two-week-old Ler-0 wild type and *pme6* seedlings. Error bars represent RQ_{MIN} and RQ_{MAX} and constitute the acceptable error level for a 95% confidence level according to a student's t-test.

the mutant to assess if the mutants did display a decrease in transcript expression which would be expected if the insertion was present. qPCR analysis showed similar levels of *PME6* transcript expression in both wild type and *pme6* plants (Figure 5.2D), suggesting that PME6 was unaffected in these plants, which would explain why no guard-cell phenotypes were observed as described in Amsbury *et al*. (2016).

5.2.1.3 Freezing sensitivity of pme6 *in the Col-0 background*

Because the Landsberg *pme6* insertion line displayed no decrease in transcript levels and no clear guard cell phenotype, a set of putative *pme6* insertion lines was obtained in the Colombia-0 background. DNA analysis carried out identified a potential homozygous insertion line that was taken forward for analysis (see Appendix D). Despite DNA analysis showing presence of the putative insertion, qPCR showed a marked increase in *pme6* expression in the Col-0 *pme6* insertion line (Figure 5.3A). A repeat analysis is required to verify this is the case, but as the insertion was found in the promotor, it may be the case that regulation of the gene was diminished, resulting in a massive increase in gene expression. Considering this finding, analysis was carried out to determine if overexpression of the *PME6* resulted in the opposite effects to guard cell dynamics to that described in Amsbury *et al.* (2016) for a mutant. A leaf drying assay showed no difference in water loss between wild type and plants with the insertion line (Figure 5.3B). Similarly, an electrolyte leakage assay showed no particular differences between wild type and insertion line; there appeared to be a slight decrease in leakage in the insertion line at the middle temperature, but repeat experiments are required to show if this is significant (Figure 5.3C). These results suggest that overexpression of the *PME6* gene does not affect guard cell dynamics or freezing tolerance.

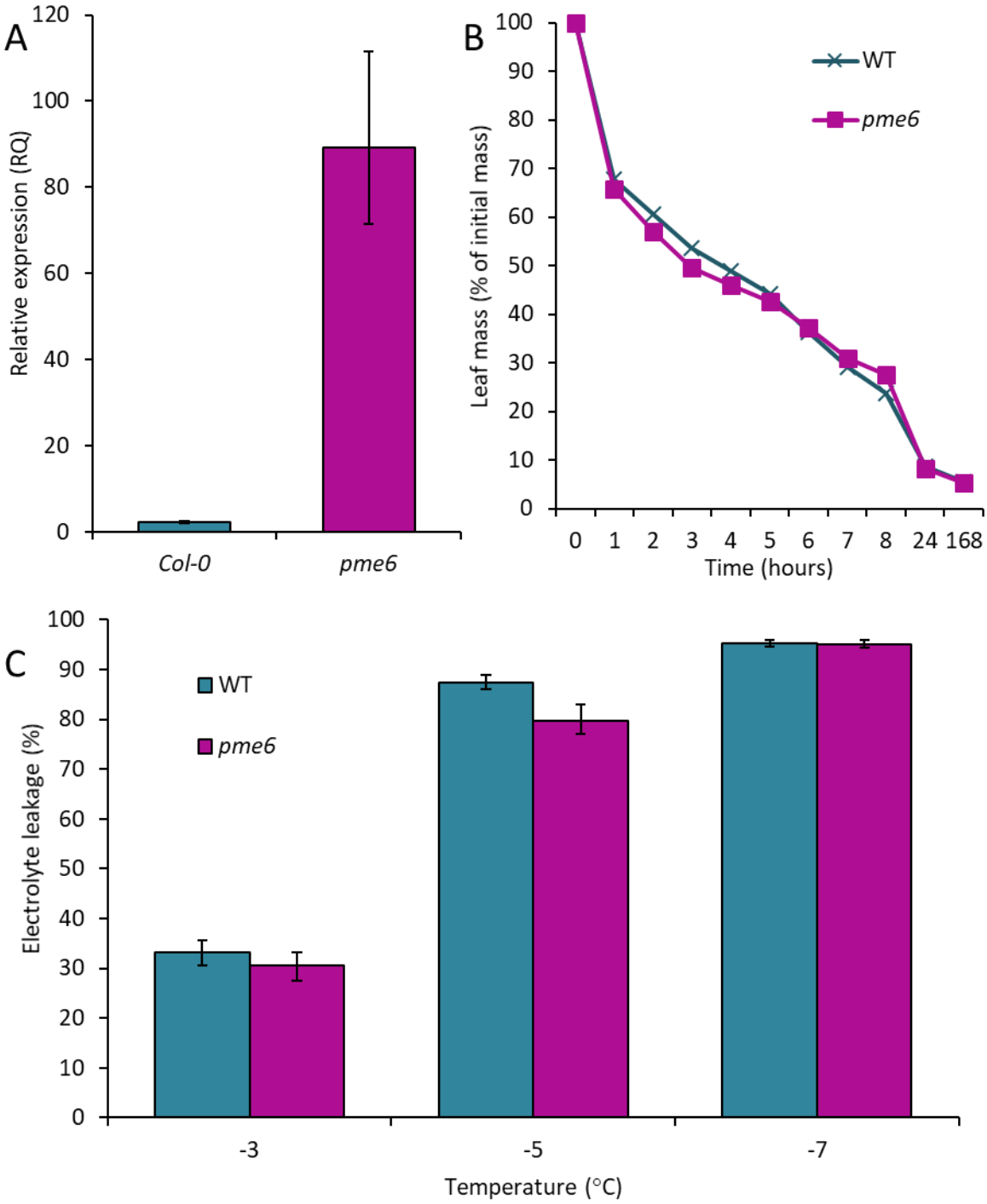

Figure 5.3: Electrolyte leakage and mutational analysis of the *pme6* mutant in the Columbia background. A) Relative expression of *PME6* in two-week-old Col-0 wild type and *pme6* seedlings. Error bars represent RQ_{MIN} and RQ_{MAX} and constitute the acceptable error level for a 95% confidence level according to a student's t-test. **B**) Percentage mass of leaves excised from mature Col-0 wild type and *pme6* plants weighed every hour for 8 hours then at 24 hours and 7 days, relative to original mass. **C**) Electrolyte leakage in five-week-old wild type and *pme6* mutant *Arabidopsis thaliana*. Values represent percentage loss of electrolytes from leaf discs when exposed to temperatures of -3, -5 and -7°C. Each data point represents the average of six replicate tubes per genotype per temperature, with three leaf discs per tube. Error bars represent +/- 1 S.E. calculated from arcsine transformed data, then converted back to percentage data.

5.2.2 Electrolyte leakage of IPCS RNAi lines

There is evidence that as well as forming borate bridges between two monomeric domains, RG-II can also form boron-mediated cross-links with plasma membrane embedded proteins known as glycosylinositol phosphorylceramides (GIPCs) (Voxeur & Fry 2014). GIPCs are the major sphingolipids in the plant membrane and are an integral component of lipid rafts (Gronnier *et al.* 2016). It is possible that if RG-II domains bind GIPCs via a borate-ester linkage the same way that they bind other RG-II domains (i.e. via the apiosyl residue of side chain A), that these cross-links could also be disrupted in *sfr8* and *mur1-1* mutants. This could then have some influence on the decrease in freezing tolerance observed in *sfr8*, as the plasma membrane and wall-membrane interactions are suggested to be an important aspect in mediating freezing tolerance (Murai & Yoshida 1998b; Yamada *et al.* 2002).

Unfortunately, the precise GIPC protein/proteins that RG-II is hypothesised to form cross-links with are unknown, therefore it was not possible to find mutants in which the GIPC-RG-II cross-linking was likely to be disrupted. However, the availability of RNA interference (RNAi) lines of inositol phosphoryl ceramide synthase (IPCS), the first enzyme in the GIPC synthesis pathway, were an interesting starting point. In these lines, the expression of one or more of the three isoforms of IPCS was significantly decreased (Pinneh 2017). Phenotypic analyses of these lines also found that leaves were smaller and inflorescence stems were weaker (Pinneh 2017), however, this was only observed in the At2 RNAi 1 line (Figure 5.4Aiii), whereas the other two lines had similar or perhaps larger rosettes that wild type plants (Figure 5.3A).

An electrolyte leakage assay was carried out on three different RNAi lines targeting ICPSs. Of the three lines chosen which targeted each of the three IPCS isoforms differentially, only one displayed a significantly different leakage compared to wild type plants. At1 RNAi 7 plants had significantly reduced electrolyte leakage compared to wild type, whereas the other two lines did not (one-way ANOVA/LSM, *, $P \leq 0.05$, Figure 5.4B). This suggests that At1 RNAi 7 was more freezing tolerant. If GIPC-RG-II cross-links are indeed inhibited in these RNAi lines, this could suggest that wall-membrane attachments are detrimental to freezing tolerance, and that removing these attachments increases freezing tolerance.

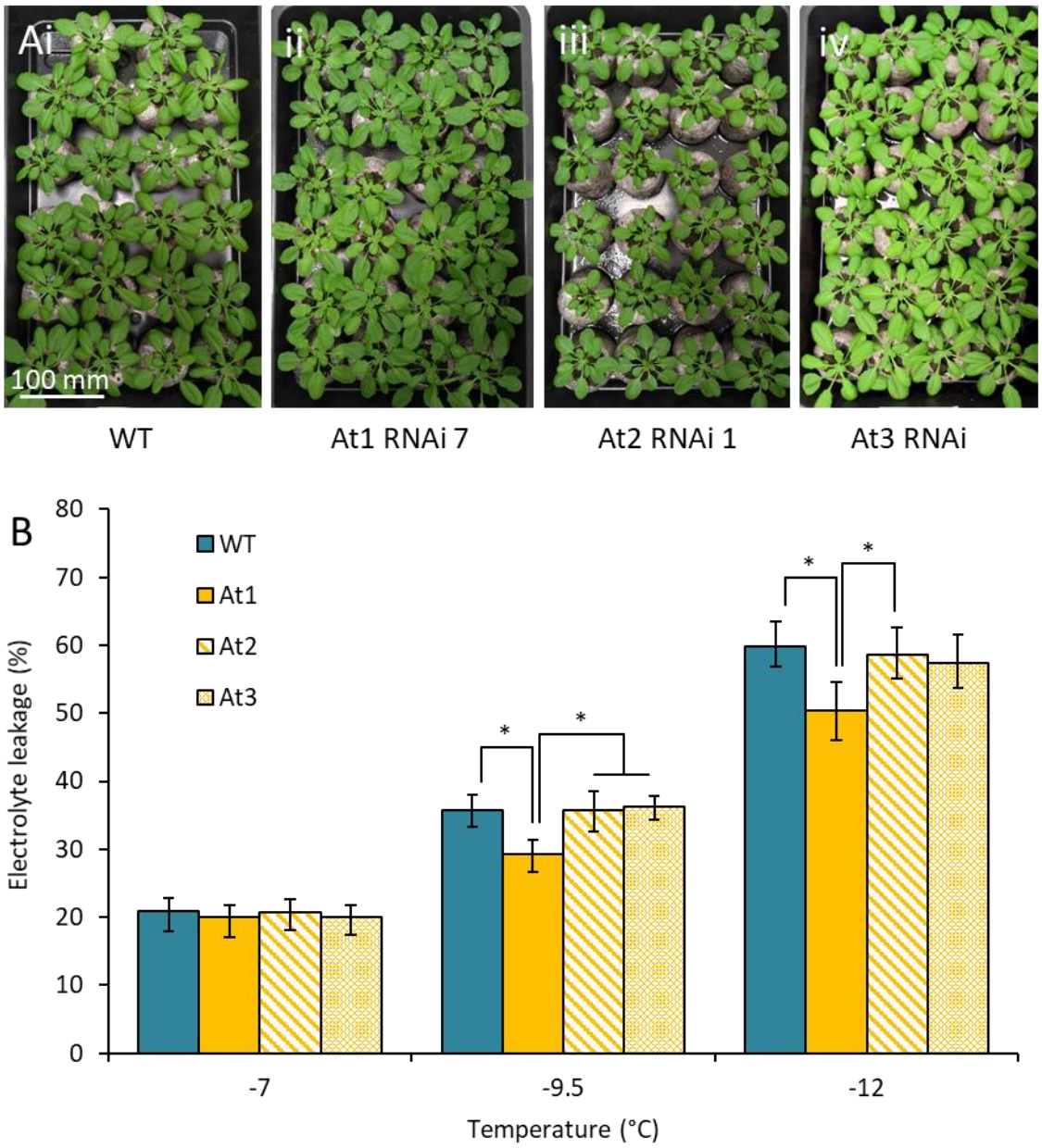

Figure 5.4: Visual analysis and electrolyte leakage in IPCS RNAi lines. A) Five-week-old rosette stage plants of Col-0 wild type (WT) plants and three RNA interference lines targeting different isoforms of the enzyme IPCS, the first enzyme in the GIPC synthesis pathway. **B**) Electrolyte leakage in Col-0 wild type (WT), At1 RNAi 7 (At1), At2 RNAi 1 (At2) and At3 RNAi (At3) *Arabidopsis thaliana*. Plants were grown for five weeks before acclimating at 5°C for two weeks. Values represent percentage loss of electrolytes from leaf discs when exposed to temperatures of -7, -9.5 and -12°C. Each data point represents the average of two separate biological replicate experiments. Each experiment used six replicate tubes per genotype per temperature, with three leaf discs per tube. Arcsine transformed percentage leakage data were analysed by a least-squares means comparison at each temperature point (*, $P < 0.05$). Error bars represent +/- 1 S.E. calculated from arcsine transformed data, then transformed back to percentage data.

5.2.3 Droplet freezing assay

5.2.3.1 Freezing of RG-II monomer and dimer fractions

Studies have shown that dimerisation of RG-II decreases the limiting pore size of plant cell walls (Fleischer *et al.* 1999), and that smaller pore size decreases the temperature at which ice can nucleate (Ashworth & Abeles 1984). It is possible that RG-II could play some role in the nucleation of ice within these pores, whether to prevent it or induce it, and there are suggestions that polysaccharides may influence ice nucleation and growth (Olien & Smith 1981). In order to test this, a droplet freezing assay was carried out using the method described by Whale *et al.* (2015) to assess the ice nucleation capabilities of monomeric and dimeric RG-II by observing at what temperature ice nucleation occurred.

Microlitre droplets of 0.1 µg/µL of RG-II monomer and dimer solutions were pipetted onto a glass slide and placed into a cryocooler which was cooled at a controlled rate. The temperature at which each droplet froze was recorded and results expressed as the fraction of droplets frozen at a specific temperature. The results showed that RG-II monomer and dimer did not differ from each other in relation to freezing temperature. Moreover, the temperature did not differ from that of pure water, suggesting there was nothing additional in the solution capable of nucleating ice (Figure 5.5). The experiment was repeated using a higher concentration of 1 µg/µl monomer and dimer solution, however, the results were the same as at the lower concentration (data not shown). These results would suggest that RG-II itself does not act as a nucleator, either in monomer or dimer form.

It was possible that the solution still did not contain a biologically relevant amount of RG-II and did not necessarily rule out the possibility that RG-II may act as a nucleator *in vivo*. More likely, however, it is the structures that are created from RG-II dimerisation along with interactions with other polysaccharides that could influence nucleation. For this reason, the droplet assay was carried out again on ground plant tissue to measure freezing in an *in vivo* environment, using a modification of the method that had not previously been explored.

5.2.3.2 Freezing of whole leaf extracts

To assess ice nucleation in whole plant extracts that represented a more realistic RG-II structure, a known weight of plant leaves was ground in a pestle and mortar with 10 mL of deionised water to form a semi-homogenous mixture of plant material. Microlitre droplets were cooled on a cryocooler as before and the temperature at which each droplet froze recorded. The initial

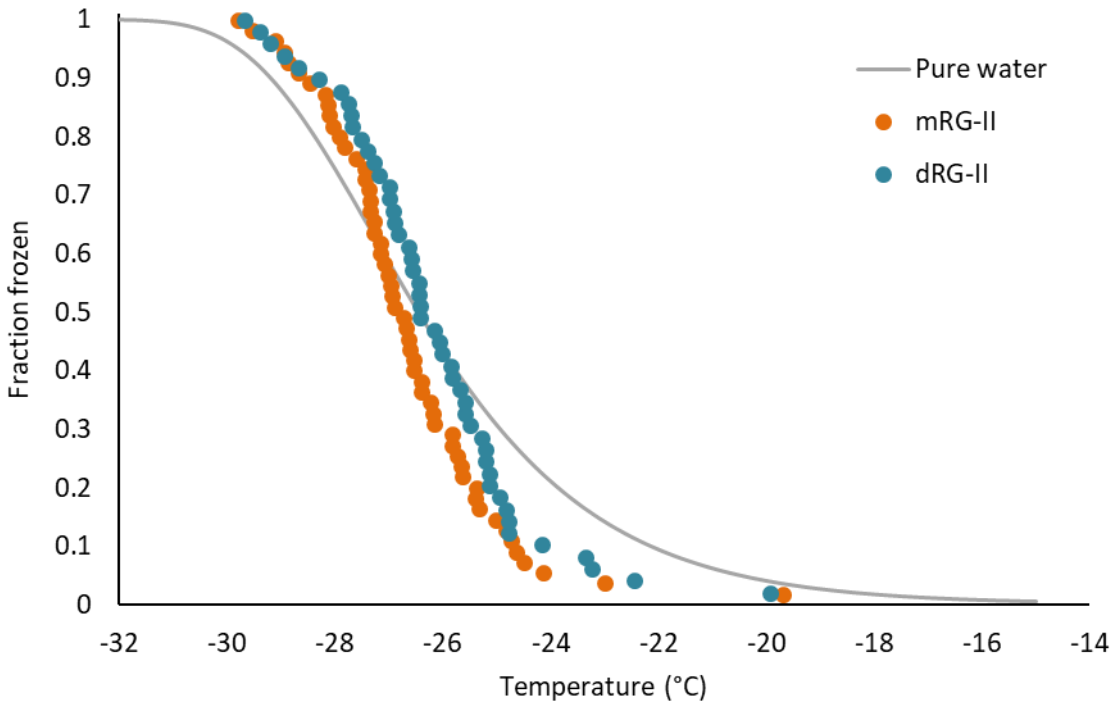

Figure 5.5: Ice nucleation in solutions of monomeric and dimeric RG-II. Droplet freezing assays carried out on 0.1 µg/mL solutions of RG-II monomer and dimer. Microlitre droplets of solutions were pipetted onto a glass slide and frozen in a cryo-cooler. The temperature at which each droplet froze was recorded and results expressed as the fraction of droplets frozen at a specific temperature.

experiment carried out showed a difference in the freezing point of the samples; the acclimated wild type sample froze at a higher temperature than the non-acclimated wild type, and the *sfr8* sample froze at a much lower temperature than both of these. There was also some difference observed in the way that each froze; wild type and acclimated wild type followed a very steady rate of freezing, whereas the freezing of *sfr8* droplets was much more sporadic and encompassed a greater range of temperatures (Figure 5.6A). All samples did freeze at a higher temperature than that of pure water (nucleation of water in the droplet freezing assay is shown in Figure 5.4) suggesting that something in these preparations was initiating ice nucleation.

A repeat experiment carried out showed the opposite pattern to that observed in Figure 5.6A. The *sfr8* solution froze at the highest temperature, followed by wild type, and then cold acclimated wild type. There was also a greater difference in the temperature at which the droplets of wild type and cold acclimated wild type samples froze. All samples began to freeze at higher temperatures than in the first experiment (Figure 5.6B).

5.2.3.3 Troubleshooting

In order to assess what may have been the cause for the differences in patterns observed between the repeat droplet freezing experiments, some test experiments were carried out. Firstly, repeat freezing experiments were carried out on wild type and *sfr8* preparations from the second set of experiments to make sure the results were repeatable between different cooling cycles. Results showed that although the samples froze at approximately the same temperature, there were variations in droplet freezing, which may have resulted from the differences in amount of ground tissue present in each droplet (Figure 5.7A). This hypothesis is supported by the freezing of the supernatant of wild type and *sfr8* samples, which had solid material removed via centrifuging, freezing at comparable temperatures (Figure 5.7B). The freezing temperatures of wild type and *sfr8* supernatant were more comparable than the freezing temperatures of a repeat of the same sample, highlighting the difficulty in obtaining true results of freezing from ground tissue samples in this method. The results of the freezing of supernatant also suggest that there was nothing in the water-soluble component of plant material of wild type and *sfr8* that differs in nucleation ability.

It was concluded that unless it were possible to achieve an extract of ground plant tissue that contained exactly the same amount and size of homogenous material, the droplet freezing assay is not the most ideal method to measure differences in nucleation due to changes in cell wall

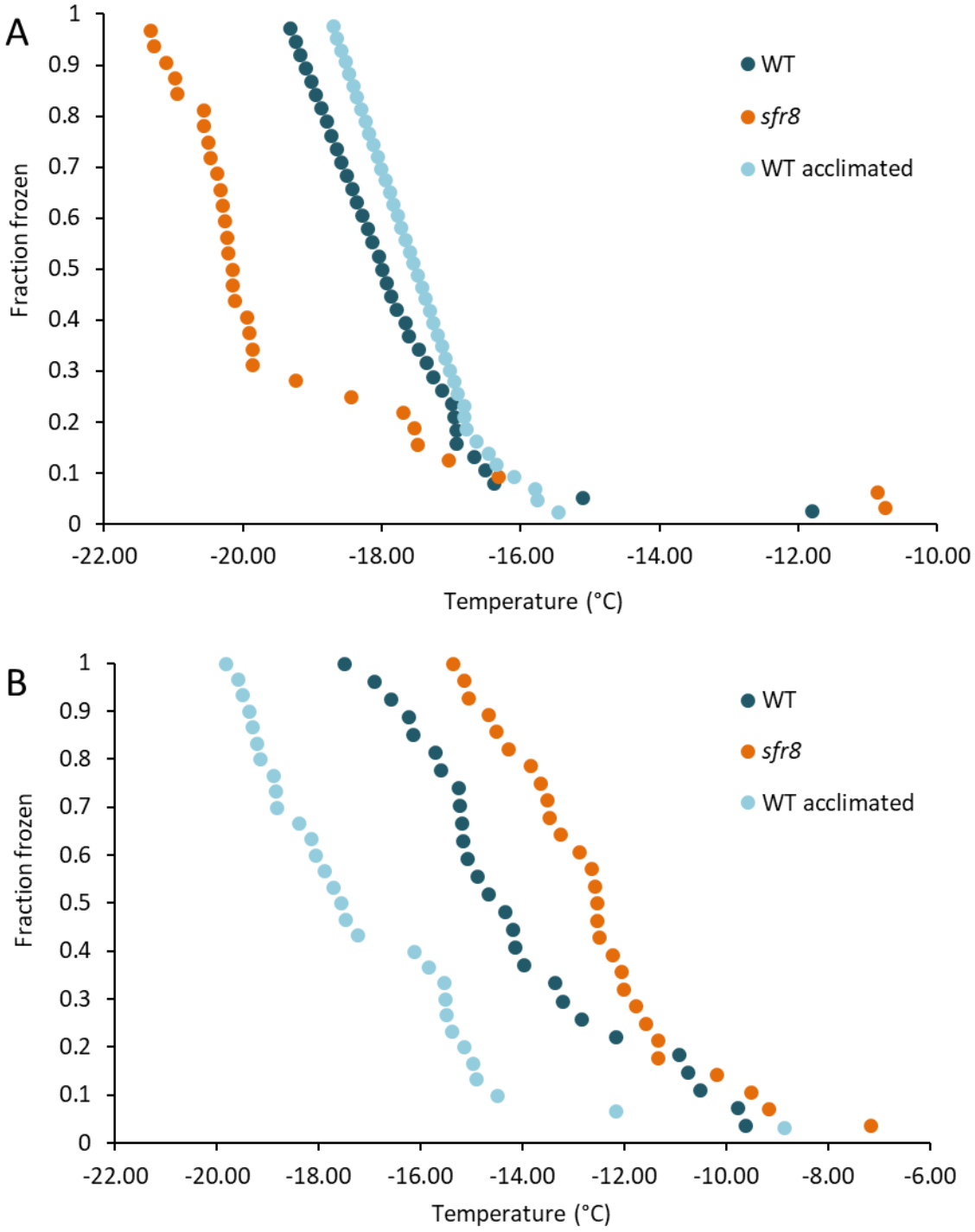

Figure 5.6: Ice nucleation in whole leaf extracts of wild type, *sfr8* and cold acclimated wild type plants. Droplet freezing assays carried out on ground tissue of five-week-old Col-0 wild type (WT), *sfr8* and wild type plants cold acclimated at 5°C for two weeks (WT acclimated). Microlitre droplets were pipetted onto a glass slide and frozen in a cryo-cooler. The temperature at which each droplet froze was recorded and results expressed as the fraction of droplets frozen at a specific temperature. **A**) Approximately 3.1 to 3.2 g of leaf tissue was ground in 10 mL of deionised water using a pestle and mortar. **B**) Approximately 5 g of leaf tissue was ground in 10 mL of deionised water using a homogeniser.

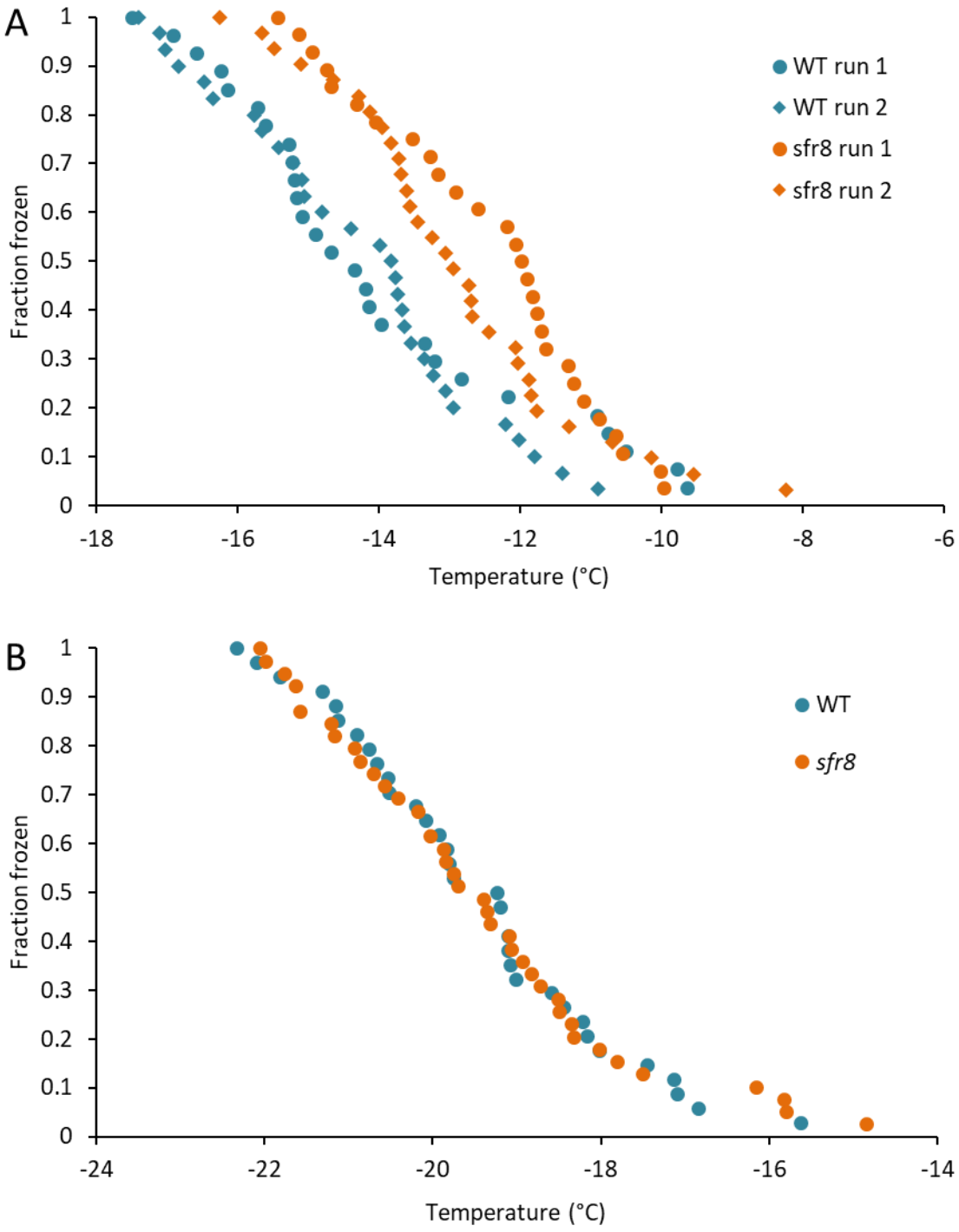

Figure 5.7: Ice nucleation in whole leaf extracts and soluble leaf material of wild type and *sfr8* plants. Droplet freezing assays carried out on ground tissue of five-week-old Col-0 wild type (WT) and *sfr8* plants. Microlitre droplets were pipetted onto a glass slide and frozen in a cryo-cooler. The temperature at which each droplet froze was recorded and results expressed as the fraction of droplets frozen at a specific temperature. **A**) Droplet freezing comparing two separate freezing experiments of wild type and *sfr8* using the same tissue but with separate cooling cycles. **B**) Freezing of supernatant of wild type and *sfr8* samples. Samples were centrifuged for 1 minute at 10000 *g* and supernatant was used in the droplet freezing assay.

structure. The next step was to therefore look at a more relevant material of intact cells in epidermal peels.

5.2.4 Ice nucleation in epidermal peels

In order to observe and analyse ice nucleation in intact cells, a new method was designed for the freezing of epidermal peels. The epidermis was peeled from leaves and placed onto a glass slide in a similar method to that carried out in Chapter 4. A compartment was constructed to maintain atmosphere and moisture content to prevent the peel drying out (see Figure 2.2A). This was then placed onto a cryoplate attached to a microscope with a high-speed camera as shown in Figure 2.2B. The temperature of the plate and thus the sample was decreased at a controlled rate, and the point of freezing captured with a high-speed the camera. Freezing was indicated by a colour change in the cells which become darker (Figure 5.8A and B), as observed in the droplet freezing assay. This phenomenon has previously been described in the freezing of plant cells (Levitt 1980).

The temperature at which ice nucleated and spread was recorded for each sample, and results showed that there was a much larger range for wild type and cold acclimated wild type samples than *sfr8*. The mean nucleation temperature for *sfr8* peels was lower than that of both wild type and wild type cold acclimated peels, of which the cold-acclimated was lower than the non-acclimated (Figure 5.8C). This finding does not fit with the hypothesis that a smaller pore size reduces freezing temperature, as this would have seen wild type plants freeze at lower temperatures than *sfr8*, if indeed a loss of RG-II dimerisation does increase pore size in the *sfr8* mutant as the literature would suggest.

The process of ice nucleation in each of the samples was analysed, considering how and where the ice was seen to nucleate (if this could be deduced), how fast it spread throughout the cells, and whether there were any other outstanding differences between genotypes/treatments. In general, freezing was observed to take place in a number of stages. In the first stage, a darkening occurred that seemed to follow the outline of the cells, which could suggest ice nucleation and growth in the apoplast and intercellular spaces. This was followed by a darkening of the whole cells which could suggest either intracellular freezing (a possibility if the cells were damaged during peeling) or plasmolysis/cytorrhysis of the cell. There were some differences observed between samples, for examples, during the first freezing stage in wild type, ice appeared to form in larger globules, whereas in *sfr8* and acclimated wild type, the first stage happened very

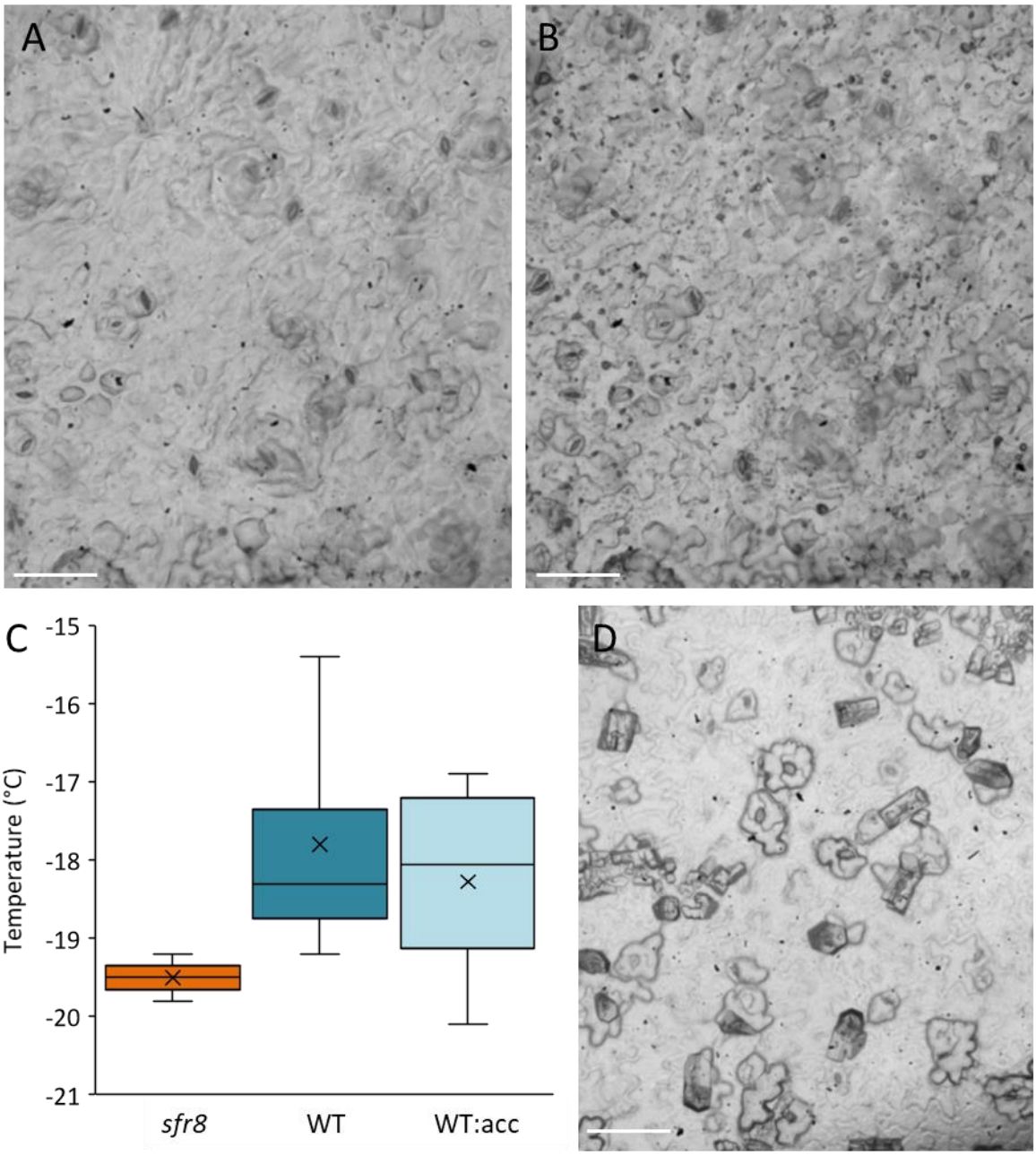

Figure 5.8: Freezing of wild type, *sfr8* and cold acclimated wild type epidermal peels. Epidermal peel from Col-0 wild type leaf before (**A**) and after (**B**) freezing occurred. **C**) Temperature at which freezing of epidermal peels occurred in *sfr8,* wild type (WT) and cold acclimated wild type (WT:acc). Results show average and spread of data from four separate experiments. For boxplots, coloured box represents inter-quartile range with centre line representing median, 'x' representing mean and bars represent maximum and minimum values. **D**) Growth of ice crystals from stomata at -25°C in a wild type epidermal peel. Scale bar for all figures equals 100 µm.

quickly, and large globules were not observed. In these samples, attributes of the second stage of freezing also seemed to happen much quicker, overlapping with the first stage. In all samples ice appeared to grow from several different areas. These results could suggest that wild type plants were able to maintain ice growth in the apoplast for longer, however the similarities between *sfr8* and acclimated wild type samples do not hint at any differences functionally significant for freezing tolerance (see attached CD-ROM).

Interestingly, at lower temperatures of approximately -25°C, ice was observed to grow and crystallise out of the stomata (Figure 5.8B). This may suggest that the substomatal cavity is a space in which ice is able to grow, since it is likely that ice is largely excluded from the cell wall due to small pore size. This could explain the finding of ice in the substomatal cavity shown by Pearce and Ashworth (1992), perhaps providing evidence against ice growing through stomata triggering nucleation within the leaf.

5.2.5 Radiolabelling of wild type leaves to measure synthesis of RG-II during cold acclimation

The freezing-sensitive phenotype of *mur1-1* was correlated with a decrease in RG-II dimerisation, due to the finding that BA was able to restore wild-type levels of electrolyte leakage. If RG-II dimerisation is important for freezing tolerance, it may be the case that the amount of RG-II in the cell wall is increased during cold acclimation as a mechanism to increase freezing tolerance. In order to assess whether the plant up-regulates RG-II production during cold acclimation, two approaches were taken. The first was measuring the level of RG-II synthesis after transfer to cold temperatures, and the second was the measurement of cell wall RG-II content after exposure to cold temperatures for varying lengths of time.

The first approach utilised [^{14}C]-fructose as a source of carbon for the synthesis of sugar residues within the plant that would then be incorporated into cell wall polysaccharides such as RG-II. The level of radioactivity present in cell wall extracts would then give a measure of how much new cell wall synthesis had taken place during the initial transfer to 5°C. Looking at RG-II specific sugars such as apiose (see Figure 1.4) would provide an indication of whether RG-II synthesis had increased after exposure to the cold when compared to samples kept at ambient temperature.

A new method was designed in which leaves of wild type plants were fed with [^{14}C]-fructose (see section 2.4.2.4). The treatments were as follows: 5-week-old plants kept at ambient

temperature (A); 7-week-old plants kept at ambient temperature (B); 5-week-old plants placed in the cold (C); 5-week-old plants plus 2 weeks of cold acclimation kept in the cold (D), four leaves were used in each treatment (designated A1, A2 etc. see Figure 5.9). Separate cell wall extracts were then obtained from leaves (L) and petioles (P) and digested with endo-polygalacturonase (EPG). Chromatography was then carried out on the digested products and autoradiograms of the migrated products were made by exposing the paper chromatograms to film which were then developed and imaged (Figure 5.9). The experiment was carried out three times, denoted by the number following the L or P. The expected galacturonic acid products (GalA, $GalA_2$ and $GalA_3$) of homogalacturonan digestion migrated along the chromatography paper, indicated by the yellow lines, whereas undigested RG-I and RG-II should have remained at the origin. However, acid hydrolysis of the origins did not yield monosaccharides characteristic of RG-II (especially apiose) (data not shown), suggesting that RG-II had been partially degraded during the prolonged incubation in EPG. Thus, further analysis was carried out on the mobile regions (Figure 5.9). Two representative tracks were chosen (P1C1 and P3A1) and each zone cut out and oligosaccharides acid hydrolysed. The monosaccharide products were run on chromatography paper and the radioactivity assessed (Figures 5.10 and 5.11). Many of the zones yielded [^{14}C]-galacturonic acid and some of them in addition gave some or all of [^{14}C]-Gal, [^{14}C]-Ara and [^{14}C]-Rha, supporting the idea that they arose from rhamnogalacturonans. However, all samples yielded [^{14}C]-glucose, which is not found in pectins, and some of them gave [^{14}C]-xylose, which is not a major monosaccharide of pectins, indicating that zones 1–24 included non-pectic oligosaccharides. None of the zones on acid hydrolysis gave [^{14}C]-apiose, so there was no evidence for fragments of RG-II.

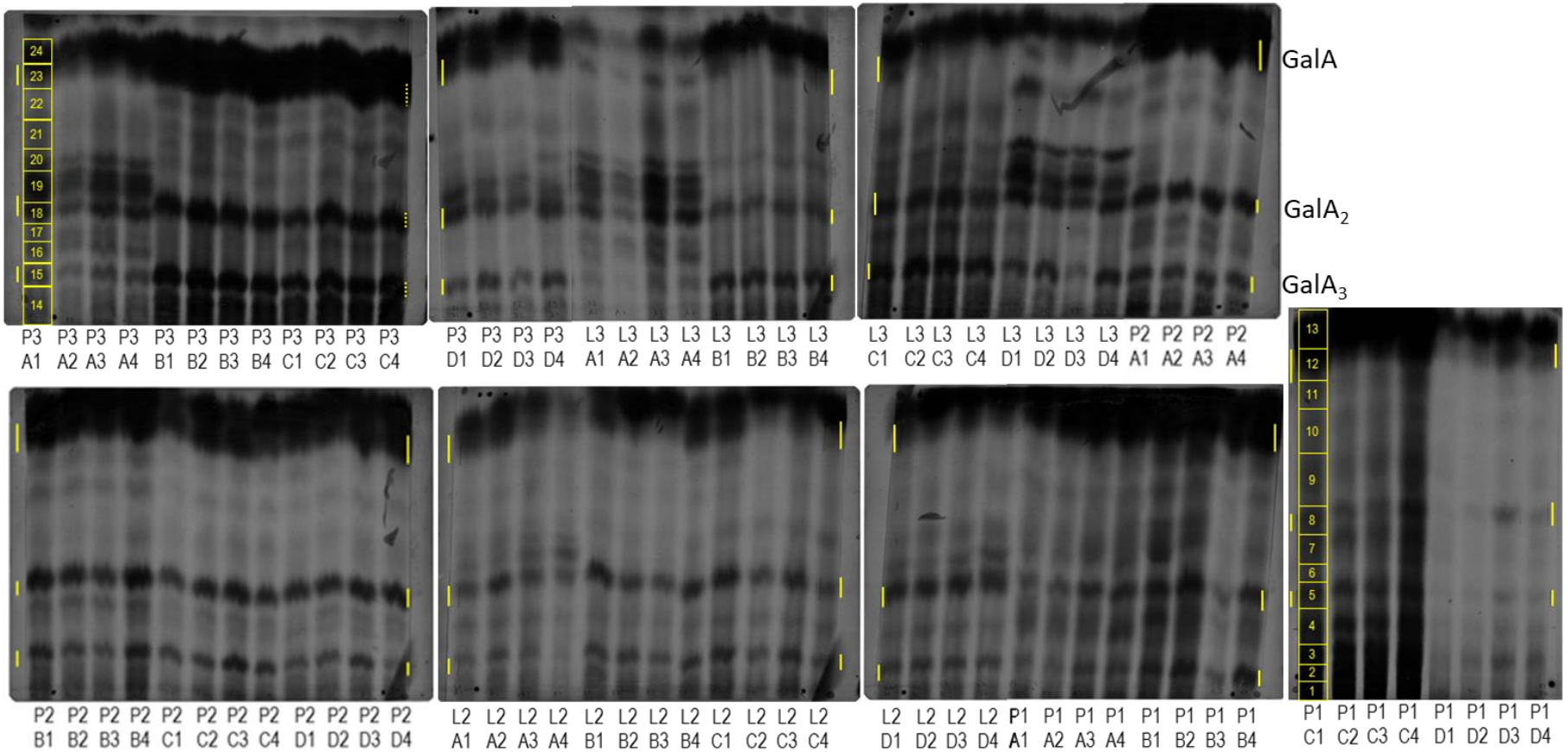

Figure 5.9: Autoradiograms of [^{14}C]-fructose labelled cell wall products. Excised leaves of Col-0 wild type plants were fed with [^{14}C]-fructose, and AIR and EPG digestion carried out on leaves (L) and petioles (P). Treatments were as follows; 5-week-old plants kept at ambient temperature (A); 7-week-old plants kept at ambient temperature (B); 5-week-old plants placed in the cold (C); 5-week-old plants plus 2 weeks of cold acclimation kept in the cold (D). Four leaves were used for each treatment and labelled 1-4 (denoted A1, A2 etc.) The experiment was repeated three times, with the experiment denoted by the number after the L or P. Products were run on chromatography paper and autoradiograms made by exposing the chromatograms to film which were then developed and imaged. Galacturonic acid products (GalA, $GalA_2$ and $GalA_3$) are marked with yellow lines and labelled on the top right autoradiogram.

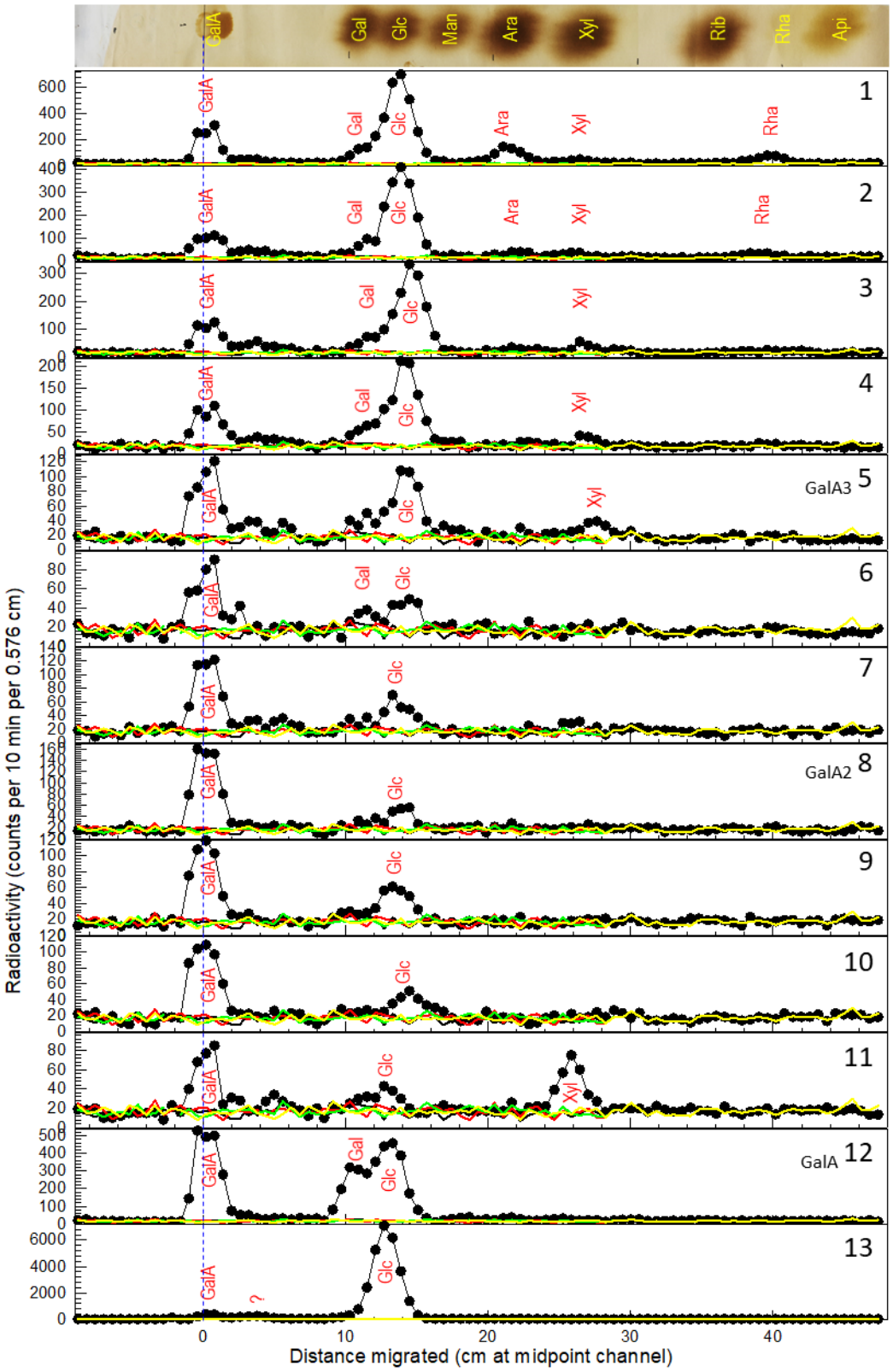

Figure 5.10: Products from acid hydrolysed migratory fractions of track P1C1. Products from lanes 1-13 shown in Figure 5.9 were acid hydrolysed, run on chromatography paper and their radioactivity measured. Positions of sugars is shown at the top by sugar markers and peaks are labelled in red. The lanes in which galacturonic acid was found are labelled on the right.

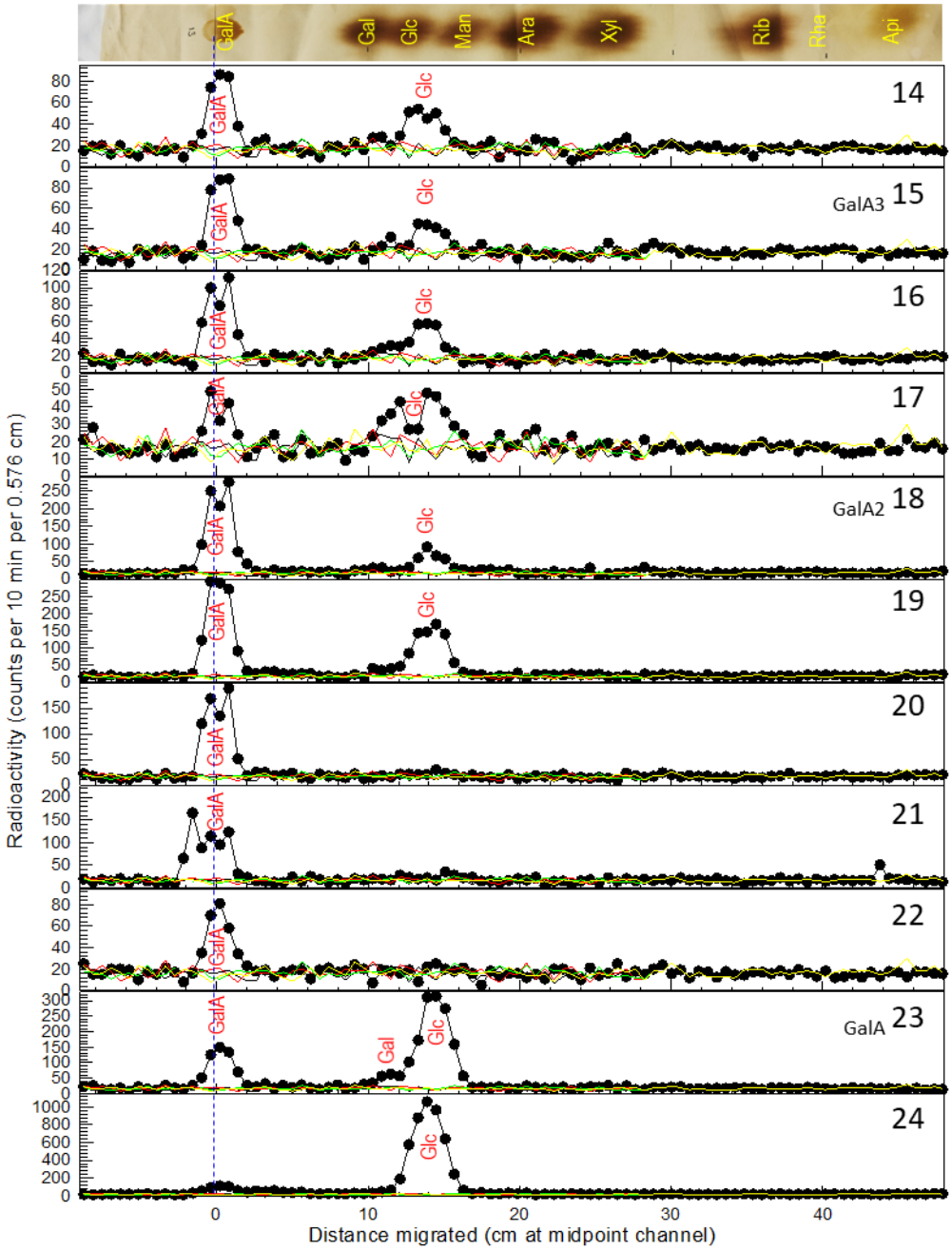

Figure 5.11: Products from acid hydrolysed migratory fractions of track P3A1. Products from lanes 14-24 shown in Figure 5.9 were acid hydrolysed, run on chromatography paper and their radioactivity measured. Positions of sugars is shown at the top by sugar markers and peaks are labelled in red. The lanes in which galacturonic acid was found are labelled on the right.

5.2.6 Measurement of RG-II levels after cold acclimation

5.2.6.1 Separation of monomer and dimer using peptide columns

The second approach used to assess RG-II cell wall content with cold induction was the direct measurement of RG-II within the cell wall after various stages of cold acclimation. Previous studies have measured levels of RG-II monomer and dimer using size exclusion chromatography methods followed by mass spectroscopy procedures (Fleischer *et al.* 1999; O'Neill *et al.* 2001; Séveno *et al.* 2009). Wild type plants were grown for five weeks as previously described and then acclimated at 5°C for 3, 12 and 48 hours, and 7 and 14 days. Leaves were harvested from these plants along with control plants of the same age maintained at ambient temperature. Cell-wall material was isolated via the production of AIR and digested with endo-polygalacturonase (EPG) as previously described (see Chapter 3). These samples were then vacuum dried and resuspended in water and used in the high-performance liquid chromatography (HPLC) column detection method using a Dionex system described in Chapter 2 and previously used to measure cell-wall xyloglucan content (Vanzin *et al.* 2002). To see which peaks related to RG-II, monomer and dimer standards were also run through the system. However, traces showed that both the RG-II monomer and dimer eluted at the same time (Figure 5.12), meaning values could not be obtained for them separately. Therefore, it was tested whether RG-II monomer and dimer could be separated via gel filtration.

A concentrated solution of digested cell wall product was run though several different gel filtration columns designed to separate molecules by size; Superdex S200, Superdex peptide and Superdex G75. Eluted fractions were collected and freeze-dried and resuspended in 40 µL of water. PAGE analysis was carried out on the samples to determine which fractions contained RG-II monomer and which contained the dimer. Unfortunately, the gels showed that none of the columns were successful in separating the monomer and dimer domains of RG-II, as both products appeared in the same fractions (Figure 5.13A-C). Although previous research has used Superdex-75 (Fleischer *et al.* 1999) and Sephadex G-75 (Séveno *et al.* 2009) columns to separate monomer and dimer successfully, these were unavailable for the research carried out here. For this reason, the decision was taken to carry out quantification of samples using the Dionex HPLC system but take the combined measurement of RG-II monomer and dimer obtained and assess if any differences were apparent between ambient and cold treated samples.

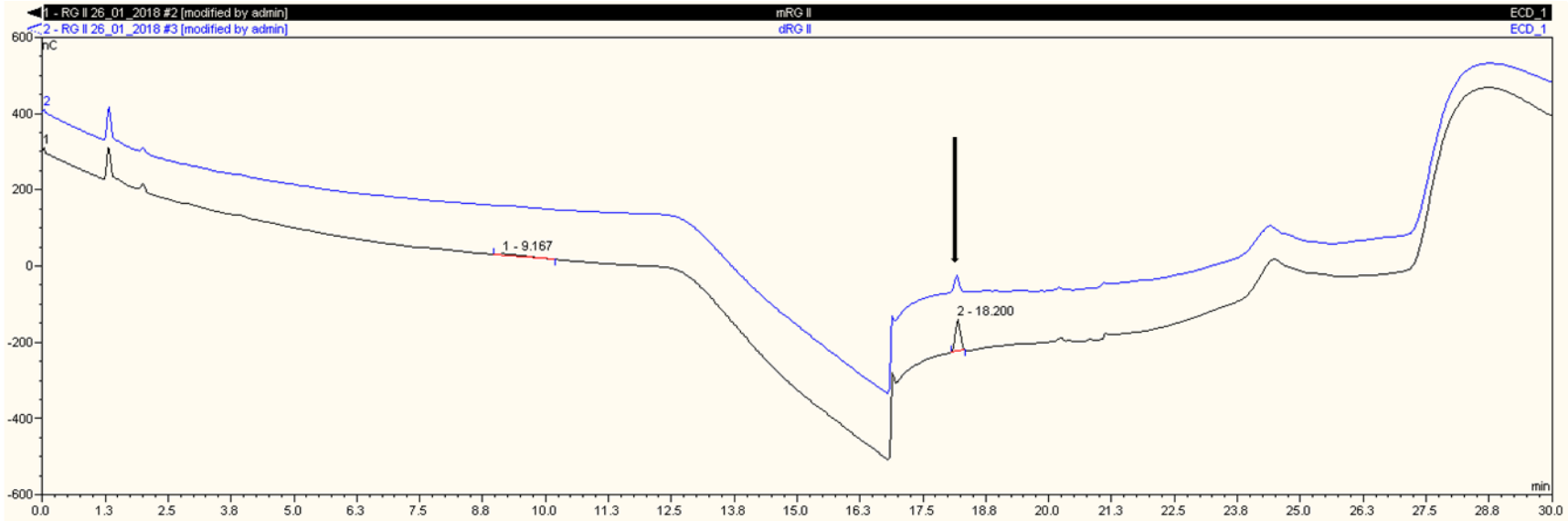

Figure 5.12: HPLC analysis of RG-II monomer and dimer standards. High-performance liquid chromatography (HPLC) analysis using a Dionex system of RG-II monomer (black) and dimer (blue) standards from isolated from sugar beet. RG-II peaks are indicated by the black arrow, showing same elution times of the monomer and dimer.

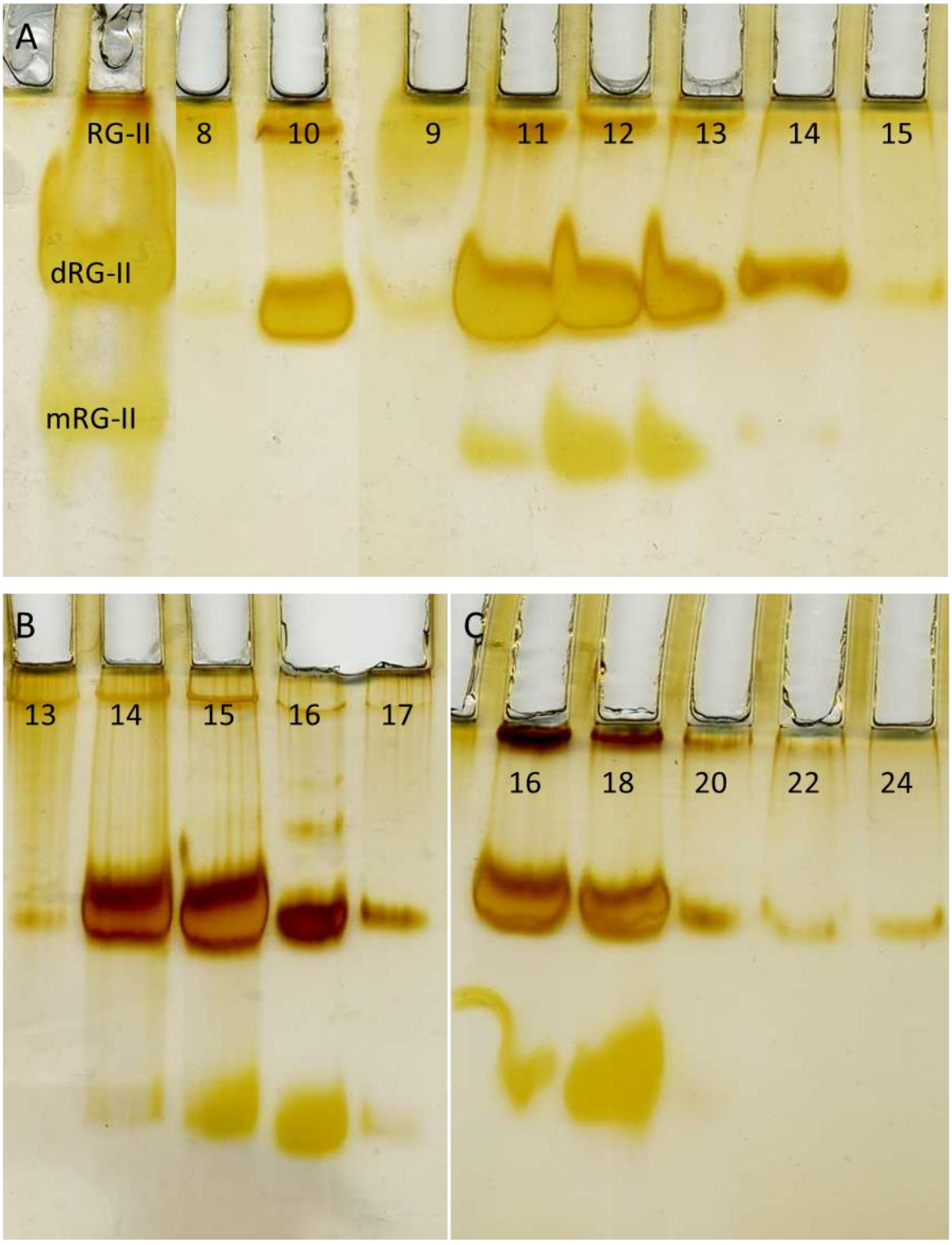

Figure 5.13: PAGE analysis of RG-II products from column separation. Cell wall extracts treated with EPG and run through a Superdex S200 column (**A**) and a Superdex peptide column (**B**) and a Superdex G75 column (**C**) to separate fractions. Numbers represent the fraction eluted from the column. PAGE analysis was carried out on separated fractions to visualise RG-II monomer and dimer. RG-II monomer and dimer standards are shown in **A**.

5.2.6.2 Measurements of RG-II with a Dionex

Although attempts to separate RG-II monomer and dimer proved unsuccessful, it may have been possible to measure the combined levels of RG-II monomer and dimer to see if any differences in total RG-II could be observed between samples. Therefore, the extracted cell wall products were digested in EPG as before, vacuum dried and re-eluted in 25 µL of water and quantification carried out. The traces of fractions obtained showed the presence of monosaccharide and di-saccharide peaks when compared to sugar standards (not shown). However, consistent peaks for RG-II were not observed, as shown in Figure 5.14. This was exacerbated by the high baseline that increased with ionic strength, a consequence that does not seem to have hindered previous studies (as previously referred to). It was therefore not possible to gain a quantitative measure of RG-II within the cell wall under various cold treatments. It was thus attempted to gain a qualitative measure of RG-II levels by PAGE analysis of the digested cell wall samples.

5.2.6.3 Measurements of RG-II monomer and dimer using PAGE analysis

Despite the inability to quantitatively measure cell wall RG-II content, a qualitative measurement could be obtained using the PAGE analysis techniques used in Chapter 3. This was carried out by running the samples on a polyacrylamide gel and staining with silver nitrate to visualise RG-II monomer and dimer bands as previously described. From the staining, it is clear that comparisons between samples was difficult to carry out, and even qualitative analysis is unlikely to highlight any differences as patterns were not repeatable between repeat experiments (Figure 5.15A and B).

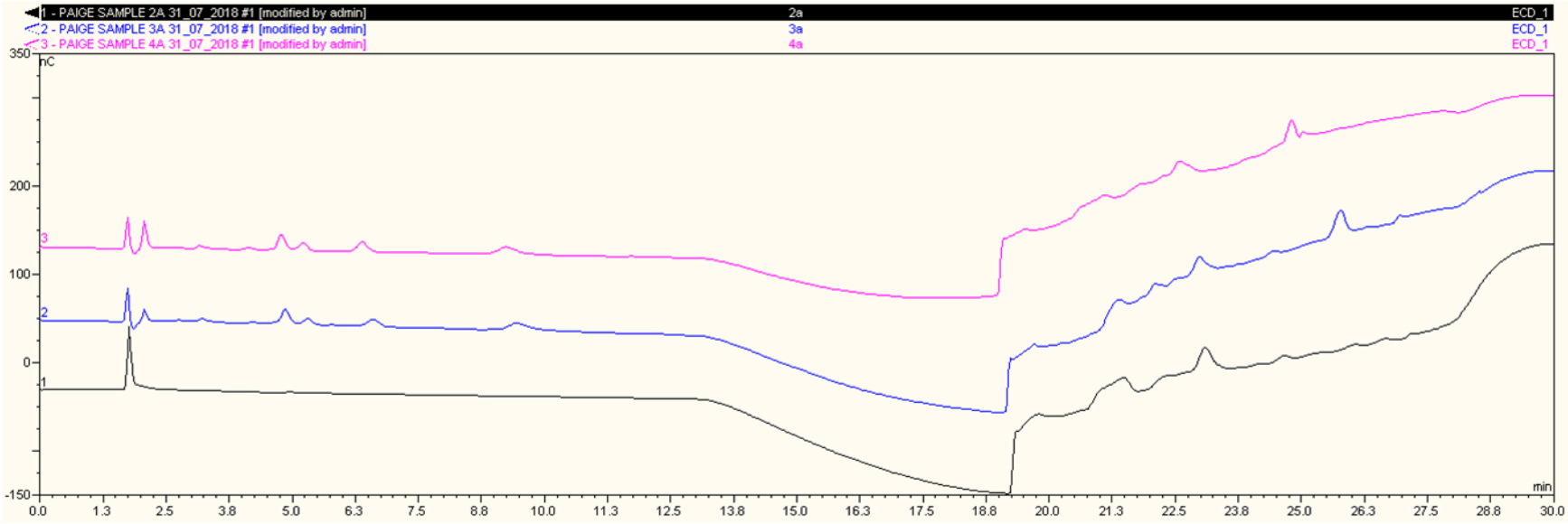

Figure 5.14: HPLC analysis of EPG digested cell wall extracts. High-performance liquid chromatography (HPLC) analysis using a Dionex system of cell-wall extracts treated with endo-polygalacturonase (EPG). Traces show differential elution of peaks that may relate to RG-II, as shown in Figure 5.13.

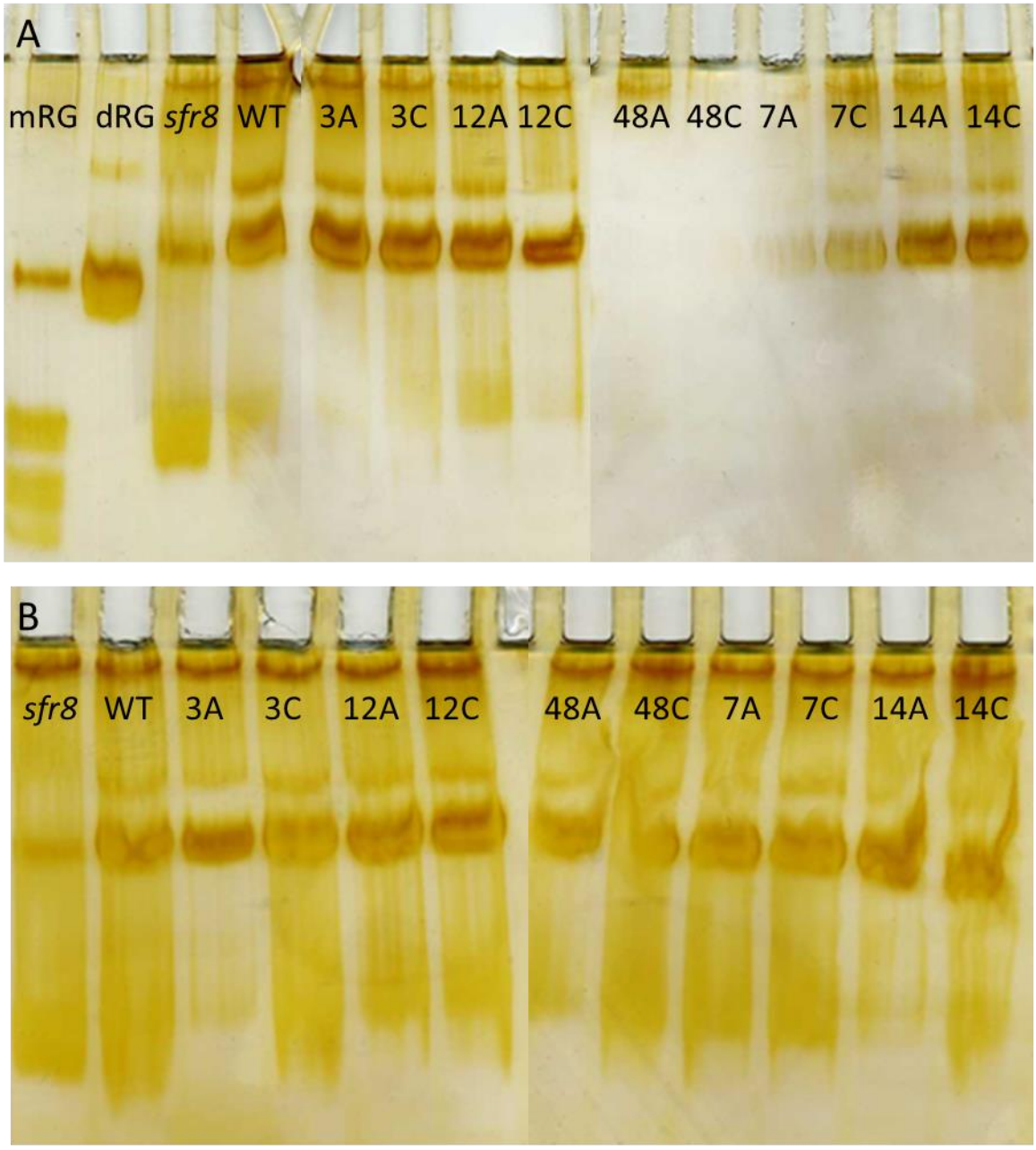

Figure 5.15: PAGE analysis of RG-II monomer and dimer from cold acclimated wild type plants. Analysis of RG-II monomer (mRG) and dimer (dRG) levels after cold acclimation. Five-week-old plants were harvested after cold acclimation at 5°C for 3, 12 and 48 hours, 7 and 14 days (C) along with control samples at ambient temperature (A) and Col-0 wild type (WT) and *sfr8* samples taken before plants were transferred to the cold. Cell wall extracts were digested with EPG and samples run on a polyacrylamide gel followed by silver staining to visualise monomer and dimer RG-II bands. **A** and **B** show results from two separate repeat experiments.

5.3 Discussion

5.3.1 Guard cell dynamics may not be correlated with freezing tolerance

There is some evidence to suggest that alterations to guard cell dynamics (Chapter 4), and the freezing-sensitive phenotype observed in the *sfr8* mutant (Chapter 3) could be correlated. Studies utilising infrared thermography to visualise ice nucleation events in plants have suggested that the stomata could act as an entry point for ice, thus allowing ice growth and concomitant damage within the plant (Wisniewski & Fuller 1999; Pearce & Fuller 2001). Studies to assess freezing in leaves also arrived at this hypothesis due to the presence of ice in substomatal cavities of frozen leaves (Pearce & Ashworth 1992). It has been shown that exposure to cold temperatures can induce stomatal closure (Allen *et al.* 2000), suggesting it is favourable for plants to close their stomata if freezing events are likely to occur. This may also be beneficial to prevent water loss to mitigate damage due to freeze-induced dehydration as well as regulating other plant processes, as photosynthesis and respiration are reduced in cold temperatures (Decker 1944; Keys *et al.* 1977), meaning stomata do not need to be as open for the transfer of gases.

In order to test the hypothesis that open stomata could allow ice entry and thus result in greater freezing damage, a mutant with alterations to guard cell dynamics was obtained. The *PME6* gene is highly expressed in guard cells (Yang *et al.* 2008), and a mutant with an insertion in the *PME6* gene was shown to have a decrease in methyl-esterification of homogalacturonan pectin chains believed to lead to a decrease in the stomatal closure response, similar to that seen in *sfr8* upon treatment with ABA, CO_2 and drought. The study showed that pectin modifications in the mutant were guard cell specific, thus unlike *sfr8*, other cells would not be affected (Amsbury *et al.* 2016).

An electrolyte leakage assay showed no significant difference in leakage between wild type and *pme6* plants, suggesting that the alterations in guard cell dynamics had no effect on freezing tolerance (Figure 5.1). However, analysis suggested *pme6* did not have the same alterations to guard cell dynamics as *sfr8*; a leaf drying assay and infrared thermography of cut rosettes suggested that the *pme6* mutation did not affect guard cell dynamics on the scale that the *sfr8* and *mur1-1* mutations did (Figure 5.2). This may have been due to the finding that *PME6* expression was not decreased in the insertion line, contrary to the findings of Amsbury *et al.* (2016) and may in fact not have contained an insertion at all (Appendix D). This led to investigations using a different putative insertion line of *pme6* in a Columbia background, which rather than showing decreased expression of *PME6*, actually showed a large increase in

transcript expression. It could be suggested that increased expression would have resulted in observations opposite to those described by Amsbury *et al.* (2016) in the mutant; namely an increase in pectin methyl-esterification and thus a decrease in cross-linking, perhaps resulting in guard cells that are more sensitive to closure signals than wild type plants. However, as no significant difference was observed in leaf drying characteristics, guard cell dynamics are inferred to be insensitive to *PME6* levels above that of the wild type. An electrolyte leakage assay may hint at a slight decrease in leakage compared to wild type, but repeat experiments are needed to verify this (Figure 5.3). Thus, it is not possible from these experiments to form a definitive link between enhanced guard cell dynamics and freezing tolerance.

As previously suggested, it is certainly possible that open stomata provide an entry for ice nucleation into the plant – water frozen on the surface of the leaf may spread through nucleation of surrounding water vapour, including water vapour in the substomatal cavity, thus allowing ice growth into the leaf. However, there are other factors that would affect this process, such as the probability that ice will nucleate on the surface of the leaf. This is related to the presence of ice-nucleation active substances (INAS) such as ice-nucleating bacteria (Maki *et al.* 1974; Hirano & Upper 2000) and the amount of water captured and retained on leaf surfaces, also known as wettability. Interestingly, leaf wettability has been correlated with nucleation temperature; making leaf surfaces hydrophobic reduced the nucleation temperature by delaying entry of ice into the leaf (Fuller *et al.* 2003), and the presence of a water droplet on tomato leaves resulted in freezing at -2°C compared to -6°C of dry tomato leaves (Wisniewski, Glenn & Fuller 2002). Plants that are more likely to experience freezing such as those at high altitudes have also been shown to frequently have reduced leaf wettability (Aryal & Neuner 2010). In order to directly correlate the freezing sensitivity of *sfr8* and *mur1-1* mutants with the observed alteration to guard cell dynamics, it would be necessary to analyse the freezing tolerance of other open stomata mutants. Care would need to be taken when choosing such mutants, as often this is due to an insensitivity to ABA (Murata *et al.* 2001). As ABA is also associated with cold acclimation (Gusta *et al.* 2005), results would mask or exacerbate any correlation between guard cell dynamics and freezing tolerance.

5.3.2 IPCS RNAi lines display no increase in sensitivity to freezing

A significant decrease in freezing tolerance was observed in an RNA interference line of IPCS (inositol phosphoryl ceramide synthase) – the first enzyme in the synthesis pathway of plasma membrane sphingolipids, GIPCs (Bromley *et al.* 2003). GIPCs have been shown to form

connections with RG-II molecules via a borate diester linkage in cultures of *Rosa* cells (Voxeur & Fry 2014), which could suggest a role for GIPCs and RG-II in wall-membrane attachment. A decrease in IPCS expression is predicted to alter GIPC structure and thus function within the plasma membrane (Pinneh 2017). It is likely in these lines that the amount of GIPCs within the plasma membrane would decrease resulting in a decrease in the number of GIPC-RG-II cross-links. This would then suggest that wall-membrane attachments are detrimental to freezing tolerance as an increase in freezing tolerance was observed in one of the IPCS RNAi lines (Figure 5.4). This agrees with data obtained from experiments using cells of Jerusalem artichoke tubers, in which tight attachments of the plasma membrane to the cell wall resulted in whole cell collapse and irreversible damage to the membrane, possibly due to mechanical stress imposed by the cell wall (Murai & Yoshida 1998b). It is also possible that rather than acting as a point of wall-membrane attachment, GIPCs facilitate the transfer of RG-II to the apoplast, perhaps acting as an intermediate for the dimerisation of two RG-II molecules, as addition of GIPCs was found to increase the rate of cross-linking (Voxeur & Fry 2014).

A problem thus presents itself; neither of these proposed roles fits with the freezing sensitivity observed in *sfr8* and *mur1-1* mutants. A decrease in GIPCs in the membrane would decrease the number of attachments to the cell wall. As this is suggested to be beneficial in freezing tolerance, *sfr8* plants should display an increase in freezing tolerance as the disruption of RG-II dimerisation would also more than likely result in disruption of GIPC-RG-II cross-links. This is, however, not the case. Similarly, if GIPC acted as an intermediate for RG-II dimerisation, a decrease in GIPCs would likely result in a decrease of dRG-II within the cell wall. If RG-II dimerisation is indeed important for freezing tolerance, this would likely result in more freezing-sensitive plants, but this is not observed here. This could suggest that the disruption of GIPC-RG-II cross-links either does not occur in *sfr8* mutants, or that other disruptions out-way any beneficial consequences. The decrease in electrolyte leakage was only observed in one RNAi line, which showed a reduction in IPCS isoform 2 expression in particular, and a slight increase in isoform 1 compared to wild type. However, no particular conclusions can be drawn from this, as the At2 line also had decreased expression of isoform 2 and a slight increase of isoforms 1 and 3 (Pinneh 2017). Without knowing the exact consequences of reducing IPCS expression, it is only possible to speculate as to what the consequences are for cell-wall structure. One way to begin rectifying this would be to assess the amount of mRG-II and dRG-II within the cell wall of the RNAi lines, which may also hint as to what role GIPCs play in relation to the cell wall. Although Voxeur and Fry (2014) show that GIPCs can bind RG-II via a borate ester bond *in vitro*, confirmation is still

required that this cross-link occurs *in vivo*. There is partial evidence for this, in that RG-II in the cell wall is found predominantly located next to the plasma membrane (Matoh *et al.* 1998).

5.3.3 Experiments suggest that ice nucleation may differ in wild type and sfr8 *plants*

Droplet freezing assays carried out on whole plant extracts were inconclusive, and it was difficult to draw conclusions from experiments using epidermal peels (Figures 5.5 to 5.8). The recorded temperature of freezing point in the epidermal peels would suggest, however, that nucleation is impacted in the *sfr8* mutant that may be related to RG-II dimerisation, since BA in particular was found to reverse the freezing-sensitive phenotype of *mur1-1* plants (see Chapter 1). There is evidence that cell-wall structures play a role in inhibiting ice nucleation, as RG-II dimerisation has been shown to affect cell wall pore size (Fleischer *et al.* 1999) which is a determinant of ice nucleation temperature (Ashworth & Abeles 1984). Fleischer *et al.* (1999) reported that pore size of boron-deficient *C. album* cells decreased from 5.1-6.2 nm to 3.3-3.7 nm with the addition of BA, concomitant with an increase in the dimerisation of RG-II. In their calculations of freezing temperatures of water occupying pores of different sizes, Ashworth and Abeles (1984) predicted that pores with a diameter less than 4 nm would depress the freezing temperature to between -15 and -25°C, suggesting wild type plants would freeze at lower temperatures. This range agrees with the freezing temperatures observed in droplet freezing assays and freezing of epidermal peels.

However, contrary to these predictions, the *sfr8* plants were observed here to nucleate at lower temperatures than wild type. It is possible that the temperature of the point of ice nucleation measured in peels is an artefact of the experimental set-up. Freezing in cells is influenced by several factors such as water availability, cell packing and the presence of intercellular spaces (Pearce 2001). The peeling of the epidermis from the leaf is likely to have altered cell structure and is of course not representative of the whole leaf (Roelfsema & Hedrich 2002). In preliminary experiments where a chamber was not constructed around the peel it was observed that the drying out of the leaf affected freezing temperature (data not shown). The water content of the peel is likely to be altered with the removal from the leaf, so may well have affected the results even when contained inside a chamber. Further investigation is required to determine whether ice nucleation in *sfr8* plants is altered and whether this is as a result of a decrease in RG-II dimerisation. Pore size would also need to be assessed in wild type and *sfr8*/*mur1-1* mutant plants as this has not yet been measured in *Arabidopsis*.

There are specific factors within the plant that can inhibit ice nucleation or growth; ice-binding proteins (IBPs, also known as anti-freeze proteins or AFPs) adsorb to ice crystals and prevent growth of ice-nuclei, as well as preventing ice nucleation by bacteria (Griffith *et al.* 2005; Bredow & Walker 2017). There is also evidence that plants may contain intrinsic INAS in the form of proteins or even polysaccharides (Zachariassen & Kristiansen 2000; Wisniewski *et al.* 2014). Some examples include ice nucleating properties of a polysaccharide in the wood of *Prunus* (Gross, Proebsting & Maccrindle-Zimmerman 1988), and more recently a polysaccharide from birch pollen that displayed both ice-nucleating and ice-binding properties (Dreischmeier *et al.* 2017). Interestingly, the addition of borate diminished both of these functions, although the authors do not speculate that this could link the ice-nucleating/binding properties to RG-II, but it is certainly possible that this is the case. It would be interesting to carry out infrared thermography on *sfr8* plants under freezing conditions, as this has previously been used to much success to show the point at which ice nucleation occurs (Wisniewski, Lindow & Ashworth 1997; Fuller & Wisniewski 1998; Wisniewski & Fuller 1999; Pearce & Fuller 2001). This would highlight any differences in ice nucleation between wild type and *sfr8* on a whole plant scale that is less likely to be subject to artefacts that may have occurred in the droplet and epidermal peel freezing assays. These experiments may also contribute to verifying the hypothesis that guard cell dynamics influence ice nucleation and thus freezing damage in *sfr8* by measuring nucleation of leaves with and without the presence of water droplets on the leaf (Wisniewski *et al.* 2002).

5.3.4 Measurements of RG-II synthesis and cell-wall content during and after cold acclimation were inconclusive

Two different approaches were taken in order to assess the possibility that RG-II synthesis and levels of RG-II in the cell wall are increased during cold acclimation. If this were observed, it would support the hypothesis that RG-II plays a particular role in the cell wall to protect against freezing damage. Unfortunately, quantitative analysis using size-exclusion chromatography and HPLC techniques was unsuccessful in this study (Figures 5.12-5.14), and qualitative analysis of poly-acrylamide gels was nearly impossible due to effects of differential staining and possibly inaccurate measurements of RG-II (Figure 5.15). Previous studies have successfully measured cell-wall RG-II content or ratios of RG-II monomer and dimer (Fleischer *et al.* 1999; O'Neill *et al.* 2001; Séveno *et al.* 2009), suggesting further investigation may yield these measurements. Radiolabelling and subsequent chromatography also showed no differences between RG-II synthesis of ambient and cold treated leaves (Figures 5.9-5.11). This arose mainly due to the

inability to detect apiose in the chromatography assays, which may have been as a result of a limited amount of tissue. As this was a new method, modification of the technique may yet yield interesting results.

Previous studies have reported the increase of pectin or pectin modifying enzymes in the cell walls of various species including *Pisum sativum* (Weiser *et al.* 1990; Baldwin *et al.* 2014), *Brassica napus* (Kubacka-Zebalska & Kacperska 1999; Solecka *et al.* 2008), *Miscanthus spp.* (Domon *et al.* 2013) and *Triticum sp.* (Willick *et al.* 2018), after exposure to cold temperatures. The increase of side chains such as arabinan and galactan indicative of RG-I and RG-II, could suggest that RG-II cell wall content is increased during cold acclimation (Baldwin *et al.* 2014), but there is no direct evidence of this as yet. If direct measurement of RG-II domains is not yet possible, it would be conceivable to assess the levels of RG-II specific sugars in the cell wall such as apiose or D-KDO which have successfully been identified in early analysis into the structure of RG-II domains (Darvill *et al.* 1978a). This would provide evidence as to whether cell-wall RG-II content is increased during cold acclimation.

5.3.5 Functional significance of increased cell wall RG-II content

Considering the roles RG-II has been found to play in the cell wall, there is evidence for functional significance if the cell-wall content of RG-II is indeed increased during cold acclimation. This includes not only the effect on pore size discussed previously, but also the effect of pectins on cell wall stiffness which has been previously alluded to (Jones *et al.* 2003; Ryden *et al.* 2003; Moore, Farrant & Driouich 2008; Amsbury *et al.* 2016). Evidence for alterations to cell-wall stiffness and strength come from a study by Ryden *et al.* (2003), who showed that tensile strength and tensile modulus were decreased in hypocotyls of *mur1-1* and *mur1-2* mutants. This suggests that stiffness and strength are decreased in mutant cell walls. There are some studies that have shown that cold acclimation induces an increase in cell-wall strength (Rajashekar & Lafta 1996; Solecka *et al.* 2008), but whether this is related to an increase or decrease in stiffness is unclear. In apple and grape cells, an increase in cell-wall strength after cold acclimation resulted in an increase in the pressure required to rupture cells, suggesting these cells could resist collapse during freezing events (Rajashekar & Lafta 1996). Indeed, it has been hypothesised that increased rigidity of cell walls allows plants to resist freeze-induced dehydration which may limit cellular damage during freezing (Rajashekar & Burke 1996). It could be suggested then that cell-wall strength is an important factor for freezing tolerance, and that a decrease in strength and/or stiffness of the cell wall in *sfr8* mutants results in the freezing

sensitivity observed. It is important to note, however, that resistance to cell collapse during freezing has been suggested to lead to the development of negative pressures within the cell (Hansen & Beck 1988; Zhu *et al.* 1989; Zhu & Beck 1991), and negative pressures have been correlated with cavitation which can lead to cell death (Tyree & Dixon 1986; Tyree & Sperry 1989). Although cavitation is generally limited to xylem tissues, this observation provides evidence that more rigid tissues do not automatically infer increased freezing tolerance, and it may be that having cell walls that are too stiff actually results in decreased freezing tolerance. It is possible that cell-wall stiffness is highly regulated during freezing events in order to reduce damage from freeze-induced dehydration but also prevent damage from cavitation.

Interestingly, pore size has also been linked to cell-wall strength, as *C. album* cells cultured in boron deficient medium were more likely to rupture than those supplemented with BA (Fleischer *et al.* 1998), suggesting that smaller pores make the cell wall stronger. Since this was later linked to RG-II dimerisation (Fleischer *et al.* 1999) it is possible that both characteristics (RG-II dimerisation and cell-wall pore size) influence cell-wall strength as a consequence of being linked. These measurements need to be carried out in cells of mature plants of *sfr8* in order for a direct link to be made to experiments carried out in this research.

5.4 Conclusions

This section has explored some of the possible mechanisms that may result in the freezing-sensitive phenotype observed in *sfr8* and *mur1-1* mutants. The impact of the guard cell phenotype observed in *sfr8* (see Chapter 4) was investigated via electrolyte leakage assessment of other putative guard cell mutants. However, no conclusion could be drawn from these experiments thus, it is not yet possible to accept or reject the hypothesis that structural aspects of RG-II influences plant freezing tolerance. The impact of a decrease in RG-II dimerisation on nucleation temperature was also assessed, and results suggest that a decrease in RG-II dimerisation may depress the freezing temperature of plant tissues. Further study is required to ascertain if this is applicable to whole plants. It was not possible to conclude whether RG-II synthesis or cell content increases in the cold, but there is evidence to suggest that an increase would be functionally significant for freezing tolerance.

CHAPTER 6

DISCUSSION AND CONCLUSIONS

6.1 Implications of the work

The cell wall is an integral component of plant cells, contributing to cell strength, integrity and growth (Cosgrove 2005). It has long been believed, and there is some evidence to show that, the cell wall is also necessary for freezing tolerance in the plant. There are suggestions that the cell wall can act as a barrier to ice nucleation and growth, perhaps through the control of cell-wall pore size (Ashworth & Abeles 1984; Wisniewski, Davis & Schaffer 1991; Yamada *et al.* 2002). There is also research to show that cell-wall composition is modified during cold acclimation, and that this can lead to increased cell-wall stiffness (Solecka *et al.* 2008), which may be functionally significant to protect cells during freezing events (Rajashekar & Burke 1996). However, the precise mechanisms via which the cell wall influences freezing tolerance are not yet fully understood. Mutants deficient in cell-wall monosaccharides have proven a useful tool for studying cell-wall polysaccharide function (Reiter *et al.* 1997), and through the use of such a mutant, this study has provided a link and suggested a possible mechanism via which the cell wall regulates freezing tolerance. A possible link has also been made between cell-wall structure and guard cell dynamics, with implications for drought tolerance and growth. This study therefore highlights the cell wall as an important target for modification to enhance response to abiotic stresses in order to protect crop yield in the future.

6.2 *sensitive to freezing8* mutants are deficient in cell-wall fucose and RG-II dimerisation

As has been shown previously in *mur1-1* mutants, *sfr8* plants displayed a decrease in cell-wall fucose (Reiter *et al.* 1993), stemming from a mutation in the *MUR1* gene which encodes an enzyme active in the GDP-L-fucose biosynthesis pathway in plants (Bonin *et al.* 1997). In this study, the freezing-sensitive phenotype of *sfr8* was correlated with cell-wall fucose deficiency by the finding that plants treated with a fucosyl-transferase inhibitor were also freezing sensitive. Fucose is mainly found as a component of cell-wall polysaccharides such as xyloglucan, RG-I and RG-II, as well as in *N*-linked glycans and glycolipids (Ebert, Rautengarten & Heazlewood 2017). There is little evidence to suggest that free fucose has any specific role within the plant,

and it is likely that any free L-fucose would be incorporated into a salvage pathway and formed into the active form of GDP-L-fucose (Bar-Peled & O'Neill 2011). Direct measurements showed that fucose residues were lost from polysaccharides in *mur1-1* mutants (Zablackis *et al.* 1996; Pabst *et al.* 2013), suggesting that the freezing-sensitive phenotype of *sfr8* and *mur1-1* could occur as a result of fucose-deficiency in any of these cell-wall components.

Previous studies have shown that supplementing *mur1-1* plants with boric acid has the ability to reverse the morphological phenotypes of mutants, and that this was correlated with the rescue of RG-II dimerisation in the cell wall, which was decreased in *mur1-1* mutants due to loss of the L-fucose residue in side chain A (O'Neill *et al.* 2001). BA treatment was also able to restore cell-wall tensile strength and modulus, which were both decreased in *mur1-1* and *mur1-2* hypocotyls (Ryden *et al.* 2003). Other studies have shown that a deficiency in cell wall L-galactose also decreases the ability of RG-II to dimerise in tomato and *Arabidopsis*, and supplementing these plants with BA had the ability to restore RG-II dimerisation (Voxeur *et al.* 2011; Sechet *et al.* 2018 respectively). As RG-II domains are believed to be the exclusive binding site for boron (Matoh *et al.* 1996), it is likely that the phenotypes that are reversible with BA occur as a result of a decrease in RG-II dimerisation. In this study, *sfr8* and *mur1-1* plants were also shown to contain primarily monomeric RG-II. However, BA-supplemented plants were not directly observed to recover RG-II dimerisation, although this may have been due to aberrant techniques and the instability of the *sfr8*/*mur1-1* RG-II molecule (O'Neill *et al.* 2001). It may be that the mass-spectroscopy detection methods used in these studies was more reliable at measuring the extent of RG-II dimerisation in fucose and galactose-deficient mutants than the PAGE analysis utilised here.

Despite the uncertainty in the efficacy of BA to restore cell-wall RG-II dimerisation, in this study BA was shown to have the ability to return electrolyte leakage to wild type levels in *mur1-1* mutants (*sfr8* was not used here due to the discovery of contamination with wild type in the seed stock). By taking into consideration the structural role that boron plays within the plant (see section 1.4.4 and 3.3.5), this provides a key link between RG-II dimerisation and freezing tolerance. BA supplementation also appeared to partially reverse the morphological phenotypes of *mur1-1* such as the rounded leaves and shortened petioles, but not to the extent of that seen in the study by O'Neill *et al.* (2001), where *mur1-1* plants treated with BA were almost identical to wild type. This may be due to BA application methods, as in this study BA was applied with water direct to the roots, whereas in O'Neill *et al.* (2001), BA was applied by spraying. Also, in

this study, plants exhibited boron toxicity, which was not apparent in O'Neill's study even though the morphological phenotypes were fully reversed.

Interestingly, boron-deficiency has been linked to the inability to acquire freezing tolerance in Norway Spruce trees, which the authors have linked to the possibility that increased pore size of boron-deficient cell walls limits the capacity of plants to supercool (Raisanen *et al.* 2006; Räisänen, Repo & Lehto 2007). Cell-wall pore size has been linked to extracellular ice nucleation, as well as RG-II dimerisation, providing evidence that dimerisation is important for freezing tolerance.

6.3 Cell-wall structure is important to attain normal freezing tolerance

6.3.1 Cell-wall pore size

Ice nucleation experiments using droplets and epidermal peels suggested that nucleation temperature may differ in *sfr8* plants compared to wild type. The epidermal peel experiments showed that nucleation of wild type peels occurred at higher temperatures than in *sfr8* plants, which could suggest that RG-II dimerisation preferentially nucleates ice in specific areas of the cell wall, perhaps in order to restrict ice damage. Previous studies have highlighted the presence of nucleation factors in plant leaves (Kaku 1973), and recent work has even highlighted a polysaccharide with ice-nucleating properties in pollen that were diminished with the additions of borate (Dreischmeier *et al.* 2017). However, if this were related to RG-II, it would suggest that the monomer has ice-nucleating properties, which does not fit with the results from ice nucleation in epidermal peels. These findings are also contradictory to the idea that plants, including *Arabidopsis*, generally limit ice nucleation by supercooling to prevent damage from freezing (Reyes-Diaz *et al.* 2006), for example by producing ice-binding proteins (Bar Dolev *et al.* 2016). Ashworth and Abeles (1984) showed that water in small pores froze at lower temperatures than water in larger pores, and that smaller pores may also impede the spread of ice. This would reduce damage to the plant from ice growth and dehydration during freezing events, if the freezing point is depressed. Cell-wall pore size has been linked to dimerisation of RG-II, as treatment of boron-deficient cells with BA led to rapid RG-II dimerisation and a concomitant decrease in pore size (Fleischer *et al.* 1999). Pore size has also been shown to decrease during cold acclimation, suggesting it is functionally significant for freezing tolerance (Rajashekar & Lafta 1996). From this information, it would be logical to observe nucleation at an increased temperature in *sfr8* plants if indeed the decrease in RG-II dimerisation does result in

increased pore size, but this is not observed in epidermal peels. However, it is possible that the epidermal peels did not represent a typical *in vivo* cell wall environment, as the very process of peeling the epidermis can affect cell structure and water content (Zhu *et al.* 2015). This can be a determinant of freezing temperature (Mazur 1963), and may mask the singular effect of changing cell-wall pore size. Cell-wall pore size, particularly that of the pit membranes whose structure was shown to be regulated by pectins (Wisniewski & Davis 1995), has also been shown to influence water movement and may limit water loss during freezing events, thus limiting freeze-induced dehydration (Wisniewski *et al.* 1987).

The contradictions may arise in this argument due to the fact that it is not certain whether plants specifically initiate or prevent ice nucleation within their tissues. It is highly likely that different species and even different tissues employ different mechanisms to prevent freezing injury, either preventing ice nucleation, or initiating ice nucleation in specific areas of the plant that will limit damage. It is unlikely that one cover-all mechanism can be applied to all plants, and this must be taken into account when investigating freeze survival mechanisms.

6.3.2 Cell wall-plasma membrane attachments

Alterations to the freezing sensitivity of RNAi lines affecting GIPC synthesis suggests that RG-II monomer may be important for freezing tolerance. Research has shown that RG-II may form boron cross-links with plasma membrane localised GIPCs; this could be functionally significant for tethering the plasma membrane to the cell wall, or act as a platform to catalyse RG-II dimerisation, as the addition of GIPCs to RG-II monomer was shown to increase dimer formation (Voxeur & Fry 2014). An observation of weakened inflorescence stems in RNAi lines affecting GIPC synthesis (Pinneh 2017) suggested that cell walls may also be weakened in these lines in a similar way to *mur1-1* mutants. However, analysis of freezing tolerance displayed no difference compared to wild type, with one line even displaying slightly decreased electrolyte leakage. This could suggest that either PM-cell wall adhesion is detrimental for freezing tolerance which has been suggested by previous work (Murai & Yoshida 1998b), or that it is better to have less RG-II dimer in the cell wall if GIPCs do facilitate cross-linking, which does not necessarily fit with the freezing sensitivity observed in *sfr8* and *mur1-1* mutants. However, the exact role of GIPCs in RG-II cross-linking *in vivo* is not fully understood, nor is the impact of altered GIPC synthesis on GIPC-RG-II cross-links, so further research is necessary to determine the nature of these connections and what impacts they have on freezing tolerance. Again, it is necessary to ask the question of whether it is better for the plasma membrane to stay in close contact with the wall

during freezing, or whether it is better for it to be able to pull away. There is still debate as to whether plasmolysis actually occurs during *in vivo* freezing events (Levitt 1980; Oparka 1994). It is also still unclear as to which event would cause damage, as the surface area changes that occur during observed plasmolysis is known to result in membrane injury (Oparka 1994), but tight adhesions of the wall to the membrane are thought to impart a mechanical stress that is also damaging (Murai & Yoshida 1998b). Once again, it may be that different species utilise different mechanisms for preventing membrane injury, which may be dependent on the lipid modifications made during cold acclimation (see section 1.2.4.1).

6.3.3 Cell-wall composition

Although it was not possible to directly show that RG-II synthesis and dimerisation is modified during cold acclimation in this study, there is ample evidence to show that cell-wall composition of other polysaccharides is altered during cold acclimation (Solecka *et al.* 2008; Domon *et al.* 2013; Baldwin *et al.* 2014; Bilska-Kos *et al.* 2017; Willick *et al.* 2018). Although there is some discrepancy between these studies as to what cell-wall components are increased or decreased, particularly in terms of cell-wall remodelling enzymes (see section 1.5.1) there is a consensus that cell-wall pectin content in particular increases during cold acclimation. This provides further evidence that pectins, which could include RG-II, are a necessary component of freezing tolerance. These modifications likely alter cell-wall structure and may form part of the mechanism for the resistance of freezing damage in terms of pore size and cell strength.

6.4 Alterations to cell-wall stiffness in sfr8 mutants may impact upon both freezing tolerance and guard cell dynamics

6.4.1 Freezing tolerance

In order to understand the mechanical consequences of changing cell wall structure and composition, it is useful to begin by defining a set of measurable cell-wall tensile properties. These are commonly probed by measuring the tensile force per unit area (stress) required to achieve a given fractional elongation (strain), illustrated in Figure 6.1. Two common regions observed in cell wall stress-strain behaviour are the elastic region, where removal of the applied stress results in complete recovery of the original cell-wall shape, and the plastic region, where after removal of the applied force, the cell wall has been permanently elongated. The elastic and plastic modulii are the gradients of the stress-strain curve in each respective region and represent the stiffness of the cell wall: a larger modulus means the cell wall is stiffer, and harder

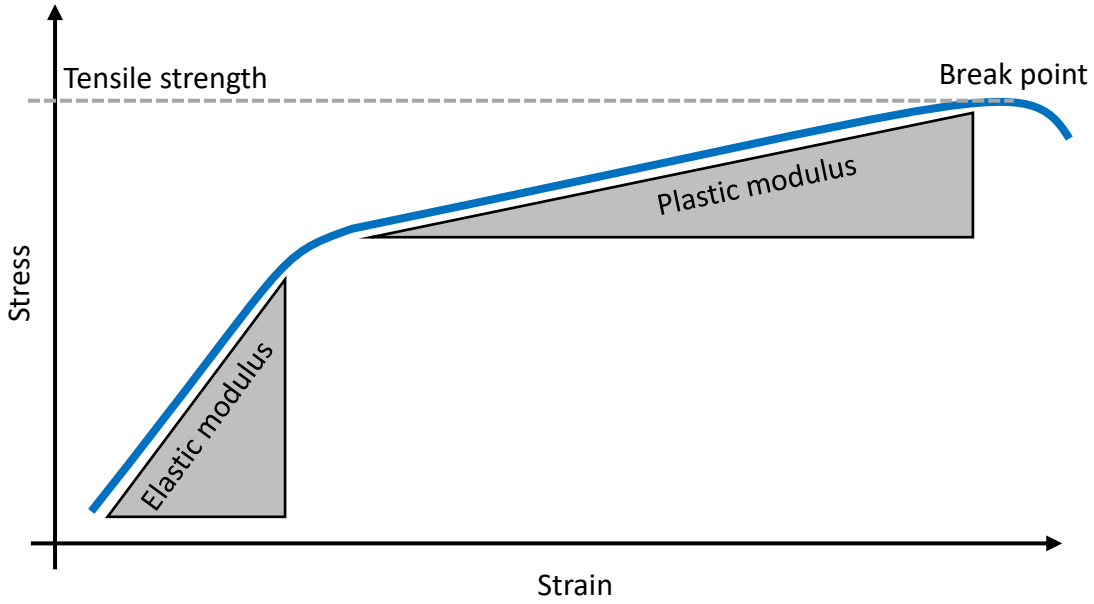

Figure 6.1: Stress-strain graph. A stress-strain graph showing the regions of elastic modulus, plastic modulus and tensile strength.

to deform. The maximum stress which can be applied to the cell wall is termed the tensile strength, and the point at which the cell wall ruptures is called the break point.

Previous evidence suggests that cell-wall stiffness may be correlated with the level of RG-II dimerization, which may be modified during freezing events. Stiffer tissues have been shown to reduce damage from freeze-induced dehydration (Rajashekar & Burke 1996). RG-II has been related to both of these properties, with *mur1-1* mutants displaying a decrease in both cell-wall tensile strength and tensile modulus that was reversible with BA supplementation (Ryden *et al.* 2003). One of the first descriptions of *mur1-1* tissues was an increase in brittleness (Reiter *et al.* 1993), referring to the break point occurring after only small plastic deformations. Boron-deficient tissues have been described as having similar properties to those with a decrease in RG-II dimerisation. Boron-deficient *C. album* cells were shown to rupture as they aged due to overexpansion (Fleischer *et al.* 1998), suggesting a decrease in cell-wall tensile strength as walls required less force to break. Boron deficiency in roots of squash and bean was shown to reduce the cell-wall elasticity modulus (Findeklee & Goldbach 1996; Findeklee *et al.* 1997), and hypocotyls of boron-deficient squash were shown to have more brittle and rigid tissues (Hu & Brown 1994). In this study, the authors also demonstrated that tissues had reduced elastic and plastic extensibilities (the inverse of the elastic modulii), suggesting boron-deficiency also impacted on cell wall growth, and not just its ability to resist mechanical force. It is unclear exactly how these properties may influence freezing tolerance of the cell as there are conflicting

theories as to whether stiffness is beneficial or detrimental for freezing tolerance (see section 6.5).

6.4.2 Guard cell dynamics

This study has revealed a link between fucose-deficiency and guard cell dynamics, suggested to be due to a decrease in RG-II dimerisation. Utilising measurements of stomatal aperture in response to ABA treatment, thermal imaging under changes in humidity and drought stress, and stomatal conductance changes in response to changing CO_2 concentrations, *sfr8* stomata were shown to have a reduced response to opening and closure signals (Chapter 4). The fact that this phenotype is observed in response to several different stimuli suggests it is not a signalling problem, but rather a mechanical problem, providing further evidence that cell-wall structure is important for normal guard cell function. Mutants deficient in homogalacturonan methyl-esterification and normal arabinan structure have also displayed aberrant guard cell dynamics (Jones *et al.* 2003; Amsbury *et al.* 2016). This is suggested to occur due to an increased stiffness of the cell wall (Woolfenden *et al.* 2017), causing a resistance to deformation. However, there is now an inherent discrepancy between the model presented from the guard cell measurement data which suggests increased stiffness, and measurements in the literature on RG-II and freezing stress that suggest mutants cell walls have a decreased stiffness. It is of course possible that the stomatal phenotype of *sfr8* is not linked to a decrease in RG-II and BA supplementation is proposed as an experiment to elucidating this, but the fact that other mutants with modified pectin structure display a similar phenotype adds credence to this theory. There are thus two competing theories; the mutant cell walls have either increased or decreased stiffness, but the successful theory must be consistent with both the observations of decreased freezing tolerance, and reduced rate of guard cell dynamics.

If cell walls are stiffer, it may be that the guard cell phenotype impacts upon freezing tolerance by allowing ice growth through the stomatal pores. However, in the context of the electrolyte leakage assay, the fact that discs are cut from the leaf automatically provides a wounded entrance for ice to enter into the leaf, which would likely mask any effects of open stomata. Assessment of freezing tolerance of *pme6* mutants unfortunately did not provide any answers to this hypothesis. It is possible that a stiffer cell wall that is able to resist collapse could result in cell cavitation during freezing events, however this is typically seen in rigid xylem vessels which are unlikely to be affected by changes in RG-II dimerisation (see section 6.5) (Tyree & Dixon 1986).

If the walls are less stiff, it is possible that this *decrease* in stiffness affects guard cell dynamics, by preventing the guard cell poles from being able to stiffen and allow the stomatal pore to open (Carter *et al.* 2017). This recent work by Carter *et al*. (2017) proposed that polar stiffening of guard cells was mediated at least in part by the accumulation of de-esterified pectins. Stiffening limited extension of the stomatal complex under opening conditions, which allowed the acquisition of a greater response in pore aperture per change in guard cell turgor. The authors also demonstrated that treating guard cell walls with polygalacturonase led to a loss of polar stiffening and a decrease in aperture for a given pressure (Carter *et al.* 2017). These findings compliment the phenotypes observed in *sfr8* mutants and provide a theory for the loss of guard cell dynamics. This suggestion also highlights a potential target for engineering of enhance stomatal regulation in order to improve water loss under water-limited conditions.

6.5 Limitations of the work

Although mutants deficient in monosaccharides are useful tools for studying cell-wall function, they are likely to contain structural alterations in several different polysaccharides. This makes it difficult to pin-point the specific structures responsible for the exhibited phenotypes, as has been the case for the *sfr8* and *mur1-1* mutants. Although the influence of RG-II dimerisation is implied when BA is able to rescue *mur1-1* phenotypes, it does not provide a direct correlation. Another problem that is recently gaining more attention, is the possibility that the plant attempts to overcome alterations to cell-wall integrity (CWI) that would confound the direct effects of cell wall defects (Cosgrove 2018). Research has shown that plants can monitor cell-wall architecture and induce compensatory changes in the cell wall (Voxeur & Höfte 2016). For example, a mutant with defects in cellulose synthesis was also shown to have alterations to methyl-esterification status of pectins (Sorek *et al.* 2015). In another study, inhibition of pectin de-methyl-esterification in the cell wall was shown to result in compensatory brassinosteroid signalling (Wolf *et al.* 2014). If compensatory mechanisms similar to this are induced in *sfr8* and *mur1-1* plants, this could go some way to explaining the observed growth phenotype. These cell wall integrity mechanisms may stem from the trade-off between growth and protection from abiotic stress (Bechtold & Field 2018). Indeed, it is possible that *mur1-1* plants do display some form of compensatory mechanism, as the mutant was recently shown to have increased expression of genes involved in lignin synthesis that led to altered lignin structure in stem tissues, as well as defects in cell-cell adhesions associated with the induction of lignified tissues (Voxeur *et al.* 2017). The authors do attribute the observed phenotype to RG-II as a similar

phenotype was observed in a mutant of the boron transporter *bor1-3* (Voxeur *et al.* 2017). It is difficult to hypothesise what impact these alterations may have on freezing-tolerance, although, as described in Chapter 1, the knock down of genes involved in lignin synthesis resulted in a decrease in cell wall lignin content and an increase in freezing tolerance (Lefebvre *et al.* 2011; Ji *et al.* 2015a). It could thus be speculated that the increase in lignin observed in *mur1-1* plants is correlated with the decrease in freezing tolerance. However, it is likely that the alterations to cell-cell adhesion may also impact upon freezing tolerance, among the other theories already discussed in relation to a loss of RG-II dimerisation. Further investigation is therefore necessary to understand what structural attributes contribute to the freezing sensitivity of *sfr8* and *mur1-1*.

6.6 Future work

6.6.1 Verification of the link between RG-II dimerisation and freezing tolerance

Although analysis of electrolyte leakage of BA supplemented *mur1-1* plants showed that freezing tolerance could be restored, further analysis is needed to ascertain if RG-II dimerisation is restored in these tissues and thus cement the link between RG-II dimerisation and freezing tolerance. PAGE analysis showed that BA was not able to restore RG-II dimerisation in *mur1-1* plants, but it is possible that because RG-II dimers from *mur1-1* plants are known to be less stable (O'Neill *et al.* 2001), that this is an artefact of the technique. Indeed, in this study by O'Neill *et al.* (2001), dimerised RG-II was monomerised with the addition of 1 M HCl, showing that the borate-ester is sensitive to acidic conditions. It may be that the acetic acid used to neutralise the cell wall extract during the extraction procedure, was enough to break some of the borate-ester bonds (see section 2.4.2.1). Measurements of the level of cell-wall RG-II dimerisation have previously been carried out via size exclusion chromatography and mass spectroscopy techniques (O'Neill *et al.* 2001; Voxeur *et al.* 2011; Sechet *et al.* 2018). Although this was attempted in this study, lack of the correct column for RG-II separation meant measurement was not possible. This method could be used to provide evidence for the link between RG-II dimerisation and rescue of the freezing-sensitive phenotype. Although experiments assessing the effects of BA supplementation suggest that it is RG-II that impacts upon freezing tolerance, there is evidence that boron has other roles within the cell (as discussed in Chapter 1). Thus, it would be necessary to eliminate the possibility that a loss of fucose on other cell-wall polysaccharides results in freezing sensitivity.

Another level of verification would come from assessing the freezing tolerance of plants deficient solely in RG-II cross-linking. The process of RG-II biosynthesis has not yet been fully characterised, although a set of RG-II synthesis enzymes have been described. Interestingly, a mutation in one of these genes led to lethal root and pollen tubes defects (Fangel *et al.* 2011; Liu *et al.* 2011), suggesting it may not be possible to assess freezing sensitivity in wholly RG-II deficient plants. It would be necessary to know which specific enzyme or suite of enzymes is important for cross-linking in order to assess this directly in a mutant, and until these have been discovered it would not be possible to utilise mutants for this purpose. Recent advances into the metabolism of human gut bacteria have led to the discovery of novel enzymes that catalyse the breakdown of specific bonds of RG-II (Ndeh *et al.* 2017). One or several of these enzymes could be expressed in plants to phenocopy the *sfr8*/*mur1-1* mutation, without affecting other cell-wall polysaccharides. A resulting freezing-sensitive phenotype would provide strong evidence that RG-II cross-linking via a borate-ester in particular is necessary for freezing tolerance.

Another interesting area of enquiry would be to investigate what the consequences of a decrease in the dimerisation of RG-II in *mur1-1* mutants (as alluded to in section 6.5). A study using mutants deficient in cell-wall arabinan suggested that a consequence of this was the cross-linking of homogalacturonan chains that reduced cell-wall flexibility (Jones *et al.* 2003). It is possible that a decrease in RG-II dimerisation may also result in similar consequences, allowing homogalacturonan chains to come together and cross-link, although alterations to cell-wall thickness and increase in pore size would suggest that a loss of cross-linking results in HG chains that are further apart in the *mur1-1* mutant (Fleischer *et al.* 1999; Ishii *et al.* 2001a). Assessing freezing sensitivity of *pme* or *pmei* mutants could reveal whether HG cross-linking is important for freezing tolerance, although recent research suggests that a decrease in methyl-esterification status does not necessarily result in increased HG cross-linking (Hocq *et al.* 2017). It is likely that CWI mechanisms may confound hypothesised alterations to cell wall structure in cell wall mutants. Thus, a general assessment of structure and polysaccharide orientation within the cell wall may be necessary to understand the overall alterations. This could be achieved via the use of polysaccharide-specific or pectin modification-specific antibodies (Knox 2008; Pattathil *et al.* 2010; Lee, Marcus & Knox 2011) or possibly via AFM, which has previously been used to gain insight into cell-wall structural attributes and could highlight specific attachments between cell-wall polysaccharides (Zdunek *et al.* 2014; Zhang *et al.* 2016b).

6.6.2 How does a loss of RG-II dimerisation result in freezing-sensitivity?

If RG-II is indeed necessary for freezing tolerance, it is still unclear what structural properties of the cell wall that RG-II dimerisation influences may be important. Assessment of Norway spruce buds suggests boron-deficiency may influence freezing tolerance by preventing the supercooling of buds (Räisänen *et al.* 2007), which could be controlled by RG-II dimerisation, perhaps via pore size (Ashworth & Abeles 1984). Refined ways of assessing differences in ice nucleation temperature between wild type and *sfr8* are required, and this could be achieved through the use of infrared thermography (Fuller & Wisniewski 1998). This could suggest whether RG-II dimerisation depresses the freezing point in plants, perhaps by maintaining small cell-wall pores, or if nucleation occurs earlier in mutant plants due to the presence of open stomata. Assessment of other open stomata mutants would also further suggest if alterations to guard cell dynamics are detrimental to freezing, although care must be taken when choosing these mutants as some are as a result of an insensitivity to ABA, which would also impact upon cold acclimation and thus freezing tolerance (Merlot *et al.* 2002).

Visualisation or measurement of ice growth, such as that carried out in Chapter 5 with increased resolution, could suggest if ice growth is prevented in wild type compared to mutants, and may reveal whether a decrease in pore size inhibits the growth of ice and thus reduces damage from freezing (Ashworth & Abeles 1984). There is a suggestion that pit membranes may also play a role in preventing the spread of ice, and also slowing water movement to sites of extracellular freezing (Wisniewski *et al.* 2004). Given the possibly that RG-II is believed to affect xylem cell-wall structure (Voxeur *et al.* 2017), it would be interesting to observe if ice growth or water movement through the vascular tissue is more or less prevalent in the mutant compared to wild type.

6.6.3 Measurements of cell-wall stiffness

There are several studies that highlight the changes to the mechanical properties of the cell wall with alterations to RG-II dimerisation or associated boron-deficiency (Hu & Brown 1994; Findeklee & Goldbach 1996; Findeklee *et al.* 1997; Ryden *et al.* 2003). These studies report that tissues deficient in RG-II dimerisation have decreased tensile strength and decreased tensile modulus. This hypothesis is supported by the theory that the alterations to guard cell dynamics occur as a result of the inability for the guard cell poles to stiffen during opening (Carter *et al.* 2017).

In the past decade, the process of atomic force microscopy (AFM) has gained more and more interest, and many different measurements can now be obtained from their use. It would thus be interesting to use AFM to take measurements of cell-wall mechanical parameters such as elasticity i.e. tensile modulus (Peaucelle *et al.* 2011; Braybrook, Hofte & Peaucelle 2012) to verify the theory that tensile modulus is decreased in the stomata thus preventing opening. It may also be possible to correlate the tensile modulus with freezing tolerance and may highlight whether the increased lignin content has an effect on wall stiffness. It may be that measurements are different in different tissues, as it has been shown that different cells contain different levels of pectins (Hadfield & Bennett 1998; Caffall & Mohnen 2009). It may be necessary therefore, to first understand which tissues are damaged during freezing events; electrolyte leakage assays would suggest that damage does occur in leaf tissue, which rules out the possibility that damage is restricted to root, reproductive or apical tissue. Verifying the effect of RG-II dimerisation in cell wall mechanics could imply whether an increased stiffness is beneficial for freezing tolerance, as has previously been implied (Rajashekar & Burke 1996; Rajashekar & Lafta 1996), or detrimental. It may still prove difficult to directly link changes in cell-wall tensile modulus to *sfr8* freezing sensitivity, especially considering the various other consequences of a decrease in RG-II dimerisation. It may be necessary to assess freezing tolerance of various mutants or enzyme treated plants that also have altered wall tensile modulus to correlate these two properties.

It is also important to be aware of the drawbacks of AFM; although micro-scale indentation techniques can provide measurements of tensile modulus, these are not comparable to the stress-strain assays typically used, for example by Ryden *et al.* (2003). In these assays, a tensile force in the plane of the wall is resisted by cellulose microfibrils, whereas this is not the case in indentation assays which probe smaller areas of the wall (Cosgrove 2016b). This may not hinder the comparison of two tissues with altered pectin structure, but there are other limits that need to be considered when using AFM techniques, such as the effect of turgor pressure, the size and shape of the tip used, and the force applied which is important in terms of knowing whether the wall is being deformed locally or whether indentation alters the whole cell shape globally. These parameters would need to be assessed and controlled for to obtain the most relevant measurements for the question being asked (Braybrook 2015).

6.6.4 Is RG-II synthesis or dimerisation up-regulated during cold acclimation?

Analysis of RG-II content in the cell wall after cold acclimation would provide further evidence that RG-II is utilised during freezing tolerance if it is found to increase. This could be carried out as described in several studies (O'Neill *et al.* 2001; Voxeur *et al.* 2011; Sechet *et al.* 2018). However, it may also be possible to measure sugars that are specific to RG-II such as apiose or D-KDO using the method described in section 2.4.1. Analysis of the ratio of monomer to dimer would be very interesting, as this would provide evidence as to whether RG-II monomer plays any role in freezing tolerance, if the ratio of monomer:dimer is found to increase, perhaps as an element of cell wall-plasma membrane attachments (Voxeur & Fry 2014). A modification of the radiolabelling method could still show whether RG-II synthesis is increased. One improvement may be to use cell cultures rather than leaf tissue which has been used in previous investigations into RG-II dimerisation (Chormova *et al.* 2014a), as this would allow better access of the [^{14}C]-fructose, which may have been a limiting factor in the technique used in this study. Analysis of gene expression of RG-II specific synthesis genes *RGXT1-4* would also suggest whether there is an up-regulation of RG-II synthesis with cold exposure.

BIBLIOGRAPHY

Achard, P., Gong, F., Cheminant, S., Alioua, M., Hedden, P. & Genschik, P. (2008) The Cold-Inducible CBF1 Factor–Dependent Signaling Pathway Modulates the Accumulation of the Growth-Repressing DELLA Proteins via Its Effect on Gibberellin Metabolism. *The Plant Cell*, **20**, 2117–2129.

Agarwal, M., Hao, Y., Kapoor, A., Dong, C.-H., Fujii, H., Zheng, X. & Zhu, J.-K. (2006) A R2R3 Type MYB Transcription Factor Is Involved in the Cold Regulation of CBF Genes and in Acquired Freezing Tolerance. *The Journal of Biological Chemistry*, **281**, 37636–37645.

Akamura, A.N., Uruta, H.F., Aeda, H.M. & Akao, T.T. (2002) Structural Studies by Stepwise Enzymatic Degradation of the Main Backbone of Soybean Soluble Polysaccharides Consisting of Galacturonan and Rhamnogalacturonan. *Bioscience, Biotechnology, and Biochemistry*, **66**, 1301–1313.

Allen, G.J., Chu, S.P., Schumacher, K., Shimazaki, C.T., Vafeados, D., Kemper, A., Hawke, S.D., Tallman, G., Tsien, R.Y., Harper, J.F., Chory, J. & Schroeder, J.I. (2000) Alteration of Stimulus-Specific Guard Cell Calcium Oscillations and Stomatal Closing in Arabidopsis det3 Mutant. *Science*, **289**, 2338–2342.

Amsbury, S., Hunt, L., Elhaddad, N., Baillie, A., Lundgren, M., Verhertbruggen, Y., Scheller, H. V, Knox, J.P., Fleming, A.J. & Gray, J.E. (2016) Stomatal Function Requires Pectin De-methyl-esterification of the Guard Cell Wall. *Current Biology*, **26**, 1–8.

Araújo, W.L., Fernie, A.R. & Nunes-Nesi, A. (2011) Control of stomatal aperture: A renaissance of the old guard. *Plant Signaling & Behavior*, **6**, 1305–1311.

Arias, N.S., Bucci, S.J., Scholz, F.G. & Goldstein, G. (2015) Freezing avoidance by supercooling in Olea europaea cultivars: the role of apoplastic water, solute content and cell wall rigidity. *Plant, Cell and Environment*, **38**, 2061–2070.

Arioli, T., Peng, L., Betzner, A.S., Burn, J., Wittke, W., Herth, W., Camilleri, C., Hofte, H., Plazinski, J., Birch, R., Cork, A., Glover, J., Redmond, J. & Williamson, R.E. (1998) Molecular Analysis of Cellulose Biosynthesis in Arabidopsis. *Science*, **279**, 717–720.

Arnon, D.I. & Stout, P.R. (1939) The essentiality of certain elements in minute quantity for plants with special reference to copper. *Plant Physiology*, **14**, 371–375.

Artus, N.N., Uemura, M., Steponkus, P.L., Gilmour, S.J., Lin, C. & Thomashow, M.F. (1996) Constitutive expression of the cold-regulated Arabidopsis thaliana COR15a gene affects both chloroplast and protoplast freezing tolerance. *Proceedings of the National Academy of Sciences of the United States of America*, **93**, 13404–13409.

Aryal, B. & Neuner, G. (2010) Leaf wettability decreases along an extreme altitudinal gradient. *Oecologia*, **162**, 1–9.

Asahina, E. (1956) The Freezing process of Plant Cell. *Contribution from the Institute of Low Temperature Science Hokkaido University*, **10**, 83–126.

Ashworth, E.N. & Abeles, F.B. (1984) Freezing Behavior of Water in Small Pores and the Possible Role in the Freezing of Plant Tissues. *Plant Physiology*, **76**, 201–204.

Baldwin, L., Domon, J.M., Klimek, J.F., Fournet, F., Sellier, H., Gillet, F., Pelloux, J., Lejeune-

Hénaut, I., Carpita, N.C. & Rayon, C. (2014) Structural alteration of cell wall pectins accompanies pea development in response to cold. *Phytochemistry*, **104**, 37–47.

Bar-Peled, M. & O'Neill, M.A. (2011) Plant Nucleotide Sugar Formation, Interconversion, and Salvage by Sugar Recycling. *Annual Review of Plant Biology*, **62**, 127–155.

Bar Dolev, M., Braslavsky, I. & Davies, P.L. (2016) Ice-Binding Proteins and Their Function. *Annual Review of Biochemistry*, **85**, 515–542.

Baron-Epel, O., Gharyal, P.K. & Schindler, M. (1988) Pectins as mediators of wall porosity in soybean cells. *Planta*, **175**, 389–395.

Bassil, E. (2004) Use of Phenylboronic Acids to Investigate Boron Function in Plants. Possible Role of Boron in Transvacuolar Cytoplasmic Strands and Cell-to-Wall Adhesion. *Plant Physiology*, **136**, 3383–3395.

Bauer, W.D., Talmadge, K.W., Keegstra, K. & Albersheim, P. (1973) The Structure of Plant Cell Walls II. The hemicellulose of the walls of suspension-cultured sycamore cells. *Plant Physiology*, **51**, 174–187.

Bechtold, U. & Field, B. (2018) Molecular mechanisms controlling plant growth during abiotic stress. *Journal of Experimental Botany*, **69**, 2753–2758.

Bigg, E.K. (1953) The Supercooling of Water. *Proceedings of the Physical Society. Section B*, **66**, 688–694.

Bilska-Kos, A., Solecka, D., Dziewulska, A., Ochodzki, P., Jonczyk, M., Bilski, H. & Sowinski, P. (2017) Low temperature caused modifications in the arrangement of cell wall pectins due to changes of osmotic potential of cells of maize leaves (Zea mays L.). *Protoplasma*, **254**, 713–724.

Blatt, M.R. (2000) Cellular Signaling and Volume Control in Stomatal Movements in Plants. *Annual Review of Cell Developmental Biology*, **16**, 221–241.

Blevins, D.G. & Lukaszewski, K.M. (1998) Boron in Plant Structure and Function. *Annual review of plant physiology and plant molecular biology*, **49**, 481–500.

Bonin, C.P., Freshour, G., Hahn, M.G., Vanzin, G.F. & Reiter, W.-D. (2003) The GMD1 and GMD2 Genes of Arabidopsis Encode Isoforms of GDP-D-Mannose 4,6-Dehydratase with Cell Type-Specific Expression Patterns. *Plant Physiology*, **132**, 883–892.

Bonin, C.P., Potter, I., Vanzin, G.F. & Reiter, W.D. (1997) The MUR1 gene of Arabidopsis thaliana encodes an isoform of GDP-D-mannose-4,6-dehydratase, catalyzing the first step in the de novo synthesis of GDP-L-fucose. *Proceedings of the National Academy of Sciences of the United States of America*, **94**, 2085–90.

Braybrook, S.A. (2015) Measuring the elasticity of plant cells with atomic force microscopy. *Biophysical Methods in Cell Biology*, **125**, 237–254.

Braybrook, S.A., Hofte, H. & Peaucelle, A. (2012) Probing the mechanical contributions of the pectin matrix. *Plant Signaling & Behavior*, **7**, 1037–1041.

Bredow, M., Vanderbeld, B. & Walker, V.K. (2016) Knockdown of Ice-binding proteins in brachypodium distachyon demonstrates their role in Freeze protection. *PLoS ONE*, **11**, 1–23.

Bredow, M., Vanderbeld, B. & Walker, V.K. (2017) Ice-binding proteins confer freezing tolerance in transgenic Arabidopsis thaliana. *Plant Biotechnology Journal*, **15**, 68–81.

Bredow, M. & Walker, V.K. (2017) Ice-Binding Proteins in Plants. *Frontiers in Plant Science*, **8**, 1–15.

Brett, C. & Waldron, K. (1996) *Physiology and Biochemistry of Plant Cell Walls*, Second (eds M Black and B Charlwood). Chapman and Hall.

Bromley, P.E., Li, Y.O., Murphy, S.M., Sumner, C.M. & Lynch, D. V. (2003) Complex sphingolipid synthesis in plants: characterization of inositolphosphorylceramide synthase activity in bean microsomes. *Archives of Biochemistry and Biophysics*, **417**, 219–226.

Brown, P.H. & Hu, H. (1993) Boron uptake in sunflower, squash and cultured tobacco cells: Studies with stable isotope and ICP-MS. *Plant and Soil*, **155**, 147–150.

Burke, M.J., Gusta, L. V, Quamme, H.A., Weiser, C.J. & Li, P.H. (1976) FREEZING AND INJURY IN PLANTS. *Annual Review of Plant Physiology*, **27**, 507–28.

Burke, D., Kaufman, P., McNeil, M. & Albersheim, P. (1974) The Structure of Plant Cell Walls VI. A survey of the walls of suspension-cultured monocots. *Plant Physiology*, **54**, 109–115.

Caffall, K.H. & Mohnen, D. (2009) The structure, function, and biosynthesis of plant cell wall pectic polysaccharides. *Carbohydrate Research*, **344**, 1879–1900.

Cai, S., Papanatsiou, M., Blatt, M.R. & Chen, Z.-H. (2017) Speedy Grass Stomata : Emerging Molecular and Evolutionary Features. *Molecular Plant*, **10**, 912–914.

Camacho-Cristobal, J.J. & Gonzalez-Fontes, A. (1999) Boron deficiency causes a drastic decrease in nitrate content and nitrate reductase activity, and increases the content of carbohydrates in leaves from tobacco plants. *Planta*, **34**, 528–536.

Camacho-cristóbal, J.J., Rexach, J. & González-Fontes, A. (2008) Boron in Plants: Deficiency and Toxicity. *Journal of Integrative Plant Biology*, **50**, 1247–1255.

Campbell, M.M. & Sederoff, R.R. (1996) Variation in Lignin Content and Composition. *Plant physiology*, **1996**, 3–13.

Canny, M.J. (1995) APOPLASTIC WATER AND SOLUTE MOVEMENT: New Rules for an Old Space. *Annual Review of Plant Physiology and Plant Molecular Biology*, **46**, 215–236.

Carpita, N.C. & Gibeaut, D.M. (1993) Structural models of primary cell walls in flowering plants: consistency of molecular structure with the physical properties of the walls during growth. *The Plant Journal*, **3**, 1–30.

Carpita, N., Sabularse, D., Montezinos, D. & Delmer, D.P. (1979) Determination of the Pore Size of Cell Walls of Living Plant Cells. *Science*, **205**, 1144–1147.

Carter, R., Woolfenden, H., Baillie, A., Amsbury, S., Carroll, S., Healicon, E., Sovatzoglou, S., Braybrook, S., Gray, J.E., Hobbs, J., Morris, R.J. & Fleming, A.J. (2017) Stomatal Opening Involves Polar, Not Radial, Stiffening Of Guard Cells. *Current Biology*, **27**, 2974–2983.

Chambers, R. & Hale, H.P. (1932) The Formation of Ice in Protoplasm. *Proceedings of the Royal Society*, **B110**, 337–352.

Chater, C., Peng, K., Movahedi, M., Dunn, J.A., Walker, H.J., Liang, Y., Mclachlan, D.H., Casson,

S., Isner, J.C., Wilson, I., Neill, S.J., Hedrich, R., Gray, J.E. & Hetherington, A.M. (2015) Elevated CO2-Induced Responses in Stomata Require ABA and ABA Signaling. *Current Biology*, **25**, 2709–2716.

Chen, J., Chen, X., Zhang, Q., Zhang, Y., Ou, X., An, L., Feng, H. & Zhao, Z. (2018) A cold-induced pectin methyl-esterase inhibitor gene contributes negatively to freezing tolerance but positively to salt tolerance in Arabidopsis. *Journal of Plant Physiology*, **222**, 67–78.

Chormova, D. & Fry, S.C. (2016) Boron bridging of rhamnogalacturonan-II is promoted in vitro by cationic chaperones, including polyhistidine and wall glycoproteins. *New Phytologist*, **209**, 241–251.

Chormova, D., Messenger, D.J. & Fry, S.C. (2014a) Boron bridging of rhamnogalacturonan-II, monitored by gel electrophoresis, occurs during polysaccharide synthesis and secretion but not post-secretion. *Plant Journal*, **77**, 534–546.

Chormova, D., Messenger, D.J. & Fry, S.C. (2014b) Rhamnogalacturonan-II cross-linking of plant pectins via boron bridges occurs during polysaccharide synthesis and/or secretion. *Plant Signalling and Behaviour*, **9**, 8–10.

Chou, Y.-H., Pogorelko, G. & Zabotina, O.A. (2012) Xyloglucan Xylosyltransferases XXT1, XXT2, and XXT5 and the Glucan Synthase CSLC4 Form Golgi-Localized Multiprotein Complexes. *Plant Physiolgy*, **159**, 1355–1366.

Clarke, S.H. (1938) Fine Structure of the Plant Cell Wall. *Nature*, **142**, 899–904.

Cocuron, J.-C., Lerouxel, O., Drakakaki, G., Alonso, A.P., Liepman, A.H., Keegstra, K., Raikhel, N. & Wilkerson, C.G. (2007) A gene from the cellulose synthase-like C family encodes a B-1,4 glucan synthase. *PNAS*, **104**, 8550–8555.

Cosgrove, D.J. (1993) How Do Plant Cell Walls Extend? *Plant Physiology*, **102**, 1–6.

Cosgrove, D.J. (2000) Loosening of plant cell walls by expansins. *Nature*, **407**, 321–326.

Cosgrove, D.J. (2005) GROWTH OF THE PLANT CELL WALL. *Nature*, **6**, 850–861.

Cosgrove, D.J. (2015) Plant expansins: diversity and interactions with plant cell walls. *Current Opinion in Plant Biology*, **25**, 162–172.

Cosgrove, D.J. (2016a) Catalysts of plant cell wall loosening. *F1000Research*, **5**, 1–13.

Cosgrove, D.J. (2016b) Plant cell wall extensibility: connecting plant cell growth with cell wall structure, mechanics, and the action of wall-modifying enzymes. *Journal of Experimental Botany*, **67**, 463–476.

Cosgrove, D.J. (2018) Diffuse Growth of Plant Cell Walls. *Plant Physiology*, **176**, 16–27.

Cossins, A.R. (1994) Homeoviscous adaptation of biological membranes and its functional significance. *Temperature Adaptation of Biological Membranes* (ed A.R. Cossins), pp. 63–76.

Costa, J.M., Grant, O.M. & Chaves, M.M. (2013) Thermography to explore plant-environment interactions. *Journal of Experimental Botany*, **64**, 3937–3949.

Daloso, D.M. & Fernie, A.R. (2016) Roles of sucrose in guard cell regulation. *New Phytologist*, **211**, 809–818.

Darvill, A.G., McNeil, M. & Albersheim, P. (1978a) Structure of Plant Cell Walls VIII. A new pectic polysaccharide. *Plant Physiology*, **62**, 418–422.

Darvill, A.G., McNeil, M. & Albersheim, P. (1978b) Structure of Plant Cell Walls VIII. A New Pectic Polysaccharide. *Plant Physiology*, **62**, 418–422.

Daszkowska-Golec, A. & Szarejko, I. (2013) Open or close the gate - stomata action under the control of phytohormones in drought stress conditions. *Frontiers in Plant Science*, **4**, 1–16.

Decker, J.P. (1944) Effect of Temperature on Photosynthesis and Photorespiration in Red and Loblolly Pines. *Plant Physiology*, 679–688.

Dell, B. & Huang, L. (1997) Physiological response of plants to low boron. *Plant and Soil*, **193**, 103–120.

Doblin, M.S., Kurek, I., Jacob-Wilk, D. & Delmer, D.P. (2002) Cellulose Biosynthesis in Plants: from Genes to Rosettes. *Plant Cell Physiology*, **43**, 1407–1420.

Domon, J.-M., Baldwin, L., Acket, S., Caudeville, E., Arnoult, S., Zub, H., Gillet, F., Lejeune-Hénaut, I., Brancourt-Hulmel, M., Pelloux, J. & Rayon, C. (2013) Cell wall compositional modifications of Miscanthus ecotypes in response to cold acclimation. *Phytochemistry*, **85**, 51–61.

Dong, C.-H., Agarwal, M., Zhang, Y., Xie, Q. & Zhu, J.-K. (2006) The negative regulator of plant cold responses, HOS1, is a RING E3 ligase that mediates the ubiquitination and degradation of ICE1. *Proceedings of the National Academy of Sciences of the United States of America*, **103**, 8281–8286.

Dong, M.A., Farré, E.M. & Thomashow, M.F. (2011) CIRCADIAN CLOCK-ASSOCIATED 1 and LATE ELONGATED HYPOCOTYL regulate expression of the C-REPEAT BINDING FACTOR (CBF) pathway in Arabidopsis. *Proceedings of the National Academy of Sciences of the United States of America*, **108**, 7241–7246.

Dordas, C. & Brown, P.H. (2001) Evidence for channel mediated transport of boric acid in squash (Cucurbita pepo). *Plant and Soil*, **235**, 95–103.

Dordas, C., Chrispeels, M.J. & Brown, P.H. (2000) Permeability and Channel-Mediated Transport of Boric Acid across Membrane Vesicles Isolated from Squash Roots. *Plant Physiology*, **124**, 1349–1361.

Dowgert, M.F. & Steponkus, P.L. (1984) Behavior of the Plasma Membrane of Isolated Protoplasts during a Freeze-Thaw Cycle. *Plant Physiology*, **75**, 1139–1151.

Drake, P.L., Froend, R.H. & Franks, P.J. (2013) Smaller, faster stomata: scaling of stomatal size, rate of response, and stomatal conductance. *Journal of Experimental Botany*, **64**, 495–505.

Dreischmeier, K., Budke, C., Wiehemeier, L., Kottke, T. & Koop, T. (2017) Boreal pollen contain ice-nucleating as well as ice-binding 'antifreeze' polysaccharides. *Nature Scientific Reports*, **7**, 1–13.

Dumont, M., Lehner, A., Bardor, M., Burel, C., Vauzeilles, B., Lerouxel, O., Anderson, C.T., Mollet, J.-C. & Lerouge, P. (2015) Inhibition of fucosylation of cell wall components by 2-fluoro 2-deoxy-L-fucose induces defects in root cell elongation. *The Plant Journal*.

Dumont, M., Lehner, A., Bouton, S., Kiefer-Meyer, M.C., Voxeur, A., Pelloux, J., Lerouge, P. & Mollet, J.-C. (2014) The cell wall pectic polymer rhamnogalacturonan-II is required for

proper pollen tube elongation: implications of a putative sialyltransferase-like protein. *Annals of Botany*, **114**, 1177–1188.

Ebert, B., Rautengarten, C. & Heazlewood, J.L. (2017) GDP-L-fucose transport in plants: The missing piece. *Channels*, **11**, 8–10.

Edwards, K., Johnstone, C. & Thompson, C. (1991) A simple and rapid method for the preparation of plant genomic DNA for PCR analysis. *Nucleic Acids Research*, **19**, 1349.

Egelund, J., Damager, I., Faber, K., Olsen, C.-E., Ulvskov, P. & Peterson, B.L. (2008) Functional characterisation of a putative rhamnogalacturonan II specific xylosyltransferase. *FEBS*, **582**, 3217–3222.

Egelund, J., Petersen, B.L., Motawia, M.S., Damager, I., Faik, A., Olsen, C.E., Ishii, T., Clausen, H., Ulvskov, P. & Geshi, N. (2006) Arabidopsis thaliana RGXT1 and RGXT2 Encode Golgi-Localized (1,3)-alpha-D-Xylosyltransferases Involved in the Synthesis of Pectic Rhamnogalacturonan-II. *The Plant Cell*, **18**, 2593–2607.

Engineer, C., Hashimoto-Sugimoto, M., Negi, J., Israelsson-Nordstrom, M., Azoulay-Shemer, T., Rappel, W.-J., Iba, K. & Schroeder, J. (2017) CO2 sensing and CO2 regulation of stomatal conductance: advances and open questions. *Trends in Plant Science*, **21**, 16–30.

Fangel, J.U., Petersen, B.L., Jensen, N.B., Willats, W.G.T., Bacic, A. & Egelund, J. (2011) A putative Arabidopsis thaliana glycosyltransferase, At4g01220, which is closely related to three plant cell wall-specific xylosyltransferases, is differentially expressed spatially and temporally. *Plant Science*, **180**, 470–479.

Farquhar, G.D., Dubbe, D.R. & Raschke, K. (1978) Gain of the Feedback Loop Involving Carbon Dioxide and Stomata. *Plant Physiology*, **62**, 406–412.

Findeklee, P. & Goldbach, H.E. (1996) Rapid effects of boron deficiency on cell wall elasticity modulus in Cucurbita pepo roots. *Bot. Acta.*, **109**, 463–465.

Findeklee, P., Wimmer, M. & Goldbach, H.E. (1997) Early effects of boron deficiency on physical cell wall parameters, hydraulic conductivity and plasmamlemma-bound reductase activities in young C. pepo and V. faba roots. *Boron in Soils and Plants* (eds R.W. Bell), & B. Rerkasem), pp. 221–222. Kluwer Academic Publishers.

Fleischer, A., O'Neill, M.A. & Ehwald, R. (1999) The Pore Size of Non-Graminaceous Plant Cell Walls Is Rapidly Decreased by Borate Ester Cross-Linking of the Pectic Polysaccharide Rhamnogalacturonan II 1. *Plant Physiology*, **121**, 829–838.

Fleischer, A., Titel, C. & Ehwald, R. (1998) The Boron Requirement and Cell Wall Properties of Growing and Stationary Suspension-Cultured Chenopodium album L. Cells. *Plant Physiology*, **117**, 1401–1410.

Fourrier, N., Bedard, J., Lopez-Juez, E., Barbrook, A., Bowyer, J., Jarvis, P., Warren, G. & Thorlby, G. (2008) A role for SENSITIVE TO FREEZING2 in protecting chloroplasts against freeze-induced damage in Arabidopsis. *The Plant Journal*, **55**, 734–745.

Fowler, S.G., Cook, D. & Thomashow, M.F. (2005) Low Temperature Induction of Arabidopsis CBF1 , 2 , and 3 Is Gated by the Circadian Clock 1. *Plant Physiology*, **137**, 961–968.

Franková, L. & Fry, S.C. (2013) Biochemistry and physiological roles of enzymes that 'cut and paste' plant cell-wall polysaccharides. *Journal of Experimental Botany*, **64**, 3519–3550.

Franks, P.J. & Farquhar, G.D. (2007) The Mechanical Diversity of Stomata and Its Significance in Gas-Exchange Control. *Plant Physiology*, **143**, 78–87.

Fry, S.C., Smith, R.C., Renwick, K.F., Martin, D.J., Hodge, S.K. & Matthews, K.J. (1992) Xyloglucan endotransglycosylase, a new wall-loosening enzyme activity from plants. *Biochemical Journal*, **282**, 821–828.

Fuller, M.P., Hamed, F., Wisniewski, M. & Glenn, D.M. (2003) Protection of plants from frost using hydrophobic particle film and acrylic polymer. *Association of Appled Biologists*, **143**, 93–97.

Fuller, M.P. & Wisniewski, M. (1998) The use of infrared thermal imaging in the study of ice nucleation and freezing of plants. *Journal of Thermal Biology*, **23**, 81–89.

Gardiner, J.C., Taylor, N.G. & Turner, S.R. (2003) Control of Cellulose Synthase Complex Localization in Developing Xylem. *The Plant Cell*, **15**, 1740–1748.

Gardner, K.H. & Blackwell, J. (1974) The structure of native cellulose. *Biopolymers*, **13**, 1975–2001.

George, M.F. & Burke, M.J. (1976) The occurrence of deep supercooling in cold hardy plants. *Current Advances in Plant Science*, **22**, 349–360.

Georgelis, N., Nikolaidis, N. & Cosgrove, D.J. (2015) Bacterial expansins and related proteins from the world of microbes. *Applied Microbiology and Biotechnology*, **99**, 3807–3823.

Gilmour, S.J., Fowler, S.G. & Thomashow, M.F. (2004) Arabidopsis transcriptional activators CBF1, CBF2 and CBF3 have matching functional activities. *Plant Molceular Biology*, **54**, 767–781.

Gilmour, S.J., Zarka, D.G., Stockinger, E.J., Salazar, M.P., Houghton, J.M. & Thomashow, M.F. (1998) Low temperature regulation of the Arabidopsis CBF family of AP2 transcriptional activators as an early step in cold-induced COR gene expression. *The Plant Journal*, **16**, 433–442.

Goldbach, H.E. & Wimmer, M.A. (2007) Boron in plants and animals: Is there a role beyond cell-wall structure? *Journal of Plant Nutrition and Soil Science*, **170**, 39–48.

Goldbach, H.E., Yu, Q., Wingender, R., Schulz, M., Wimmer, M., Findeklee, P. & Baluska, F. (2001) Rapid response reactions of roots to boron deprivation. *Journal of Plant Nutrition and Soil Science*, **164**, 173–181.

Goldberg, R., Morvan, C. & Roland, J.C. (1986) Composition, Properties and Localisation of Pectins in Young and Mature Cells of the Mung Bean Hypocotyl. *Plant Cell Physiol.*, **27**, 417–429.

Goldberg, R. & Prat, R. (1982) Involvement of Cell-Wall Characteristics in Growth-Processes Along the Mung Bean Hypocotyl. *Plant and Cell Physiology*, **23**, 1145–1154.

Gonçalves, B., Maugarny-calès, A., Adroher, B., Cortizo, M., Borrega, N., Blein, T., Hasson, A., Gineau, E., Mouille, G., Laufs, P. & Arnaud, N. (2017) GDP-L-fucose is required for boundary definition in plants. *Journal of Experimental Botany*, **68**, 5801–5811.

González-Fontes, A., Rexach, J., Navarro-Gochicoa, M.T., Herrera-Rodríguez, M.B., Beato, V.M., Maldonado, J.M. & Camacho-Cristóbal, J.J. (2008) Is boron involved solely in structural roles in vascular plants? *Plant Signaling & Behavior*, **3**, 24–26.

Gonzalez-Guzman, M., Pizzio, G.A., Antoni, R., Vera-Sirera, F., Merilo, E., Bassel, G.W., Fernández, M.A., Holdsworth, M.J., Perez-Amador, M.A., Kollist, H. & Rodriguez, P.L. (2012) Arabidopsis PYR/PYL/RCAR Receptors Play a Major Role in Quantitative Regulation of Stomatal Aperture and Transcriptional Response to Abscisic Acid. *The Plant Cell*, **24**, 2483–2496.

Gordon-Kamm, W.J. & Steponkus, P.L. (1984a) Lamellar-to-hexagona-ll phase transitions in the plasma membrane of isolated protoplasts after freeze-induced dehydration. *Proceedings of the National Academy of Sciences of the United States of America*, **81**, 6373–6377.

Gordon-Kamm, W.J. & Steponkus, P.L. (1984b) The Influence of Cold Acclimation on the Behavior of the Plasma Membrane Following Osmotic Contraction of Isolated Protoplasts. *Protoplasma*, **123**, 161–173.

Gotow, K., Tanaka, K., Kondo, N., Kobayashi, K. & Syono, K. (1985) Light Activation of NADP-Malate Dehydrogenase in Guard Cell Protoplasts from Vicia faba L. *Plant Physiology*, **79**, 829–832.

Griffith, M., Ala, P., Yang, D.S.C., Hon, W. & Moffatt, B.A. (1992) Antifreeze Protein Produced Endogenously in. , 593–596.

Griffith, M., Lumb, C., Wiseman, S.B., Wisniewski, M., Johnson, R.W. & Marangoni, A.G. (2005) Antifreeze Proteins Modify the Freezing Process In Planta. *Plant Physiology*, **138**, 330–340.

Gronnier, J., Germain, V., Gouguet, P., Cacas, J.-L. & Mongrand, S. (2016) GIPC: Glycosyl Inositol Phospho Ceramides, the major sphingolipids on earth. *Plant Signaling & Behavior*, **11**, e1152438.

Gross, D.C., Proebsting, E.L. & Maccrindle-Zimmerman, H. (1988) Development, Distribution, and Characteristics of Intrinsic, Nonbacterial Ice Nuclei in Prunus Wood. *Plant Physiology*, **88**, 915–922.

Gu, L., Hanson, P.J., Post, W. Mac, Kaiser, D.P., Yang, B., Nemani, R., Pallardy, S.G. & Meyers, T. (2008) The 2007 Eastern US Spring Freeze: Increased Cold Damage in a Warming World? *BioScience*, **58**, 253–262.

Gusta, L. V., Burke, M.J. & Kapoor, A.C. (1975) Determination of Unfrozen Water in Winter Cereals at Subfreezing Temperatures. *Plant Physiology*, **56**, 707–709.

Gusta, L. V., Trischuk, R. & Weiser, C.J. (2005) Plant Cold Acclimation: The Role of Abscisic Acid. *Journal of Plant Growth Regulation*, **24**, 308–318.

Guy, C., Haskell, D. & Li, Q.-B. (1998) Association of Proteins with the Stress 70 Molecular Chaperones at Low Temperature: Evidence for the Existence of Cold Labile Proteins in Spinach. *Cryobiology*, **36**, 301–314.

Guy, C.L. & Li, Q.-B. (1998) The Organization and Evolution of the Spinach Stress 70 Molecular Chaperone Gene Family. *The Plant Cell*, **10**, 539–556.

Guy, C.L., Niemi, K.J. & Brambl, R. (1985) Altered gene expression during cold acclimation of spinach. *Proceedings of the National Academy of Sciences of the United States of America*, **82**, 3673–7.

Hadfield, K.A. & Bennett, A.B. (1998) Polygalacturonases: Many Genes in Search of a Function. *Plant Physiology*, **117**, 337–343.

Hannah, M.A., Heyer, A.G. & Hincha, D.K. (2005) A global survey of gene regulation during cold acclimation in Arabidopsis thaliana. *PLoS genetics*, **1**, 172–196.

Hansen, J. & Beck, E. (1988) Evidence for ideal and non-ideal equilibrium freezing of leaf water in frosthardy ivy (Hedera helix) and winter barley (Hordeum vulgare). *Botanica acta*, **101**, 76–82.

Hasson, A., Plessis, A., Blein, T., Adroher, B., Grigg, S., Tsiantis, M., Boudaoud, A., Damerval, C. & Laufs, P. (2011) Evolution and Diverse Roles of the CUP-SHAPED COTYLEDON Genes in Arabidopsis Leaf Development. *The Plant Cell*, **23**, 54–68.

Hayashi, T. (1989) Xyloglucans in the Primary Cell Wall. *Annual Review of Plant Physiology and Plant Molecular Biology*, **2**, 1–19.

Hayashi, T., Marsden, M.P.F. & Delmer, D.P. (1987) Pea Xyloglucan and Cellulose V. Xyloglucan-Cellulose Interactions In Vitro and In Vivo. *Plant Physiology*, **83**, 384–389.

Hayes, J.E. & Reid, R.J. (2004) Boron Tolerance in Barley Is Mediated by Efflux of Boron from the Roots. *Plant Physiology*, **136**, 3376–3382.

Heath, O.V.S. (1948) Control of Stomatal Movement by a Reduction in the Normal Carbon Dioxide Content of the Air. *Nature*, **161**, 179–181.

Heber, U., Schmitt, J.M., H., K.G., J., K.R. & A., S.K. (1981) Freezing damage to thylakoid membranes in vitro and in vivo. *Effects of Low Temperature on Biological Membranes* (eds G.J. Morris), & A. Clarke), pp. 264–287. Academic Press, London, New York.

Hemsley, P., Hurst, C.H., Kaliyadasa, E., Lamb, R., Knight, M.R., De Cothi, E., Steele, J.F. & Knight, H. (2014) The Arabidopsis mediator complex subunits MED16, MED14, and MED2 regulate mediator and RNA polymerase II recruitment to CBF-responsive cold-regulated genes. *The Plant cell*, **26**, 465–84.

van Hengel, A.J. & Roberts, K. (2002) Fucosylated arabinogalactan-proteins are required for full root cell elongation in arabidopsis. *The Plant Journal*, **32**, 105–113.

Hetherington, A.M. (2001) Guard Cell Signaling. *Cell*, **107**, 711–714.

Hetherington, A.M. & Woodward, F.I. (2003) The role of stomata in sensing and driving environmental change. *Nature*, **424**, 901–908.

Hincha, D.K., Heber, U. & Schmitt, J.M. (1990) Proteins from frost-hardy leaves protect thylakoids against mechanical freeze-thaw damage in vitro. *Planta*, **180**, 416–419.

Hirano, S.S. & Upper, C.D. (2000) Bacteria in the Leaf Ecosystem with Emphasis on Pseudomonas syringae - a Pathogen, Ice Nucleus, and Epiphyte. *Microbiology and Molecular Biology Reviews*, **64**, 624–653.

Hocq, L., Pelloux, J. & Lefebvre, V. (2017) Connecting Homogalacturonan-Type Pectin Remodelling to Acid Growth. *Trends in Plant Science*, **22**, 20–29.

Höfte, H. & Voxeur, A. (2017) Plant cell walls. *Current Biology*, **27**, R865–R870.

Homshaw, L.G. (1980) Freezing and melting temperature hysteresis of water in porous materials: Application to the study of pore form. *European Journal of Soil Science*, **31**, 399–414.

Hooke, R. (1665) *Micrographia: Some Physiological Descriptions of Minute Bodies Made by Magnifying Glasses. With Observations and Inquiries Thereupon*. The Royal Society, Great Britain.

Hosy, E., Vavasseur, A., Mouline, K., Dreyer, I., Gaymard, F., Poree, F., Boucherez, J., Lebaudy, A., Bouchez, D., Very, A.-A., Simonneau, T., Thibaud, J.-B. & Sentenac, H. (2003) The Arabidopsis outward K+ channel GORK is involved in regulation of stomatal movements and plant transpiration. *Proceedings of the National Academy of Sciences of the United States of America*, **100**, 5549–5554.

House, C.R. (1974) *Water Transport in Cells and Tissues*. Edward Arnold, London, UK.

Houston, K., Tucker, M.R., Chowdhury, J., Shirley, N. & Little, A. (2016) The Plant Cell Wall: A Complex and Dynamic Structure As Revealed by the Responses of Genes under Stress Conditions. *Frontiers in Plant Science*, **7**, 1–18.

Hu, H. & Brown, P.H. (1994) Localization of Boron in Cell Walls of Squash and Tobacco and Its Association with Pectin. *Plant Physiology*, **105**, 681–689.

Hu, H. & Brown, P.H. (1997) Absorption of boron by plant roots. *Plant and Soil*, **193**, 49–58.

Huang, Y.-C., Wu, H.-C., Wang, Y.-D., Liu, C.-H., Lin, C.-C., Luo, D.-L. & Jinn, T.-L. (2017) PECTIN METHYLESTERASE34 Contributes to Heat Tolerance through Its Role in Promoting Stomatal Movement. *Plant Physiology*, **174**, 748–763.

Hudson, M.A. & Idle, D.B. (1962) The Formation of Ice in Plant Tissues. *Planta*, **57**, 718–730.

Huner, N.P.A., Palta, J.P., Li, P.H. & Carter, J. V. (1981) Anatomical Changes in Leaves of Puma Rye in Response to Growth at Cold-Hardening Temperatures. *Botanical Gazette*, **142**, 55–62.

Inaba, M., Suzuki, I., Szalontai, B., Kanesaki, Y., Los, D.A., Hayashi, H. & Murata, N. (2003) Gene-engineered Rigidification of Membrane Lipids Enhances the Cold Inducibility of Gene Expression in Synechocystis. *The Journal of Biological Chemistry*, **278**, 12191–12198.

Ishii, T. (1997) O-Acetylated Oligosaccharides from Pectins of Potato Tuber Cell Walls. *Plant Physiology*, **113**, 1265–1272.

Ishii, T. & Matsunaga, T. (1996) Isolation and characterization of a boron-rhamnogalacturonan-II complex from cell walls of sugar beet pulp. *Carbohydrate Research*, **284**, 1–9.

Ishii, T. & Matsunaga, T. (2001) Pectic polysaccharide rhamnogalacturonan II is covalently linked to homogalacturonan. *Phytochemistry*, **57**, 969–974.

Ishii, T., Matsunaga, T. & Hayashi, N. (2001a) Formation of Rhamnogalacturonan II-Borate Dimer in Pectin Determines Cell Wall Thickness of Pumpkin Tissue. *Plant Physiology*, **126**, 1698–1705.

Ishii, T., Matsunaga, T. & Hayashi, N. (2001b) Formation of Rhamnogalacturonan II-Borate Dimer in Pectin Determines Cell Wall Thickness of Pumpkin Tissue. *Plant Physiology*, **126**, 1698–1705.

Ishii, T., Matsunaga, T., Pellerin, P., O'Neill, M.A., Darvill, A. & Albersheim, P. (1999) The Plant Cell Wall Polysaccharide Rhamnogalacturonan II Self-assembles into a Covalently Cross-linked Dimer. *The Journal of Biological Chemistry*, **274**, 13098–13104.

Jaglo-Ottosen, K.R., Gilmour, S.J., Zarka, D.G., Schabenberger, O. & Thomashow, M.F. (1998) Arabidopsis CBF1 Overexpression Induces COR Genes and Enhances Freezing Tolerance. *Science*, **280**, 104–107.

Janská, A., Aprile, A., Zámečník, J., Cattivelli, L. & Ovesná, J. (2011) Transcriptional responses of winter barley to cold indicate nucleosome remodelling as a specific feature of crown tissues. *Functional and Integrative Genomics*, **11**, 307–325.

Jarvis, M.C. (1984) Structure and properties of pectin gels in plant cell walls. *Plant, Cell and Environment*, **7**, 153–164.

Jezek, M. & Blatt, M.R. (2017) The Membrane Transport System of the Guard Cell and Its Integration for Stomatal Dynamics. *Plant Physiology*, **174**, 487–519.

Ji, H., Wang, Y., Cloix, C., Li, K., Jenkins, G.I., Wanf, S., Shang, Z., Shi, Y., Yang, S. & Li, X. (2015a) The Arabidopsis RCC1 Family Protein TCF1 Regulates Freezing Tolerance and Cold Acclimation through Modulating Lignin Biosynthesis. *PLOS Genetics*, 1–25.

Ji, H., Wang, Y., Cloix, C., Li, K., Jenkins, G.I., Wang, S., Shang, Z., Shi, Y., Yang, S. & Li, X. (2015b) The Arabidopsis RCC1 Family Protein TCF1 Regulates Freezing Tolerance and Cold Acclimation through Modulating Lignin Biosynthesis. *PLOS Genetics*, 1–25.

Jones, H.G. (1999) Use of thermography for quantitative studies of spatial and temporal variation of stomatal conductance over leaf surfaces. *Plant, Cell and Environment*, **22**, 1043–1055.

Jones, L., Milne, J.L., Ashford, D., McCann, M.C. & McQueen-Mason, S.J. (2005) A conserved functional role of pectic polymers in stomatal guard cells from a range of plant species. *Planta*, **221**, 255–264.

Jones, L., Milne, J.L., Ashford, D. & McQueen-Mason, S.J. (2003) Cell wall arabinan is essential for guard cell function. *PNAS*, **100**, 11783–11788.

Kaewthai, N., Gendre, D., Eklof, J.M., Ibatullin, F.M., Ezcurra, I., Bhalerao, R.P. & Brumer, H. (2013) Group III-A XTH Genes of Arabidopsis Encode Predominant Xyloglucan Endohydrolases That Are Dispensable for Normal Growth. *Plant Physiology*, **161**, 440–454.

Kaku, S. (1973) High ice nucleating ability in plant leaves. *Plant and Cell Physiol.*, **14**, 1035–1038.

Kaneko, S., Ishii, T. & Matsunaga, T. (1997) A BORON-RHAMNOGALACTURONAN-II COMPLEX FROM BAMBOO SHOOT CELL WALLS. *Phytochemistry*, **44**, 243–248.

Kendall, E.J. & McKersie, B.D. (1989) Free radical and freezing injury to cell membranes of winter wheat. *Physiologia Plantarum*, **76**, 86–94.

Keys, A.J., Sampaio, E.V.S.B., Cornelius, M.J. & Bird, I.F. (1977) Effect of Temperature on Photosynthesis and Photorespiration of Wheat Leaves. *Journal of Experimental Botany*, **28**, 525–533.

Kimura, S., Laosinchai, W., Itoh, T., Cui, X., Linder, C.. R. & Brown Jr., R.M. (1999) Immunogold Labeling of Rosette Terminal Cellulose-Synthesizing Complexes in the Vascular Plant Vigna angularis. *The Plant Cell*, **11**, 2075–2085.

Kinoshita, T., Nishimura, M. & Shimazaki, K. (1995) Cytosolic Concentration of Ca2+ Regulates the Plasma Membrane H+-ATPase in Guard Cells of Fava Bean. *The Plant Cell*, **7**, 1333–1342.

Klusener, B., Young, J.J., Murata, Y., Allen, G.J., Mori, I.C., Hugouvieux, V. & Schroeder, J.I. (2002) Convergence of Calcium Signaling Pathways of Pathogenic Elicitors and Abscisic Acid in Arabidopsis. *Plant Physiology*, **130**, 2152–2163.

Knight, M.R., Campbell, A.M., Smith, S.M. & Trewavas, A.J. (1991) Transgenic plant aequorin reports the effects of touch and cold-shock and elicitors on cytoplasmic calcium. *Nature*, **352**, 524–526.

Knight, M.R. & Knight, H. (2012) Low-temperature perception leading to gene expression and cold tolerance in higher plants. *New Phytologist*, **195**, 737–751.

Knight, H., Mugford, S.G., Ulker, B., Gao, D., Thorlby, G. & Knight, M.R. (2009) Identification of SFR6, a key component in cold acclimation acting post-translationally on CBF function. *The Plant journal : for cell and molecular biology*, **58**, 97–108.

Knight, H., Trewavas, A.J. & Knighta, M.R. (1996) Cold Calcium Signaling in Arabidopsis lnvolves Two Cellular Pools and a Change in Calcium Signature after Acclimation. , **8**, 489–503.

Knight, H., Veale, E.L., Warren, G.J. & Knight, M.R. (1999) The sfr6 Mutation in Arabidopsis Suppresses Low-Temperature Induction of Genes Dependent on the CRT / DRE Sequence Motif. , **11**, 875–886.

Knight, H., Zarka, D.G., Okamoto, H., Thomashow, M.F. & Knight, M.R. (2004) Abscisic Acid Induces CBF Gene Transcription and Subsequent Induction of Cold-Regulated Genes via the CRT Promoter Element. *Plant Physiology*, **135**, 1710–1717.

Knox, J.P. (2008) Revealing the structural and functional diversity of plant cell walls. *Current Opinion in Plant Biology*, **11**, 308–313.

Kobayashi, M., Matoh, T. & Azuma, J. (1996) Two Chains of Rhamnogalacturonan II Are Cross-Linked by Borate-Diol Ester Bonds in Higher Plant Cell Walls. *Plant Physiology*, **110**, 1017–1020.

Kollist, H., Nuhkat, M. & Roelfsema, M.R.G. (2014) Closing gaps: linking elements that control stomatal movement. *New Phytologist*, **203**, 44–62.

Kubacka-Zebalska, M. & Kacperska, A. (1999) Low temperature-induced modifications of cell wall content and polysaccharide composition in leaves of winter oilseed rape (Brassica napus L. var. oleifera L.). *Plant Science*, **148**, 59–67.

Kuprian, E., Briceno, V.F., Wagner, J. & Neuner, G. (2014) Ice barriers promote supercooling and prevent frost injury in reproductive buds , flowers and fruits of alpine dwarf shrubs throughout the summer. *Environmental and Experimental Botany*, **106**, 4–12.

Kuznetsova, A., Brockhoff, P.B. & Christensen, R.H.B. (2016) lmerTest: Tests in Linear Mixed Effects Models.

Lau, J.M., McNeil, M., Darvill, A.G. & Albersheim, P. (1985) Structure of the Backbone of Rhamnogalacturonan I, a Pectic Polysaccharide in the Primary Cell Walls of Plants. *Carbohydrate Research*, **137**, 111–125.

Lawson, T. & Blatt, M.R. (2014) Stomatal Size, Speed, and Responsiveness Impact on Photosynthesis and Water Use Efficiency. *Plant Physiology*, **164**, 1556–1570.

Lawson, T. & Vialet-Chabrand, S. (2018) Speedy stomata, photosynthesis and plant water use efficiency. *New Phytologist*.

Lee, K.J.D., Marcus, S.E. & Knox, J.P. (2011) Cell Wall Biology: Perspectives from Cell Wall Imaging. *Molecular Plant*, **4**, 212–219.

Lefebvre, V., Fortabat, M.N., Ducamp, A., North, H.M., Maia-Grondard, A., Trouverie, J., Boursiac, Y., Mouille, G. & Durand-Tardif, M. (2011) ESKIMO1 disruption in Arabidopsis alters vascular tissue and impairs water transport. *PLoS ONE*, **6**.

Lendzian, K.J. & Kerstiens, G. (1991) Sorption and transport of gases and vapours in plant cuticles. *Reviews of Environmental Contamination and Toxicology*, **121**, 65–128.

Lennon, K.A. & Lord, E.M. (2000) In vivo pollen tube cell of Arabidopsis thaliana I. Tube cell cytoplasm and wall. *Protoplasma*, **214**, 45–56.

Lenth, R. V. (2016) Least-Squares Means: The R Package lsmeans. *Journal of Statistical Software*, **69**, 1–33.

Levitt, J. (1941) *Frost Killing and Hardiness of Plants*. Burgess Publishing Company, Minneapolis.

Levitt, J. (1956) *The Hardiness of Plants*. Academic Press, New York.

Levitt, J. (1980) *Responses of Plants to Environmental Stresses I: Chilling, Freezing and High Temperature Stresses*, 2nd Editio. Academic Press.

Levy, S., Maclachlan, G. & Staehelin, L.A. (1997) Xyloglucan sidechains modulate binding to cellulose during in vitro binding assays as predicted by conformational dynamics simulations. *The Plant Journal*, **11**, 373–386.

Lewis, B.D. & Spalding, E.P. (1998) Membrane Biology Nonselective Block by La3+ of Arabidopsis Ion Channels Involved in Signal Transduction. *The Journal of Membrane Biology*, **90**, 81–90.

Li, S., Assmann, S.M. & Albert, R. (2006) Predicting Essential Components of Signal Transduction Networks: A Dynamic Model of Guard Cell Abscisic Acid Signaling. *PLoS Biology*, **4**, e312.

Li, S., Bashline, L., Zheng, Y., Xin, X., Huang, S., Kong, Z., Kim, S.H., Cosgrove, D.J. & Gu, Y. (2016a) Cellulose synthase complexes act in a concerted fashion to synthesize highly aggregated cellulose in secondary cell walls of plants. *PNAS*, **113**, 11348–11353.

Li, Q., Liu, Y., Pan, Z., Xie, S. & Peng, S. (2016b) Boron deficiency alters root growth and development and interacts with auxin metabolism by influencing the expression of auxin synthesis and transport genes. *Biotechnology & Biotechnological Equipment*, **30**, 661–668.

Liang, Y., Xie, X., Lindsay, S.E., Wang, Y.B., Masle, J., Williamson, L., Leyser, O. & Hetherington, A.M. (2010) Cell wall composition contributes to the control of transpiration efficiency in Arabidopsis thaliana. *The Plant Journal*, **64**, 679–686.

Lindow, S.E., Arny, D.C. & Upper, C.D. (1982) Bacterial Ice Nucleation: A Factor in Frost Injury to Plants. *Plant Physiology*, **70**, 1084–1089.

Lintunen, A., Holtta, T. & Kulmala, M. (2013) Anatomical regulation of ice nucleation and cavitation helps tress to survive freezing and drought stress. *Scientific Reports*, **3**, 1–7.

Liu, G., Dong, X., Liu, L., Wu, L., Peng, S. & Jiang, C. (2014) Boron deficiency is correlated with changes in cell wall structure that lead to growth defects in the leaves of navel orange plants. *Scientia Horticulturae*, **176**, 54–62.

Liu, Q., Kasuga, M., Sakuma, Y., Abe, H., Miura, S., Yamaguchi-Shinozaki, K. & Shinozaki, K. (1998) Two Transcription Factors, DREB1 and DREB2, with an EREBP/AP2 DNA Binding Domain Separate Two Cellular Signal Transduction Pathways in Drought- and Low- Temperature-Responsive Gene Expression, Respectively, in Arabidopsis. *The Plant Cell*, **10**, 1391–1406.

Liu, X.-L., Liu, L., Niu, Q.-K., Xia, C., Yang, K.-Z., Li, R., Chen, L.-Q., Zhang, X.-Q., Zhou, Y. & Ye, D. (2011) MALE GAMETOPHYTE DEFECTIVE 4 encodes a rhamnogalacturonan II xylosyltransferase and is important for growth of pollen tubes and roots in Arabidopsis. *The Plant Journal*, **65**, 647–660.

Livingston III, D.P. & Henson, C.A. (1998) Apoplastic Sugars, Fructans, Fructan Exohydrolase, and Invertase in Winter Oat: Responses to Second-Phase Cold Hardening. *Plant Physiology*, **116**, 403–408.

Loomis, W.D. & Durst, R.W. (1992) Chemistry and Biology of Boron. *Biofactors*, **3**, 229–239.

Lynch, D. V. & Steponkus, P.L. (1987) Plasma Membrane Lipid Alterations Associated with Cold Acclimation of Winter Rye Seedlings (Secale cereale L. cv Puma). *Plant Physiology*, **83**, 761–7.

Lyons, J.M. (1973) CHILLING INJURY IN PLANTS. *Annual Review of Plant Physiology*, **24**, 445–466.

Maercker, U. (1965) Mikroautoradiographischer Nachweis tritiumhaltigen Transpirationswassers. *Naturwissenschaften*, **52**, 15–16.

Majewska-Sawka, A., Mu, A. & Rodriguez-Garcia, M.I. (2002) Guard cell wall: immunocytochemical detection of polysaccharide components. *Journal of Experimental Botany*, **53**, 1067–1079.

Maki, L.R., Galyan, E.L., Chang-Chien, M.-M. & Caldwell, D.R. (1974) Ice Nucleation Induced by Pseudomonas syringae. *Applied Microbiology*, **28**, 456–459.

Marx-Figini, M. (1966) Comparison of the Biosynthesis of Cellulose in vitro and in vivo in Cotton Bolls. *Nature*, **210**, 754–755.

Matoh, T., Ishigaki, K.I., Ohno, K. & Azuma, J.-I. (1993) Isolation and Characterization of a Boron-Polysaccharide Complex from Radish Roots. *Plant and Cell Physiology*, **34**, 639–642.

Matoh, T., Kawaguchi, S. & Kobayashi, M. (1996) Ubiquity of a Borate-Rhamnogalacturonan II Complex in the Cell Walls of Higher Plants. *Plant Cell Physiology*, **37**, 636–640.

Matoh, T., Takasaki, M., Takabe, K. & Kobayashi, M. (1998) Immunocytochemistry of Rhamnogalacturonan II in Cell Walls of Higher Plants. *Plant Cell Physiology*, **39**, 483–491.

Matsunaga, T., Ishii, T., Matsumoto, S., Higuchi, M., Darvill, A., Albersheim, P. & O'Neill, M.A. (2004) Occurrence of the Primary Cell Wall Polysaccharide Rhamnogalacturonan II in Pteridophytes, Lycophytes, and Bryophytes. Implications for the Evolution of Vascular Plants. *Plant Physiology*, **134**, 339–351.

Mazeau, K. & Perez, S. (1998) The preferred conformations of the four oligomeric fragments of Rhamnogalacturonan II. *Carbohydrate Research*, **311**, 203–217.

Mazur, P. (1963) Kinetics of Water Loss from Cells at Subzero Temperatures and the Likelihood of Intracellular Freezing. *The Journal of General Physiology*, **47**, 347–369.

Mazur, P. (1965) The role of cell membranes in the freezing of yeast and other single cells. *Annals*

of the New York Academy of Sciences, **125**, 65–676.

Mcausland, L., Vialet-Chabrand, S., Davey, P., Baker, N.R., Brendel, O. & Lawson, T. (2016) Effects of kinetics of light-induced stomatal responses on photosynthesis and water-use efficiency. *New Phytologist*, **211**, 1209–1220.

Mccann, M.C., Wells, B. & Roberts, K. (1990) Direct visualization of cross-links in the primary plant cell wall. *Journal of Cell Science*, **96**, 323–334.

Mckersie, B.D., Chen, Y., de Beus, M., Bowley, S.R., Bowler, C., Inzé, D., D'Halluin, K. & Botterman, J. (1993) Superoxide Dismutase Enhances Tolerance of Freezing Stress in Transgenic Alfalfa (Medicago safiva L.). *Plant Physiology*, **103**, 1155–1163.

McNeil, M., Darvill, A.G., Fry, S.C. & Albersheim, P. (1984) Structure and function of the primary cell walls of plants. *Annual Review of Biochemistry*, **53**, 625–663.

Meents, M.J., Watanabe, Y. & Samuels, A.L. (2018) The cell biology of secondary cell wall biosynthesis. *Annals of Botany*, **121**, 1107–1125.

Merlot, S., Mustilli, A.-C., Genty, B., North, H., Lefebvre, V., Sotta, B., Vavasseur, A. & Giraudat, J. (2002) Use of infrared thermal imaging to isolate Arabidopsis mutants defective in stomatal regulation. *The Plant Journal*, **30**, 601–609.

Miura, K., Jin, J.B., Lee, J., Yoo, C.Y., Stirm, V., Miura, T., Ashworth, E.N., Bressan, R.A., Yun, D.-J. & Hasegawa, P.M. (2007) SIZ1-Mediated Sumoylation of ICE1 Controls CBF3/DREB1A Expression and Freezing Tolerance in Arabidopsis. *The Plant Cell*, **19**, 1403–1414.

Miwa, K., Takano, J., Omori, H., Seki, M., Shinozaki, K. & Fujiwara, T. (2007) Plants Tolerant of High Boron Levels. *Science*, **318**, 1417.

Miwa, K., Wakuta, S., Takada, S., Ide, K., Takano, J., Naito, S., Omori, H., Matsunaga, T. & Fujiwara, T. (2013) Roles of BOR2, a boron exporter, in cross linking of rhamnogalacturonan II and root elongation under boron limitation in Arabidopsis. *Plant physiology*, **163**, 1699–709.

Modlibowska, I. & Rogers, W.S. (1955) Freezing of Plant Tissues under the Microscope. *Journal of Experimental Botany*, **6**, 384–391.

Moellering, E.R., Muthan, B. & Benning, C. (2010) Freezing Tolerance in Plants Requires Lipid Remodeling at the Outer Chloroplast Membrane. *Science*, **330**, 226–228.

Moffat, C.S., Ingle, R.A., Wathugala, D.L., Saunders, N.J., Knight, H. & Knight, M.R. (2012) ERF5 and ERF6 Play Redundant Roles as Positive Regulators of JA/Et-Mediated Defense against Botrytis cinerea in Arabidopsis. *PLoS ONE*, **7**, e35995.

Mohl, H. V. (1856) Welches ursachen bewirken die erweiterung und veregung fer spaltoeffnungen. *Bot. Z.*, **14**, 713–721.

Mohnen, D. (2008) Pectin structure and biosynthesis. *Current Opinion in Plant Biology*, **11**, 266–277.

Molisch, H. (1897) *Untersuchungen Uber Das Erfrieren Der Pflanzen*. Fischer, Jena.

Monroy, A.F. & Dhindsa, R.S. (1995) LowTemperature Signal Transduction: lnduction of Cold Acclimation-Specific Genes of Alfalfa by Calcium at 25°C. *The Plant Cell*, **7**, 321–331.

Moore, J.P., Farrant, J.M. & Driouich, A. (2008) A role for pectin-associated arabinans in maintaining the flexibility of the plant cell wall during water deficit stress. *Plant Signaling & Behavior*, **3**, 102–104.

Moore, P.J. & Staehelin, L.A. (1988) Immunogold localization of the cell- wall-matrix polysaccharides rhamnogalacturonan I and xyloglu- can during cell expansion and cytokinesis cytokinesis inTrifolium pratense L.; implication for secretory pathways. *Planta*, **174**, 433–445.

Muhlung, K.H., Wimmer, M. & Goldbach, H.E. (1998) Apoplastic and membrane-associated Ca in leaves and roots as affected by boron deficiency. *Physiologia Plantarum*, **102**, 179–184.

Murai, M. & Yoshida, S. (1998a) Vacuolar membrane lesions induced by a freeze-thaw cycle in protoplasts isolated from deacclimated tubers of Jerusalem artichoke (Helianthus tuberosus L.). *Plant and Cell Physiology*, **39**, 87–96.

Murai, M. & Yoshida, S. (1998b) Evidence for the Cell Wall Involvement in Temporal Changes in Freezing Tolerance of Jerusalem Artichoke (Helianthus tuberosus L.) Tubers during Cold Acclimation. *Plant Cell Physiology*, **39**, 97–105.

Murata, N. & Los, D.A. (1997) Membrane Fluidity and Temperature Perception. *Plant Physiology*, **115**, 875–879.

Murata, Y., Pei, Z.-M., Mori, I.C. & Schroeder, J. (2001) Abscisic Acid Activation of Plasma Membrane Ca2+ Channels in Guard Cells Requires Cytosolic NAD(P)H and Is Differentially Disrupted Upstream and Downstream of Reactive Oxygen Species Production in abi1-1 and abi2-1 Protein Phosphatase 2C Mutants. *The Plant Cell*, **13**, 2513–2523.

Nable, R.O., Banuelos, G.S. & Paull, J.G. (1997) Boron toxicity. *Plant and Soil*, **193**, 181–198.

Nagao, M., Arakawa, K., Takezawa, D. & Fujikawa, S. (2008) Long- and short-term freezing induce different types of injury in Arabidopsis thaliana leaf cells. *Planta*, **227**, 477–489.

Ndeh, D., Rogowski, A., Cartmell, A., Luis, A.S., Baslé, A., Gray, J., Venditto, I., Briggs, J., Zhang, X., Labourel, A., Terrapon, N., Buffetto, F., Nepogodiev, S., Xiao, Y., Field, R.A., Zhu, Y., O'Neill, M.A., Urbanowicz, B.R., York, W.S., Davies, G.J., Abbott, D.W., Ralet, M.-C., Martens, E.C., Henrissat, B. & Gilbert, H.J. (2017) Complex pectin metabolism by gut bacteria reveals novel catalytic functions. *Nature*, **544**, 65–70.

Ninagawa, T., Eguchi, A., Kawamura, Y., Konishi, T. & Narumi, A. (2016) A study on ice crystal formation behavior at intracellular freezing of plant cells using a high-speed camera. *Cryobiology*, **73**, 20–29.

Noguchi, K., Ishii, T., Matsunaga, T., Kakegawa, K., Hayashi, H. & Fujiwara, T. (2003) Biochemical properties of the cell wall in the Arabidopsis mutant bor1-1 in relation to boron nutrition. *Journal of Plant Nutrition and Soil Science*, **166**, 175–178.

Noguchi, K., Yasumori, M., Imai, T., Naito, S., Matsunaga, T., Oda, H., Hayashi, H., Chino, M. & Fujiwara, T. (1997) bor1-1, an Arabidopsis thaliana Mutant That Requires a High Level of Boron. *Plant Physiology*, **115**, 901–906.

Notman, R., Noro, M., O'Malley, B. & Anwar, J. (2006) Molecular Basis for Dimethylsulfoxide (DMSO) Action on Lipid Membranes. *Journal of the American Chemical Society*, **128**, 13982–13983.

Novillo, F., Alonso, J.M., Ecker, J.R. & Salinas, J. (2004) CBF2/DREB1C is a negative regulator of CBF1/DREB1B and CBF3/DREB1A expression and plays a central role in stress tolerance in Arabidopsis. *Proceedings of the National Academy of Sciences of the United States of America*, **101**, 3985–3990.

Novillo, F., Medina, J. & Salinas, J. (2007) Arabidopsis CBF1 and CBF3 have a different function than CBF2 in cold acclimation and define different gene classes in the CBF regulon. *Proceedings of the National Academy of Sciences of the United States of America*, **104**, 21002–21007.

O'Neill, M.A., Eberhard, S., Albersheim, P. & Darvill, A.G. (2001) Requirement of Borate Cross-Linking of Cell Wall Rhamnogalacturonan II for Arabidopsis Growth. *Science*, **294**, 846–849.

O'Neill, M.A., Ishii, T., Albersheim, P. & Darvill, A.G. (2004) RHAMNOGALACTURONAN II: Structure and Function of a Borate Cross-Linked Cell Wall Pectic Polysaccharide. *Annual Review of Plant Biology*, **55**, 109–139.

O'Neill, M.A., Warrenfeltz, D., Kates, K., Pellerin, P., Doco, T., Darvill, A.G. & Albersheim, P. (1996) Rhamnogalacturonan-II, a pectic polysaccharide in the walls of growing plant cell, forms a dimer that is covalently cross-linked by a borate ester. In vitro conditions for the formation and hydrolysis of the dimer. *Journal of Biological Chemistry*, **271**, 22923–22930.

Oakenfull, R.J., Baxter, R. & Knight, M.R. (2013) A C-Repeat Binding Factor Transcriptional Activator (CBF/DREB1) from European Bilberry (Vaccinium myrtillus) Induces Freezing Tolerance When Expressed in Arabidopsis thaliana. *PLOS ONE*, **8**, e54119.

Olien, C.R. & Smith, M.N. (1977) Ice Adhesions in Relation to Freeze Stress. *Plant Physiology*, **60**, 499–503.

Olien, C.R. & Smith, M.N. (1981) Protective systems that have evolved in plants. *Analysis and Improvement of Plant Cold Hardiness* (eds C.R. Olien), & M.N. Smith), pp. 61–87. Boca Raton: CRC Press.

Oparka, K.J. (1994) Plasmolysis: new insights into an old process. *New Phytologist*, **126**, 571–591.

Ortega, J.K.E. (2017) Dimensionless number is central to stress relaxation and expansive growth of the cell wall. *Scientific Reports*, **7**, 1–16.

Orvar, B.L., Sangwan, V., Omann, F. & Dhindsa, R.S. (2000) Early steps in cold sensing by plant cells: the role of actin cytoskeleton and membrane fluidity. *The Plant Journal*, **23**, 785–794.

Özparpucu, M., Rüggeberg, M., Gierlinger, N., Cesarino, I., Vanholme, R., Boerjan, W. & Burgert, I. (2017) Unravelling the impact of lignin on cell wall mechanics: a comprehensive study on young poplar trees downregulated for CINNAMYL ALCOHOL DEHYDROGENASE (CAD). *Plant Journal*, **91**, 480–490.

Pabst, M., Fischl, R.M., Brecker, L., Morelle, W., Fauland, A., Kofeler, H., Altmann, F. & Leonard, R. (2013) Rhamnogalacturonan II structure shows variation in the side chains monosaccharide composition and methylation status within and across different plant species. *The Plant Journal*, **76**, 61–72.

Pantin, F., Monnet, F., Jannaud, D., Costa, J.M., Renaud, J., Muller, B., Simonneau, T. & Genty, B. (2013) The dual effect of abscisic acid on stomata. *New Phytologist*, **197**, 65–72.

Pattathil, S., Avci, U., Baldwin, D., Swennes, A.G., Mcgill, J.A., Bootten, T., Albert, A., Davis, R.H., Chennareddy, C., Dong, R., O'Shea, B., Rossi, R., Leoff, C., Freshour, G., Narra, R., O'Neill, M.A., York, W.S. & Hahn, M.G. (2010) A Comprehensive Toolkit of Plant Cell Wall. *Plant Physiology*, **153**, 514–525.

Pauly, M., Gille, S., Liu, L., Mansoori, N., de Souza, A., Schultik, A. & Xiong, G. (2013) Hemicellulose biosynthesis. *Planta*, **238**, 627–642.

Pauly, M. & Keegstra, K. (2016) Biosynthesis of the Plant Cell Wall Matrix Polysaccharide Xyloglucan. *Annual Review of Plant Biology*, **67**, 235–259.

Pearce, R.S. (1988) Extracellular ice and cell shape in frost-stressed cereal leaves: A low-temperature scanning-electron-microscopy study. *Planta*, **175**, 313–324.

Pearce, R.S. (2001) Plant Freezing and Damage. *Annals of Botany*, **87**, 417–424.

Pearce, R.S. & Ashworth, E.N. (1992) Cell-shape and localisation of ice in leaves of overwintering wheat during frost stress in the field. *Planta*, **188**, 324–331.

Pearce, R.S. & Fuller, M.P. (2001) Freezing of Barley Studied by Inrared Video Thermography. *Plant Physiology*, **125**, 227–240.

Pearce, R.S. & Willison, J.H.M. (1985) A freeze-etch study of the effects of extracellular freezing on cellular membranes of wheat. *Planta*, **163**, 304–316.

Peaucelle, A., Braybrook, S.A., Guillou, L. Le, Bron, E., Kuhlemeier, C. & Hofte, H. (2011) Pectin-Induced Changes in Cell Wall Mechanics Underlie Organ Initiation in Arabidopsis. *Current Biology*, **21**, 1720–1726.

Peier, A.M., Moqrich, A., Hergarden, A.C., Reeve, A.J., Andersson, D.A., Story, G.M., Earley, T.J., Dragoni, I., McIntyre, P., Bevan, S. & Patapoutian, A. (2002) A TRP Channel that Senses Cold Stimuli and Menthol. *Cell*, **108**, 705–715.

Pellerin, P., Doco, T., Vidal, S., Williams, P., Brillouet, J.-M. & O'Neill, M.A. (1996) Structural characterization of red wine rhamnogalacturonan II. *Carbohydrate Research*, **290**, 183–197.

Pelloux, J., Rustérucci, C. & Mellerowicz, E.J. (2007) New insights into pectin methylesterase structure and function. *Trends in Plant Science*, **12**, 267–277.

Penfield, S. (2008) Temperature perception and signal transduction in plants. *New Phytologist*, **179**, 615–628.

Perrin, R.M. (2003) Analysis of Xyloglucan Fucosylation in Arabidopsis. *Plant Physiology*, **132**, 768–778.

Perrin, R.M., DeRocher, A.E., Bar-Peled, M., Zeng, W., Norambuena, L., Orellana, A., Raikhel, N. V. & Keegstra, K. (1999) Xyloglucan Fucosyltransferase, an Enzyme Involved in Plant Cell Wall Biosynthesis. *Science*, **284**, 1976–1980.

Petersen, B.L., Egelund, J., Damager, I., Faber, K., Jensen, J.K., Yang, Z., Bennett, E.P., Scheller, H.V. & Ulvskov, P. (2009) Assay and heterologous expression in Pichia pastoris of plant cell wall type-II membrane anchored glycosyltransferases. *Glycoconj J*, **26**, 1235–1246.

Philippe, F., Pelloux, J. & Rayon, C. (2017) Plant pectin acetylesterase structure and function: New insights from bioinformatic analysis. *BMC Genomics*, **18**, 1–18.

Phyo, P., Wang, T., Kiemle, S.N., O'Neill, H., Pingali, S.V., Hong, M. & Cosgrove, D.J. (2017) Gradients in wall mechanics and polysaccharides along growing inflorescence stems. *Plant Physiology*, **175**, pp.01270.2017.

Pinneh, E. (2017) *Targeting a Promising New Herbicide Mode of Action: Chemical and Genetic Approaches to Elucidate the Role of PIC Synthase in Plants*. Durham University.

Plieth, C. (1999) Temperature Sensing by Plants: Calcium-Permeable Channels as Primary Sensors - A Model. *The Journal of Membrane Biology*, **172**, 121–127.

Popper, Z.A. & Fry, S.C. (2008) Xyloglucan-pectin linkages are formed intra-protoplasmically, contribute to wall-assembly, and remain stable in the cell wall. *Planta*, **227**, 781–794.

Proseus, T.E. & Boyer, J.S. (2005) Turgor Pressure Moves Polysaccharides into Growing Cell Walls of Chara corallina. *Annals of Botany*, **95**, 967–979.

R-Core-Team. (2016) R: A language and environment for statistical computing.

Räisänen, M., Repo, T. & Lehto, T. (2007) Cold acclimation was partially impaired in boron deficient Norway spruce seedlings. *Plant and Soil*, **292**, 271–282.

Raisanen, M., Repo, T., Rikala, R. & Lehto, T. (2006) Does ice crystal formation in buds explain growth disturbances in boron-deficient Norway spruce? *Trees*, **20**, 441–448.

Rajashekar, C.B. & Burke, M.J. (1982) Liquid water during slow freezing based on cell water relations and limited experimental testing. *Plant Cold Hardiness and Freezing Stress, Vol 11* (eds H. Li, P), & A. Sakai), pp. 211–220. Academic Press, New York.

Rajashekar, C.B. & Burke, M.J. (1996) Freezing Characteristics of Rigid Plant Tissues: Development of Cell Tension during Extracellular Freezing. *Plant Physiology*, **111**, 597–603.

Rajashekar, C.B. & Lafta, A. (1996) Cell-Wall Changes and Cell Tension in Response to Cold Acclimation and Exogenous Abscisic Acid in Leaves and Cell Cultures. *Plant Physiology*, **111**, 605–612.

Raven, J.A. (1980) SHORT- AND LONG-DISTANCE TRANSPORT OF BORIC ACID IN PLANTS. *New Phytologist*, **84**, 231–249.

Raven, J.A. (2014) Speedy small stomata? *Journal of Experimental Botany*, **65**, 1415–1424.

Ray, P.M., Green, P.B. & Cleland, R. (1972) Role of Turgor in Plant Cell Growth. *Nature*, **239**, 163–164.

Rayle, D.L. & Cleland, R.E. (1992) The Acid Growth Theory of Auxin-induced Cell Elongation Is Alive and Well. *Plant Physiology*, **99**, 1271–1274.

Rayon, C., Cabanes-Macheteau, M., Loutelier-Bourhis, C., Salliot-Maire, I., Lamoine, J., Reiter, W.-D., Lerouge, P. & Faye, L. (1999) Characterization of N-Glycans from Arabidopsis. Application to a Fucose-Deficient Mutant. *Plant Physiology*, **119**, 725–733.

Redondo-Nieto, M., Maunoury, N., Mergaert, P., Kondorosi, E., Bonilla, I. & Bolaños, L. (2012) Boron and calcium induce major changes in gene expression during legume nodule organogenesis. Does boron have a role in signalling? *New Phytologist*, **195**, 14–19.

Refregier, G., Pelletier, S., Jaillard, D. & Hofte, H. (2004) Interaction between Wall Deposition and Cell Elongation in Dark-Grown Hypocotyl Cells in Arabidopsis. *Plant Physiology*, **135**,

959–968.

Reid, R. (2014) Understanding the boron transport network in plants. *Plant and Soil*, **385**, 1–13.

Reid, R.J., Hayes, J.E., Post, A., Stangoulis, J.C.R. & Graham, R.D. (2004) A critical analysis of the causes of boron toxicity in plants. *Plant, Cell and Environment*, **25**, 1405–1414.

Reiter, W.D., Chapple, C.C. & Somerville, C.R. (1993) Altered growth and cell walls in a fucose-deficient mutant of Arabidopsis. *Science*, **261**, 1032–1035.

Reiter, W.D., Chapple, C. & Somerville, C.R. (1997) Mutants of Arabidopsis thaliana with altered cell wall polysaccharide composition. *Plant Journal*, **12**, 335–345.

Reuhs, B.L., Glenn, J., Stephens, S.B., Kim, J.S., Christie, D.B., Glushka, J.G., Zablackis, E., Albersheim, P., Darvill, A.G. & O'Neill, M.A. (2004) L-Galactose replaces L-fucose in the pectic polysaccharide rhamnogalacturonan II synthesized by the L-fucose-deficient mur1 Arabidopsis mutant. *Planta*, **219**, 147–157.

Reyes-Diaz, M., Ulloa, N., Zuniga-Feest, A., Gutierrez, A., Gidekel, M., Alberdi, M., Corcuera, L.J. & Bravo, L.A. (2006) Arabidopsis thaliana avoids freezing by supercooling. *Journal of Experimental Botany*, **57**, 3687–3696.

Richmond, T.A. & Somerville, C.R. (2000) The Cellulose Synthase Superfamily. *Plant Physiology*, **124**, 495–498.

Ridley, B.L., O'Neill, M.A. & Mohnen, D. (2001) Pectins: structure, biosynthesis, and oligogalacturonide-related sugnaling. *Phytochemistry*, **57**, 929–967.

Roelfsema, M.R.G. & Hedrich, R. (2002) Studying guard cells in the intact plant: modulation of stomatal movement by apoplastic factors. *New Phytologist*, **153**, 425–431.

Rudolph, A.S. & Crowe, J.H. (1985) Membrane stabilization during freezing: The role of two natural cryoprotectants, trehalose and proline. *Cryobiology*, **22**, 367–377.

Rui, Y. & Anderson, C.T. (2016) Functional Analysis of Cellulose and Xyloglucan in the Walls of Stomatal Guard Cells of Arabidopsis. *Plant Physiology*, **170**, 1398–1419.

Rui, Y., Xiao, C., Yi, H., Kandemir, B., Wang, J.Z., Puri, V.M. & Anderson, C.T. (2017) POLYGALACTURONASE INVOLVED IN EXPANSION3 Functions in Seedling Development, Rosette Growth, and Stomatal Dynamics in Arabidopsis thaliana. *The Plant Cell*, **29**, 2413–2432.

Rui, Y., Yi, H., Kandemir, B., Wang, J.Z., Puri, V.M. & Anderson, C.T. (2016) Integrating cell biology, image analysis, and computational mechanical modeling to analyze the contributions of cellulose and xyloglucan to stomatal function. *Plant Signaling & Behavior*, **11**, e1183086.

Ryden, P., Sugimoto-Shirasu, K., Smith, A.C., Findlay, K., Reiter, W.D. & McCann, M.C. (2003) Tensile properties of Arabidopsis cell walls depend on both a xyloglucan cross-linked microfibrillar network and rhamnogalacturonan II-borate complexes. *Plant Physiology*, **132**, 1033–1040.

Sadava, D., Walker, F. & Chrispeels, M.J. (1973) Hydroxyproline-rich cell wall protein (extensin): Biosynthesis and accumulation in growing pea epicotyls. *Developmental Biology*, **30**, 42–48.

Sakai, A. & Larcher, W. (1987) *Frost Survival of Plants: Responses and Adaptation to Freezing*

Stress. Ecological Studies.

Salt, R.W. & Kaku, S. (1967) Ice nucleation and propagation in spruce needles. *Canadian Journal of Botany*, **45**, 1335–1346.

Sarria, R., Wagner, T.A., Neill, M.A.O., Faik, A., Wilkerson, C.G., Keegstra, K. & Raikhel, N. V. (2001) Characterization of a Family of Arabidopsis Genes Related to Xyloglucan Fucosyltransferase1. *Plant Physiology*, **127**, 1595–1606.

von Schaewen, A., Sturm, A., O'Neill, J. & Chrispeels, M.J. (1993) lsolation of a Mutant Arabidopsis Plant That Lacks N-Acetyl Glucosaminyl Transferase I and Is Unable to Synthesize Golgi-Modified Complex N-Linked Glycans. *Plant Physiology*, **102**, 1109–1118.

Scheller, H.V. & Ulvskov, P. (2010) Hemicelluloses. *Annual Review of Plant Biology*, **61**, 263–289.

Scholz, F.G., Bucci, S.J., Arias, N., Meinzer, F.C. & Goldstein, G. (2012) Osmotic and elastic adjustments in cold desert shrubs differing in rooting depth: coping with drought and subzero temperatures. *Oecologia*, **170**, 885–897.

Schroeder, J.I. (1988) K+ Transport Properties of K+ Channels in the Plasma Membrane of Vicia faba. *The Journal of General Physiology*, **92**, 667–683.

Schroeder, J.I., Allen, G.J., Hugouvieux, V., Kwak, J.M. & Waner, D. (2001a) Guard Cell Signal Transduction. *Annual Review of Plant Physiology and Plant Molecular Biology*, **52**, 627–658.

Schroeder, J.I., Kwak, J.M. & Allen, G.J. (2001b) Guard cell abscisic acid sgnaling and engineering drought hardiness in plants. *Nature*, **410**, 327–330.

Sechet, J., Htwe, S., Urbanowicz, B., Agyeman, A., Feng, W., Ishikawa, T., Colomes, M., Kumar, K.S., Kawai-Yamada, M., Dinneny, J.R., O'Neill, M.A. & Mortimer, J.C. (2018) Suppressing Arabidopsis GGLT1 affects growth by reducing the L-galactose content and borate cross-linking of rhamnogalacturonan II. *Plant Journal*.

Séveno, M., Voxeur, A., Rihouey, C., Wu, A.-M., Ishii, T., Chevalier, C., Ralet, M.C., Driouich, A., Marchant, A. & Lerouge, P. (2009) Structural characterisation of the pectic polysaccharide rhamnogalacturonan II using an acidic fingerprinting methodology. *Planta*, **230**, 947–957.

Shafi, A., Dogra, V., Gill, T., Ahuja, P.S. & Sreenivasulu, Y. (2014) Simultaneous Over-Expression of PaSOD and RaAPX in Transgenic Arabidopsis thaliana Confers Cold Stress Tolerance through Increase in Vascular Lignifications. *PLOS One*, **9**, e110302.

Shimazaki, K., Doi, M., Assmann, S.M. & Kinoshita, T. (2007) Light Regulation of Stomatal Movement. *Annual Review of Plant Biology*, **58**, 219–247.

Shimazaki, K. & Kondo, N. (1987) Plasma Membrane H+-ATPase in Guard-Cell Protoplasts from Vicia faba L. *Plant Cell Physiology*, **28**, 893–900.

Shinwari, Z.K., Nakashima, K., Miura, S., Kasuga, M., Seki, M., Yamaguchi-Shinozaki, K. & Shinozaki, K. (1998) An Arabidopsis Gene Family Encoding DRE/CRT Binding Proteins Involved in Low-Temperature-Responsive Gene Expression. *Biochemical and Biophysical Research Communications*, **250**, 161–170.

Shorrocks, V.M. (1997) The occurrence and correction of boron deficiency. *Plant and Soil*, **193**, 121–148.

Showalter, A.M. (1993) Structure and Function of Plant Cell Wall Proteins. *The Plant Cell*, **5**, 9–23.

Shtein, I., Shelef, Y., Marom, Z., Zelinger, E., Schwartz, A., Popper, Z.A., Bar-On, B. & Harpaz-Saad, S. (2017) Stomatal cell wall composition: distinctive structural patterns associated with different phylogenetic groups. *Annals of Botany*, **119**, 1021–1033.

Siminovitch, D. (1979) Protoplasts Surviving Freezing to -196 C and Osmotic Dehydration in 5 Molar Salt Solutions Prepared from the Bark of Winter Black Locust Trees. *Plant Physiology*, **63**, 722–725.

Singh, J. (1979) Freezing of Protoplasts Isolated from Cold-Hardened and Non-Hardened Winter Rye. *Plant Science Letters*, **16**, 195–201.

Solecka, D., Zebrowski, J. & Kacperska, A. (2008) Are Pectins Involved in Cold Acclimation and De-acclimation of Winter Oil-seed Rape Plants? *Annals of Botany*, **101**, 521–530.

Sorek, N., Szemenyei, H., Sorek, H., Landers, A., Knight, H., Bauer, S., Wemmer, D.E. & Somerville, C.R. (2015) Identification of MEDIATOR16 as the Arabidopsis COBRA suppressor MONGOOSE1. *Proceedings of the National Academy of Sciences*, **112**, 16048–16053.

Spencer, F.S. & Maclachlan, G.A. (1972) Changes in Molecular Weight of Cellulose in the Pea Epicotyl during Growth. *Plant Physiology*, **49**, 58–63.

Starlfelt, M.G. (1966) The Role of Epidermal Cells in the Stomatal Movements. *Physiologia Plantarum*, **19**, 241–256.

Stefanowska, M., Kuras, M., Kubacka-Zebalska, M. & Kacperska, A. (1999) Low Temperature Affects Pattern of Leaf Growth and Structure of Cell Walls in Winter Oilseed Rape (Brassica napus L., var. oleifera L.). *Annals of Botany*, **84**, 313–319.

Steponkus, P.L. (1984) ROLE OF THE PLASMA MEMBRANE IN FREEZING INJURY AND COLD ACCLIMATION. *Annual Review of Plant Physiology*, **35**, 543–584.

Steponkus, P.L., Garber, M.P., Myers, S.P. & Lineberger, R.D. (1977) Effects of cold acclimation and freezing on structure and function of chloroplast thylakoids. *Cryobiology*, **14**, 303–321.

Steponkus, P.L., Uemura, M., Joseph, R.A., Gilmour, S.J. & Thomashow, M.F. (1998) Mode of action of the COR15a gene on the freezing tolerance of Arabidopsis thaliana. *Proceedings of the National Academy of Sciences of the United States of America*, **95**, 14570–14575.

Sterling, J.D., Atmodjo, M.A., Inwood, S.E., Kolli, V.S.K., Quigley, H.F., Hahn, M.G. & Mohnen, D. (2006) Functional identification of an Arabidopsis pectin biosynthetic homogalacturonan galacturonosyltransferase. *PNAS*, **103**, 5236–5241.

Sterling, J.D., Quigley, H.F., Orellana, A. & Mohnen, D. (2018) The Catalytic Site of the Pectin Biosynthetic Enzyme a-1,4-Galacturonosyltransferase Is Located in the Lumen of the Golgi. *Plant Physiology*, **127**, 360–371.

Stevenson, T.T., Darvill, A.G. & Albersheim, P. (1988) STRUCTURAL FEATURES OF THE PLANT CELL-WALL POLYSACCHARIDE RHAMNOGALACTURONAN-II. *Carbohydrate Research*, **182**, 207–226.

Stockinger, E.J., Gilmour, S.J. & Thomashow, M.F. (1997) Arabidopsis thaliana CBF1 encodes an AP2 domain-containing transcriptional activator that binds to the C-repeat/DRE, a cis-acting DNA regulatory element that stimulates transcription in response to low

temperature and water deficit. *Proceedings of the National Academy of Sciences of the United States of America*, **94**, 1035–1040.

Stout, D.G., Majak, W. & Reaney, M. (1980) In Vivo Detection of Membrane Injury at Freezing Temperatures. *Plant Physiology*, **66**, 74–77.

Strauss, G. & Hauser, H. (1986) Stabilization of lipid bilayer vesicles by sucrose during freezing. *Proceedings of the National Academy of Sciences of the United States of America*, **83**, 2422–2426.

Szymanski, D.B. & Cosgrove, D.J. (2009) Dynamic Coordination of Cytoskeletal and Cell Wall Systems during Plant Cell Morphogenesis. *Current Biology*, **19**, R800–R811.

Tahtiharju, S., Sangwan, V., Monroy, A.F., Dhindsa, R.S. & Borg, M. (1997) The induction of kin genes in cold-acclimating Arabidopsis thaliana. Evidence of a role for calcium. *Planta*, **203**, 442–447.

Takano, J., Miwa, K., Yuan, L., von Wiren, N. & Fujiwara, T. (2005) Endocytosis and degradation of BOR1, a boron transporter of Arabidopsis thaliana, regulated by boron availability. *Proceedings of the National Academy of Sciences of the United States of America*, **102**, 12276–12281.

Takano, J., Noguchi, K., Yasumori, M., Kobayashi, M., Gajdos, Z., Miwa, K., Hayashi, H., Yoneyama, T. & Fujiwara, T. (2002) Arabidopsis boron transporter for xylem loading. *Nature*, **420**, 337–340.

Takano, J., Wada, M., Ludewig, U., Schaaf, G., von Wiren, N. & Fujiwara, T. (2006) The Arabidopsis Major Intrinsic Protein NIP5;1 Is Essential for Efficient Boron Uptake and Plant Development under Boron Limitation. *The Plant Cell*, **18**, 1498–1509.

Tanaka, M., Wallace, I.S., Takano, J., Roberts, D.M. & Fujiwara, T. (2008) NIP6;1 Is a Boric Acid Channel for Preferential Transport of Boron to Growing Shoot Tissues in Arabidopsis. *The Plant Cell*, **20**, 2860–2875.

Tanner, C.B. (1963) Plant Temperatures. *Agronomy Journal*, **55**, 210–211.

Tao, D.-L., Li, P.H. & Carter, J. V. (1983) Role of cell wall in freezing tolerance of cultured potato cells and their protoplasts. *Physiologia Plantarum*, **58**, 527–532.

Tao, D.-L., Oquist, G. & Wingsle, G. (1998) Active Oxygen Scavengers during Cold Acclimation of Scots Pine Seedlings in Relation to Freezing Tolerance. *Cryobiology*, **37**, 38–45.

Taylor-Teeples, Lin, Lucas, Turco, Toal, Gaudinier, Young, Trabucco, Veling, Lamothe, Handakumbura, Xiong, Wang, Corwin, Tsoukalas, Zhang, Ware, Pauly, Kliebenstein, Dehesh, Tagkopoulos, Breton, Pruneda-Paz, Ahnert, Kay, Hazen & Brady. (2015) An Arabidopsis Gene Regulatory Network for Secondary Cell Wall Synthesis. *Nature*, **517**, 571–575.

Tenhaken, R. (2015) Cell wall remodeling under abiotic stress. *Frontiers in Plant Science*, **5**, 1–9.

Thomas, J.R., Darvill, A.G. & Albersheim, P. (1989) ISOLATION AND STRUCTURAL CHARACTERIZATION OF THE PECTIC POLYSACCHARIDE RHAMNOGALACTURONAN II FROM WALLS OF SUSPENSION-CULTURED RICE CELLS. *Carbohydrate Research*, **185**, 261–277.

Thomashow, M.F. (1998) Role of Cold-Responsive Genes in Plant Freezing Tolerance. *Plant Physiology*, **118**, 1–7.

Thomashow, M.F. (1999) PLANT COLD ACCLIMATION: Freezing Tolerance Genes and Regulatory Mechanisms. *Annual Review of Plant Physiology and Plant Molecular Biology*, **50**, 571–599.

Thonar, C., Liners, F. & Van Cutsem, P. (2006) Polymorphism and modulation of cell wall esterase enzyme activities in the chicory root during the growing season. *Journal of Experimental Botany*, **57**, 81–89.

Thorlby, G., Veale, E., Butcher, K. & Warren, G. (1999) Map positions of SFR genes in relation to other freezing-related genes of Arabidopsis thaliana. *The Plant Journal*, **17**, 445–452.

Trejo, Carlos, L., Davies, W.J. & Ruiz, L. del M.P. (1993) Sensitivity of Stomata to Abscisic Acid. *Plant Physiology*, **102**, 497–502.

Tyree, M.T. & Dixon, M.A. (1986) Water stress induced cavitation and embolism in some woody plants. *Physiologia Plantarum*, **66**, 397–405.

Tyree, M.T. & Sperry, J.S. (1989) Vulnerability of Xylem to Cavitation and Embolism. *Annual Review of Plant Physiology and Plant Molecular Biology*, **40**, 19–38.

Uemura, M., Joseph, R.A. & Steponkus, P.L. (1995) Cold Acclimation of Arabidopsis thaliana. Effect on Plasma Membrane Lipid Composition and Freeze-induced Lesions. *Plant Physiology*, **109**, 15–30.

Uemura, M., Tominaga, Y., Nakagawara, C., Shigematsu, S., Minami, A. & Kawamura, Y. (2006) Responses of the plasma membrane to low temperatures. *Physiologia Plantarum*, **126**, 81–89.

Vanzin, G.F., Madson, M., Carpita, N.C., Raikhel, N. V., Keegstra, K. & Reiter, W.-D. (2002) The mur2 mutant of Arabidopsis thaliana lacks fucosylated xyloglucan because of a lesion in fucosyltransferase AtFUT1. *PNAS*, **99**, 3340–3345.

Verhertbruggen, Y., Marcus, S.E., Haeger, A., Verhoef, R., Schols, H.A., Mccleary, B. V., Mckee, L., Gilbert, H.J. & Knox, J.P. (2009) Developmental complexity of arabinan polysaccharides and their processing in plant cell walls. *The Plant Journal*, **59**, 413–425.

Vialet-Chabrand, S.R.M., Matthews, J.S.A., Mcausland, L., Blatt, M.R., Griffiths, H. & Lawson, T. (2017) Temporal Dynamics of Stomatal Behavior: Modeling and Implications for Photosynthesis and Water Use. *Plant Physiology*, **174**, 603–613.

Villalobos, J.A., Yi, B.R. & Wallace, I.S. (2015) 2-Fluoro-L-Fucose Is a Metabolically Incorporated Inhibitor of Plant Cell Wall Polysaccharide Fucosylation. *Plos One*, **10**.

Voxeur, A. & Fry, S.C. (2014) Glycosylinositol phosphorylceramides from Rosa cell cultures are boron-bridged in the plasma membrane and form complexes with rhamnogalacturonan II. *The Plant Journal*, **79**, 139–149.

Voxeur, A., Gilbert, L., Rihouey, C., Driouich, A., Rothan, C., Baldet, P. & Lerouge, P. (2011) Silencing of the GDP-D-mannose 3,5-Epimerase Affects the Structure and Cross-linking of the Pectic Polysaccharide Rhamnogalacturonan II and Plant Growth in Tomato. *The Journal of Biological Chemistry*, **286**, 8014–8020.

Voxeur, A. & Höfte, H. (2016) Cell wall integrity signaling in plants: “To grow or not to grow that’s the question.” *Glycobiology*, **26**, 950–960.

Voxeur, A., Soubigou-Taconnat, L., Legee, F., Sakai, K., Antelme, S., Durand-Tardif, M., Lapierre, C. & Sibout, R. (2017) Altered lignification in mur1-1 a mutant deficient in GDP-L-fucose

synthesis with reduced RG-II cross linking. *PLoS ONE*, **12**, e0184820.

Walton, D.C. (1980) BIOCHEMISTRY AND PHYSIOLOGY OF ABSCISIC ACID. *Annual Review of Plant Physiology*, **31**, 453–489.

Wang, Y., Holroyd, G., Hetherington, A.M. & Ng, C.K.-Y. (2004) Seeing "cool" and "hot" - infrared thermography as a tool for non-invasive, high-throughput screening of Arabidopsis guard cell signalling mutants. *Journal of Experimental Botany*, **55**, 1187–1193.

Wanner, L.A. & Junttila, O. (1999) Cold-Induced Freezing Tolerance in Arabidopsis. *Plant Physiology*, **120**, 391–399.

Warington, K. (1923) The Effect of Boric Acid and Borax on the Broad Bean and certain other Plants. *Annals of Botany*, **27**, 630–670.

Warren, G., Mckown, R., Marin, A. & Teutonico, R. (1996a) Isolation of Mutations Affecting the Development of Freezing Tolerance in Arabidopsis thaliana (L.) Heynh. *Plant Physiology*, **111**, 1011–1019.

Warren, G., McKown, R., Marin, A. & Teutonico, R. (1996b) Isolation of mutations affecting the development of freezing tolerance in Arabidopsis thaliana (L.) Heynh. *Plant Physiology*, **111**, 1011–1019.

Webb, A.A.R., Mcainsh, M.R., Mansfield, T.A. & Hether. (1996) Carbon dioxide induces increase in guard cell cytosolic free calcium. *The Plant Journal*, **9**, 297–304.

Weiser, C.J. (1970) Cold Resistance and Injury in Woody Plants. *Science*, **169**, 1269–1278.

Weiser, R.L., Wallner, S.J. & Waddell, J.W. (1990) Cell Wall and Extensin mRNA Changes during Cold Acclimation of Pea Seedlings. *Plant Physiology*, **93**, 1021–1026.

Wesley-Smith, J., Berjak, P., Pammenter, N.W. & Walters, C. (2014) Intracellular ice and cell survival in cryo-exposed embryonic axes of recalcitrant seeds of Acer saccharinum: An ultrastructural study of factors affecting cell and ice structures. *Annals of Botany*, **113**, 695–709.

Whalley, H.J., Sargeant, A.W., Steele, J.F.C., Lacoere, T., Lamb, R., Saunders, N.J., Knight, H. & Knight, M.R. (2011) Transcriptomic Analysis Reveals Calcium Regulation of Specific Promoter Motifs in Arabidopsis. *The Plant Cell*, **23**, 4079–4095.

Whitcombe, A.J., O'Neill, M.A., Steffan, W., Albersheim, P. & Darvill, A.G. (1995) Structural characterization of the pectic polysaccharide, rhamnogalaturonan-II. *Carbohydrate Research*, **271**, 15–29.

Wiest, S.C. & Steponkus, P.L. (1978) Freeze-Thaw Injury to Isolated Spinach Protoplasts and Its Simulation at Above Freezing Temperatures. *Plant Physiology*, **62**, 699–705.

Willats, W.G.T. & Knox, J.P. (1996) A role for arabinogalactan-proteins in plant cell expansion: evidence from studies on the interaction of β-glucosyl Yariv reagent with seedlings of Arabidopsis thaliana. *The Plant Journal*, **9**, 919–925.

Willats, W.G.T., Orfila, C., Limberg, G., Buchholt, H.C., van Alebeek, G.-J.W.M., Voragen, A.G.J., Marcus, S.E., Christensen, T.M.I.E., Mikkelsen, J.D., Murray, B.S. & Knox, J.P. (2001) Modulation of the Degree and Pattern of Methyl-esterification of Pectic Homogalacturonan in Plant Cell Walls. *The Journal of Biological Chemistry*, **276**, 19404–19413.

Willick, I.R., Takahashi, D., Fowler, D.B., Uemura, M. & Tanino, K.K. (2018) Tissue-specific changes in apoplastic proteins and cell wall structure during cold acclimation of winter wheat crowns. *Journal of Experimental Botany*, **69**, 1221–1234.

Wisniewski, M., Ashworth, E. & Schaffer, K. (1987) The Use of Lanthanum to Characterize Cell Wall Permeability in Relation to Deep Supercooling and Extracellular Freezing in Woody Plants: II. Intrageneric Comparisons Between Betula lenta and Betula papyrifera. *Protoplasma*, **141**, 160–168.

Wisniewski, M. & Davis, G. (1995) Immunogold localization of pectins and glycoproteins in tissues of peach with reference to deep supercooling. *Trees*, **9**, 253–260.

Wisniewski, M., Davis, G. & Schaffer, K. (1991) Mediation of deep supercooling of peach and dogwood by enzymatic modifications in cell-wall structure. *Planta*, **184**, 254–260.

Wisniewski, M., Filler, M., Palta, J., Carter, J. & Arora, R. (2004) Ice Nucleation, Propagation, and Deep Supercooling in Woody Plants. *Journal of Crop Improvement*, **10**, 5–16.

Wisniewski, M. & Fuller, M. (1999) Ice nucleation and deep supercooling in plants: new insights using infrared thermography. *Cold-Adapted Organisms*, 105–118.

Wisniewski, M., Glenn, D.M. & Fuller, M.P. (2002) Use of a Hydrophobic Particle Film as a Barrier to Extrinsic Ice Nucleation in Tomato Plants. *Journal of American Society of Horticultural Science*, **127**, 358–364.

Wisniewski, M., Gusta, L. & Neuner, G. (2014) Adaptive mechanisms of freeze avoidance in plants: A brief update. *Environmental and Experimental Botany*, **99**, 133–140.

Wisniewski, M., Lindow, S.E. & Ashworth, E.N. (1997) Observations of Ice Nucleation and Propagation in Plants Using lnfrared Video Thermography. *Plant Physiology*, **113**, 327–334.

Wolf, S., van der Does, D., Ladwig, F., Sticht, C., Kolbeck, A., Schürholz, A.-K., Augustin, S., Keinath, N., Rausch, T., Greiner, S., Schumacher, K., Harter, K., Zipfel, C. & Höfte, H. (2014) A receptor-like protein mediates the response to pectin modification by activating brassinosteroid signaling. *Proceedings of the National Academy of Sciences*, **111**, 15261–15266.

Wong, S.C., Cowan, I.R. & Farquhar, G.D. (1979) Stomatal conductance correlates with photosynthetic capacity. *Nature*, **282**, 424–426.

Woolfenden, H.C., Baillie, A.L., Gray, J.E., Hobbs, J.K., Morris, R.J. & Fleming, A.J. (2018) Models and Mechanisms of Stomatal Mechanics. *Trends in Plant Science*, **23**, 822–832.

Woolfenden, H.C., Bourdais, G., Kopischke, M., Miedes, E., Molina, A., Robatzek, S. & Morris, R.J. (2017) A computational approach for inferring the cell wall properties that govern guard cell dynamics. *The Plant Journal*, **92**, 5–18.

Xin, Z. & Browse, J. (1998) eskimo1 mutants of Arabidopsis are constitutively freezing-tolerant. *Proceedings of the National Academy of Sciences of the United States of America*, **95**, 7799–7804.

Xin, Z., Mandaokar, A., Chen, J., Last, R.R. & Browse, J. (2007) Arabidopsis ESK1 encodes a novel regulator of freezing tolerance. *The Plant Journal*, **49**, 786–799.

Xu, Z., Jiang, Y., Jia, B. & Zhou, G. (2016) Elevated-CO2 Response of Stomata and Its Dependence on Environmental Factors. *Frontiers in Plant Science*, **7**, 1–15.

Yamada, T., Kuroda, K., Jitsuyama, Y., Takezawa, D., Arakawa, K. & Fujikawa, S. (2002) Roles of the plasma membrane and the cell wall in the responses of plant cells to freezing. *Planta*, **215**, 770–778.

Yamaguchi-Shinozaki, K. & Shinozaki, K. (1994) A Novel cis-Acting Element in an Arabidopsis Gene is lnvolved in Responsiveness to Drought, Low-Temperature, or High-Salt Stress. *The Plant Cell*, **6**, 251–264.

Yamazaki, T., Kawamura, Y. & Uemura, M. (2009) Extracellular freezing-induced mechanical stress and surface area regulation on the plasma membrane in cold-acclimated plant cells. *Plant signaling behavior*, **4**, 231–233.

Yang, Y., Costa, A., Leonhardt, N., Siegel, R.S. & Schroeder, J.I. (2008) Isolation of a strong Arabidopsis guard cell promotor and its potential as a research tool. *Plant Methods*, **4**.

Yapo, B.M., Lerouge, P., Thibault, J.-F. & Ralet, M.-C. (2007) Pectins from citrus peel cell walls contain homogalacturonans homogenous with respect to molar mass, rhamnogalacturonan I and rhamnogalacturonan II. *Carbohydrate Polymers*, **69**, 426–435.

Yoo, C.Y., Pence, H.E., Jin, J.B., Miura, K., Gosney, M.J., Hasegawa, P.M. & Mickelbart, M. V. (2010) The Arabidopsis GTL1 Transcription Factor Regulates Water Use Efficiency and Drought Tolerance by Modulating Stomatal Density via Transrepression of SDD1. *The Plant Cell*, **22**, 4128–4141.

Yoshida, S. & Uemura, M. (1990) Responses of the Plasma Membrane to Cold Acclimation and Freezing Stress. *The Plant Plasma Membrane* (eds C. Larsson), & I.M. Moller), p. Springer-Verlag, Berlin, Heidelberg.

Yuan, S. (2001) A Fungal Endoglucanase with Plant Cell Wall Extension Activity. *Plant Physiology*, **127**, 324–333.

Zablackis, E., Huang, J., Müller, B., Darvill, A.G. & Albersheim, P. (1995) Characterization of the Cell-Wall Polysaccharides of Arabidopsis thaliana Leaves. *Plant Physiology*, **107**, 1129–1138.

Zablackis, E., York, W.S., Pauly, M., Hantus, S., Reiter, W.-D., Chapple, C.C.S., Albersheim, P. & Darvill, A. (1996) Substitution of L-Fucose by L-Galactose in Cell Walls of Arabidopsis mur1. *Science*, **272**, 1808–1810.

Zachariassen, K.E. & Kristiansen, E. (2000) Ice Nucleation and Antinucleation in Nature. *Cryobiology*, **41**, 257–279.

Zarka, D.G., Vogel, J.T., Cook, D. & Thomashow, M.F. (2003) Cold Induction of Arabidopsis CBF Genes Involves Multiple ICE (Inducer of CBF Expression) Promoter Elements and a Cold-Regulatory Circuit That Is Desensitized by Low Temperature. *Plant Physiology*, **133**, 910–918.

Zdunek, A., Koziol, A., Pieczywek, P.M. & Cybulska, J. (2014) Evaluation of the Nanostructure of Pectin, Hemicellulose and Cellulose in the Cell Walls of Pears of Different Texture and Firmness. *Food Bioprocessing Technology*, **7**, 3525–3535.

Zeiger, E. (1983) The Biology of Stomatal Guard Cells. *Annual Review of Plant Physiology*, **34**, 441–75.

Zhang, C. (2009) Identification and characterization of cold- responsive genes in perennial

ryegrass.

Zhang, Y.-J., Bucci, S.J., Arias, N.S., Scholz, F.G., Hao, G.-Y., Cao, K.-F. & Goldstein, G. (2016a) Freezing resistance in Patagonian woody shrubs: the role of cell wall elasticity and stem vessel size. *Tree Physiology*, **36**, 1007–1018.

Zhang, G.F. & Staehelin, L.A. (1992) Functional Compartmentation of the Golgi Apparatus of Plant Cells. *Plant Physiology*, **99**, 1070–1083.

Zhang, T., Vavylonis, Di., Durachko, D.M. & Cosgrove, D.J. (2017) Nanoscale movements of cellulose microfibrils in primary cell walls. *Nature Plants*, **3**, 1–6.

Zhang, T., Zheng, Y. & Cosgrove, D.J. (2016b) Spatial organization of cellulose microfibrils and matrix polysaccharides in primary plant cell walls as imaged by multichannel atomic force microscopy. *Plant Journal*, **85**, 179–192.

Zhao, C., Zhang, Z., Xie, S., Si, T., Li, Y. & Zhu, J.-K. (2016) Mutational Evidence for the Critical Role of CBF Transcription Factors in Cold Acclimation in Arabidopsis. *Plant Physiology*, **171**, 2744–2759.

Zhu, J.-J. & Beck, E. (1991) Water Relations of Pachysandra Leaves during Freezing and Thawing. *Plant Physiology*, **97**, 1146–1153.

Zhu, M., Jeon, B.W., Geng, S., Yu, Y., Balmant, K., Chen, S. & Assmann, S.M. (2015) Preparation of Epidermal Peels and Guard Cell Protoplasts for Cellular, Electrophysical, and-Omics Assays of Guard Cell Function. *Plant Signal Transduction: Methods and Protocols* (eds J.R. Botella), & M.A. Botella), p. Springer, New York.

Zhu, J., Shi, H., Lee, B. -h., Damsz, B., Cheng, S., Stirm, V., Zhu, J.-K., Hasegawa, P.M. & Bressan, R.A. (2004) An Arabidopsis homeodomain transcription factor gene, HOS9, mediates cold tolerance through a CBF-independent pathway. *Proceedings of the National Academy of Sciences*, **101**, 9873–9878.

Zhu, J.J., Steudle, E. & Beck, E. (1989) Negative Pressures Produced in an Artificial Osmotic Cell by Extracellular Freezing. *Plant Physiology*, **91**, 1454–1459.

APPENDIX A

Nucleotide and amino acid sequence of MUR1 showing the SNPs and amino acid substitutions on the mutants of *mur1-1, mur1-2, mur1-3* and *sfr8* (*mur1-4*). (Skipsey, Knight and Knight, unpublished).

```
Protein      1  M  A  S  E  N  N  G  S  R  S  D  S  E  S  I  T  A  P  K  A
DNA          1 ATGGCGTCAGAGAACAACGGATCCAGATCCGATTCCGAATCCATCACCGCTCCCAAAGCT

            21  D  S  T  V  V  E  P  R  K  I  A  L  I  T  G  I  T  G  Q  D
            61 GATTCCACCGTCGTTGAACCGAGGAAGATAGCTCTGATCACCGGAATCACCGGCCAGGAC

            41  G  S  Y  L  T  E  F  L  L  G  K  G  Y  E  V  H  G  L  I  R
           121 GGATCATACCTGACGGAGTTCCTTCTCGGAAAAGGCTACGAAGTTCATGGTCTGATCCGT

            61  R  S  S  N  F  N  T  Q  R  I  N  H  I  Y  I  D  P  H  N  V
           181 CGATCATCGAATTTCAACACCCAGCGAATCAACCATATCTACATCGATCCACACAATGTC

            81  N  K  A  L  M  K  L  H  Y  A  D  L  T  D  A  S  S  L  R  R
           241 AACAAAGCTCTGATGAAACTCCACTACGCCGATCTCACCGACGCTTCCTCTCTCCGTCGT

                                  L(mur1-2)
           101  W  I  D  V  I  K  P  D  E  V  Y  N  L  A  A  Q  S  H  V  A
           301 TGGATCGATGTGATCAAACCTGACGAAGTTTATAACCTAGCTGCTCAATCTCACGTCGCT
                                  T
           121  V  S  F  E  I  P  D  Y  T  A  D  V  V  A  T  G  A  L  R  L
           361 GTCTCCTTCGAGATCCCTGATTACACAGCCGATGTAGTCGCAACCGGTGCTCTCCGTCTC

           141  L  E  A  V  R  S  H  T  I  D  S  G  R  T  V  K  Y  Y  Q  A
           421 CTTGAAGCCGTCAGATCTCACACCATCGACAGTGGCCGTACCGTCAAGTATTACCAAGCC

                F(mur1-1)
           161  G  S  S  E  M  F  G  S  T  P  P  P  Q  S  E  T  T  P  F  H
           481 GGATCTTCGGAGATGTTTGGATCAACTCCTCCTCCACAATCGGAGACGACGCCGTTTCAC
                T
                                        V(mur1-3)
           181  P  R  S  P  Y  A  A  S  K  C  A  A  H  W  Y  T  V  N  Y  R
           541 CCCAGATCTCCTTACGCAGCTTCCAAATGCGCTGCTCATTGGTACACAGTGAATTACAGA
                                        T
                                     E(sfr8)
           201  E  A  Y  G  L  F  A  C  N  G  I  L  F  N  H  E  S  P  R  R
           601 GAGGCGTACGGTCTCTTCGCTTGTAACGGAATCTTGTTCAATCACGAGTCACCTCGCCGT
                                        A
           221  G  E  N  F  V  T  R  K  I  T  R  A  L  G  R  I  K  V  G  L
           661 GGTGAGAATTTCGTGACGAGGAAGATCACAAGAGCATTGGGAAGGATCAAGGTTGGTTTG

           241  Q  T  K  L  F  L  G  N  L  Q  A  S  R  D  W  G  F  A  G  D
           721 CAGACGAAGCTATTCCTTGGGAATTTGCAAGCGTCAAGAGATTGGGGATTTGCAGGAGAT

           261  Y  V  E  A  M  W  L  M  L  Q  Q  E  K  P  D  D  Y  V  V  A
           781 TATGTGGAAGCAATGTGGTTGATGTTGCAGCAAGAGAAGCCAGATGATTACGTTGTGGCA

           281  T  E  E  G  H  T  V  E  E  F  L  D  V  S  F  G  Y  L  G  L
           841 ACAGAGGAAGGACACACAGTGGAAGAGTTTCTTGATGTGTCATTTGGGTATTTGGGACTC

           301  N  W  K  D  Y  V  E  I  D  Q  R  Y  F  R  P  A  E  V  D  N
           901 AATTGGAAAGATTATGTTGAGATTGACCAGAGGTACTTTAGGCCTGCTGAAGTAGATAAC

           321  L  Q  G  D  A  S  K  A  K  E  V  L  G  W  K  P  Q  V  G  F
           961 CTTCAAGGAGATGCAAGCAAGGCAAAGGAAGTGTTGGGGTGGAAACCACAAGTAGGGTTT

           341  E  K  L  V  K  M  M  V  D  E  D  L  E  L  A  K  R  E  K  V
          1021 GAGAAGCTTGTGAAGATGATGGTTGATGAAGATCTTGAGCTTGCTAAGAGGGAGAAAGTG

           361  L  V  D  A  G  Y  M  D  A  K  Q  Q  P  *
          1081 CTTGTTGATGCTGGATACATGGATGCTAAGCAGCAACCTTGA
```

APPENDIX B

List of the primers used for DNA analysis and RT-qPCR analysis of *pme6* and *mur* mutants. All primers were obtained from IDT (Integrated DNA Technologies).

No.	Target	Sequence (5' to 3')	Purpose
1	Transposon	TCTGAGTCGTGTAAACGAGCC	To confirm presence of the transposon insertion in *pme6* (Ler-0 background)
2	*PME6*	CCTCTTCGTATTCAAAGTATTTCCC	
3	*PME6* promotor	TGTGGCATTACGGGAAAGGT	To confirm presence of the T-DNA insertion in *pme6* (Col-0 background)
4	*PME6* promotor	TGGGAGGTGTTAGTAGGATTTTGT	
5	GK Left border	ATATTGACCATCATACTCATTGC	To verify GK insertion line in *pme6* (Col-0 background)
6	*MUR1*	GGATCAACTCCTCCTCCACA	To verify presence of base change in *sfr8* shown in Appendix A
7	*MUR1*	CCTCTGTTGCCACAACGTAA	
8	*PME6*	GGAACGTTCAAGATGGCACG	For gene expression measurements of *PME6* (Ler-0 and Col-0 background)
9	*PME6*	TGATGTTTCTCCGGTCCTGC	
10	*MUR1*	ATCTCACGTCGCTGTCTCCT	For gene expression measurements of *MUR1* in mutants shown in Appendix C
11	*MUR1*	GAGATCTGACGGCTTCAAGG	

APPENDIX C

Relative transcript expression of the *MUR1* gene in two-week-old seedlings of Col-0 wild type (WT), *sfr8, mur1-1, mur2* and *sfr8-C.* Error bars represent RQ_{MIN} and RQ_{MAX} and constitute the acceptable error level for a 95% confidence level according to a student's t-test.

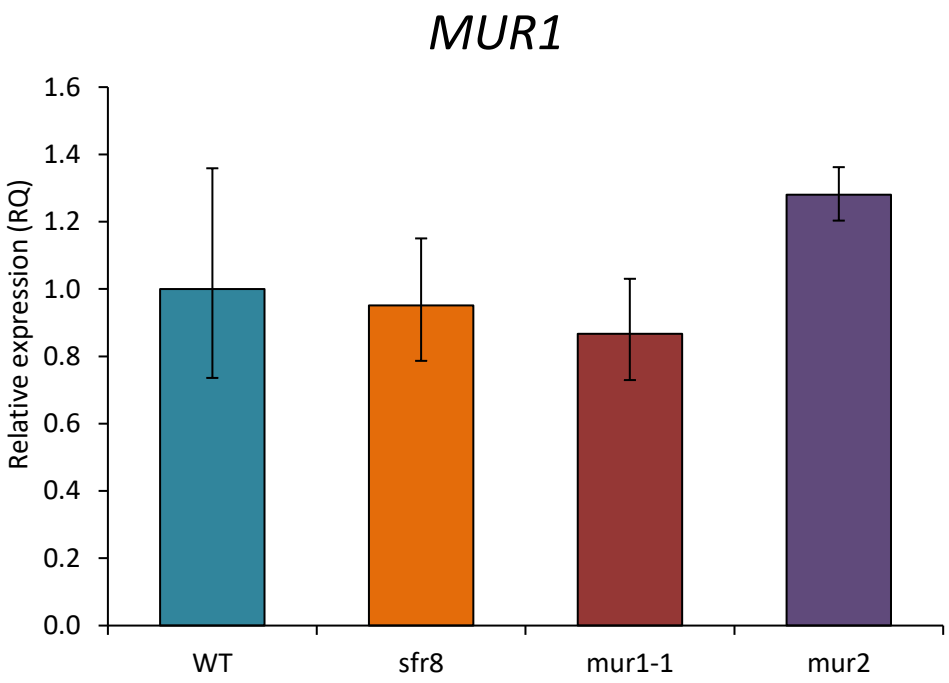

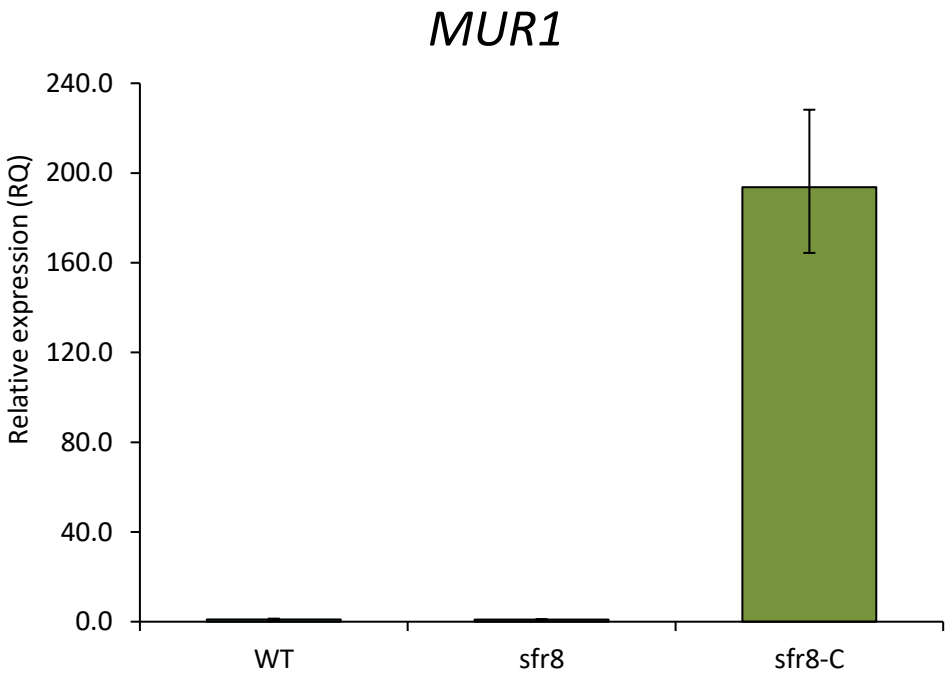

APPENDIX D

DNA analysis of putative Columbia-0 *pme6* insertion lines (1-12) using PCR and gel electrophoresis. Lane 1 contains 1 kb Hyperladder. **A**) Amplification of *pme6* DNA using primers 3 and 4 (Appendix B). Lines 1-12 were compared to Col-0 wild type (WT). A diminished band suggests presence of insertion. B) Amplification of *pme6* DNA using primers 3 and 5 (Appendix B). Lines 2,4,5,10 and 12 were compared to Col-0 wild type (WT). Presence of a band suggests presence of the insertion. DNA analysis was carried out on the Ler-0 *pme6* insertion line using primers 1 and 2 as in Amsbury *et al.* (2016), but no bands were observed for either wild type or *pme6* (data not shown).